

**An experimental study on the impact of temperature,
gasifying agents composition and pressure in the conversion
of coal chars to combustible gas products in the context of
Underground Coal Gasification**

Thesis submitted for the degree of Doctor of Philosophy

by

ELENI KONSTANTINOY, BSc, MSc

Institute of Sustainability and Environment
Cardiff School of Engineering
Cardiff University

July 2016



DECLARATION

This work has not previously been accepted in substance for any other degree and is not concurrently submitted in candidature for any other higher degree.

Signed (Eleni Konstantinou) Date 30/01/2017

STATEMENT 1

This thesis is being submitted in partial fulfillment of the requirements for the degree of Doctor of Philosophy (PhD).

Signed (Eleni Konstantinou) Date 30/01/2017

STATEMENT 2

This thesis is the result of my own independent work/investigation, except where otherwise stated. Other sources are acknowledged by explicit references

Signed (Eleni Konstantinou) Date 30/01/2017

STATEMENT 3

I hereby give consent for my thesis, if accepted, to be available for photocopying, inter-library loan and for the title and summary to be made available to outside organisations.

Signed (Eleni Konstantinou) Date 30/01/2017

SUMMARY OF THESIS

The key controlling factor in the effective energy conversion of coal to combustible gases during the UCG process is the behaviour of the pyrolysed char in the reduction zone of the UCG cavity, which has not been published in available academic literature. This study investigates the impact of the operating parameters during the reduction zone of UCG using a bespoke high pressure high temperature rig which was developed as part of this research work. This rig, operating at temperatures of up to 900 °C and at pressures up to 5.0 MPa, simulates the UCG process including each UCG zone individually for a broad range of underground conditions to a depth of 500 m. Carbon dioxide and steam were used as the primary reductants with char derived from dry steam coal and anthracite sample. Carbon dioxide and steam were injected at a variety of pressures and temperatures, plus at a range of relative H₂O/CO₂ proportions. The composition of the resulting product gas of both coals was measured and subsequently used to calculate carbon conversion (X), carbon conversion of combustible gases (Xa), cold gas efficiency (CGE) and low heating value (LHV) of the product gas.

Optimal operating conditions were determined for the dry steam coal and anthracite that produced the best gas composition both at atmospheric and elevated pressure and are unique for each UCG system. A shrinking core model was employed to describe the behaviour of the pyrolysed char to determine the activation energy and pre-exponential factor at atmospheric pressure for both coals. The evolution of the volatile matter of both coals and its contribution to the overall UCG performance was also determined. An optimum H₂O/CO₂ ratio was determined for both coals which enhanced the gasification rate of both coal chars up to the ratio of 2:1, above this ratio the effect saturated for both coals.

It was shown that pressure increases the reduction-gasification process of the chars which suggests that there is an optimum operating pressure which produces a peak in carbon conversion, CGE and LHV for the product gas over the conditions tested that differs for each coal. Therefore UCG projects aiming at reaching higher pressures will not achieve an increase in the output, unless there are some new effects occurring above 4.0 MPa. Pressure enhances the gas solid reactions and almost doubles the max carbon conversion (Xa) of combustible gases achieved at elevated pressure compared to that at atmospheric pressure. A shrinking core model was modified to take into account the effect of total pressure to the gasification rate of dry steam coal at 900 °C and pressures ranging from 0.7 to 1.65 MPa. Reaction constants for various pressures at 900 °C were determined for both coal chars.

Analysis of data shown that typical UCG operations on low rank coals provides a combustible product gas that relies heavily on releasing the volatile matter from the coal and does not depend on the carbon conversion of char to gas which justifies the high CGE and LHV of the product gas found in the field trials. It was found that carbon conversion X is not significantly affected by the type of coal and that the carbon converted during UCG is between approximately 45% for high rank coals up to 55% for low rank coals. Experimental results were used to calculate the output, size and UCG model of a potential power plant which produced realistic solutions and proves that high rank coals can be suitable for UCG projects. Anthracite can produce almost the same amount of combustible gases as the dry steam coal operating under specific conditions but with a lower CGE and LHV which suggests that anthracite may be found to be more suitable for producing hydrocarbons with UCG than energy.

ACKNOWLEDGEMENTS

I would like to thank the Engineering school of Cardiff University for giving me the opportunity to study and carry out this research work which I thoroughly enjoyed. I would also like to thank the Seren project for funding this research work.

I would like to thank my supervisors Devin Sapsford, especially a big thank you to Richard Marsh for his positive approach, his constructive criticism, his support in hard times and for being present and available.

An enormous thanks to my lovely husband, Alun, for being my rock. Without his continuous support, assistance and understanding, particularly during the last year, I wouldn't have managed to complete my PhD.

I would like to express my gratitude to the technicians of the combustion lab, especially Malcom Seabourne, for being always eager to assist me throughout this study.

I would like to dedicate this PhD to my father whom I sadly lost recently and whose memory was my driving force for the completion of this thesis.

“I expect nothing. I fear nothing. I am free.”

Nikos Kazantzakis

TABLE OF CONTENTS

LIST OF FIGURES	IX
LIST OF TABLES	XIV
NOMENCLATURE	XV
CHAPTER I: INTRODUCTION	1
1.1 Background	1
1.2 How UCG works	3
1.2.1 Chemical processes of UCG	4
1.2.2 Operating parameters of UCG	7
1.2.2.1 Coal rank	7
1.2.2.2 Gasifying agents	8
1.2.2.3 Temperature	9
1.2.2.4 Pressure	9
1.3 Research work	10
1.3.1 Aim of the research work	10
1.3.2 Objectives of the research work	10
1.4 Thesis overview	11
CHAPTER II: LITERATURE REVIEW	
2.1 Introduction	14
2.2 Medium to large laboratory scale experiments (particle size of coal blocks from 0.25x0.20x0.16 m up to 0.40x0.40x2.00 m)	15
2.2.1 UCG experiments performed at atmospheric pressure	15
2.2.2 UCG experiments at elevated pressure	19
2.3 Experiments on the pyrolysis, coal activity for CO ₂ and CO ₂ gasification in the context of UCG	20
2.3.1 Experiment on UCG pyrolysis	20
2.3.2 Experiment on coal activity for CO ₂	20
2.3.3 Experiment on CO ₂ gasification during UCG	21
2.4 UCG past and current pilot projects	22
2.4.1 Current UCG field trials at low and elevated pressure	24
2.4.1.1 Thulin, Belgium (1986-1987)	24
2.4.1.2 El Tremedal, Spain (1989-1998)	24
2.4.1.3 Rocky Mountain 1, Wyoming, USA (1987-1988)	25
2.4.1.4 Centralia, USA (1981-1985)	25
2.4.2 Effect of pressure on the gas composition of the product gas	25
2.5 Experiments on coal char reactivity at low and high pressures during gasification	28
2.5.1 Chars prepared at atmospheric pressure	30
2.5.2 Chars prepared at pressure	35
2.5.3 Effect of coal type on the gasification rate	38
2.6 Gas solid reactions	39
2.6.1 Coal gasification process	39
2.6.2 Characteristics of coal chars	40
2.6.3 Active or reaction sites	41
2.6.4 Regimes of gas solid reactions	41
2.6.5 Mechanism of char with CO ₂ and H ₂ O at low and high pressures	43

2.6.5.1	Reaction of char with CO ₂	43
2.6.5.2	Reaction of char with H ₂ O	44
2.6.6	Kinetic models	45
2.6.7	Arrhenius Law	47
2.7	Chapter Summary	48
CHAPTER III: EXPERIMENTAL APPARATUS		52
3.1	Introduction	52
3.2	Experimental Apparatus	56
3.3	Gas supply system	56
3.3.1	Gas cylinders	56
3.3.2	Gas lines	56
3.3.3	HPLC pump (High Performance Liquid Chromatography)	57
3.3.4	Mass flow controllers (MFC)	59
3.4	The reacting system	60
3.4.1	Pressure Vessel (reactor) and Heating system	60
3.4.2	Pressure gauges and pressure relief valves	65
3.5	Gas analysis system	65
3.5.1	Gas Liquid Separator	65
3.5.2	Back pressure regulator	66
3.5.3	Coriolis mass flow meter (MFM)	67
3.5.4	Gas analyser	68
CHAPTER IV: MATERIALS AND METHODS		69
4.1	Introduction	69
4.2	Coal samples	69
4.2.1	Preparation of the crushed and powdered coal samples	69
4.2.2	Preparation of the core coal samples	70
4.3	Coal characterisation tests	71
4.3.1	Proximate analysis	71
4.3.2	Ultimate analysis	73
4.3.3	Calorimeter bomb	73
4.4	Description of the experimental process	75
4.4.1	Char preparation	75
4.4.2	Char gasification at atmospheric pressure	76
4.4.3	Char gasification at elevated pressure	76
4.4.4	Shutdown procedure	77
4.4.5	Post experimental procedure	77
4.5	Measurements methods	78
4.6	Preliminary experiments to determine the impact of flowrate, sample size and particle size	80
CHAPTER V: EXPERIMENTAL RESULTS AT VARIOUS TEMPERATURES AND COMPOSITIONS OF GASIFYING AGENTS		84
5.1	Introduction	84
5.2	Effect of temperature	85
5.2.1	Experiments with dry steam coal and anthracite at various temperatures	86
5.2.2	Coal samples before and after gasification at atmospheric pressure	89
5.2.3	Experimental results / Discussion	90
5.2.3.1	Effect of temperature on carbon conversion, LHV and CGE	90
5.2.3.2	Effect of temperature on gasification reaction rate	91

5.2.3.3	Kinetic calculations	94
5.2.3.4	Summary	99
5.3	Effect of gasifying agent composition	100
5.3.1	Experiments with dry steam coal and anthracite at various compositions of gasifying agents	100
5.3.1.1	Experimental results / Discussion	104
5.3.1.2	Effect of gasifying agent composition on gasification reaction rate	104
5.3.1.3	Effect of gasifying agent composition on carbon conversion, LHV and CGE	106
5.3.1.4	Summary	111
5.4	Comparison with other studies	112
5.5	Experiments at the oxidation and drying - pyrolysis zone	114
5.5.1	Experimental results / Discussion	116
5.5.2	Summary	118
5.6	Chapter summary	119

CHAPTER VI: EXPERIMENTAL RESULTS OF PRESSURISED GASIFICATION

		122
6.1	Introduction	122
6.2	Effect of pressure	122
6.2.1	Pressurised gasification experiments with dry steam coal and anthracite	122
6.2.2	Coal samples before and after pressurised gasification	125
6.3	Experimental results / Discussion	126
6.3.1	Pressurised gasification	126
6.3.2	Effect of pressure on gasification reaction rate	130
6.3.3	Reaction mechanism at pressure	133
6.3.4	Kinetic calculations at pressure	135
6.3.5	Effect of pressure on Carbon Conversion, LHV & CGE at pressure	141
6.3.5.1	Carbon Conversion X and Xa	141
6.3.5.2	LHV of product gas	144
6.3.5.3	Cold Gas Efficiency	147
6.4	Comparison with other studies at pressure	149
6.5	Chapter Summary	150

Chapter VII: ENERGY AND MASS BALANCE IN ORDER TO DEMONSTRATE PRACTICAL FEASIBILITY OF REAL UCG OPERATIONS

		154
7.1	Introduction	154
7.2	Mass and energy balance	154
7.2.1	Energy balance	154
7.2.2	Mass balance	156
7.3	Application of data to UCG field trials	157
7.4	Commercialisation of UCG	161
7.4.1	Advance drilling technology (CRIP method)	161
7.4.2	UCG model	162
7.4.3	Coal resources gasified per panel and energy produced by panel	164
7.4.4	Calculating the output of small and large UCG power plants	165
7.5	Chapter Summary	169

Chapter VIII: CONCLUSIONS AND RECOMMENDATIONS

		171
8.1	Conclusions	171
8.1.1	Experimental apparatus	171

8.1.2	Effect of temperature and gasifying agents composition at atmospheric pressure	171
8.1.3	Effect of pressure	174
8.1.4	Application of data to UCG field trials	177
8.1.5	Overall conclusions	178
8.2	Recommendations	181

LIST OF FIGURES

Figure 1.1: World coal reserves by region and type. (Source: IEA-CCT).	1
Figure 1.2: World energy consumption for each fuel. (Source: BP statistical review of World Energy 2015)	2
Figure 1.3: UCG process	3
Figure 1.4: Schematic representation of UCG reaction zones	4
Figure 1.5: Gasified coal in the reduction zone	7
Figure 2.1: Past (yellow dot) and current (green dot) UCG projects (Source: Solid Energy-Huntly project in New Zealand)	23
Figure 2.2: UCG gas composition produced by UCG field trials [17]	26
Figure 2.3: UCG gas composition and heating value variation with pressure (LLNL)	27
Figure 2.4: UCG product gas calorific value with gas pressure [63]	28
Figure 2.5: Coal gasification process	40
Figure 2.6: Gas-solid reaction rate in temperature regimes	43
Figure 2.7: Reaction of a particle under chemical control with the progressive conversion model [45]	46
Figure 2.8: Reaction of a particle under chemical control with the shrinking unreacted core model [45]	48
Figure 3.1: Schematic of the bespoke high pressure high temperature rig showing the gas supply system (lines of O ₂ , CO ₂ , N ₂ and steam with mass flow controllers, filters and non-return valves-blue line), the reacting system (reactor and furnace with pressure gauges and pressure relief valves before and after the reactor-red line) and the gas analysis system (tar trap, water cooled condenser, cooler, mass flow meter, gas analyser and PC with logging and software control-green line).	53
Figure 3.2: Image of the bespoke high pressure high temperature rig and associated control and analysis hardware	55
Figure 3.3: The cylinder cupboard with the O ₂ , CO ₂ and CO gas cylinders	56
Figure 3.4: Part of the gas supply system showing the gas lines and the HPLC pump. The pressure relief valve and the pressure gauge are also visible	57
Figure 3.5: The HPLC pump with a glass bottle filled with deionised water	58
Figure 3.6: The 1/16" liquid stream line inserted into a 1/4" gas line passed to the reactor	58
Figure 3.7: The mass flow controllers of the experimental setting	59
Figure 3.8: MFC and flow sensor operational diagram	60
Figure 3.9: The reactor sitting on the HST furnace and its right head opening from where the boat with the coal sample was inserted	61
Figure 3.10: A view inside of the reactor from the right head opening	62
Figure 3.11: Image of the removable sample holder referred as quartz boat with a cylindrical coal sample	62
Figure 3.12: Procedure of the preparation of the boat with the coal sample and its insertion in the reactor	62
Figure 3.13: Equipment which was used to connect the right screw cap end of the reactor with the gas line	63
Figure 3.14: The right screw cap ending of the reactor connected to the gas line	63
Figure 3.15: The tubular pressure vessel (reactor) sitting in the Horizontal Split Tube furnace	64
Figure 3.16: Temperature controller of the Horizontal Split Tube (HST) furnace.	64
Figure 3.17: A pressure gauge (left) and a pressure relief valve (right)	65

Figure 3.18: The gas liquid separator (tar trap) (on the left) and the cooler (on the right)	66
Figure 3.19: Back pressure regulator	67
Figure 3.20: Coriolis flow meter	67
Figure 3.21: The X-Stream Enhanced XEGP-General Purpose Gas Analyser (left) and its calibration gas (right)	68
Figure 4.1: Angular sizes blocks and crushed coal 3-4 mm	70
Figure 4.2: Image of the diamond core drill	71
Figure 4.3: Image of the cylindrical coal samples	71
Figure 4.5: Crucibles for determining the moisture and ash content	72
Figure 4.6: Crucibles for determining the volatile matter	72
Figure 4.7: Image of the sulfur and carbon analyser	73
Figure 4.8: Image and schematic of the bomb calorimeter	74
Figure 4.8: The tar trap put into a bucket with ice cubes to drop its temperature	76
Figure 4.8: Optimum CO ₂ /C ratio for dry steam coal at fixed CO ₂ flowrate=0.4 l/min	80
Figure 4.9: Optimum CO ₂ /C ratio for the anthracite at fixed CO ₂ flowrate=0.4 l/min	81
Figure 5.1: Measured rig data showing the variation of concentration of the produced gases (Vol %) over time at a) 750°C, b) 800°C, c) 850°C and d) 900°C under the flow of CO ₂ +H ₂ O (H ₂ O/CO ₂ =2 (m/m), 0.1 MPa) during gasification of the dry steam coal.	87
Figure 5.2: Measured rig data showing the variation of concentration of the produced gases (Vol %) over time at a) 760°C, b) 800°C, c) 850°C and d) 900°C under the flow of CO ₂ +H ₂ O (H ₂ O/CO ₂ =2 (m/m), 0.1 MPa) during gasification of anthracite.	88
Figure 5.3: Coal samples and coal char samples of the dry steam coal and anthracite before and after gasification at 0.1 MPa under the flow of CO ₂ + H ₂ O (900°C, H ₂ O / CO ₂ =2:1).	89
Figure 5.4: Calculated carbon conversion X_a of char to combustible gases (CO + CH ₄) over time during CO ₂ +H ₂ O gasification of the dry steam coal at 750 °C, 800 °C, 850 °C and 900 °C from (H ₂ O/CO ₂ =2, 0.1 MPa) from raw rig data.	92
Figure 5.5: Calculated carbon conversion X_a of char to combustible gases (CO + CH ₄) over time during CO ₂ +H ₂ O gasification of anthracite at 760 °C, 800 °C, 850 °C and 900 °C (H ₂ O/CO ₂ =2, 0.1 MPa) from raw rig data.	93
Figure 5.6: Calculated reaction rate of dry steam and anthracite coal char as a function of carbon conversion X_a under the flow of CO ₂ +H ₂ O at 900 °C (H ₂ O/CO ₂ =2, 0.1 MPa).	93
Figure 5.7: Comparison of the conversion X_a at 900 °C of the experimental data with the shrinking core model and the progressive conversion model for the dry steam coal.	95
Figure 5.8: Comparison of the conversion X_a at 900 °C of the experimental data with the shrinking core model and progressive conversion model for the anthracite.	95
Figure 5.9: Calculated conversion data $3(1-(1-X_a)^{1/3})$ versus reaction time of dry steam coal for CO ₂ + H ₂ O gasification at a total system pressure of 0.1 MPa.	97
Figure 5.10: Calculated conversion data $3(1-(1-X_a)^{1/3})$ versus reaction time of anthracite for CO ₂ + H ₂ O gasification at a total system pressure of 0.1 MPa.	97
Figure 5.11: Arrhenius plot of the reaction constant k for CO ₂ + H ₂ O gasification of the dry steam coal-char at 900 °C, 850 °C, 800 °C and 750 °C (H ₂ O/CO ₂ =2, 0.1 MPa).	98

Figure 5.12: Arrhenius plot of the reaction constant k for $\text{CO}_2 + \text{H}_2\text{O}$ gasification of the anthracite coal-char at 900 °C, 850 °C, 800 °C and 760 °C ($\text{H}_2\text{O}/\text{CO}_2=2$, 0.1 MPa).	98
Figure 5.13: Measured rig data showing the variation of concentration of the produced gases (Vol %) during gasification of the dry steam coal char over time for ratio of $\text{H}_2\text{O} / \text{CO}_2$ of a)1:1 , b) 1.5:1, c) 2:1, d)2.5:1, e) 3:1 and f) 3.5:1 under the flow of $\text{CO}_2 + \text{H}_2\text{O}$ (900°C, 0.1 MPa).	102
Figure 5.14: Measured rig data showing the variation of concentration of the produced gases (Vol %) during gasification of anthracite char over time for ratio of $\text{H}_2\text{O} / \text{CO}_2$ of a)1:1 , b) 1.5:1, c) 2:1, d)2.5:1 and e) 3:1 under the flow of $\text{CO}_2 + \text{H}_2\text{O}$ (900°C, 0.1 MPa).	102
Figure 5.15: Calculated carbon conversion X_a of combustible gases ($\text{CO} + \text{CH}_4$) over time for various ratios of $\text{H}_2\text{O}/\text{CO}_2$ (900°C, 0.1 MPa) during gasification of the dry steam coal.	105
Figure 5.16: Calculated carbon conversion X_a of combustible gases ($\text{CO} + \text{CH}_4$) over time for various ratios of $\text{H}_2\text{O}/\text{CO}_2$ (900°C, 0.1 MPa) during gasification of anthracite.	105
Figure 5.17: Calculated gas production (mol/kg of sample) during gasification of dry steam coal char for various ratios of $\text{H}_2\text{O} / \text{CO}_2$ (900°C, 0.1 MPa).	109
Figure 5.18: Calculated LHV (MJ/Nm^3) of the produced gas during gasification of dry steam coal char for various ratios of $\text{H}_2\text{O} / \text{CO}_2$ (900°C, 0.1 MPa), expressed as the relative contributions of each gas.	109
Figure 5.19: Calculated gas production (mol/kg of sample) during gasification of anthracite for various ratios of $\text{H}_2\text{O} / \text{CO}_2$ (900°C, 0.1 MPa).	110
Figure 5.20: Calculated LHV (MJ/Nm^3) of the produced gas during gasification of anthracite char for various ratios of $\text{H}_2\text{O} / \text{CO}_2$ (900°C, 0.1 MPa), expressed as the relative contributions of each gas.	110
Figure 5.21: Percentage composition of gaseous products during oxygen lignite seam gasification phase. [76]	114
Figure 5.22: Measured rig data showing the variation of concentration of the produced gases (Vol %) during combustion of dry steam coal char over time under the flow of $\text{O}_2 = 0.4\text{l}/\text{min}$ (900°C, 0.1 MPa).	115
Figure 5.23: Measured rig data showing the variation of concentration of the produced gases (Vol %) during combustion of anthracite coal char over time under the flow of $\text{O}_2 = 0.4\text{l}/\text{min}$ (900°C, 0.1 MPa).	115
Figure 5.24: Measured rig data showing the variation of concentration of the produced gases (Vol %) during devolatilisation of dry steam coal over time under the flow of N_2 (0.1 MPa).	116
Figure 5.25: Measured rig data showing the variation of concentration of the produced gases (Vol %) during devolatilisation of anthracite coal over time under the flow of N_2 (0.1 Mpa).	116
Figure 6.1: Measured rig data showing variation of concentration of the produced gases (Vol %) during gasification of the dry steam coal over time for a) 0.7 , b) 0.9 , c) 1.65, d) 2.2, e) 3.0 and f) 3.9 MPa under the flow of $\text{CO}_2 + \text{H}_2\text{O}$ (900°C, $\text{H}_2\text{O} / \text{CO}_2=2:1$)	123
Figure 6.2: Measured rig data showing variation of concentration of the produced gases (Vol %) during gasification of anthracite over time for a) 0.8, b)1.0 , c) 1.65, d) 2.1, e) 3.0 and f) 4.0 MPa under the flow of $\text{CO}_2 + \text{H}_2\text{O}$ (900°C, $\text{H}_2\text{O} / \text{CO}_2=2:1$)	124
Figure 6.3: Coal samples and coal char samples of the dry steam coal before and after gasification at 1.65 MPa under the flow of $\text{CO}_2 + \text{H}_2\text{O}$ (900°C, $\text{H}_2\text{O} /$	

CO ₂ =2:1)	125
Figure 6.4: Coal sample and coal char sample of anthracite before and after gasification at 1.65 MPa under the flow of CO ₂ + H ₂ O (900°C, H ₂ O / CO ₂ =2:1).	126
Figure 6.5: Calculated concentrations (Vol %) of the combustible product gases over pressure of dry steam coal from measured rig data.	129
Figure 6.6: Calculated concentrations (Vol %) of the combustible product gases over pressure of anthracite from measured rig data.	129
Figure 6.7: Calculated carbon conversion X_a of combustible gases (CO + CH ₄) over time normalised to the total product gas flowrate during CO ₂ + H ₂ O gasification of dry steam coal at 900°C and 0.7, 0.9, 1.65, 2.2, 3.0 and 3.9 MPa from measured rig data.	131
Figure 6.8: Calculated carbon conversion X_a of combustible gases (CO + CH ₄) over time normalised to the total product gas flowrate during CO ₂ + H ₂ O gasification of anthracite at 900°C and 0.8, 1.0, 1.65, 2.1, 3.0 and 4.0 MPa from measured rig data.	131
Figure 6.9: Calculated comparison of the conversion X_a at 1.65 MPa and 900°C of the experimental data with the shrinking core model and the progressive reaction model for the dry steam coal from measured rig data.	136
Figure 6.10: Calculated comparison of the conversion X_a at 1.0 MPa and 900 °C of the experimental data with the shrinking core model and the progressive reaction model for the anthracite from measured rig data.	136
Figure 6.11: Calculated carbon conversion X_a of combustible gases (CO + CH ₄) over time during CO ₂ + H ₂ O gasification of dry steam coal at 0.1, 0.7, 0.9, 1.65, 2.2, 3.0 and 3.9 MPa (900°C, H ₂ O/CO ₂ =2:1) from measured rig data.	137
Figure 6.12: Calculated carbon conversion X_a of combustible gases (CO + CH ₄) over time during CO ₂ + H ₂ O gasification of anthracite coal at 1.0, 1.65, 2.1, 3.0 and 4.0 MPa (900°C, H ₂ O/CO ₂ =2:1) from measured rig data.	137
Figure 6.13: Pressure over the reaction constant k for CO ₂ + H ₂ O gasification of dry steam coal char at 0.1, 0.7, 0.9, 1.65, 2.2, 3.0 and 3.9 MPa and anthracite at 0.1, 0.8, 1.0, 1.65, 2.1, 3.0 and 4.0 MPa (900°C, H ₂ O/CO ₂ =2:1) from measured raw data.	139
Figure 6.14: Calculated carbon conversion X and X_a at 900°C as a function of pressure for the dry steam (H ₂ O/CO ₂ =2:1) from measured rig data.	142
Figure 6.15: Calculated carbon conversion X and X_a at 900°C as a function of pressure for anthracite (H ₂ O/CO ₂ =2:1) from measured rig data.	142
Figure 6.16: Calculated LHV of the gas produced versus pressure during the reduction zone of a simulated UCG process expressed as energy contribution to the overall heating value of the resultant product gas of dry steam coal from measured rig data.	145
Figure 6.17: Gas production (mass/ kg of coal sample) during gasification of dry steam coal sample for various pressures at 900 °C.	145
Figure 6.18: Calculated LHV of the gas produced versus pressure during the reduction zone of a simulated UCG process expressed as energy contribution to the overall heating value of the resultant product gas of anthracite from measured rig data.	146
Figure 6.19: Gas production (mass/ kg of coal sample) during gasification of anthracite for various pressures at 900 °C.	
Figure 6.20: Calculated CGE as function of pressure at 900 °C for both coal chars from measured rig data.	148
Figure 6.21: Calculated CGE as function of pressure at 900 °C for both coals from measured rig data.	149

Figure 7.1: Energy balance of the experimental process presented in a Sankey diagram.	155
Figure 7.2: Mass balance of the experimental procedure presented in a Sankey diagram.	156
Figure 7.3: Gas composition of Centralia field trial, Rocky Mountain 1 field trial together with the study of the dry steam coal at 0.7 MPa and anthracite at 0.8 MPa.	160
Figure 7.4: Gas composition of El Tremedal field trial together with the study of the dry steam coal at 3.9 MPa and anthracite at 4.0 MPa.	160
Figure 7.5: Schematic of the CRIP method [16].	161
Figure 7.6: Multiple gasification cavities produced by the CRIP technique [16].	162
Figure 7.7: UCG model underground by employing the CRIP method.	163
Figure 7.8: UCG module	163

LIST OF TABLES

Table 1.1: Principal overall reactions participating in the coal gasification process	6
Table 4.1: Proximate, ultimate analysis and LHV of the coal and char samples	74
Table 4.2: LHV of gases	79
Table 4.3: Calculated reactivity from experiments with different sizes of coal samples at atmospheric pressure	82
Table 4.4: Calculated reactivity from experiments with different sizes of coal samples at elevated pressure	83
Table 5.1: Calculated average gas compositions as % vol of dry steam coal and anthracite during the reduction zone for different temperatures at ratio of $H_2O/CO_2 = 2$ (m/m) and 0.1 MPa.	90
Table 5.2: Calculated gasification parameters of dry steam coal at different temperatures from the rig data ($H_2O/CO_2=2$ (m/m), 0.1 MPa)	91
Table 5.3: Calculated gasification parameters of anthracite at different temperatures from the rig data ($H_2O/CO_2=2$ (m/m), 0.1 MPa)	91
Table 5.4: Reaction constants k for $CO_2 + H_2O$ gasification of the bituminous coal-char at 900 °C, 850 °C, 800 °C and 750 °C ($H_2O/CO_2=2$, 0.1 MPa)	96
Table 5.5: Reaction constants k for $CO_2 + H_2O$ gasification of the anthracite at 900 °C, 850 °C, 800 °C and 760 °C ($H_2O/CO_2=2$, 0.1 MPa)	96
Table 5.6: Activation energies and pre-exponential factors for the two coal chars in $CO+H_2O$ at 0.1 MPa and ratio of $H_2O/CO_2=2$ (m/m)	99
Table 5.7: Calculated average gas compositions as % vol of dry steam coal and anthracite during the reduction zone for different ratios of H_2O/CO_2 at 900 °C and 0.1 MPa	104
Table 5.8: Calculated gasification parameters of the chars of dry steam coal and anthracite for different H_2O/CO_2 ratios (900 °C, 0.1 MPa)	107
Table 5.9: Compositions of product gas (% V) of other studies and of this study	112
Table 5.10: Calculated gasification parameters during the reduction, oxidation and drying-pyrolysis zone for the dry steam coal and anthracite at 900 °C and 0.1 MPa	118
Table 6.1: Calculated average gas composition and LHV of product gas in $CO_2 + H_2O$ gasification at 900°C of dry steam coal at a range of pressures from measured rig data	127
Table 6.2: Calculated average gas composition and LHV of product gas in $CO_2 + H_2O$ gasification at 900°C of anthracite at a range of pressures from measured rig data	128
Table 6.3: The values of the reaction constant k for the dry steam coal at various pressures (900°C, $H_2O/CO_2=2:1$)	138
Table 6.4: The values of the reaction constant k for anthracite at various pressures (900°C, $H_2O/CO_2=2:1$)	138
Table 7.1 Information determined for the 120 MWth power plant	169
Table 7.2: Information determined for the 500 MWth power plant	168

NOMENCLATURE

A	Activation energy
Ca	Carbon in CO + CH ₄
CCS	Carbon capture and storage
CGE	Cold gas efficiency
C(O)	Oxygen surface complex
CRIP	Controlled Retracting Injection Point
DTF	Drop tube furnace
dX_a / dt	Reaction rate
E	Pre-exponential factor
F.C.	Fixed Carbon
$f(x)$	Structure factor
HHV	High heating value
HPLC	High performance liquid chromatography
k	Reaction constant
LHV	Low heating value
m	Correlation exponent of total system pressure
M	Moisture
MFC	Mass flow controller
MFM	Mass flow metre
Mtoe	Million tons of oil equivalent
MPa	Mega pascal
n	Reaction order
OEA	Oxygen enriched air
P_{CO_2}	CO ₂ concentration
P_g	Partial pressure of the reactant
P_{total}	Total system pressure
PBBR	Packed bed balance reactor
PDTF	Pressurised drop tube furnace
r	Reactivity
R	Ideal gas constant
STP	Standard temperature pressure
T	Temperature (Kelvin)

TGA	Thermo gravimetric analyzer
UCG	Underground coal gasification
V.M.	Volatile matter
W	Final mass of carbon in the char
W_0	Initial mass of carbon in the char
X	Carbon conversion
X_a	Carbon conversion in CO + CH ₄
ΔW	Initial mass in char-final mass in char

CHAPTER I

INTRODUCTION

1.1 Background

Climate change and global warming is forcing industry worldwide to reduce their greenhouse gas emissions, one of which is carbon dioxide mainly produced by burning fossil fuels for energy. Therefore industry is trying to develop low-carbon technologies which will provide the required energy demand. In Europe, the European Commission's target is to reduce the green house gas (GHG) emissions to 80-95% below 1990 levels by 2050 by developing secure, affordable and climate-friendly energy. A diversified supply of technologies is in the agenda which includes large scale renewable mainly for heating and cooling (onshore wind, hydro and solar power), nuclear power for electricity, biomass for heating, electricity and transport (bio fuels), shale gas and clean coal technologies for electricity and alternative fuels (electrical vehicles, synthetic fuels, methane, LPG) and last but not least carbon capture and storage to manage the CO₂ emissions.

There are different scenarios for which technologies of energy mix will proceed and at what scale. This will depend on a market basis and on each country's indigenous sources of energy. One of the most widely spread sources is coal [16, 71] as shown in Figure 1.1 which illustrates the world coal reserves that are economically recoverable by region and type.

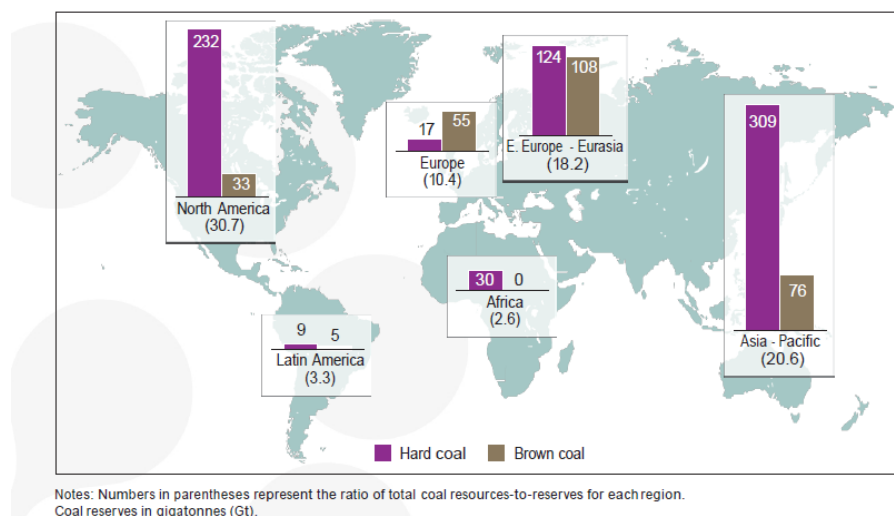


Figure 1.1: World coal reserves by region and type. (Source: IEA-CCT)

According to the International Energy Agency (IEA) the world's proved reserves which are economically recoverable using conventional mining technologies were estimated at the end of 2005 to be just under 850 Gt by the World Energy Council (2007) and 900 Gt by BP (2007). Studies suggest that coal seams that cannot be mined with conventional mining because they are deep, thin or steeply dipping could increase the world's coal reserves by 600 Gt (World Energy Council 2007) which is a 70% increase [11]. In total there is around 18 Tt of coal resources all around the world that are unmined [11]. In 2013 the world energy demand was supplied mainly by the fossil fuels of oil, coal and gas as shown in Figure 1.2 with coal having the second highest consumption after oil at 3.9 Billion Mtoe. In addition, sufficient coal reserves exist for another 150 years of generation at current consumption rates compared to oil and gas resources which will last around 54 and 60 years respectively [34].

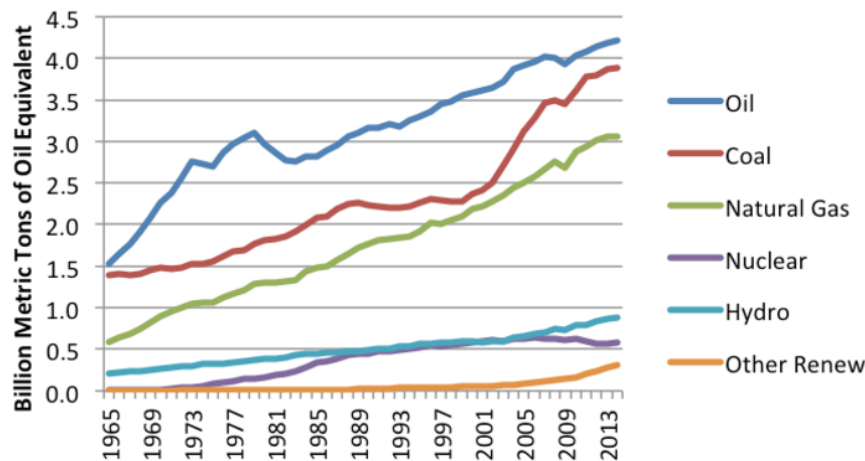


Figure 1.2: World energy consumption for each fuel.
(Source: BP statistical review of World Energy 2015)

So industry is currently heavily dependent on coal for energy production and according to the European's Committee report "Energy roadmap 2050", coal can add to the future diversified energy portfolio and continue to contribute to the security of supply. With the development of carbon capture and storage (CCS) and other emerging clean coal technologies, coal could continue to play an important role in the future sustainable and secure supply of energy [20, 21]. One of the clean coal technologies that exploits coal is Underground coal gasification (UCG). UCG converts coal resources in-situ into a gas product which can be combusted for power generation and industrial heating or used for the production of hydrogen, synthetic

natural gas, transport fuels (diesel) and chemicals (fertilisers, etc). UCG produces energy with 30% less CO₂ emissions than a conventional power plant and if combined with carbon storage is a very cost effective option. Furthermore UCG eliminates coal mining, coal transportation and the need for ash disposal after gasification. UCG's footprint is smaller than conventional mining and less costly according to relevant studies [10]. Therefore if UCG and CCS are going to be commercialised, then UCG can provide in short term the required low-carbon energy, as well as chemicals and transport fuels which will be needed in the long term [16, 25].

1.2 How UCG works

Underground coal gasification (UCG) exploits coal resources that are either uneconomical to mine with conventional mining methods or are inaccessible due to depth, geology or other mining and safety considerations. Coal seams are accessed from the surface via boreholes. An injection borehole introduces oxygen or air to the coal seam to combust a proportion of the coal in-situ, which in addition to water added to the system, drives the gasification of the remaining coal producing a mixture of gases (known as 'syngas') that is extracted via a second borehole (Figure 1.3). This mixture of gases mainly consists of H₂, CO, CH₄ and CO₂ whose proportions depend on the coal rank, temperature, pressure conditions and the reactant gases injected [7, 12, 71]. In this study the syngas will be called product gas.

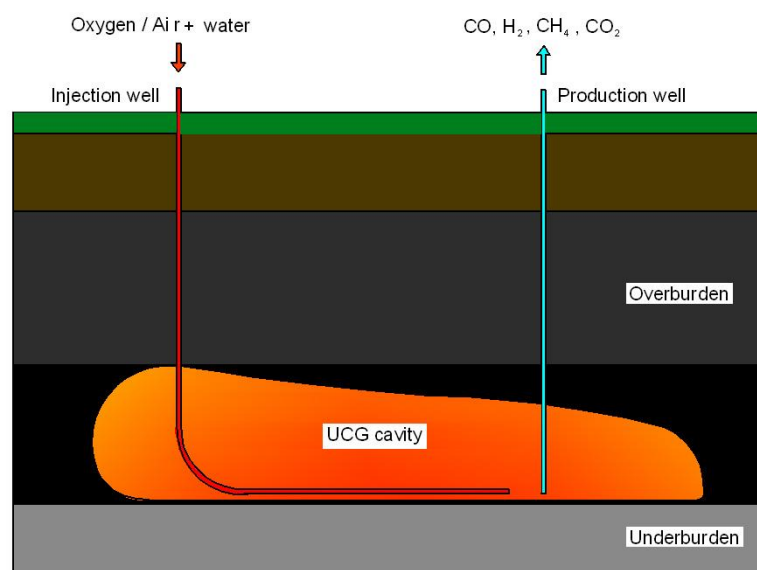


Figure 1.3: UCG process

1.2.1 Chemical Processes of UCG

The overall chemistry underlying coal gasification processes is reasonably well understood. In the gasification channel three different reaction zones are created during underground coal gasification as shown in Figure 1.4, the drying and pyrolysis zone where the volatiles are released, the oxidation zone where combustion is completed and the reduction zone where gasification takes place [94, 96].

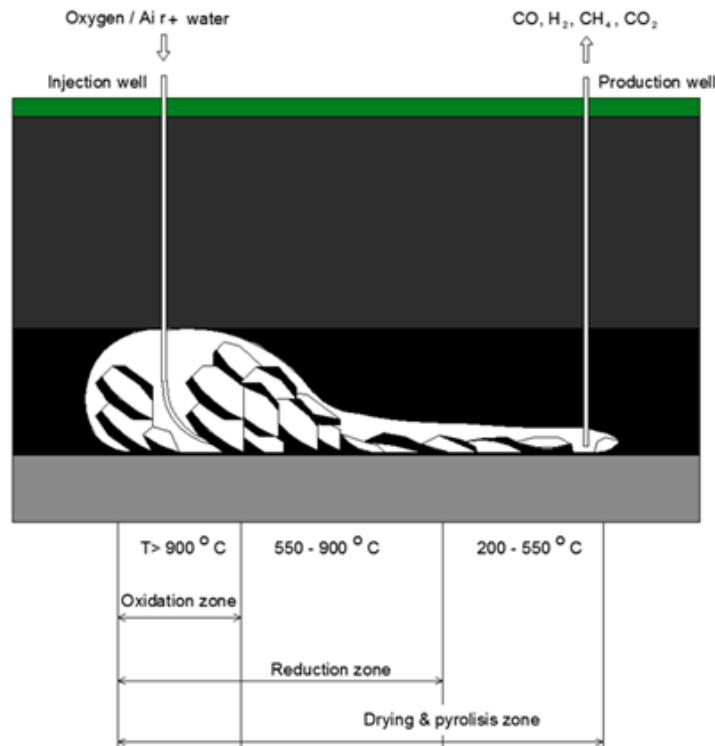


Figure 1.4: Schematic representation of UCG reaction zones.

A fire is initiated at the start of the UCG process to increase the underground temperature and as the temperature reaches 100°C the coal dries and its moisture content evaporates to steam. As the temperature continues to increase, between 200 to 550°C pyrolysis takes place where coal loses its weight and generates volatile matters, ash and a solid called char. The volatile matters decompose to tar, coal gas and chemical water. When the temperature is stabilised, oxygen is injected which reacts with the generated char within a short distance from the injection point resulting in combustion and creates the oxidation zone. The reactions that take place are the oxidation reactions 1 and 2 shown in Table 1.1 where CO and mainly CO₂ are produced. These two reactions are exothermic and produce the heat required by

raising the temperature to the required one for reasonable combustion reaction rates (1000-1300°K) for the next zone to proceed which is the gasification zone [7, 13, 64, 94, 96].

The gasification zone is created by big lumps of coal falling into the cavity as the consumption of the coal carries on in the oxidation zone. As more coal falls into the growing cavity a high coal surface area pyrolysed from the evolved heat, is available for reaction and permits contact between the hot gases and the char [11, 12]. This area is the final reduction zone (550-900°C) where the two main gasification reactions 3 and 4 take place (Table 1.1) which are solid phase reactions and kinetically and mass-transfer controlled [98]. Reaction 3 is the Boudouard reaction which converts the excess CO₂ produced in the oxidation zone to CO and is responsible for the uniform quality of the product gas [11, 12, 27, 28, 75, 95]. Reaction 4 is the steam-carbon reaction through which char reacts with the injected steam in the cavity in order for the excess heat to be used and increase the efficiency of the process by producing H₂ and more CO. These two reactions are endothermic and decrease the temperature in the cavity so the product gas enters the next zone which is the drying and pyrolysis zone (200-550 °C) where devolatilisation of the coal takes place and the product gas reacts with the volatiles released from the coal and the char.

The primary reactions at the drying/pyrolysis zone are Reactions 5, 6 and 7 as shown in Table 1.1. Reaction 5 produces CH₄ through the reaction of char with H₂ which increases the heating value of the product gas. This reaction also takes place during the gasification zone but not to a great extent; mainly it occurs at low temperatures and high pressures and during pyrolysis. Reactions 6 and 7 are gas-phase reactions through which the produced gases react between themselves, and reduce the heating value of the product gas, especially the water-gas shift reaction 6 which is equilibrium controlled [10, 11, 27, 61, 85, 90, 94]. The R6 has influence on the CO/H₂ ratio which can be important depending on the use of the gas. Where the temperature is high enough the reverse reaction R6 takes place and the amount of CO increases at the expense of hydrogen resulting in a decrease in the heating value of the product gas, pressure has no effect on this reaction [91]. As for reaction R7, at low temperatures and high pressures the reverse reaction takes place where 3 molecules of H₂ and one molecule of CO are exchanged with one molecule of CH₄ [91] which also results in a decrease in the product gas heating value.

Table 1.1 below summarizes the most important overall reactions participating in the coal gasification process.

Table 1.1: Principal overall reactions participating in the coal gasification process [11,64]

Reaction		Reaction heat	
1. Oxidation (combustion)	$C + O_2 = CO_2$	-393 kJ/mol^{-1}	(R1)
2. Partial oxidation	$C + 1/2O_2 = CO$	-111 kJ/mol^{-1}	(R2)
3. Boudouard reaction	$C + CO_2 = 2CO$	$+172 \text{ kJ/mol}^{-1}$	(R3)
4. Steam-carbon	$C + H_2O = 2H_2 + CO$	$+131 \text{ kJ/mol}^{-1}$	(R4)
4a. Steam-carbon a	$C + 2H_2O = H_2 + CO_2$	-90 kJ/mol^{-1}	(R4a)
5. Hydrogasification	$C + 2H_2 = CH_4$	-75 kJ/mol^{-1}	(R5)
6. Water-gas-shift reaction	$CO + H_2O = H_2 + CO_2$	-41 kJ/mol^{-1}	(R6)
7. Methanation	$CH_4 + H_2O = CO + 3H_2$	-206 kJ/mol^{-1}	(R7)

About 60% of the product gas is produced during the char gasification and combustion phases [16] but measurement of the upstream gas composition in the oxidation zone has shown comparatively low heating values which demonstrate that the reactions in the oxidation zone do not have a significant effect on the product gas composition [11, 12]. Furthermore the combustion reactions occur at the base of the injection well where a pile of the big lumps of coal have fallen in the cavity is formed which, according to other studies, is because the O_2 is consumed fairly quickly since the reaction of O_2 with C which produces CO_2 is very fast [11, 12, 18, 75]. Also the reaction of char with oxygen is unlikely to occur at the side wall because any oxygen that is not consumed at the base of the reactor will probably react before it reaches the char on the side wall [92]. So what is mainly left in the cavity to react with pyrolised char in the next zone, which is the reduction zone, is CO_2 which reacts with C and produces 2 moles of CO. When stable gasification is achieved H_2O is injected to enhance the performance by using the extra heat available in the cavity with Reaction 4, which explains why steam is used as the gasifying agent. So the two reactions that mainly take place during the reduction zone, which is the longest in duration and where the majority of the gases are produced, is the Boudouard Reaction 3 and the steam-carbon Reaction 4. These two

gasification reactions are the slowest and therefore control the gasification rate and the conversion of coal char to gas.

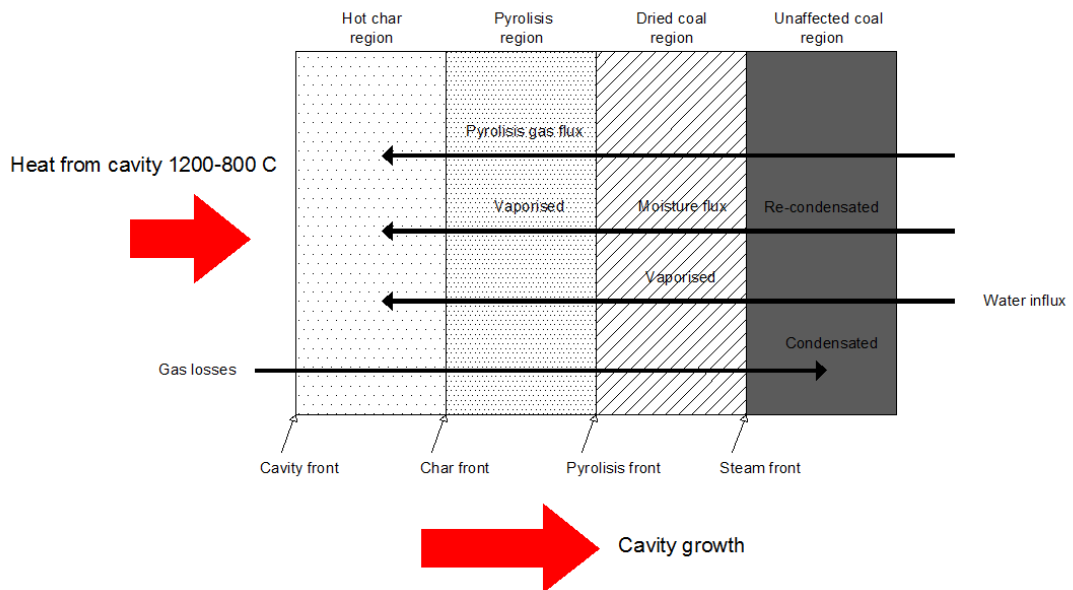


Figure 1.5: Gasified coal in the reduction zone [57].

The processes that happen at the reduction zone are shown in Figure 1.5, where moist coal undergoes drying, pyrolysis and then gasification due to the heat and mass transfer from the cavity. The coal that participates at the gasification in the reduction zone is the char that has fallen into the cavity which creates a big surface area for reaction (reduction zone) plus the char at the side wall of the cavity.

The reactivity of the char to O_2 , H_2O , CO_2 and H_2 determines the rates at which the desired gases of the product gas are formed [11, 62]. This mixture of gases is affected by the main operating parameters of the UCG process which are coal rank, temperature, composition of the oxidant gases and pressure

1.2.2 Operating parameters of UCG

The main operating parameters of UCG which affect the product gas composition are discussed below.

1.2.2.1 Coal rank

Coal rank is important in terms of reactivity, permeability, structural strength, water and ash content. Almost all the coal types are suitable for UCG except the coals which swell on heating because the passage between the injection and production

well can be blocked. Preferably low rank coals which are more reactive than high rank coals are more suitable for UCG because there is an increase in reactivity with decreasing coal rank, with lignite being the most reactive and anthracite the least. High permeability is desirable as well because more gases can penetrate into the pores of the coal which increases coal seam fractures and the diffusion of gas into the bulk seam and the moving velocity of the reaction face. Finally ash and water content should be less than 50% to allow adequate gasification [49].

Previous UCG trials have been carried out mainly on low rank coal, characterised by a high reactivity and high moisture content. Much less information exists on UCG of medium to high rank coals with the only relevant trials being in Belgium at Thulinon (which was on semi-anthracite coal) and at Lisichansk in Russia, and Pricetown in USA (both on bituminous coal) [7, 10].

1.2.2.2 Gasifying agents

The gasifying agents and their composition determine the product gas composition and its heating value. Air was the only gasifying agent used in initial UCG trials and the calorific value of the product gas was low, around 10% of that of natural gas, because the product gas was diluted by the nitrogen in the air. However more recently, oxygen and steam have been used as oxidants which produced a product gas with a medium calorific value which is a third of that of natural gas [34]. In addition there are significant environmental disadvantages of using air instead of oxygen due to nitrogen within the air increasing the production of ammonia compounds and promoting the synthesis of HCN (hydrogen cyanide).

Knowledge of supply rates of gases and their ratio is important because these determine the composition of the product gas [23, 74, 76]. If there is excess gas the feed mixture is diluted and excess steam decreases the temperature which decreases the performance [14]. Every underground coal gasification system is different due to the different chemical and physical variations so it is not possible to derive an optimum O_2/H_2O ratio which would apply to all different systems. Each underground coal gasification system has its own individually ratio of O_2/H_2O and operating parameters which need to be determined [28].

1.2.2.3 Temperature

Temperature affects the gasification process and the product gas composition. It is very important to maintain the temperature in the cavity between 600 to 900 °C for the gasification to proceed and the combustible gases to be produced. The combustion of coal is necessary because the oxidation reactions raise the temperature for gasification to take place. Injection of too much water or uncontrolled water influx from the surrounding strata can drop the temperature and affect the gasification process. The temperature in the cavity can be increased by increasing the proportion of oxygen injected, however excessive temperatures reduces the product gas calorific value and the gasification efficiency since combustion occurs and not gasification [61].

1.2.2.4 Pressure

Pressure is a key factor in the operation of UCG. Previous studies indicate that pressure has an impact on the gasification performance [28, 32] because the chemical kinetics are improved. At low pressures the kinetics of the gasification reactions are limited and this has an impact on the product gas heating value [5]. At high temperatures and pressures (50 bar, 900°C) the gases in the cavity reach equilibrium rapidly but at low temperatures and pressures the time needed for the gases to reach equilibrium exceeds their residence time so the heating value of the product gas decreases [11]. Hence increasing pressure expedites the formation of the combustible gases and the increase in calorific value of the product gas up to the limits of the chemical equilibrium [12].

Furthermore the operational pressure in the cavity should not exceed the hydrostatic pressure in order to allow water to enter into the cavity for the gasification to proceed and also control the amount of water influx because too much water will cease the gasification process. In addition contaminants will be kept in the cavity and avoid groundwater pollution.

Most research into UCG has concentrated on coals at relatively shallow depth and low pressures. Recent work, particularly in Europe where there are substantial coal resources at depth, has focused on the exploitation of UCG in deep coals accessed using advanced guided drilling techniques. UCG in deep coal seams can operate at high pressures up to the hydrostatic pressure for the reasons mentioned above and

the maximum pressure at which it can operate is determined by the depth of the coal seam. For every 10 m depth the pressure rises 1 bar=0.1 MPa so for a 500 m deep coal seam the maximum pressure should be below 50 bar=5 MPa which is the hydrostatic pressure. Field trials at Thulin in Belgium (1986-1987) at 860 m and subsequently at 'El Tremedal' in Spain (1993-1998), which was at 500 m deep, demonstrated the technical feasibility of UCG at depth [9, 10].

1.3 Research work

1.3.1 Aim of the research work

The aim of the research work is to obtain a better understanding of the behaviour of the pyrolysed coal (char) in the reduction zone of the UCG cavity which is one of the key controlling factors in the conversion and yield of the UCG process. The behaviour of the pyrolysed char in the reduction zone of UCG has not been studied before and was achieved by using carbon dioxide and steam simultaneously as the primary reactants. Pyrolysed chars at atmospheric pressure derived from a dry steam coal and anthracite were gasified at a variety of pressure and temperature levels, plus at a range of relative H₂O/CO₂ proportions. The coal samples that were used are cylindrical blocks of approximately 2 cm diameter x 4 cm length. The composition of the resulting product gas was measured and subsequently used to calculate important parameters which evaluate the performance of the UCG process such as the heating value of the product gas, cold gas efficiency and carbon conversion. Furthermore a better insight into the impact of pressure on the gasification performance of UCG will be provided which is not understood very well yet. Finally information on UCG of high rank coals from bituminous to anthracite will be provided which does not yet exist.

1.3.2 Objectives of the research work

In order to address the aim of this study the following objectives are set:

1. To review the current literature to gain an up to date understanding of the main operating parameters that affect the gas composition of the product gas and the effective energy conversion of coal to gas during char gasification in the context of Underground coal gasification.

2. To develop an appropriate apparatus to simulate the reduction zone of a UCG process which can be used to determine operation parameters such as temperature, gasifying agent composition and pressure.
3. To design an experimental procedure to determine the effect of the main operation parameters on the gas composition of the product gas.
4. To provide information about how the main operating conditions affect the gas composition and determine optimal gasification conditions which can be useful for future UCG trials or future research. In addition important parameters will be calculated to evaluate the UCG performance such as the heating value of the product gas, the cold gas efficiency and the carbon conversion.
5. To study the behaviour of pyrolised char with the gases and the kinetics of the char-gas reactions at atmospheric and elevated pressures and to define a model which describes the behaviour of carbon with $\text{CO}_2+\text{H}_2\text{O}$ and calculate parameters which could be useful for numerical simulations of UCG process.
6. To obtain a better understanding of the amount of carbon conversion to gas for dry steam coal and anthracite and quantify the required coal resources for a potential UCG project.
7. To better understand the behaviour of high rank coals during the UCG gasification and to provide information about their suitability for a potential UCG project depending on the end use of the product gas.

1.4 Thesis overview

This thesis consists of 8 chapters, after introducing the thesis in Chapter I, a review of the literature will be presented in Chapter II. The aim of the literature review is first to review up-to date experimental work and to understand how the main operation parameters affect the gas composition of the product gas and the efficient energy conversion of coal to gas during a UCG process. Furthermore a brief review of the history of UCG will be presented with field trials reviewed, the procedures followed during their UCG process and the composition of the product gas that was achieved.

In addition the char gasification with CO_2 and with H_2O at high pressure has been studied previously widely and this study analyses some of these. The gas solid

reactions of char gasification with CO_2 and with H_2O were also briefly reviewed together with the most widely accepted mechanism under which they occur at low and high pressure. Finally some kinetic models mostly used to describe these reactions are also mentioned.

Chapter III presents the experimental apparatus that was developed as part of this study and the considerations that took place during the design process in order to select equipment with the appropriate specifications for the required experiments. The specifications of the major components and the specific features of the commissioned experimental set-up are also provided in this chapter.

Chapter IV describes the materials and methods used in the experimental investigation of this study. Specifically the properties of the coal samples and the methods that were used to determine them are presented. Furthermore the preparation methods of the different coal samples are provided and the experimental procedure that was developed and the measurement methods that were utilised are described. Finally a series of preliminary experiments are included for both coals which were performed to test the presence of any effect of particle size, sample size and flowrate of oxidants to enable the sample size (C content), particle size and the flowrate of CO_2 to be determined in order to design the experimental matrix presented in Chapter V and VI.

In Chapter V the results of the experiments performed at atmospheric pressure in order to determine the impact of temperature and gasifying agents composition on the composition of the product gas in the reduction zone are presented and analysed through discussion. Also other important parameters were calculated which are carbon conversion, cold gas efficiency and heating value. Section 5.2 presents the results conducted at different temperatures for both coals and section 5.3 determines the impact of gasifying agents composition (ratio of $\text{H}_2\text{O}/\text{CO}_2$) on the composition of the product gas at the optimum temperature that was determined in the experiments described in Section 5.2. Furthermore kinetic calculations take place in order to describe the gasification on coal particles and comparison with other studies is carried out to assess the results of this study. Finally experiments were conducted in order to understand how char reacts at the oxidation and during the

drying/devolatilisation zone under simulating conditions and there results are presented and analysed.

Chapter VI presents the results of the experiments conducted at elevated pressure in order to determine the impact of pressure on the composition of the product gas and the efficient energy conversion of coal to gas during the reduction zone in terms of carbon conversion, cold gas efficiency and heating value of the product gas. The optimum values of temperature and $\text{CO}_2/\text{H}_2\text{O}$ ratio which were determined for each coal at atmospheric pressure in chapter V formed a baseline and were used to perform these experiments at elevated pressures. The kinetics are investigated in order to determine which model describes better the behaviour of the two pyrolysed chars with $\text{CO}_2 + \text{H}_2\text{O}$ under total pressure, to understand the mechanism involved and derive an equation for each coal expressing the reaction rate of their char under total pressure.

The purpose of this Chapter VII is to evaluate the experimental results of this study and the operation of the bespoke high pressure high temperature rig using a mass and energy balance which was developed. In addition the data of this study is compared with the data from UCG field trials and parameters which determine the performance of the UCG process, such as carbon conversion, CGE and LHV of the product gas, are discussed. Finally the LHV and CGE determined in this study are used to calculate the output of small and large potential UCG power plants in order to demonstrate practical feasibility of real UCG operations. Information about the required coal resources and the size of the UCG models are also provided.

Finally Chapter VIII includes the conclusions drawn from the findings of this research study and also recommendations for future work.

CHAPTER II

LITERATURE REVIEW

2.1 Introduction

A literature review took place in order to find studies conducting experiments with similar conditions or close to those used in the experiments of this study in the context of Underground coal gasification.

It was found that there is only a small number of studies which have been conducted experiments on UCG under large scale laboratory conditions using coal blocks from 0.25 x 0.20 x 0.16 m to 0.55 x 0.70 x 2.50 m size which are discussed in Section 2.2. Two of these studies are performed under pressure and are presented in Section 2.2.1 Furthermore there are a few studies that have been carried out on the pyrolysis, coal activity for CO₂ and CO₂ gasification in the context of underground coal gasification which are presented in Section 2.3. In addition a brief review of the history of UCG was carried out plus some UCG field trials which were relevant to this study, there are also described in Section 2.4 including the effect of pressure on the product gas composition.

The char gasification with CO₂ and with H₂O at high pressure have been studied in the literature for a wide range of coal char types at temperatures from 700 to 1100°C and at pressures up to 5 MPa using various high pressure apparatuses. The diameter of the coal sample particle in these studies was from 106 to 2400 μm. A number of the above mentioned studies are analysed in Section 2.5. The gas solids reactions of the char gasification with CO₂ and with H₂O were also briefly reviewed including the regimes under which these reactions take place, where these reactions occur on the solid particle and the most widely accepted mechanism under which they occur at low and high pressure. Finally some kinetic models mostly used to describe these reactions are also mentioned in section 2.6.

2.2 Medium to large laboratory scale experiments (particle size of coal blocks from 0.25x0.20x0.16 m up to 0.40x0.40x2.00 m)

2.2.1 UCG experiments performed at atmospheric pressure

Stanczyk, K et al. (2011) [75] simulated underground coal gasification in ex-situ reactors in order to explore lignite and hard coal gasification process with oxygen and air and to compare the results to determine the optimal operation conditions. The gasifying agents were oxygen, air and oxygen enriched air (OEA). The experimental gasifier (reactor) had a rectangular shape with external dimensions of 3 m (length) x 1.4 m (width) x 1.5 m (height). The walls of the reactor were made of 0.2 m thick refractory concrete. The lignite coal seam gasified was simulated by a coal sample with dimensions of 0.55 m (width) x 0.70 m (height) x 2.50 m (length). The hard coal seam was simulated with a coal sample with dimensions of 0.55 m (width) x 0.45 m (height) x 2.50 m (length).

The experiment ran at ambient pressure and in three phases. In the first phase oxygen was supplied in order to heat up the coal and accumulate sufficient amount of thermal energy. In the second phase oxygen was replaced by air in order to find the optimal air flow rate for hydrogen rich production on direct observations on product gas compositions. At the final phase oxygen enriched air (OEA) was supplied and the best ratio was determined considering the gas composition. The results showed that the best gas composition is obtained with the OEA.

The average per volume % gas composition produced by the lignite gasification at a volume ratio of oxygen/air=4:2 was H₂=23.1%, CO=6.3%, CH₄=2.3% and the calorific value of product gas was 4.18 MJ/m³. For the hard coal at a ratio of oxygen/air=2:3 the average per volume % gas composition was H₂=18.7%, CO=17.3%, CH₄=4.2% and the calorific value of the product gas was 5.74MJ/m³. The calorific value of lignite was less than that of hard coal due to the high moisture content of 53% for the lignite which dropped the temperature in the cavity. Furthermore due to the high carbon content of hard coal, its progress in the reaction zone was slower than that of lignite.

Daggupati et al. (2011) [14] studied the feasibility of in-situ gasification of coal in a similar scale laboratory reactor set up under conditions relevant for field practice of UCG using an oxygen-steam mixture as the feed gas. The cross section dimensions of the coal blocks were 0.25x 0.20 m and the length was 0.16, 0.20, 0.24 and 0.28 m. The flow rate of oxidants was 800, 1000 and 1250 ml/min. First ignition was generated and then oxygen was introduced and the combustion reaction was carried out for 3 hours until steam was introduced at 150 °C, but the concentrations of CO and H₂ were low which showed that gasification was insignificant under the conditions employed because, the steam dropped the temperature in the cavity below 600°C. In order to overcome this problem the initial combustion time was prolonged from 4 to 6 hours in order to obtain sufficient large coal surface area for subsequent gasification. Furthermore, the steam was preheated and introduced at a sufficiently high temperature (400-600 °C) in 10 min intervals in a cyclic manner. The operation time of the experiment was from 10 to 16 hours.

The calorific value of the product gas ranged from 130 to 178 KJ/mol and the product gas composition (Vol %) for a steam/oxygen ratio equal to 2.5 was CH₄=5%, CO=10% and H₂=40%. It was found that the ratio of H₂O/O₂ is a very important parameter because excess oxygen dilutes the gasifying agents to produce excess CO₂ which drops the calorific value of the syngas and excess H₂O drops the temperature which again decreases the calorific value of the product gas.

Liu et al. (2008) [49] conducted simulated tests of UCG in order to investigate the hydrogen production of lignite. The simulated coal seam that was used for the experiment was constructed using processed block coal samples of size 0.40x0.40x0.40 m joined together with a mixture of fine coal and cement in order to form a continuous coal seam of a lateral length of 2.00 m, a depth of 0.40 m and an inclined length of 0.40 m. The coal seam was placed at an angle of 15° according to the dip of the in-situ coal seam. A firebrick layer was cast surrounding the coal seam to form an entity.

The gasifying agents were steam and oxygen and the experiment with stable gasification lasted 12 hours. After ignition, air was injected and the coal began to burn and a high temperature profile gradually was formed. The air was switched to oxygen to enhance the combustion and then combustible gas began to form with the

release of the volatile matters from the coal seam. Steam was introduced when the temperature was above 900° C. The steam flow was adjusted to find a suitable steam/oxygen ratio in order to maximise the amount of combustible gas and that ratio was $H_2O/O_2=2:1$.

The gas composition was $CH_4=3.3-4\%$, $CO=24.3-28.5\%$ and $H_2=40-45\%$. Liu et al. (2008) [50] state that H_2 is mainly produced during pyrolysis which is enhanced due to the large surface areas provided by the spanning of the coal into the UCG cavity. Furthermore H_2 is produced by the water gas shift reaction (R6) which requires a relatively long time for gases to react between them and reach equilibrium.

Stanczyk et al. (2012) [76] assessed the feasibility of a hydrogen rich gas from a simulated UCG operation on hard coal. An ex-situ reactor was constructed with dimensions 3.0 m length x 1.4 m width and 1.5 m height which was filled with two coal samples which both had cross section dimensions of 0.55 m (width) x 0.60 m (height), the first coal sample had a length of 1.25 m and the second of 1.15 m.

The procedure used was a two stage gasification process in which oxygen and steam were supplied to the reactor separately, the oxygen was supplied first to increase the temperature and heat up the coal by the reaction of oxygen with carbon which produces mainly CO_2 and CO . The temperatures were up to 1600 °C and the pressures near ambient. Each oxygen gasification lasted 2 hours and the oxygen supply was gradually increased by $1m^3/h$ from $2m^3/h$ to $5m^3/h$ every 30 min time intervals. During the oxygen stage the temperatures were 1100 to 1200 °C.

In the steam gasification stage which lasted 1 to 1.5 hours the steam was supplied to the reaction zone with the rate of $6.20 m^3/h$ for the whole experiment. The steam stage lasted until the temperature had decreased to 700-800 °C because the heating value of the product gas was declined since the concentration of the gases was reducing. The reason was that steam was dropping the temperature below the required temperature for the gasification reactions to proceed which is around 800-900 °C. This shows that the product gas of UCG is mainly produced during the reduction zone of UCG by the reactions of coal char with the reactant gases which are CO_2 produced during the oxidation zone and H_2O either injected or there is a water influx towards the cavity. The CH_4 content during the steam stage was increased from 1.55% vol to 13% as the temperature was decreasing by time. The

basic gasification stage lasted 115 hours and the maximum concentration of the gas composition during the O₂ stage was CH₄=3.05%, CO=17.58% and H₂=15.28% and during the steam stage was CH₄=9.77%, CO=15.78% and H₂=53.77%. It was shown that the composition of the product gas and its heating value depends on the thermodynamics of the process and on the composition of the reactant gases.

Yang et al. (2009) [95] studied the effect of different gasifying agents such as O₂ and O₂+H₂O in the gas quality during the UCG process with a model gasifier of 9.3 m x 1.57 m x 1.17 m. The model gasifier was filled with a coal sample of 4.45 m x 1.50 m x 0.50 m which consisted of big natural chunks in order to better simulate the underground coal seam. It was found that adding steam as a gasifying agent with the O₂ increases the heating value of the product gas by increasing the H₂ and CO production. Furthermore adding steam not only uses the excess heat but also improves the performance of the process by increasing the gas production per tonne of coal.

Yang et al. (2008) [94] also tested the effect of different ratios of H₂O/O₂ on the product gas composition and determined that when the H₂O/O₂ ratio increases the CO+H₂ concentration also increases and reaches its maximum for the H₂O/O₂ ratio between 1.5 to 2.2 (V/V). Above this ratio the CO+H₂ concentration declines mainly because the decomposition of steam absorbs large amount of heat and the following reaction occurs $2\text{H}_2\text{O} + \text{C} \rightarrow \text{CO}_2 + 2\text{H}_2$ $\Delta H = -90 \text{ MJ/kmol}$ which drops the temperature in the gasifier and as a result the quality of the product gas declines gradually. It is worth noting that the CH₄ concentration increases as the H₂O/O₂ ratio increases with its maximum achieved at around 10% (V) for the maximum H₂O/O₂ ratio of 3. At the H₂O/O₂ ratio of 2:1 (V/V), the concentration of H₂ can be considered stable at around 40% (V) and that of CO at 26% (V), basically during continuous gasification the H₂+CO concentration was between 61 to 72% with a heating value of 10-11 MJ/m³.

It was concluded that O₂-steam gasification has a great impact on the product gas composition by utilising the surplus heat and improve the energy efficiency of the process and that the H₂O/O₂ ratio can be adjusted to produce a product gas with a different desired composition according to the industry needs.

Wiatowski et al., (2016) [91] who performed an ex-situ experimental simulation of hard coal underground gasification at elevated pressure noted that the effect of pressure on coal pyrolysis is not significant compared to the effect of the chemical reactions during the UCG process. It was determined that the process gas composition at elevated pressure UCG had higher concentrations of carbon dioxide and methane and lower concentrations of carbon monoxide and hydrogen than UCG operations at atmospheric pressure.

2.2.2 UCG experiments performed at elevated pressure

Thorsness et al. (1977) [80] conducted an experiment with a 1.6 m long packed-bed combustion tube in order to predict the product gas composition. The 1.6 m reactor was a high pressure tube of 30cm diameter and it contained an inner thin walled tube of 15cm diameter where the coal was placed. The pressure of the experiment was 0.52 MPa, the temperature around 730°C, the coal was subbituminous with a particle size of 10mm and the experiment lasted around 8 hours. The gasification medium was oxygen and steam with a steam to oxygen ratio (moles) of around 5 which is 2.8 (w/w). It was found that the GCV of the product gas was about 11 MJ/m³ and the product gas composition (mol fraction) was CH₄=0.069, CO=0.190, H₂=0.446, and CO₂=0.295 for the run which best agreed with the developed mathematical model that predicts the product gas composition for given injection gas flow rates and compositions.

Wang et al. (2009) [89] conducted a semi industrial test with a coking coal (60% F.C 16% V.M., LHV 26 MJ/kg). The coal seam with dimensions around 1.00 m (thickness) x 20.00 m (width) was gasified with O₂-enriched air and steam, aiming to investigate the effect of cyclically changing the operational pressure in terms of the composition of the product gas [25]. In order to increase or change the pressure two methods were used; with the first method controlling the pressure by opening and closing cyclically the outlet flow of the product gas. The second method the inlet and outlet was opening and closing alternatively which improved the heat transfer in the gasifier by changing cyclically the direction of the gases. The average gas composition at pressures of 0.2, 0.4, 0.6, 0.8, 1.0 and 1.2 MPa was 15-25% CO, 5-

8% CH₄ and 10-30% H₂. The highest concentration of H₂ and CO was produced for the pressure of 0.8 MPa and the heating value of the product gas was increased by 26% compared with the fixed pressure. The gasification rate was 1.2 to 1.6 times higher than those under the fixed pressure operation. It was concluded that the increased pressure provides a higher gas density and improved conditions for gas-solid contact, leading to the increase of the gasification reaction rate [85, 88].

2.3 Experiments on the pyrolysis, coal activity for CO₂ and CO₂ gasification in the context of UCG

In UCG combustion of coal is very important because it provides the energy that is needed to drive the gasification reactions. The gasifying agents in UCG usually are oxygen and steam or oxygen alone. In the latter case the main product of the reaction of coal with O₂ is CO₂ which also acts as gasifying agent and mainly drives the gasification ($C+CO_2\rightarrow CO$) [53]. In the following paragraphs two studies are discussed which carried out experiments with CO₂ gasification in the context of UCG.

2.3.1 Experiment on UCG pyrolysis

Furthermore Liu et al. (2008) [49] carried out pyrolysis experiments with a quartz tube reactor in the context of underground coal gasification. Coal samples of 10 gr were placed in a quartz boat and then into a reactor which was heated from room temperature to a final temperature between 300 to 1000°C at a slow heating rate of 3.3°C /min in a N₂ atmosphere. This was because, as previously mentioned, the difference between surface gasification and underground coal gasification is the slow heating rate of the coal seam and its pyrolysis. It was found that H₂ is released from coal above 350°C and that the optimum temperature is between 725 to 825°C.

2.3.2 Experiment on coal activity for CO₂

Liu et al. (2008) [49] conducted experiments to determine the coal activity for CO₂ in the context of underground coal gasification. First char samples were prepared by placing 3-6 mm coal samples of lignite into a furnace for 1 hour at 900°C. Then the

char sample was placed in a general reactivity apparatus which was heated up to 850°C at a rate of 20-25°C /min and then CO₂ was introduced at a flow of 500 ml/min under STP conditions. The CO₂ concentration was analysed for different temperatures and the CO₂ decomposition rate was calculated. It was found that the CO₂ decomposition rate is around 50% at 850°C and 96% above 950°C and that the lignite is suitable for gasification in a seam.

2.3.3 Experiment on CO₂ gasification during UCG.

Mandapati et al. (2012) [53] conducted experiments on CO₂ gasification of four Indian coal chars in the context of underground coal gasification. It was mentioned that underground coal gasification differs from the surface gasification in the particle size of coal which in the UCG process is large and for this reason the overall rate of reaction is influenced by diffusion. Also the entire char is not directly exposed to the flowing gas.

Furthermore Mandapati et al. (2012) [53] report that the coal surface is first pyrolysed before being exposed to the gasification environment. For this reason the coal chars were obtained by pyrolyzing coal separately prior to the experiment. In order to prepare the coal chars the coal was dried initially at 30° C and crushed to a size of between 2 to 3 mm. The coal sample was then placed in a quartz tube reactor under N₂ atmosphere at 110 °C for 1 hour to remove the moisture and flush out the air in the reactor. Following this, the temperature was increased to 1000 °C at a rate of 30 °C/min and maintained at that temperature for 10 min for pyrolysis completion, the sample was then cooled down to the reaction temperature (850-1000° C) in an inert atmosphere at a rate of 30 °C/min and grounded to a size of less than 150 µm for CO₂ gasification experiments. These experiments were carried out with a TGA apparatus at a temperature range of 800-1050 °C and with different reactant gas compositions with N₂ as diluents. It was found that the lower rank coals are the most reactive and their kinetics were well predicted with the random pore model. Furthermore a kinetic process UCG model was developed in which the diffusivity in the char bed is assumed to be a linear function of char conversion or in other hands; the bed diffusivity varies with time as carbon reacts [53].

Gregg et al. (1978) [28] conducted a review on UCG with some interesting points were mentioned. When the coal is heated many chemical and physical changes take place which depend on the type of the coal. The most common ones are cracking and shrinking of the coal. Heating rates underground are rather slow around 3 °C / min so the release of volatiles is slowed down by the very fast chemical reaction and the diffusion of the gases through the solid. It is believed that UCG kinetics is controlled by chemical kinetics, adsorption and diffusion and that above 1000 °C the controlling regime is external molecular or bulk diffusion and below 1000 °C is chemical reaction and intraparticle or pore diffusion. The size of the particle will be controlled by the structure and type of coal since the coal is subject to thermal fracturing. UCG reactors are simulated as fixed bed reactors and the operation of the gasification system is a batch operation.

2.4 UCG past and current pilot projects

UCG is an old technology; the first UCG tests took place in Russia between 1900 and 1930 leading to a commercial operation in Lisichansk in 1932. Between 1944 and 1959 UCG tests were carried out in Czechoslovakia, France, Poland and Italy. In UK tests were carried out at Newman Spinney and Bayton site and a few years later a first attempt was made to develop a commercial pilot plant, the P5 Trial, but all European work stopped during the 1960's when additional oil and gas reserves were found.

The Arab oil embargo in the 1970's created concern for domestic energy security and as a result a new interest in UCG was developed, both in Europe and US with more than by 30 field tests conducted. In Europe UCG trials took place in Belgium, France and Spain (El Tremedal-supported by the European committee) and in US many field trials took place in the Rocky Mountain at Hanna, Wyoming. Currently UCG pilot plants are running in many countries such as New Zealand, Australia, China, Canada, South Africa etc. Figure 2.1 illustrates past and current UCG pilot projects. [7, 11, 34].

Currently the only commercial running UCG operation is the Angren plant in Uzbekistan which is partly feeding a power generation plant. This UCG operation still relies on 1950's technology. Most research into UCG has concentrated on coals

at relatively shallow depth and low pressures. Recent work, particularly in Europe where there are substantial coal resources at depth, has focused on the exploitation of UCG in deep coals accessed using advanced guided drilling techniques. Field trials that operated at pressure were at Thulin in Belgium (1986-1987) at 860 m and subsequently at ‘El Tremedal’ in Spain (1993-1998) at 500 m deep. Both field trials demonstrated the technical feasibility of UCG at depth [10, 11].

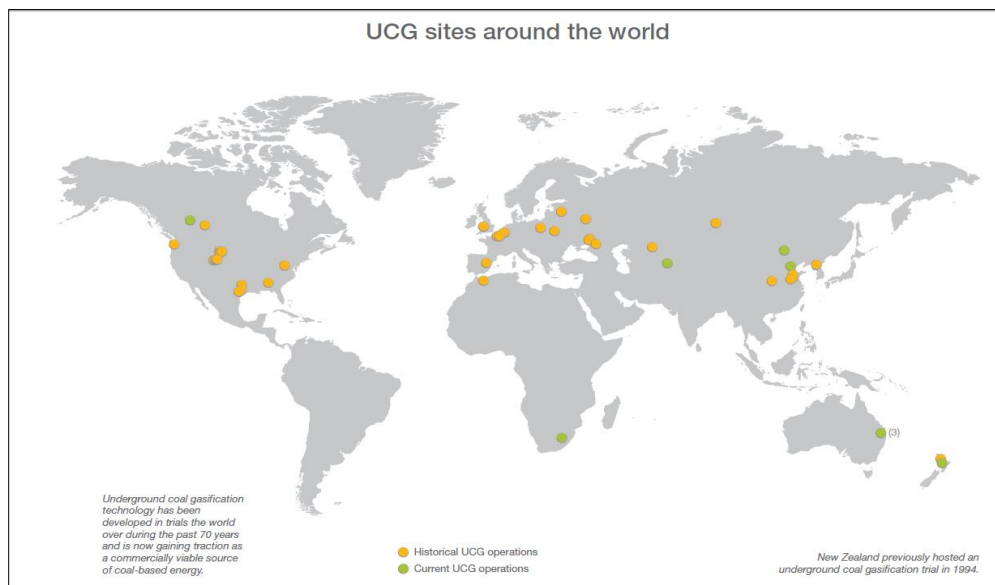


Figure 2.1: Past (yellow dot) and current (green dot) UCG projects.

(Source: Solid Energy-Huntly project in New Zealand)

Furthermore the previous UCG trials have been carried out mainly on highly reactive low rank coal with high moisture content. Little information exists on UCG of medium to high rank coals, the only relevant trials being at Thulin in Belgium, on semi-anthracite coal, and at Lisichansk in Russia, and Pricetown in US both on bituminous coal [11, 15].

Some field trials which were conducted with advanced drilling technology at low and elevated pressure are mentioned in the following paragraphs.

2.4.1 Current UCG field trials at low and elevated pressure

2.4.1.1 Thulin, Belgium (1986-1987)

A UCG pilot project took place in Tulin, Belgium at a depth of 860-870 m in a coal seam of 6 m height. The coal was semi-anthracite or a low volatile steam coal in the British classification, non swelling with a volatile content of 13.5%. The gasifying agent was air and the technique that was used was deviated drilling. The gasification took place for around 200 days at high pressure and it was calculated from the mass balance that 157 t of coal had been completely converted to gas and 183 t of semi-coke was left in the reactor, which means that around 46% of the affected coal was converted to gas. The calorific value of the product gas from several tests was between 3.3 to 11.1 MJ/m³. Finally the gasification was terminated due to a formation of a gas bypass [7, 11].

2.4.1.2 El Tremedal, Spain (1989-1998)

The target coal seam was situated at an average depth of 560 m with a 2-3 m seam thickness. The coal type was high sulphur sub bituminous (22.2 % moisture, 27.5% volatiles, 14.3 % ash, 36 % fixed carbon) with a heating value of 18 MJ/Kg. The linking method was in-seam deviated drilling (CRIP method) and the gasyfing agents were oxygen and nitrogen. The coal seam was first ignited by a burner placed at the end of the injection well, inside the in-seam liner. The gasification phases at 5.4 to 5.6 MPa lasted totally 21 days and 237.2 tonnes of coal moisture ash free was affected with a char deposit of 88 tonnes (123 tonnes of coal). This means that the total coal affected was around 360 tonnes and the gasified coal was around 65%.

The calorific value of the gas was 10.9 MJ/m³ and the composition (% mole) of the product gas was 40% CO₂, 12% CO, 25% H₂, 13 % CH₄ and 8% H₂S. The amount of CH₄ produced was the highest between the field trials conducted at pressure. During the UCG operation the high amount of water influx tried to be controlled by the increase of the back pressure at the production well position. Finally the integrity of the injection well was lost during the second gasification phase and the gasification was terminated [10].

2.4.1.3 Rocky Mountain¹, Wyoming, USA (1987-1988)

A steam/oxygen mix was injected into a coal seam 130 m deep of subbituminous coal (8.8 % moisture, 32% volatiles, 27.3 % ash, 32 % fixed carbon) with a heating value of 20 MJ/Kg. The linking of the wells took place with two different techniques, the Extended Linked Well technique (reverse combustion/hydraulic fracturing) and the CRIP technique [5, 15]. The coal seam was first ignited by a burner inside the stainless steel liner of the injection well and the gasification preceded. With the CRIP technique 60-180 tons/day of coal were gasified at 0.5-0.7 MPa with a total 9800 tonnes. The calorific value of the gas was 10.9 MJ/m³ and the composition (% mole) of the product gas was 38.2% CO₂, 11.9% CO, 36.9% H₂ and 10.3 % CH₄.

2.4.1.4 Centralia, USA (1981-1985)

A field trial took place at Centralia, USA in 1981-1985. The coal seam was 20-50 m deep, the seam thickness was 6-8 m and the coal type was sub bituminous (17.3 % moisture, 34.4% volatiles, 20.8 % ash, 27.5 % fixed carbon). The drilling method was in-seam deviated drilling (CRIP method) and the gasifying agents were steam and oxygen. The coal seam was first ignited by the use of a burner at the end of the injection well which first melted the horizontal casing and then ignited the coal seam. The gasification at 0.37-0.43 MPa lasted 6.81 days and the affected coal was 370 tonnes and the char deposit 121 tonnes. The calorific value of the gas was 8.7 MJ/m³ and the composition (% mole) of the product gas was 34.9% CO₂, 20.8% CO, 38.1% H₂ and 4.7 % CH₄ [10].

2.4.2 Effect of pressure to the gas composition of the product gas

Figure 2.2 shows the gas composition produced by various field trials. The CO₂ concentration is between 20 to 45%, the concentration of CH₄ is between 5 to 25% and that of H₂+CO is between 50 to 80%. It is evident that the heating value of the gas produced by trials which operated at high pressure like El Tremedial (57 bar), Lurgi (30 bar), Princeton (50 bar) and Thulin is higher than the trials operated at low pressure [17].

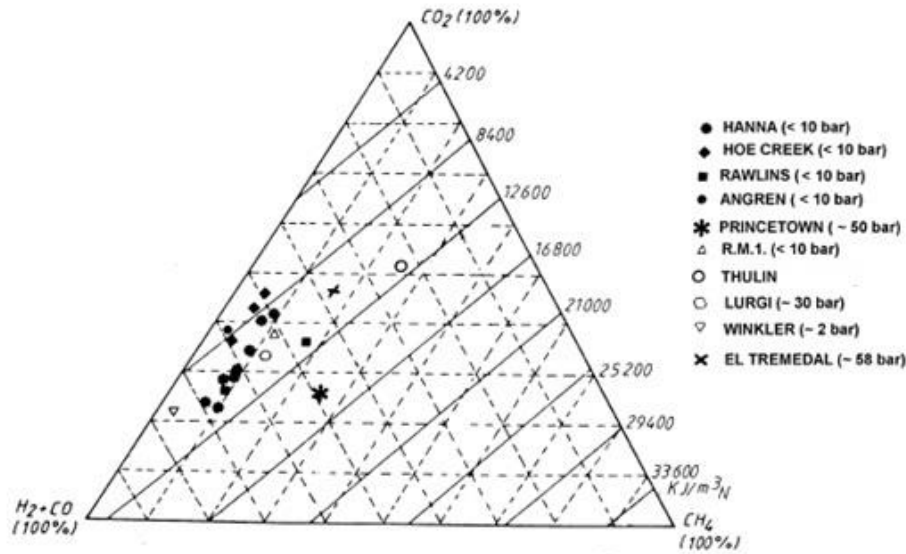


Figure 2.2: UCG gas composition produced by UCG field trials [17].

UCG in deep coal seams can operate at high pressures of up to the hydrostatic pressure and the maximum pressure that can operate is determined by the depth of the coal seam. For every 10 m depth the pressure rises 1 bar = 0.1 MPa so for a 500 m deep coal seam the maximum pressure should be below 50 bar = 5 MPa which is the hydrostatic pressure. The pressure in the cavity should not exceed the hydrostatic pressure in order for water to enter into the cavity for the gasification to proceed and also control the amount of water influx because too much water will stop the gasification process. In addition contaminants will be kept in the cavity and avoid groundwater pollution.

Figure 2.3 below shows calculated compositions of the product gas at various pressures and its heating value. It is evident that the heating value of the product gas is increasing with pressure. As is shown in Figure 2.3 the concentration of the H₂ and CO are decreasing with pressure but the concentration of CH₄ and CO₂ are increasing which means that the reactions of gases between themselves (R6 and R7 - homogeneous reactions) are favoured and that the produced gases have enough time to react between them during the pyrolysis zone and might reach equilibrium. During a UCG process the produced gases are transported through the gasification channel to the surface and have enough time to react between themselves and might reach equilibrium. In this study only the reduction zone and the gasification reactions that

take place were examined, which are the gas solid reactions of C with CO_2 and H_2O (R3 & R4) mainly and to a less extent reaction R5. It seems that the gas phase reactions (homogeneous reactions R6 & R7) do not have enough time to occur in this study or if they do occur it is to a limited extent. The results of this study are due mainly to the reaction of C with $\text{CO}_2 + \text{H}_2\text{O}$ and the main reactions that take place are reactions R4, R5 and R6.

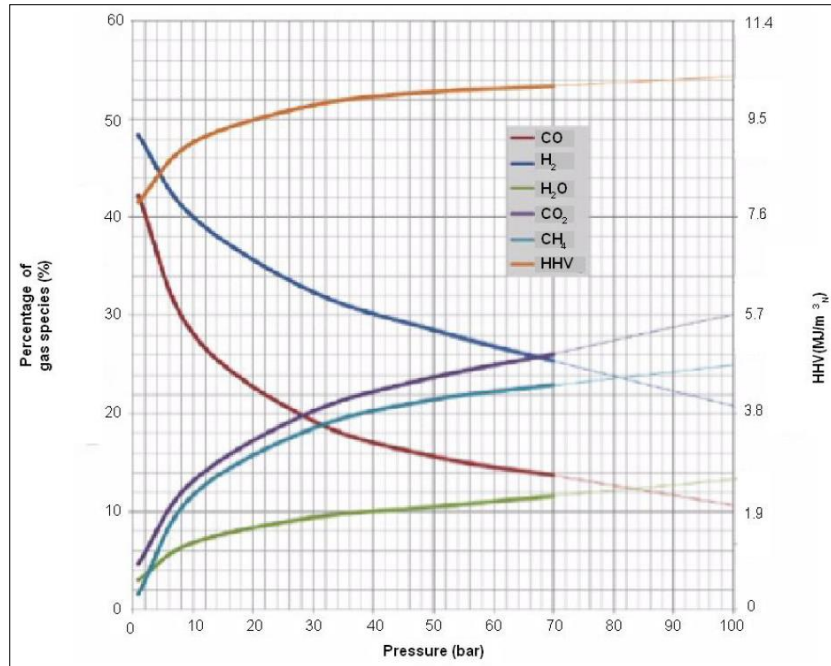


Figure 2.3: UCG gas composition and heating value variation with pressure [27]

Many studies conducting numerical simulations consider the intensity of the mixing of gases in the reaction zone adjacent to the coal/char face, which increases the gas-char contact by quantifying by the Grashof number which is proportional to the local temperature time \times pressure² [17]. This means that any increase in pressure also increases the calorific value of product gas. Perkins et al., (2008) [63] developed a steady state model for estimating the gas production from UCG and state that the calorific value of the product gas increases as the gas pressure increases which is shown in Figure 2.4.

Finally IEA Clean Coal Centre conducted a report on UCG where it was mentioned that at low pressures and temperatures carbon dioxide reactions dominate resulting in a high CO_2 concentration and a low heating value of the product gas.

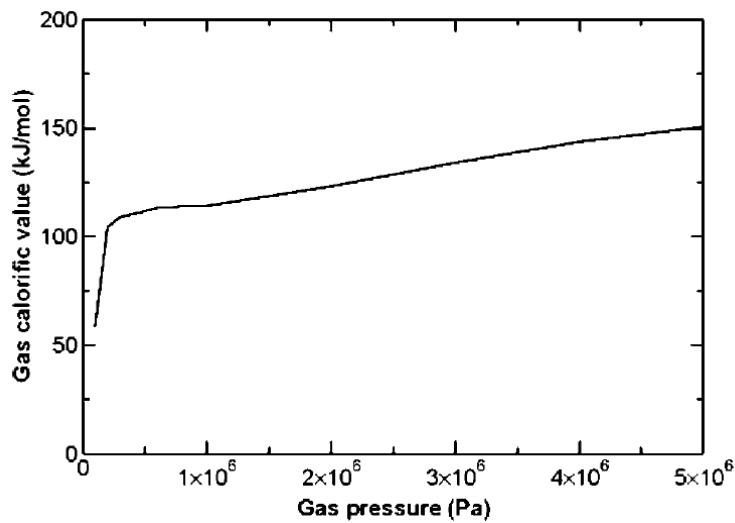


Figure 2.4: UCG product gas calorific value with gas pressure [63]

2.5 Experiments on coal char reactivity at low and high pressures during gasification

Char conversion data obtained at high temperatures and pressures are important in understanding the coal performance under any gasification conditions. Of particular importance is the reaction rate of the coal char with both CO_2 and H_2O because the slowest step in the conversion of coal to product gas is the gasification of char. The relative slow rate of these reactions determines overall coal conversion rates in a gasifier. There are many chemical and physical processes which when combined can influence the conversion rate of coal char. These processes can be gas diffusion to the char particle and through the pores of the particle, reaction at the surface and diffusion of the products away from the reaction site. These processes are associated with the consequential changes in pore structure and in some cases with the chemical composition of the char that result from the gasification of carbon. Any combination of these processes can have a controlling influence on the rate of the char conversion. The result depends on a range of process and sample properties such as temperature, reactant gas composition, pressure, particle size and char morphology [53].

Char gasification with CO_2 and H_2O at low and high pressure has been studied for a wide range of coal char types at temperatures between 700 and 1100°C at pressures

of up to 5 MPa using various high pressure apparatuses like a fixed bed reactor, tube reactor, packed bed balance reactor, thermo gravimetric analyzer (TGA), thermal balance reactor and pressurised drop tube furnace (PDTF) reactor. The diameter of the coal sample particle in these studies was from 106 up to 2400 μm .

It is mentioned in the literature that the conditions under which the char is pyrolysed, whether the coal is pyrolysed under pressure or not and whether a low or high heating rate ($^{\circ}\text{C}/\text{min}$) might affect its gasification rate. It is determined that elevated pyrolysis pressure slows down the rate of release of volatiles, increases the amount of char for gasification and alters the composition of volatile products [70, 88]. The latter shows that pressure decreases the effect of pyrolysis. Furthermore it was found that elevated pyrolysis pressures affects the apparent reaction rate and not the intrinsic reaction rate which means that pyrolysis pressures affects the physical structure of the char and not the chemical structure which is important for the char reactivity [67].

It is also mentioned in the literature that the temperature and the heating rate by which the temperature is gradually increasing during the devolatilisation of coal is important for the gasification reactivity of the produced char [38]. The difference between surface gasification and underground coal gasification is that in underground coal gasification the coal seam heats up slowly allowing for the pyrolysis taking place and the volatile matters to be released before gasification starts [49]. It is the contrary in surface gasification where coal heats up quickly and as a result pyrolysis and gasification occur simultaneously and that does not allow an amount of volatiles to be released [32]. According to Higman et al., (2008) the extent of devolatilisation depends on the final temperature, which means that at high temperatures such as 900 $^{\circ}\text{C}$ the effect of heating rate becomes insignificant. In the following paragraphs studies are presented which studied the CO_2 and H_2O gasification at low and high pressure by pyrolysing the coal under ambient or elevated pressure at a low or high temperature heating rate.

2.5.1 Chars prepared at atmospheric pressure

a. Low temperature heating rates

Ma et al. (1992) [52] studied the gasification kinetics of Jincheng anthracite coal char (F.C.=76.92%, V.M.=6.48%) with steam with a tubular fixed bed reactor over a pressure range of 0.1 to 1.42 MPa and temperatures between 868 and 1100 °C. The particle size was from 450 to 1000 µm and the char was produced by devolatilisation of the coal under N₂ environment from room temperature to 900 °C at a rate of 5 °C /min and held there for 2 hours. It was found that the reaction rates increased with an increase in steam partial pressure [52]. It is worth noting that the reaction rates at different temperatures and 0.1 MPa over time for the anthracite coal char were all mountain shaped with their maximum reaction rate achieved at the value of 0.2. This was explained by Ma et al. (1992) [52] as a reaction feature of the type of the coal and it was irrelevant with temperature and pressure. Anthracite has very low volatile matters content and so the resulting coal char has a small initial porosity. This initial porosity and pore surface area increase with reaction and the maximum surface area was obtained at reaction rate of 0.2 which is the maximum rate achieved. If the reaction continues the rate decreases since the pore surface area decreases and overlapping of the pores is taking place.

Li et al. (1994) [46] investigated the kinetics of a lignite char gasification at 1.96 MPa with CO₂, H₂ and H₂O using a packed bed balance reactor (PBBR). The char was produced by heating the coal samples from room temperature to 900 °C and holding the temperature for 1 hour, then the char was cooled down at ambient temperature and been grounded to 0.25-0.42 mm. The flow rate of the CO₂ was 40 l/min (0.66 l/sec) at temperatures between 800 and 950 °C and the flowrate of H₂O was 10 ml/h (0.16 ml/sec) + 40 l/h N₂ at temperatures between 750 and 1000 °C.

The results for the various temperatures showed that carbon conversion is very sensitive to temperature and increases as temperature increases at 1.96 MPa. This suggests that chemical reaction is probably the rate controlling step and the reaction of char with CO₂ and H₂O was interpreted well with the shrinking core model proposed by Wen (1968) [90] and good linearities of carbon conversion over time were obtained. This model suggests that the reaction initially occurs at the external

surface of the coal particle and then the reaction gradually moves inside leaving a layer of ash behind. Under the experimental conditions of low temperature below 1000 °C, only the chemical reaction at the surface is the controlling step, so the carbon conversion with time described as $1-(1-X)^{1/3}=(K_s P_A^n / R C_s) t$ (where K_s is the surface reaction rate constant, P_A^n the pressure of the reactant gas, n the reaction order, R is the initial radius of the char particle and C_s is the initial solid concentration) was substituted with $1-(1-X)^{1/3} = K t$ where K is the rate constant.

Goyal et al., (1989) [26] studied the gasification rate of a bituminous char at temperatures between 925 to 1038 °C and pressures of 0.78, 1.45 and 2.82 MPa using a high pressure high temperature thermo balance. The char was prepared under nitrogen flow at atmospheric pressure with a low heating rate of around 10 °F/min until it reached the set temperature and was maintained there for 30 min. Then the char was crushed to mesh fraction of -20 to +40 for it to be gasified for 90 min. Steam and synthesis gas mixtures (CO, CO₂, H₂ and H₂O) were used as gasifying agents. It was found that the gasification rate with steam is the highest and the rate decreased with the gas mixture due to the retardation created by H₂ and especially CO.

In addition it was observed that the gasification rate increases with temperature. The rate of carbon conversion over time is expressed by the model proposed by Johnson (1974) $dX/dt= K(1-X)^{2/3}\exp(-aX^2)$ where $\exp(-aX^2)$ determines the relative reactivity of the effective surface area which decreases with increasing conversion for positive values of a . By integrating the above equation of the model, it becomes $3[1-(1-X)^{1/3}]=Kt$. The value of $a=0$ because the plots of $3[1-(1-X)^{1/3}]$ versus time are linear and from the slope of these plots the overall rate constant K is derived. The values of the K for 0.78, 1.45 and 2.82 MPa and various concentrations of gases in the gas mixture such as 27.4-38.8% H₂, 39.4-51% H₂O, 6.1-19.3% CO and 4.1-13.0% CO₂ were from 0.00025 to 0.00051/sec.

Roberts D. G. et al., (2000) [66] studied the intrinsic and apparent reaction rates of a high volatile bituminous coal and semi-anthracite with CO₂ and H₂O by using a pressurized thermogravimetric analyzer (TGA). Chars were produced by heating sized coal samples (-1.0mm + 0.6 mm) at atmospheric pressure in ceramic containers

to 1100°C at 10°C/min under dry nitrogen for 3 hours. Char–CO₂ experiments were performed at 900°C and char–H₂O experiments at 850 °C in the TGA at 0.1, 0.5, 1, 1.5, 2 and 3 MPa pressure.

It was found that pressure increases the apparent and intrinsic rate of the char- CO₂ reaction for both chars up to 1 MPa pressure. Above this pressure the intrinsic rate for both chars is almost constant up to 3 MPa for both chars and so is the apparent rate of the bituminous coal but the apparent rate of the semi-anthracite seems to increase up to 3 MPa which this increase reducing at higher pressures. This effect was explained by the concentration of the adsorbed surface complexes C(O) and not due to a fundamental change in the reaction mechanism. At ambient pressure the reaction rate is proportional to the number of surface complexes and as pressure is increased more surface complexes are generated which result in an increase in the reaction rate. At higher pressures the surface of the char will be saturated with surface complexes and no more will be created which will lead to a decrease of the char reaction rate [67, 88]. The activation energies for the bituminous char-CO₂ reaction were 209, 211 and 220 KJ/mol at 0.1, 1 and 2 MPa respectively and those for the char-H₂O reaction were 227 and 231 KJ/mol at 0.1 and 1 MPa respectively.

Harris et al., (1991) [30] determined the intrinsic reactivity of a petroleum coke and a brown coal with CO₂ and H₂O using a fixed bed reactor under chemical control reaction regime I. The particle size was between 0.2-2 mm, the pressure atmospheric and the temperature between 500 and 980 °C. The surface area of both coals increased with reaction and the reaction of char with H₂O produced greater increase in the surface area than with CO₂. The activation energy was determined for the brown coal char for the reaction with CO₂ and H₂O at 230 and 225 KJ/mol respectively. Similarly the activation energy for the petroleum coke for the reaction with CO₂ and H₂O was found at 215 and 242 KJ/mol respectively

Ye et al., (1998) [96] conducted gasification experiments with a highly reactive low rank coal with H₂O and CO₂ in a single particle reactor at temperatures between 714 and 892 °C and ambient pressure. The particle size of the coal char was 1.6-2.4 mm. It was found that carbon conversion increases with increasing reaction time and the gasification rate of H₂O was higher than with CO₂. This was explained by Ergun et

al., (1956) cited in Ye [96] that the difference in rates of those two reactions is because the reaction of carbon with steam generates a greater number of active sites than with CO₂.

The model that Ye et al., (1998) [96] used to describe the reactions of char with H₂O and CO₂ was the volumetric model but it is worth noting that it was mentioned that different researchers claimed that both volumetric and shrinking core models describe the kinetics of char gasification well. Kwon et al., (1988) [43] determined that under the assumption of chemical reaction control both models describe the kinetics of char gasification equally well at temperatures below 700 °C and at higher temperatures the shrinking core model exhibits smaller deviations than the volumetric model. Adanez et al., (1990) studied the gasification kinetics of a high ash coal and found that both models describe the experimental data very well in the chemical reaction control regime I.

b. High temperature heating rates

Ahn et al., (2001) [1] studied the effects of gasification temperature (900-1400 °C), partial pressure of CO₂ (0.1-0.5 MPa) and total system pressure (0.5, 0.7, 1.0, 1.5 MPa) on the gasification rate of coal char with CO₂ of an Indonesian sub bituminous coal-char by performing PDRF reactor tests. The coal char was prepared in an ambient pressure at a temperature of 1400 °C with a heating rate of 10⁴ K/sec and a particle size of 45-64 μm. The experiments at different temperatures were performed at ambient pressure and CO₂ partial pressure of 0.2 MPa and it was found that the gasification rate increases as the temperature increases and the non reactive core model predicts well the conversion-timed data. The apparent reaction coefficient k was determined for the reaction regime II which is controlled by the chemical reaction and gas diffusion into the pores of the particle. The carbon conversion with time was describe with the equation $dX / dt = k P_{CO_2}^n (1-X)^{2/3}$ where n is the apparent reaction order, P_{CO_2} is the CO₂ concentration and X is the carbon conversion. Experiments were also performed at lower temperatures (900-1000 °C) for the chemical control reaction regime I and the intrinsic reaction rate was determined. The experiments at various total system pressures were performed at 1300 °C and it was found that the reaction rate decreases as the total system pressure increases since

the time to achieve a specific extent of conversion is increasing as pressure is increasing. Furthermore the value of the reaction rate coefficient k changes according to the change of total pressure so the value of k obtained at atmospheric pressure cannot be appropriate to be used to the cases of elevated pressures. The effect of pressure was explained by the assumption that the diffusion resistance of reactant gas into the pore structure of char increases as the total system pressure increases [1, 48]. The carbon conversion with time based on the shrinking core model was modified to be $dX / dt = k P_{CO_2}^n P_{total}^m (1-X)^{2/3}$ in order to describe the impact of total pressure to the gasification rate, where m is the correlation exponent which takes into account the effect of total pressure on the reaction rate. This correlation exponent was derived from the slope of the log-log plot of k versus total pressure [1].

Kajitani et al., (2002) [38] studied the gasification rates of a bituminous coal char with a pressurised drop tube furnace at 1300 °C. The coal chars were prepared by rapid pyrolysis in nitrogen using an atmospheric DTF at 1400 °C. The coal char was gasified with CO₂ and H₂O up to a total pressure of 2 MPa and it was observed that the gasification rate with CO₂ (0.2 MPa) was independent of pressure variation but with H₂O (0.05 MPa) the gasification rate increased by around 30% from 0.2 to 2 MPa. Arrhenius plots indicated that in a PDTF reactor below 1200 °C the chemical surface reaction controls the gasification and at temperatures above 1200 °C the pore diffusion controls as the reaction rate remained below the straight line. The gasification rate over time was better described by the random pore model than the grain model.

Nozaki et al., (1991) [59] studied the gasification rate of four chars ranking from sub bituminous to anthracite under CO₂ pressure of 0.02 to 0.25 MPa using a high pressure fixed bed reactor. The chars were produced in a fluidized bed pyrolyser at a heating rate of 1000 K/min under N₂ environment. The N₂ was switched over to CO₂ flow and gasification is initiated. The reactor was loaded with 10-100 mg of 0.5-0.59 mm chars and heated up to the reaction temperature of 850 °C under N₂ flow at a heating rate of 10 K/min. It was found that there is pressure dependency of the CO₂ gasification rate which increases with pressure and is stronger in the low pressures. One explanation of these results is that under pressure the surface oxide complexes

are attacked by the CO₂ molecules more often, this speeds up the desorption of the surface oxide complexes by the collisions with CO₂ molecules. Furthermore the gasification rate of anthracite char was much slower than that of low rank coals and the increase of its gasification rate between 1.0 and 2.5 MPa was very small. It seems that there is saturation of the gasification rate at high pressures for the anthracite and high rank coals with this effect being less obvious for low rank coals. The effect of pressure saturates with high rank coals such as bituminous and anthracite but no saturation is observed with low rank coals [48].

2.5.2 Chars prepared at pressure

a. Low temperature heating rates

Muhlen et al., (1985) [57] tested the reactivity of a German bituminous char with CO₂, H₂O and H₂ at pressure up to 0.7 MPa and 900°C temperature with a pressurised thermobalance apparatus at a heating rate of 10 °C/min. It was found that there is an increase in reaction rate at low pressures up to around 0.2 MPa for CO₂ and H₂O with the increase levelling off at further increases in pressure up to 0.6 MPa. The H₂O gasification rate was several times higher than that for CO₂ gasification and the inhibiting effect of the produced H₂ and CO was also observed. Muhlen et al., (1991) [58] also noted that the reactivity of chars with steam is not affected by pressure if the pyrolysis is performed under inert conditions. However, under a hydrogen atmosphere increased pressure resulted in a decrease in the steam reactivity of the resulting char.

Sha et al., (1990) [70] tested the reactivity of Chinese lignite and bituminous chars with CO₂, H₂O and H₂ at pressures from 0.12 to 3.1 MPa, temperatures of 850 to 900°C with a pressurized thermobalance. The particle size was from 420 to 840 µm and it was observed that the reaction rates increase with increasing pressure up to 1 MPa for the reaction of char with H₂O and up to 1 - 1.5 MPa for that with CO₂. Above these pressures reaction rates levelled off with higher pressures up to 3.1 MPa. It was observed that the produced gases H₂ and CO had a strong inhibiting effect on the reaction rate of carbon with H₂O which tends towards zero at higher pressures. Inhibiting effect of CO was also observed with the reaction of carbon with

CO₂. It is worth noting that Sha et al., (1990) [70] conducted experiments under pressure with a fixed tubular reactor where chars were produced under various pressures of 0.1, 2.0, 4.0 and 6.0 MPa at 800 °C and then reacted with H₂ at 900 °C and 2.0 MPa. It was found that the reaction rates and carbon conversion of the chars decreased with increased pyrolysis pressure and this levelled off at around above 4.0 MPa. It seems that the pyrolysis under pressure may bring changes in the pore structure of the char and can decrease the reactivity of the coal char produced.

Lim et al., (1996) [47] studied pressurised coal gasification of the Daw Mill coal with CO₂ by using a wire mesh (WMR) and fixed-bed 'hot-rod' (HRR) reactors at pressures between 0.1-3 MPa, at 850 and 1000 °C temperatures and coal samples of 50 mg with particle size between 106 and 150 µm. The heating rates of 10 K/sec were applied to both reactors with a hold time of 10 sec at peak temperature. It was found that the reaction rate was increasing with an increase in pressure.

Blackwood et al., (1960) [3] tested the reactivity of char coal with CO₂ and H₂O with a high pressure reactor at pressures up to 5 MPa and temperatures from 750°C to 830°C. The size of the coal samples was from 1200 to 2400 µm. It was found that the reactivity of carbon increased with an increase in the gas pressure, also the reaction rate for steam gasification was higher than that of CO₂ [3, 55].

Li and Xiao (1993) investigated the reaction rates of three Chinese coal chars with steam at pressures up to 15 bar and temperatures between 750 and 950 °C. The apparatus that was used was a packed bed balance reactor and the particle size was from 180 to 250 µm. It was found that the reactivity decreases as the coal rank increases.

b. High temperature heating rates

Moilanen and Muhlen (1985) [55] studied the CO₂ and steam gasification of a peat char of particle size 0.1 mm produced in an atmospheric drop tube reactor at a heating rate of 10⁴ K/sec. The gasification took place at pressures of 0.1, 0.5 and 1.5 MPa and temperatures between 750 and 950 °C with a pressurised thermobalance system and found that the reactivity decreases as the pressure increases. The steam

gasification rate was slightly higher than the CO₂ gasification rate and the presence of H₂ and CO inhibited the peat char gasification almost entirely.

Roberts et al., (2003) [69] focused on the coal conversion aspect of gasification and in particular the conversion of coal char following pyrolysis under pressure. Chars were devolatilized in a pressurized drop tube furnace, a horizontal tube furnace at 0.5, 1.0 and 1.5 MPa with a temperature of 1100 °C, also some chars were prepared in an atmospheric pressure tube furnace. The size of the coal samples were from -1.0 mm to 0.6 mm. The reaction rates of these chars were measured using a pressurized thermo gravimetric analyzer (TGA).

It was found that chars made at high pressures and with high heating rates have apparent reaction rates in CO₂, H₂O and O₂ that are orders of magnitude faster than those of char made from the same coal at atmospheric pressure and slow heating rate conditions. This finding was attributed to the char morphology and surface area rather than on the chemical reactivity of the char and this type of effects would influence the diffusion of reactants through the pore structure of the particle at high temperature. They never influenced the intrinsic reactivity of the char [66, 67] which is the chemical reactivity of the char itself and the reaction of char with gases and what this study is looking at.

It was noted that the data on the effect of pyrolysis pressure on the char reactivity is limited. Sha et al., (1990) [70] noted a decrease in the char reactivity as pyrolysis pressure was increased which was explained that pressure may bring changes to the pore structure. Muhlen et al., (1991) [58] also noted that the reactivity of chars with steam is not affected by pressure if the pyrolysis is performed under inert conditions. However, under a hydrogen atmosphere increased pressure resulted in a decrease in the steam reactivity of the resulting char. More recent Roberts et al., (2003) [69] found that chars made at high pressures and with high heating rates have apparent reaction rates in CO₂, H₂O and O₂ that are orders of magnitude faster than those of char made from the same coal at atmospheric pressure and slow heating rate conditions. This finding was attributed to the char morphology and surface area rather than on the chemical reactivity of the char. This suggests that pyrolysis pressure significantly influence the physical structure of coal chars but has little effect

on chemical structure where the char reacts with gases and C is converted to gas, which is what this study is looking at. In addition Wiatowski et al., (2016) [91] who performed an ex-situ experimental simulation of hard coal underground gasification at elevated pressure noted that the effect of pressure on coal pyrolysis is not significant compared to the effect of the chemical reactions during the UCG process.

From the above studies it seems that the effect of pyrolysis at elevated pressure does not affect significantly the reactivity and the chemical reaction rate of char during UCG and its effective energy conversion to gas [91]. In this study the coal samples of dry steam coal and anthracite are pyrolysed under nitrogen environment at atmospheric pressure and as shown from the literature review [58] it seems that there will be no significant impact on the reactivity of the derived coal chars with $\text{CO}_2+\text{H}_2\text{O}$.

2.5.3 Effect of coal type on the gasification rate

Wall et al., (2002) [88] summarises the effect of CO_2 and H_2O partial pressure on the gasification rates for a variety of char types. He reports that the apparent rates of different coal types vary between two orders of magnitude due to differences in the surface area, the chemical structure of the coal char and the mineral content of the coals. The intrinsic reaction rate varies by one order between different coal types. Also he mentions that the reactivity of coal chars increase as gas pressure increases but this effect becomes independent at elevated pressures due to the adsorption-desorption mechanism.

The pressure dependency on the CO_2 gasification rate is stronger in the low pressures and the effect saturates at higher pressures only for high rank coals and not for low rank coals. There was no evidence that the effect of pressure saturates with low rank coals. Finally the coal char of low rank coals is more reactive than that of high rank coals due to the catalytic mineral content of the low rank coals or due to the difference in the structure of the carbon with more active sites. Low rank coals have a disorder carbon than high rank coals which generates more active sites [48, 66].

2.6 Gas-solid reactions

The gas solids reactions of the char gasification with CO_2 and with H_2O are briefly reviewed including the regimes under which these reactions take place, where these reactions occur on the solid particle and the most widely accepted mechanism under which they occur at low and high pressure. Finally some kinetic models mostly used to describe these reactions are also described.

2.6.1 Coal gasification process

The coal gasification process consists of the following stages as shown in Figure 2.5. Initially the coal starts heating up and above 100°C it dries by losing its moisture and at a temperature above 300°C pyrolysis occurs where the volatile matter in the coal is released consisting of gas, liquid and solid products. The principal noncondensable pyrolysis gases that are released are H_2 , CO , CO_2 , CH_4 , C_2H_6 , C_3H_8 and C_2H_6 . The liquid products that are released are all the condensable gases at 273 K and 0.1 MPa which are known as tar and consists of decomposition of water and organic phase tar. The latter includes compounds of CHN, phenols, sulphur compounds, aromatics (benzene, toluene, xylene) and some pentanes and hexanes. What is left is the char and inorganic phase of minerals in the coal which both consist the solid pyrolysis product. The char is unreacted coal with a different chemical structure and elemental composition than the parent coal [8, 11,64]. In a combustion environment the volatiles and char react with O_2 which is consumed very quickly and produces CO_2 and CO . These oxidation reactions R1 and R2 provide the heat for the reaction of char with CO_2 (R3) and with H_2O (R4) to proceed and produce $\text{CO}+\text{H}_2$. These gasification reactions are the slowest and therefore control the gasification rate and the conversion of coal char to gas. Finally what is left after gasification is ash and slag [64, 90].

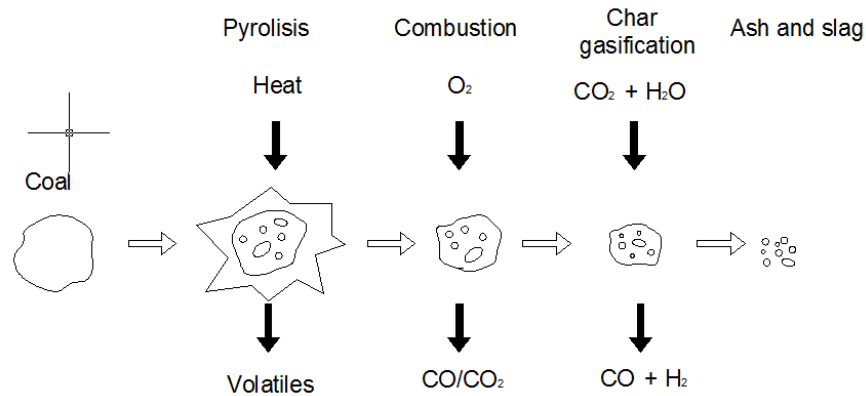


Figure 2.5: Coal gasification process

2.6.2 Characteristics of coal chars

Coals and coal chars have a trimodal pore distribution which means that there are three different types of pores with diameter from nm to mm which are the macropores, mesopores and micropores with some of the micropores being connected to the macropores and mesopores with restricted passages or being closed [35]. The rate of char gasification depends on the accessibility of the reactant gases through the macropores and mesopores to the internal surface of the porous coal where the active sites are, which are located within the micropores [86]. The diameter of the micropores is less than 1.2 nm and in order for the reactant gases to reach the active sites they must be transported by a substantial number of larger pores (feeders) connected to micropores.

The reason for that is the concentration of the gases at the micropores to approach the concentration of the gases at the external surface of the particle in order the active sites to be well utilised for reaction. Otherwise the absence of many larger pores which will feed the micropores leads to low char reactivity. Low rank coals have a larger amount of larger pores than high rank coals which contributes to an excellent utilisation of the active sites and as a result low rank coals are more reactive than high rank coals [35, 86].

At the beginning of coal gasification the volatiles are released primarily from the periphery of the particle and char is produced. The micropores in the parent coal are preserved in the char and are more accessible to the reactant gases because the loss

of volatiles increases the porosity of the char and all pore sizes allowing the reactants to be transported to the internal surface of the solid where the active sites are and enhance the char reactivity. As the reaction proceeds and the char conversion increases, more active sites are utilised and the active surface area is reducing resulting in a decrease in the char reactivity [35].

2.6.3 Active or reaction sites.

For a gas-solid reaction to occur one or all the reactants must become attached to the surface. This attachment is known as adsorption and there are two types, the physical adsorption and the chemisorptions with the latter affecting the chemical reaction rate [78, 86]. The gas-solid reaction is not taking part over the entire solid surface but only at certain active sites or centres or reaction sites. These active sites can be unsaturated atoms or unpaired electrons resulting from surface irregularities, edges and cracks of the carbon lattice or mineral matter [24, 51, 78, 83] and are capable of chemisorptions of the reacting gas forming oxygen surface complexes [83]. The reaction rate depends on the formation and removal of these oxygen surface complexes and on the number and extent of coverage of the active sites [83, 86]. The difference in the reactivity of coal types depend on the number of the active sites [83].

2.6.4 Regimes of gas-solid reactions

For a gas-carbon reaction to take place the reactants must first diffuse through the boundary layer surrounding the particle, which is also known as bulk diffusion of the reactants to the particle. Then the gas must diffuse into the pores of the particle in order for the reactants to be transported through the pores to the active sites so that the reaction of the reactants with the C can occur and finally the products of the reaction must be removed. Any of these processes can influence the reaction rate and be the controlling step in a chemical reaction which means that the chemical reaction takes place under the regime of the specific process. These regimes are the following:

Regime I

At low temperatures below 1000 °C the reaction is chemically controlled which means that the bulk diffusion of the reactants to the particle and the pore diffusion of reactants into the pores of the particle is happening very fast and that the reaction of reactants with the particle is the slowest step which determines the reaction rate [46]. In this case the reaction rate is chemical reaction control Regime I and the observed activation energy E in Regime I is the true activation energy [1, 83].

Regime II

At temperatures above 1000 °C, diffusion of the reactants into the pores of the particle is the controlling step of the chemical reaction which slows down the chemical reaction and determines the gasification rate. In this case the chemical reaction is controlled by pore diffusion Regime II. There are cases where the chemical reaction is still increasing until the diffusion of the reactant starts slowing down the reaction. In these cases the chemical reaction is a combination of chemical control and pore diffusion control Regime II [1]. The observed activation energy E in Regime II is half of the true activation energy [32].

Regime III

As the temperature increases further the chemical reaction is controlled by the diffusion of reactants to the particle surface which means that the reactants cannot be transported into the pores of the particle in order to reach the particle surface and react chemically. In this case the reaction is controlled by bulk diffusion Regime II. The observed activation energy E in Regime III is very small [32].

Figure 2.6 below illustrates the regimes of the gas-solid reaction depending on temperature

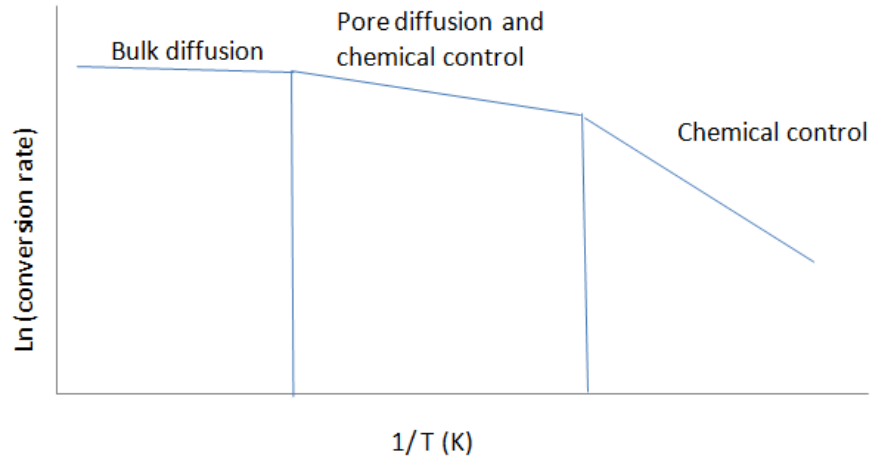


Figure 2.6: Gas-solid reaction rate in temperature regimes

2.6.5 Mechanisms of char with CO₂ and H₂O at low and high pressure

2.6.5.1 Reaction of char with CO₂

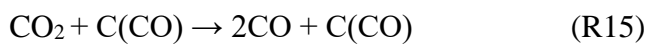
The reaction of char with CO₂ takes place through adsorption, reaction of the CO₂ with the char surface and finally desorption. The two step adsorption – desorption reaction mechanism that has been widely accepted for the heterogeneous reactions and for the CO₂ gasification at low pressure is the following [44, 81, 85, 87]:



where C(O) is an oxygen surface complex. Certain carbon atoms can detach an oxygen atom from a CO₂ mole reducing CO₂ to CO and forming an occupied site which is the C(O) (R8) [19]. At low pressures the C(O) concentration is low and the reaction mechanism is controlled by the forward adsorption reactions R8. From this reaction the C(O) that is produced is then desorbed to CO with the reactions R9. By increasing the pressure, the number of C(O) formed is increasing, resulting in an increase in the reaction rate which is proportional to the number of these oxygen surface complexes [2, 88]. The difference of the reaction rates of carbons is due to specific number of reaction sites, furthermore the reaction of char with steam

generates more active sites than the reaction of char with CO₂ [19]. There is experimental evidence that the product CO inhibit the reaction by shifting the adsorption reaction to the left [19,85].

At high pressures the formation of CO₂ has been observed which can be explained by other mechanisms proposed by different authors[2, 3, 67, 88] and are mentioned below. Reactions R12-R16 can express the reaction mechanism of the R3 reaction at higher pressures and reaction R16 shows the formation of CO₂.



According to the above set of reactions R12-R16, the C(O) and C(CO) concentration on the carbon surface approaches unity and saturation as pressure increases, which means that further increases in pressure will not lead to the formation of more C(O) and C(CO) and the reaction rate will not increase so the impact of pressure will become less significant to independent [67, 88].

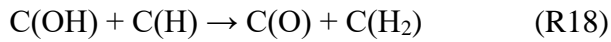
2.6.5.2 Reaction of char with H₂O

Similarly for the adsorption reaction of H₂O with C (R10), the H₂O is reduced to H₂ and an C(O) is formed.



The reaction is inhibited (retarded) by the H₂ produced and additional reactions were added to explain this inhibiting effect. Also at high pressures the formation of CH₄ has been observed which can be explained by other mechanisms proposed by different authors [2, 3, 57, 88] and are mentioned below. Reactions R17-R20 can

express the reaction mechanism of the R4 reaction at higher pressures and the reaction R20 shows the formation of CO₂.



According to the above set of reactions R17-R20, the C(O) and C(H₂) concentration on the carbon surface approaches unity and saturation as pressure increases, which means that further increases in pressure will not lead to the formation of more C(O) and C(H₂) and the reaction rate will not increase so the impact of pressure will become less significant to independent [16, 23].

2.6.6 Kinetic models

A number of previously published kinetics models were used to describe the gasification on coal particles. In this study the models that are used to interpret the conversion-time data are the progressive conversion model and the shrinking unreacted core model [45] or non-reactive core model [1] which are both based in the first order kinetics and chemical control of the reaction rate when the tested temperature is below 1000 °C. This means that the internal and external diffusion of the gases into the surrounding gas film and inside the char particle is negligible [1, 46].

The progressive conversion model assumes that the reactant gas to some extent enters and reacts with the particle, thus the particle is converted continuously with the particle size remaining constant and its density reduces as char conversion proceeds [45] as shown in Figure 2.7.

The carbon conversion with time is described with the progressive conversion model by the equation $-\ln(1-X) = k t$ where k is the first order rate constant and X is the carbon conversion of the solid.

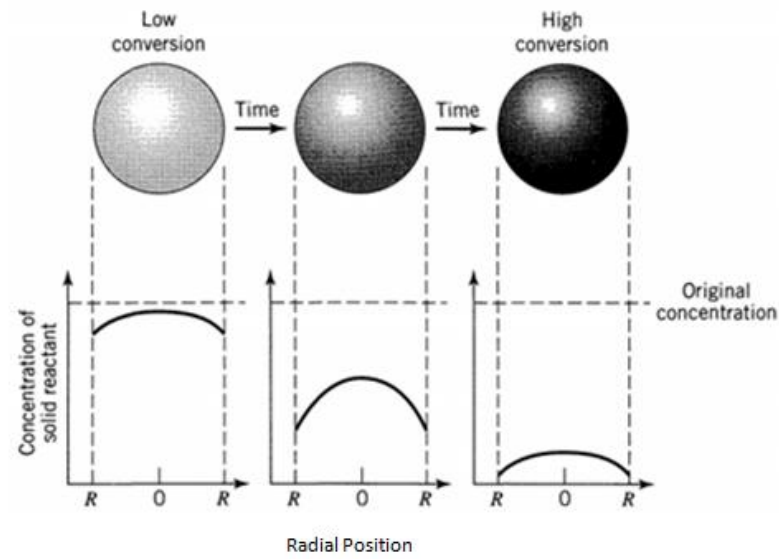


Figure 2.7: Reaction of a particle under chemical control with the progressive conversion model [45]

The shrinking unreacted core model assumes that the reaction occurs first at the outer skin of the particle and then moves into the solid leaving behind converted material and ash. As the reaction progresses the unreacted core keeps shrinking.

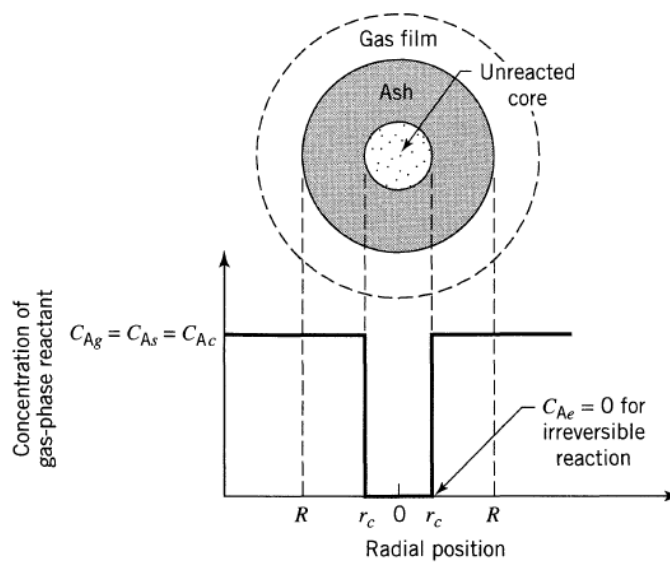


Figure 2.8: Reaction of a particle under chemical control with the shrinking unreacted core model [45]

Figure 2.8 illustrates a particle when chemical reaction is the controlling step with the shrinking unreacted core model. As shown, the concentration of the reactant passed through the gas film which is the external surface of the particle, and was then transported through the pores of the particle to the particle surface for the chemical reaction to proceed [45, 46].

The carbon conversion with time is described with the shrinking unreacted core model by the equation $3[1-(1-X)^{1/3}] = (b k^n C_{Ag} / R \rho_b) t$ where k^n is the first order rate constant, C_{Ag} is the partial pressure of the reactant gas, n is the reaction order, R is the initial radius of the char particle, b/ρ_b is the initial solid concentration (b is the mole concentration of the solid and ρ_b is the molar density of the solid) and X is the carbon conversion of solid [45].

2.6.7 Arrhenius Law

The overall reaction rate for gas-solid reactions can be expressed generally as follows:

$$dX/dt = k(P_g, T) f(x)$$

where k is the reaction rate constant, T is the temperature, P_g is the partial pressure of the reactant and $f(x)$ is a structure factor describing the chemical and physical changes of the particle during gasification [22]. Where the partial pressure of the reactant is constant then the reaction rate depends only on temperature which means that the reaction follows the Arrhenius law and that the variation of the reaction constant k with temperature can be described with the Arrhenius equation as follows:

$$k = A e^{-(E/RT)}$$

where A is a pre-exponential factor which indicates the probability that two or more molecules involved in a reaction can collide (sec^{-1}) and E is the activation energy which represents the amount of energy that has to be overcome so that the reaction can occur (KJ/mole). R is the ideal gas constant and T is temperature in K [32].

2.7 Chapter Summary

It was determined that there is no publically available data that quantifies the reduction zone of UCG by injecting $\text{CO}_2 + \text{H}_2\text{O}$, however there are relevant studies which can be used as reference such as those using $\text{O}_2 + \text{H}_2\text{O}$ as gasifying agents. Information was obtained from the medium to large laboratory scale experiments and field trials under which the experiments of this study will be conducted in terms of the operating procedure and important parameters such as temperature, ratio of gasifying agents and pressure.

With regard to the operating procedure it has been shown that the coal seam heats up slowly allowing for pyrolysis to take place and the volatile matter to be released before gasification starts during the underground coal gasification process [49, 53]. In order to simulate the UCG process it was found in some studies that the coal surface is first pyrolysed under a nitrogen atmosphere before being exposed to gasification environment. The temperature increases to the set temperature at a slow rate between 3.3 to 30 °C/min and is maintained at that temperature for a few minutes for pyrolysis completion [49, 53]. Furthermore in the UCG field trials mentioned, ignition of the coal seam takes place first which increases its temperature slowly and allows for pyrolysis to occur and for the volatiles to be released before the next stages take place which are oxidation and gasification. The CH_4 is mainly produced at low temperatures and during devolatilisation.

It was previously discussed that air or oxygen was introduced to increase the temperature and heat up the coal seam after the ignition and release of the volatile matter in order to enhance combustion [50, 75]. The reactions of oxygen with carbon produce mainly CO_2 and CO and are exothermic which means that they increase the temperature and heat up the coal. According to other studies the O_2 is consumed fairly quickly because the reaction of O_2 with C is very fast [12, 28,74]. At a later stage when the temperature was high enough, steam was introduced because it reduces the temperature and this hinders combustion and gasification Furthermore the high moisture content of low rank coals had the same impact as steam. It was found that steam was introduced in various studies when the temperature was above 900° C [49] in studies also where gasification took place in two stages, the steam

stage lasted until the temperature decreases to 700-800 °C [74] because below these temperatures the heating value of the product gas declined. In one study steam dropped the temperature in the cavity below 600°C and as a result the concentrations of CO and H₂ were low which showed that gasification was insignificant under these conditions [14]. The reason for this was that steam by dropping the temperature hindered the gasification reactions which need a temperature around 800-900 °C to proceed, hence the reactions of carbon with the reactant gases were diminishing which decreased the concentration of the produced gases.

This shows how important the reduction zone of UCG process is since the product gas is mainly produced during gasification through the reactions of coal char with the reactant gases which are mainly CO₂ produced during the oxidation zone and H₂O either injected or there is a water influx towards the cavity. These reactions are the Boudouard reaction (R3) which converts the excess CO₂ produced in the oxidation zone to CO and is responsible for the uniform quality of the product gas [12, 28, 17, 91] and the steam-carbon reaction (R4) through which char reacts with the injected steam in the cavity in order for the excess heat to be used and increase the efficiency of the process by producing H₂ and more CO.

In the UCG studies described earlier the gasifying agents used air, oxygen, enhanced oxygen, oxygen and steam either injected simultaneously or in cyclic phases if the aim is to increase the H₂ production [14, 74, 89]. Injecting oxygen with steam produced a product gas with the best composition and highest heating value compared to the other agents [13, 95]. The ratio of H₂O/O₂ is a very important parameter because excess oxygen dilutes the gasifying agents and produces excess CO₂ which drops the calorific value of the syngas, whilst excess H₂O drops the temperature which again decreases the calorific value of the product gas [14]. The steam flow was adjusted to find a suitable steam/oxygen ratio in order to maximise the amount of combustible gases and in various studies that ratio was H₂O/O₂=2:1 [14, 49, 94] whilst in one study the H₂O/O₂ ratio (moles) was around 5 [80], which is equal to 2.82 by mass. Every underground coal gasification system is different due to the different chemical and physical variations in the coal so it is not possible to derive an optimum H₂O/ O₂ ratio which could be applied to all the different systems, hence these parameters need to be derived individually for each UCG system.

There is very little information in the literature on the impact of pressure on the effective energy conversion of coal char to gas during underground coal gasification process and its performance. There are field trials that conducted UCG experiments at pressure but only one study conducted UCG tests at a range of pressures in order to assess its effect by cyclically changing the operational pressure on the gas composition of the product gas. O₂-enriched air and steam were injected into a coking coal and the operational pressure was changed by controlling the outlet flow of the product gas [89]. It was concluded in the latter study that the increased pressure increases the gasification rate and the heating value of the product gas and the best gas composition was achieved for the 0.8 MPa pressure between tested pressures from 0.2-1.2 MPa. This finding agrees with UCG field trials conducted under elevated pressure where the achieved heating value of the product gas was higher than that achieved at low pressures [64]. In addition in studies where the product gas compositions under pressure were calculated or determined by numerical simulations the effect of increasing the pressure was considered always to have a positive effect on the heating value of the product gas.

The data on the effect of pyrolysis pressure on the char reactivity is limited. It seems that the effect of pyrolysis at elevated pressure does not affect significantly the reactivity and the chemical reaction rate of char during UCG and its effective energy conversion to gas. In this study the coal samples of dry steam coal and anthracite are pyrolysed under nitrogen environment at atmospheric pressure and as shown from the literature review it seems that there will be no significant impact on the reactivity of the derived coal chars with CO₂+H₂O.

There are many studies investigating the behaviour of coal char with CO₂ and H₂O in surface gasification which look at a wide range of coal char types; different coal sample particle from 106 up to 2400 µm.; temperatures between 700 and 1100 °C; pressures of up to 5.0 MPa. However there is very little information on the behaviour of coal char with gases during underground coal gasification process and its kinetics. There is only one study which conducted CO₂ gasification experiments at 1000 °C in the context of UCG and this found that the intrinsic kinetics are better described with the random pore model and that diffusion influences the overall

gasification rate [14]. In the literature it is mentioned that the UCG kinetics are controlled above 1000 °C by external molecular or bulk diffusion and below 1000 °C by chemical reaction and intraparticle or pore diffusion [28]. It is evident that there is a lack of knowledge of how pyrolyzed char reacts with gases and its kinetics during the underground coal gasification process and hence experimental data is needed which will provide a better understanding of this. This information might help in the development of numerical models to predict the process accurately.

Each underground coal gasification system has its own individually operating parameters which need to be determined [28] in order to achieve the best gas composition and enhance the effective energy conversion of char to gas and the overall performance of the process. In addition, the previous UCG trials have mainly been carried out on highly reactive low rank coals with high moisture content, with very little information available on UCG for medium to high rank coals. It is therefore prudent to investigate the behaviour of two high rank coals in the context of underground coal gasification and their suitability for a UCG project depending on the end use of the product gas. In addition information would be provided on the oxidation and pyrolysis zone as well.

It is also shown that the composition of the product gas and its heating value depends on the thermodynamics of the process and on the composition of the reactant gases, also that the reduction zone of UCG where gasification takes place produces most of the gases and controls the product gas composition through the reactions of coal char with CO₂ and steam. Based on these findings this study investigates how temperature, pressure and composition of reactant gases impact on the effective energy conversion of coal to gas during the simulated reduction zone of UCG by injecting CO₂+H₂O.

Chapter III

EXPERIMENTAL APPARATUS

3.1 Introduction

This chapter describes the experimental apparatus that was designed, tested and commissioned as part of this PhD thesis and the considerations that took place during the design process in order to select equipment with the appropriate specifications for the required experiments. The company which provided the equipment was also responsible for the delivery and assembly of the apparatus.

3.2 Experimental Apparatus

The purpose was to design an experimental set up which will test coal under conditions which simulated aspects of the UCG process in order to be able to determine the impact of operating parameters which control the UCG process and have a better understanding of the coal-gas interactions in the UCG cavity. Figure 3.1 presents the schematic of the bespoke high pressure/high temperature rig that was developed and operated at pressures up to 5.0 MPa and 900°C. The experimental rig consists mainly of:

- a) A gas supply system
- b) The gas-solid reacting system
- c) The gas analysis system

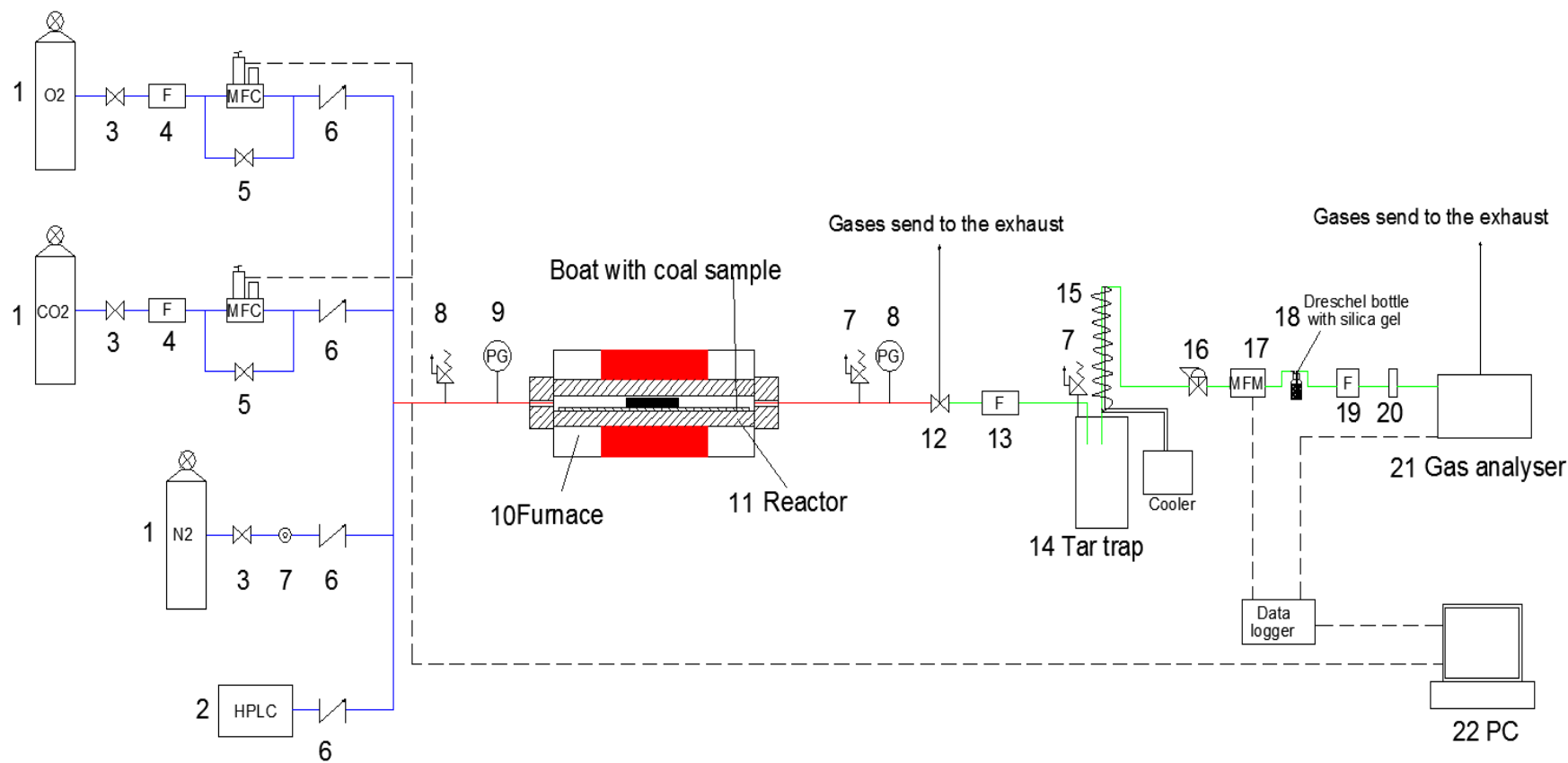


Figure 3.1: Schematic of the bespoke high pressure high temperature rig showing the gas supply system (lines of O₂, CO₂, N₂ and steam with mass flow controllers, filters and non-return valves-blue line), the reacting system (reactor and furnace with pressure gauges and pressure relief valves before and after the reactor-red line) and the gas analysis system (tar trap, water cooled condenser, cooler, mass flow meter, gas analyser and PC with logging and software control-green line)

As shown in Figure 3.1 the experimental rig consists of:

1. Gas cylinders of O₂, CO₂ and N₂ with pressure regulators
2. An HPLC water pump which injected water in the system
3. On/off valves which allow or restrict the flow of the gases
4. Filter upstream of the MFC to remove any particles in the gas flow
5. Mass flow controllers (MFC) for O₂ and CO₂ gas pipe line with by-pass on/off valve
6. Non return valves which restrict the reverse flow
7. Needle valve which controlled the flow rate of N₂
8. Pressure relief valves which safety limited the pressure within the system
9. Pressure gauges to monitor the pressure within the system
10. A horizontal split hinge furnace to heat up the reactor
11. A tubular pressure vessel (reactor) where the boat with the coal sample was placed
12. On/off valve which allow sending the gases to the exhaust without passing them through the gas analysis system
13. In-line filter (100 micron) to remove any particles carried over in the line
14. A gas liquid separator (tar trap) where volatile matter and water vapour condensed
15. A water cooled condenser which was placed on the head of the tar trap and connected to a cooler in order to drop the temperature of the tar trap
16. A back pressure regulator to govern the pressure within the system
17. A digital mass flow meter (MFM) to measure the product gas flow rate at the outlet
18. A dreschel bottle with silica gel (silica gel trap) to remove any water vapour
19. A filter to remove any particle
20. A rotameter to monitor the product gas flowrate
21. A gas analyser to quantitative analyse the product gas
22. PC with logging for the MFM and the gas analyser and control software for the MFC.

Figure 3.2 illustrates the bespoke high pressure, high temperature rig which was developed.

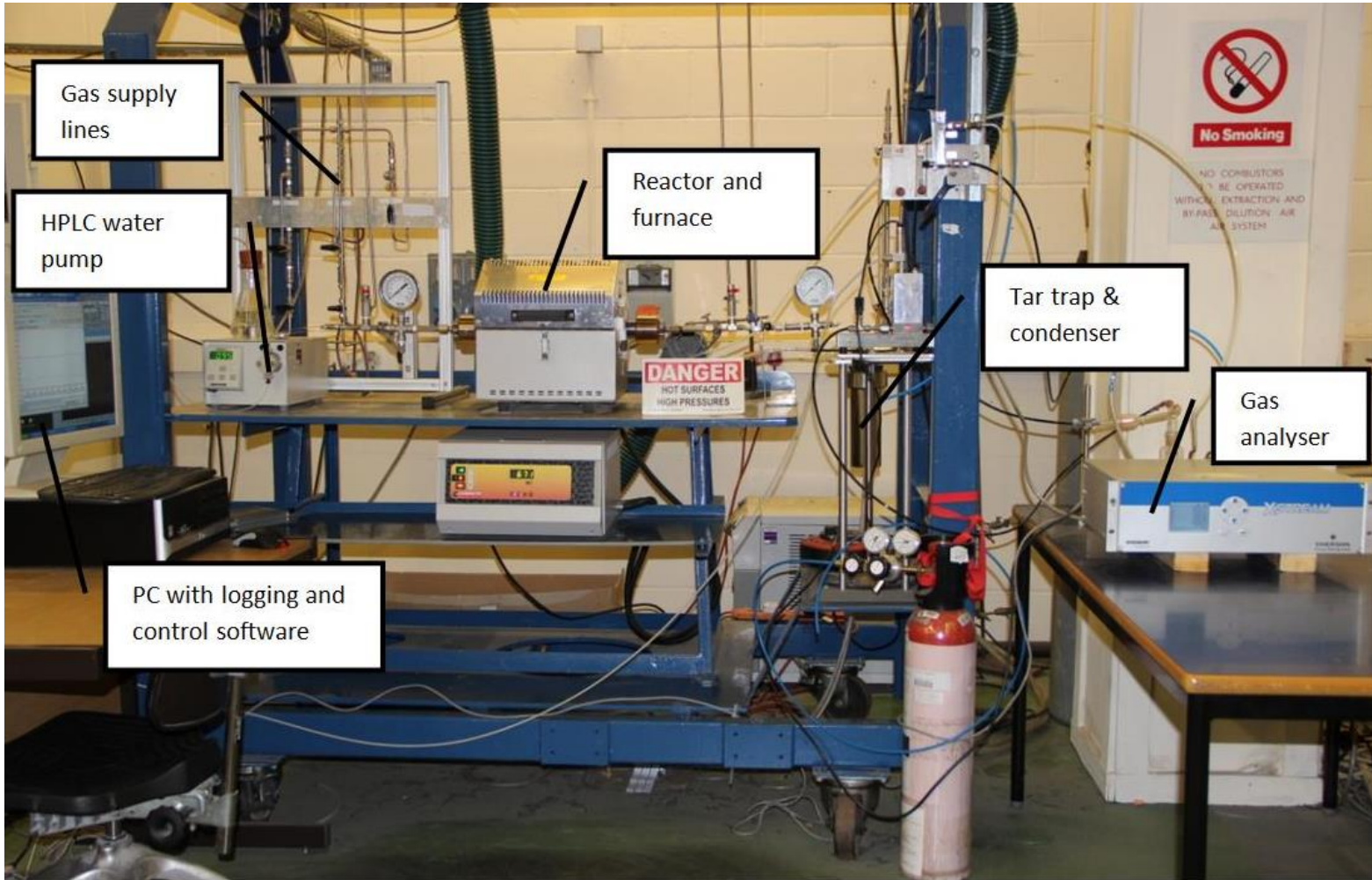


Figure 3.2: Image of the bespoke high pressure high temperature rig and associated control and analysis hardware

The main components of the experimental set up are described below in more detail.

3.3 Gas supply system

3.3.1 Gas cylinders

The gases that were used for the experiments were O₂, CO₂ and N₂. The gas cylinders of O₂, CO₂ and N₂ were placed in a cylinder cupboard as shown in Figure 3.3 and were equipped with regular gas pressure regulators which could control the pressure in the system. The two stage pressure regulators were brass construction and were manufactured by Gas-Arc Group Ltd, model Tech Master GA1500, which had an outlet pressure between the range of 0-105 bar. The CO₂ cylinder was also equipped with a Sirocco CO₂ vaporiser which heats up the liquid CO₂ in the gas cylinder in order to be injected as a vapour in the system. The Sirocco heater was manufactured by Air Liquide UK Ltd, operated at a power supply of 200 W and its maximum flow rate was 28 l/min.

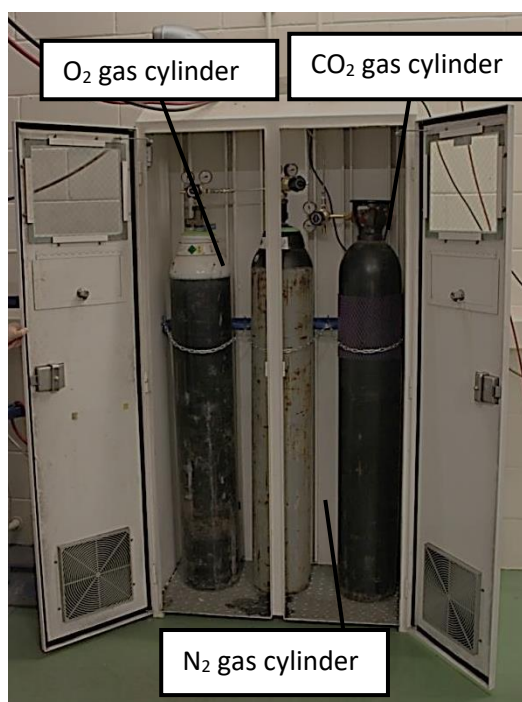


Figure 3.3: The cylinder cupboard with the O₂, CO₂ and CO gas cylinders

3.3.2 Gas lines

The purge lines of O₂, CO₂ and N₂ gases are shown in Figure 3.4 and were 1/4" stainless steel pipes which were equipped with on/off valves and non-return valves.

The N₂ gas purge line was also equipped with a needle valve which controlled the flow rate of N₂ in the system.

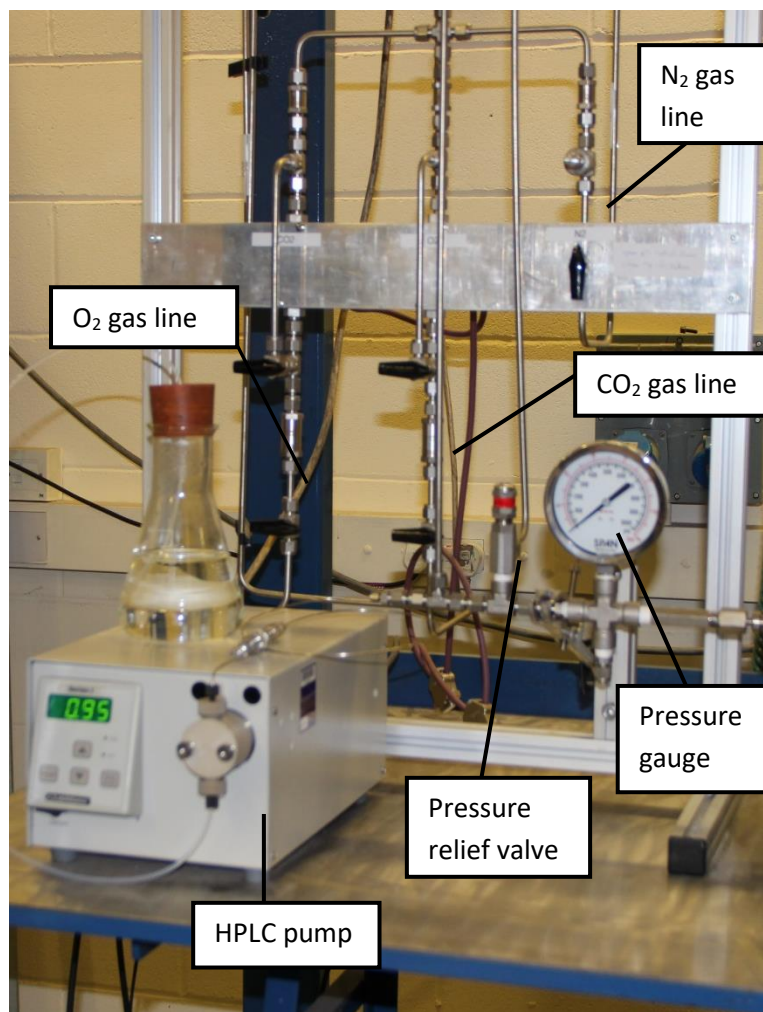


Figure 3.4: Part of the gas supply system showing the gas lines and the HPLC pump. The pressure relief valve and the pressure gauge are also visible

3.3.3 HPLC pump (High Performance Liquid Chromatography)

An HPLC pump was used to inject water in the system at high pressure. There was a need for steam to be injected in the system in order to perform the required experiments. For this reason it was decided that it is much easier to inject water in the system which would then evaporate to steam due to the high temperature in the system instead of heating up water to produce steam and then inject the steam in the system. The HPLC pump was a Series I high performance metering pump manufactured by Scientific Systems, INC and is shown in Figure 3.5. The water pump had a manual set point with a flow rate range from 0.01 up to 9.99 ml/min

measured at STP, a pressure rating of up to 2500 psi and a flow accuracy of $\pm 0.2\%$. De-ionised water was used for the experiment to avoid blocking the pump.



Figure 3.5: The HPLC pump with a glass bottle filled with deionised water

The liquid stream line was 1/16" which was inserted into the 1/4" line that was passed to the tubular pressure vessel (reactor) as shown in Figure 3.6.

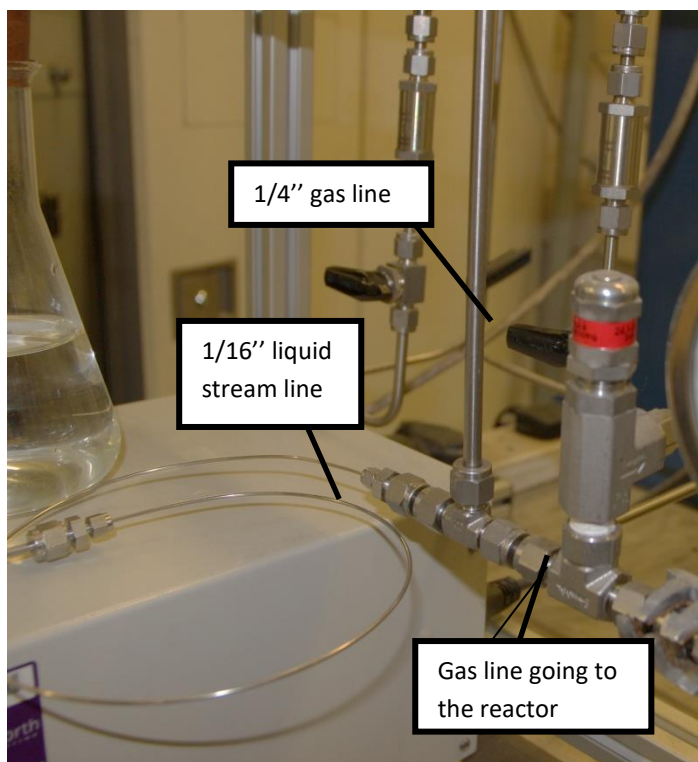


Figure 3.6: The 1/16" liquid stream line inserted into a 1/4" gas line passed to the reactor

3.3.4 Mass flow controllers (MFC)

Digital Mass Flow Controllers (MFC) on the O₂ and CO₂ gas pipe line were implemented in the system in order to control the inlet flow of the gases independent of flow temperature and pressure changes (Figure 3.7). The MFCs could also control the pressure. A filter was included upstream of each MFC to remove any particles and there was a bypass needle valve on both the O₂ and CO₂ lines to bypass the MFCs in case the system needs to be flushed with gases.

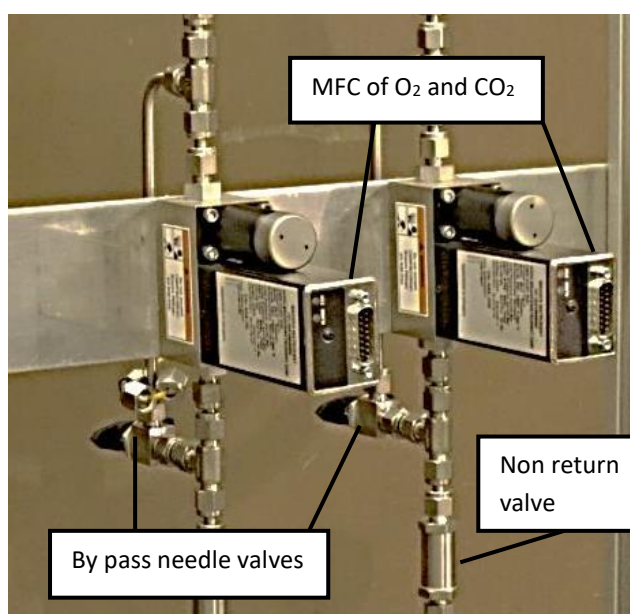


Figure 3.7: The mass flow controllers of the experimental setting

The MFCs were SLA5800 Series manufactured by Brooks Instrument B.V., their full scale flow rate was 10 l/min measured at STP they were calibrated at 50 bar and they need to remain in an ambient temperature between 0 to 65°C. The thermal mass flow measurement system of the MFCs consists of two components which are the restrictor and the flow sensor. The gas flow A+B as shown in Figure 3.8 enters into the MFC through the restrictor where it creates a pressure difference that forces gas stream A to flow into the sensor at a constant ratio of A/B and gas stream B to go straight through the restrictor. Then the gas A flows in the sensor through a thin walled stainless steel tube which has a heating element in the middle and temperature sensing elements on either side of it as shown in the enlarge view of the sensor in Figure 3.8.

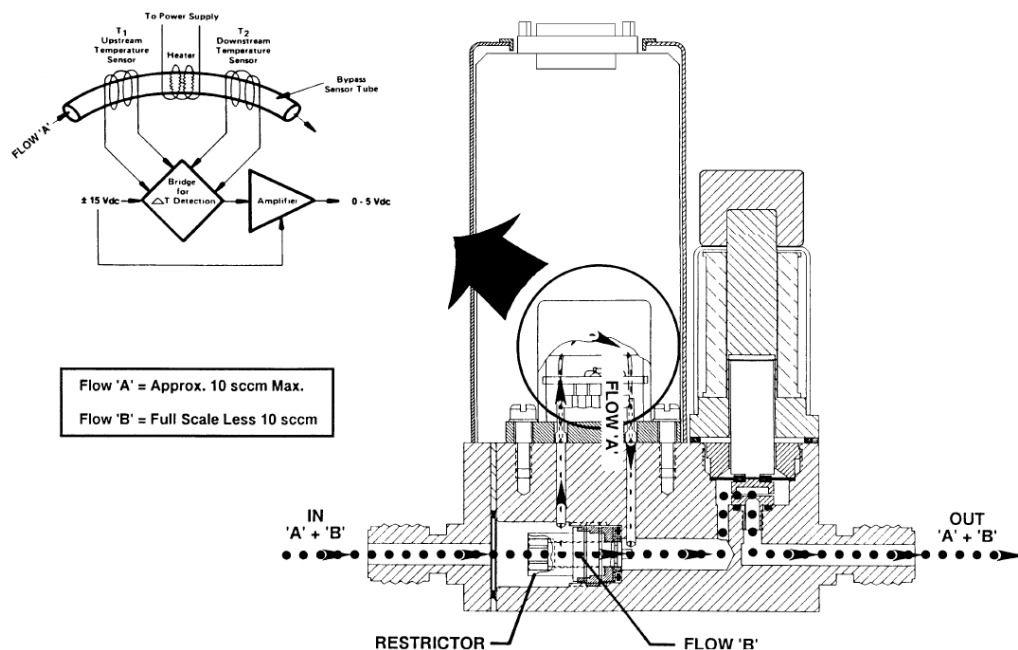


Figure 3.8: MFC and flow sensor operational diagram

As the gas A flows in the tube it carries away heat from the upstream temperature sensor to the downstream sensor. The difference in heat makes a difference in temperature which is proportional to the gas mass flow. Then a bridge circuit and a differential amplifier interpret the difference in temperature and generate an electrical signal proportionally to the gas mass flow rate. Finally flow A and B are joined again at the far side of the restrictor as shown in Figure 3.8.

3.4 The reacting system

3.4.1 Pressure Vessel (reactor) and Heating system

The reactor that was selected was a Parr tubular pressure vessel, series 4740 HP/HT manufactured in Alloy Haynes 230 by the Parr Instrument Company rated 50 bar and 900°C. The reason for this was the need to select a reactor where the coal sample could be placed in to be heated up and reacted under the flow of the gases at high temperature and high pressure conditions. Alloy Haynes 230 is a nickel (Ni)-chromium (Cr)-tungsten(W)-molybdenum (Mo) alloy with excellent high temperature strength and long term thermal stability at high pressure conditions (max allowable stress 13 bar at 900 °C). It has low thermal expansion, a pronounced resistance to grain coarsening with prolonged exposure to high temperature and excellent resistance to oxidation. Alloy Haynes 230 is covered by the ASTM product

standard B-622 for seamless pipe and tubing [31]. The reactor had two head openings after special request with screw cap ends and flexible graphoil gasket seals on each end as shown in Figure 3.10. The total internal length of the reactor was approximately 33 cm, the ID was 1" (2.54cm), the OD was 3" (7.62cm) and its volume was 0.21 L.

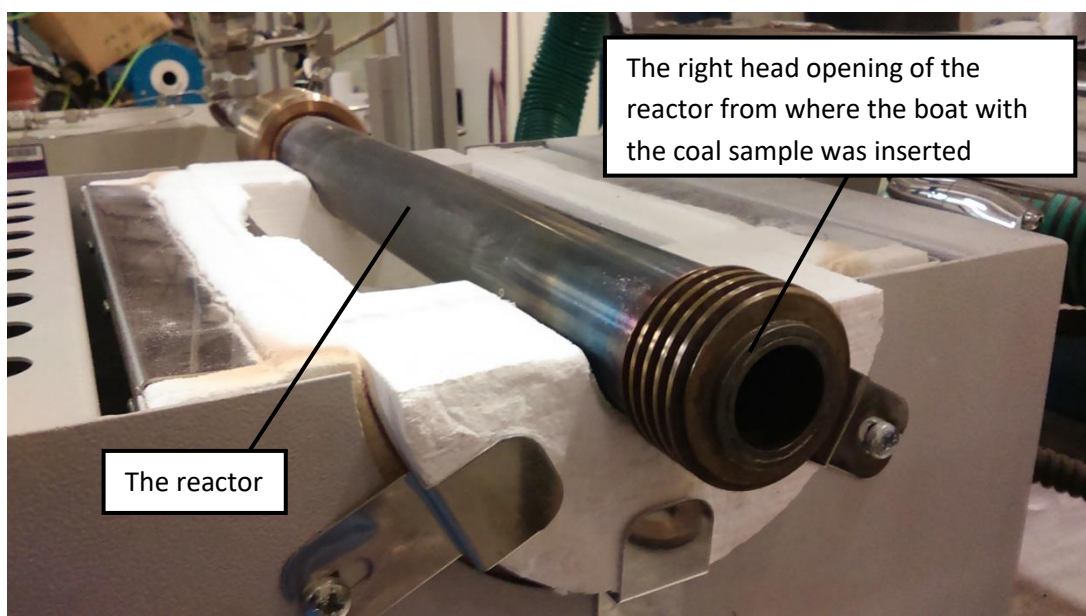
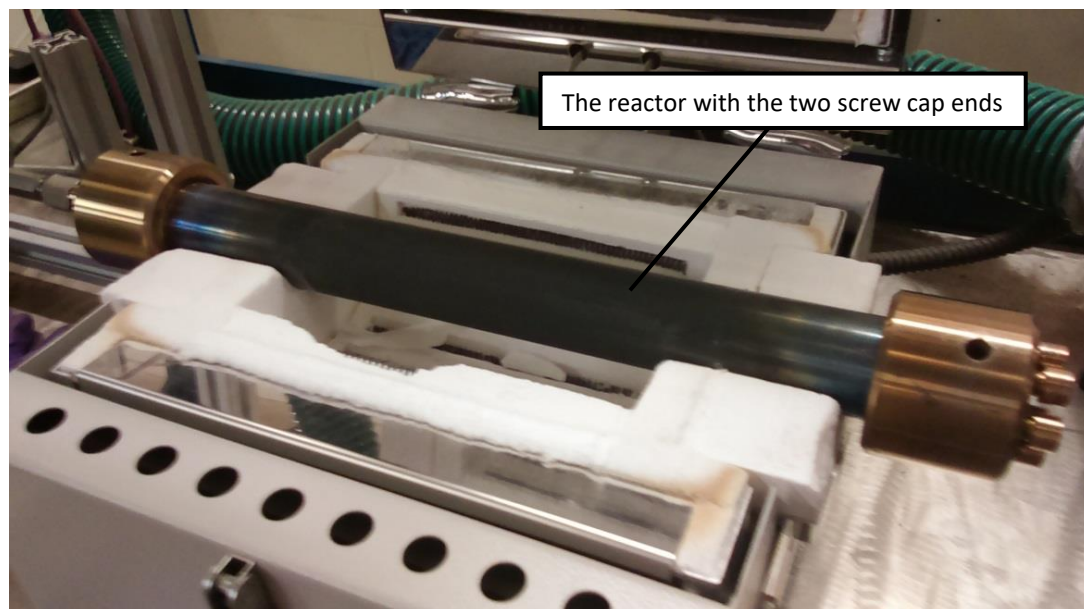


Figure 3.9: The reactor sitting on the HST furnace and its right head opening from where the boat with the coal sample was inserted

Figure 3.10 shows a view of the inside of the reactor from the right head opening where the removable sample holder (quartz boat) with the coal sample was inserted (shown in Figure 3.11). After insertion of the boat with the coal sample as shown in Figure 3.12, the right screw cap end of the reactor was assembled and then the equipment which is shown in Figure 3.13 was used to connect the right screw cap end of the reactor with the gas line as shown in Figure 3.14.



Figure 3.10: A view inside of the reactor from the right head opening



Figure 3.11: Image of the removable sample holder referred as quartz boat with a cylindrical coal sample

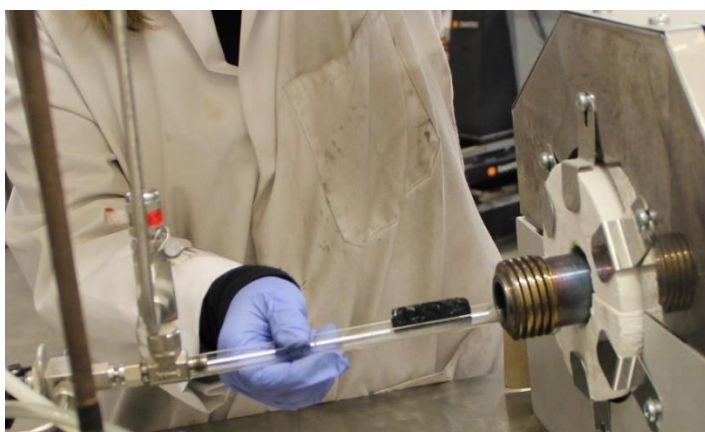


Figure 3.12: Procedure of the preparation of the boat with the coal sample and its insertion in the reactor



Figure 3.13: Equipment which was used to connect the right screw cap end of the reactor with the gas line



Figure 3.14: The right screw cap ending of the reactor connected to the gas line

The vessel sat in a Horizontal Split Tube (HST) furnace. The HST furnace comprised a furnace body which was split and hinged into two halves along its length which allowed it to be used with tubes where end flanges would make insertion into a non-split furnace difficult and this was the reason why this type of furnace was selected. The HST furnace was manufactured by Carbolite and used free radiating wire elements embedded within the insulation of the furnace body as shown in Figure 3.15. Its maximum temperature was 1200°C, the heated length was 20 cm and the tube length and OD were 30 and 11 cm respectively.

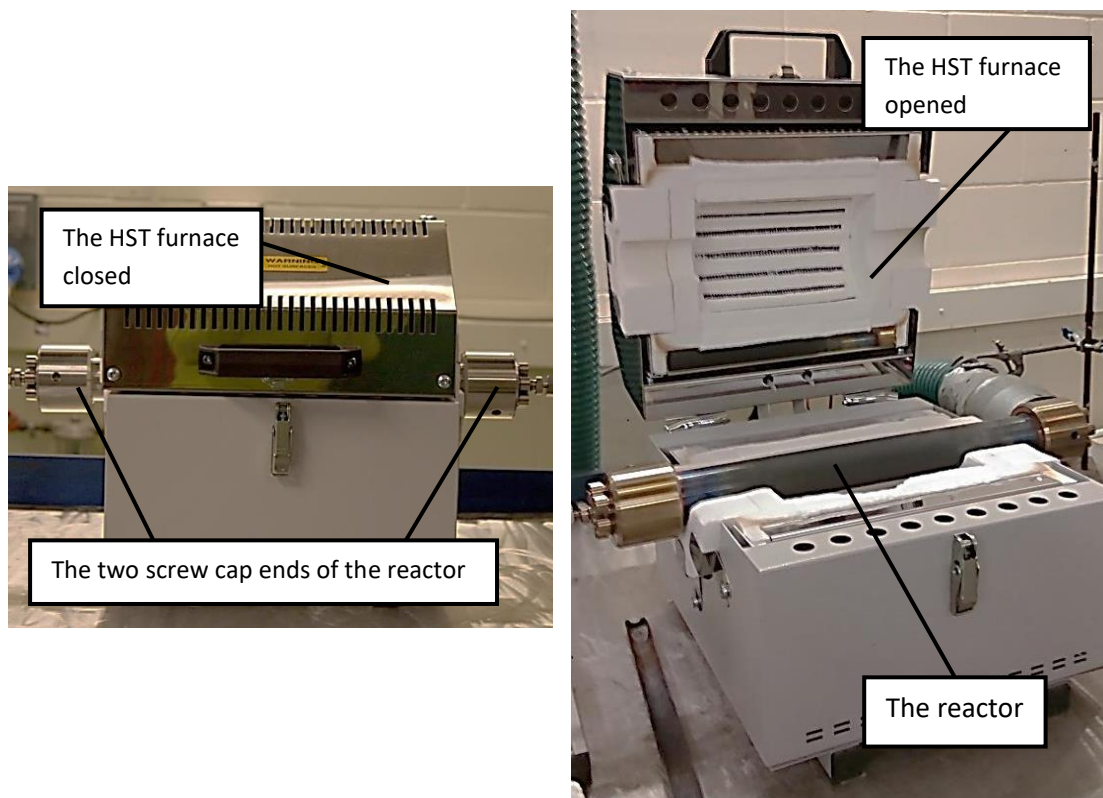


Figure 3.15: The tubular pressure vessel (reactor) sitting in the Horizontal Split Tube furnace

The HST furnace was connected to a 301 standard temperature controller in which the required temperature and the heating rate ($^{\circ}\text{C}/\text{min}$) were manually set which is shown in Figure 3.16.



Figure 3.16: Temperature controller of the Horizontal Split Tube (HST) furnace.

3.4.2 Pressure gauges and pressure relief valves

Pressure levels within the system were monitored with pressure gauges, one before and one after the pressure vessel. The pressure gauges which were calibrated were Span sealed dry series SC gauges rating from 0-72 bar with a 2.5" dial size and stainless steel cases. The pressure gauges which are shown in Figure 3.17 (left) were manufactured by Thuemling Instrument Group and were placed on both the inlet and outlet of the reactor

The pressure within the system was also safety limited by pressure relief valves. The pressure relief valves are R3A series proportional relief valves manufactured by Swagelok. The $\frac{1}{4}$ " pressure relief valves are rated at 50bar which were automatically set to release at 51 bar and they had a 0.14" (3.6 mm) fully open orifice. They were placed on both the inlet and outlet of the reactor (Figure 3.17 (right)).

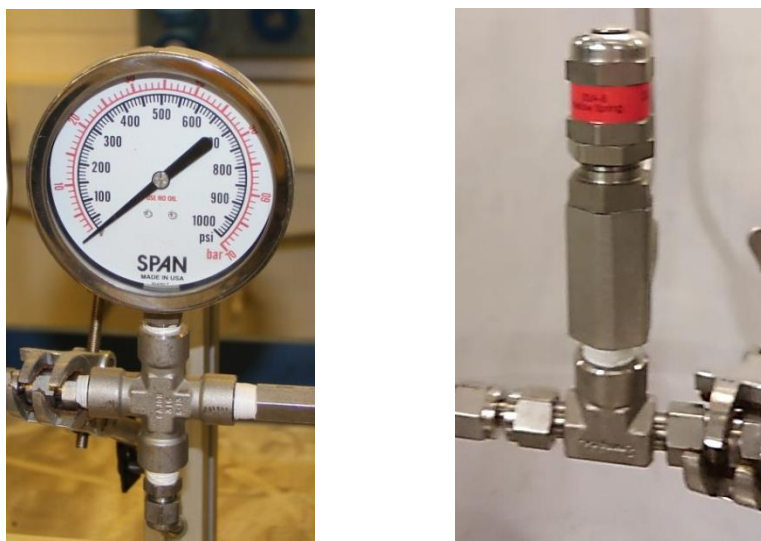


Figure 3.17: A pressure gauge (left) and a pressure relief valve (right)

3.5 Gas analysis system

3.5.1 Gas liquid separator

The gas liquid separator (tar trap) was used to condense all volatile matter and water vapour out of the gas stream coming from the reactor, which enabled the gas stream to be clean and dry before it passes through the gas analyser. The gas liquid separator was a series 4768 general purpose vessel manufactured by Parr Instrument Company. It was a 600 ml vessel with fixed head and split ring closure with cap

screws manufactured in T316SS. The vessel had a rupture disc and a pressure relief valve located on the vessel head and was rated 68.9 bar and 350°C. The vessel also had a water cooled condenser on its head which was connected to a cooler which dropped the temperature in the vessel down to 10°C. The tar trap and the cooler are shown in Figure 3.18. Upstream of the tar trap an in-line filter (100 micron) was placed to remove any particles carried over.



Figure 3.18: The gas liquid separator (tar trap) (on the left) and the cooler (on the right)

3.5.2 Back pressure regulator

The pressure within the system was governed mainly by a manually operated back pressure regulator at the exit of the gas path as shown in Figure 3.19. The back pressure regulator was closed and opened to increase and decrease the pressure upstream respectively. It was a medium-to-high-pressure piston-sensing back pressure regulator manufactured by Swagelok series KPB with a pressure control range from 0 - 68.9 bar and ¼ " female NPT inlet and outlet and gauge ports.



Figure 3.19: Back pressure regulator

3.5.3 Coriolis mass flow meter (MFM)

The exhaust gas flowrate was measured with a Coriolis digital mass flow meter. The Compact Coriolis flow meter was a mini Cori-Flow series Bronkhorst Cori-Tech B.V. and an M13-RAD-88-0-S model with a flow range between 10-500g/h and an accuracy of 0.5%. The Coriolis flow meter was rated for pressures up to 50 bar and temperatures between 15 to 20°C. When the exhaust gas flowed through the uniquely shaped single loop sensor tube in the Coriolis, a drive coil was energised and caused the tube to oscillate. This oscillated movement caused changes in amplitude and frequency which were proportional to the mass flow rate of the fluid passing through and were detected by sensors which were then fed into the integrally mounted pc-board. The resulting output signal was strictly proportional to the real mass flow rate. The Coriolis flow meter is shown in Figure 3.20.



Figure 3.20: Coriolis mass flow meter

3.5.4 Gas analyser

The exhaust gas was finally subjected to on-line quantitative analysis with analytical equipment which was an X-Stream Enhanced XEGP-General Purpose Gas Analyser manufactured by Emerson as shown in Figure 3.21. The X-Stream analyser platform comprised 5 channels in order to detect 5 gases which were CO, CO₂, CH₄, H₂ and O₂. The CO, CO₂ and CH₄ were detected with non-dispersive infrared sensors; H₂ was detected with thermal conductivity (TCD) and O₂ with paramagnetic (pO₂) sensors. It was a continuous monitoring gas analyser, its detection limit was $\leq 1\%$ and the permissible gas flow was 0.2-1.5 l/min. It comprised a web-browser interface with a data logger.



Figure 3.21: The X-Stream Enhanced XEGP-General Purpose Gas Analyser (left) and its calibration gas (right)

CHAPTER IV

MATERIALS and METHODS

4.1 Introduction

This chapter describes the properties of the coal samples that were used, how and why these coal samples were prepared. In addition this chapter describes the measurement methods that were utilised.

4.2 Coal samples

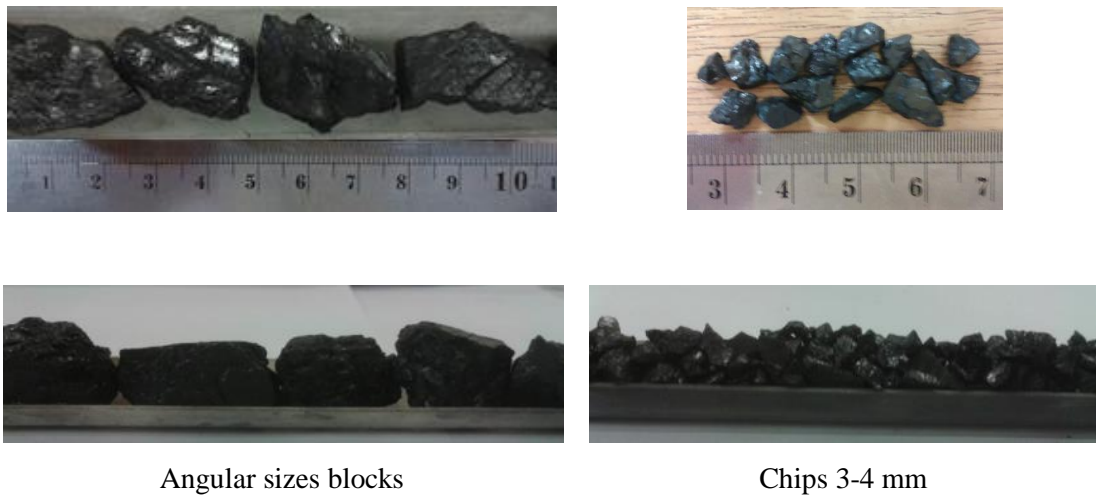
Samples from two Welsh coals, a dry steam coal and an anthracite were used in this study. The dry steam coal was chosen because of its high volatile content, preferred coals for UCG are the lower rank coals with high volatile matter content [11]. The dry steam coal was obtained from the Ffos-y-fran mine at Merthyr Tydfil in South Wales which is part of the South Wales coalfield. Coal blocks around 0.5x0.5x0.5 m were collected from the six feet coal seam located at 500 m depth. The anthracite known as Black Diamond was provided from the East Pit East Revised mine situated in the western part of the South Wales coalfield. Blocks of 0.5x0.5x0.5 m were collected from the upper white coal seam located at 150 m depth. Anthracite was tested in order to examine the coal rank dependency on UCG performance since there is much less information available for medium to high rank coals in UCG. Furthermore the majority of the coal resources in Wales is anthracite so there was a need to assess the anthracite's performance under UCG conditions and determine the available energy potential for future projects. Also much less information is available on UCG of medium to high rank coals.

Both the coal samples from the two mines were transported to the laboratory where they were placed in air-tight plastic bags, labelled and sealed until they were used to prepare the required coal samples.

4.2.1 Preparation of the crushed and powdered coal samples.

In order to prepare crushed coal samples the blocks of coal collected from the mines were first crushed by a jaw crusher manufactured by Denver Equipment Co Ltd with

a serial no BAA 12983/3 which reduced the coal samples to sizes $2^{1/4}$ to $3^{1/4}$. Then the coal samples were crushed with a cone crusher also manufactured by Denver equipment Co Ltd with serial no 09-134923-001-1/MX008 which reduced the sizes down to 6". Then they were sieved with a vibration sieving machine in order to obtain 3-3.5 cm angular sizes blocks and 3-4 mm chips which are shown in Figure 4.1. The 3-3.5 cm angular sizes blocks were shaped with the diamond saw machine in order to fit in the quartz boat. Some of the chips were ground with a Tema ring mill to obtain powder of 200 μm which was also used for coal characterisation tests.



Angular sizes blocks

Chips 3-4 mm

Figure 4.1: Angular sizes blocks and crushed coal 3-4 mm

4.2.2 Preparation of the core coal samples

Cylindrical coal samples were extracted from parent blocks of coal using a coring machine with a diamond core drill at 19mm ID which is shown in Figure 4.2. Due to the required small diameter of the coal samples it was difficult to obtain many samples and there was a lot of waste. Most of the core samples that were obtained had a length of around 40 mm and a roughly uniform size. Special care was taken not to damage the coal samples and for the specimens with the longer length, a diamond saw machine was used to obtain the required length which gave the required weight of the coal samples of around 36g per sample for the dry steam coal and 20 g for the anthracite. Core samples of the dry steam coal are shown in Figure 4.3.



Figure 4.2: Image of the diamond core drill

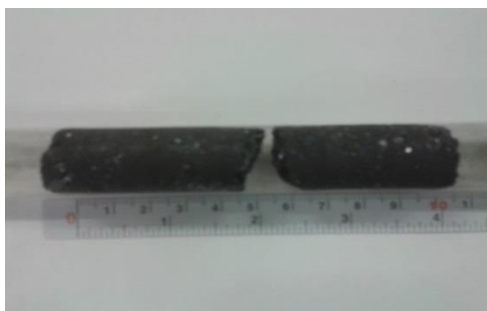


Figure 4.3: Image of the cylindrical coal samples

4.3 Coal characterisation tests

The properties of the coal types were determined by conducting proximate and ultimate analysis and by the calorimeter bomb located at the Cleer Facility of School of Engineering at Cardiff University.

4.3.1 Proximate analysis

Proximate analysis was conducted according to BS 1016-104 which determined the characteristics of the two coals comprising moisture content, volatile matter, ash content and fixed carbon of the coal samples. Mainly powders of the two coals of 500 μm size were placed in the oven to be heated up to certain temperatures according to BS 1016.

In order to determine the moisture content, first the empty crucibles with their lid were weighted before and after coal samples of 1 g were placed in them as shown in Figure 4.5. Then they were placed in an oven at 105 $^{\circ}\text{C}$ to be dried for a minimum of 60 min. After completion of the drying the crucibles were removed from the oven and placed in a dessicator with a lid in order to cool down at room temperature and avoid moisture adsorption. As soon as room temperature was reached the crucibles with the lid were weighed again. The moisture content was calculated by dividing

the difference in mass of sample, before and after drying, by the original sample weight and quote as a percentage of the original weight.



Figure 4.5: Crucibles for determining the moisture and ash content

For the volatile matter determination, first the empty crucibles with their lid were weighed before and after coal samples of 1 g were placed in them, which are shown in Figure 4.6. Then the crucibles were placed in the oven to be heated in the absence of air at 900 °C for 7 minutes. After removing them from the oven they were placed in a cold stand to cool down in order to be weighed. The volatile matter is calculated by dividing the difference in mass of the sample, before and after drying, by the original sample weight and it is expressed as a percentage of the dried sample weight.



Figure 4.6: Crucibles for determining the volatile matter

For the ash content determination the crucibles were weighed before and after a coal sample of 1 g was placed in them as shown in Figure 4.5. Then they were put in the oven at room temperature and the furnace temperature was raised to 500 °C over a period of 60 min and held at this temperature for 30 min. The heating was continued to 815 °C and held at this temperature for 60 min. Then the crucibles were removed from the oven and placed to cool down for 10 min. After 10 min the crucibles were placed in a desiccator to cool down to room temperature. Finally they were weighed again. The ash content was calculated from the weight of the ash remaining divided by the original sample weight.

The fixed carbon is defined as the carbon that is not lost as volatiles but is fixed in the sample and was determined by subtracting from 100 the moisture content, volatile matter and ash content. [54]. The results of the proximate analysis of coals and chars are presented in Table 4.1.

4.3.2 Ultimate analysis

The ultimate analysis is a quantitative analysis of the elements in the coal which are C, H, O, S and N. The ultimate analysis which was conducted according BS 1016-106, determined only the C and S content of the coal samples. The SC-144DR sulphur and carbon analyser which was used was manufactured by Leco Corporation and is shown in Figure 4.7. The coal sample within a boat was placed into the Leco analyser to be combusted under an oxygen environment at high temperature releasing CO₂ and SO₂ gases. Then IR detection cells measure the concentration of these gases and determine the C and S content of the coal sample. The analyser was controlled by an external PC. The results of the ultimate analysis are presented in Table 4.1.



Figure 4.7: Image of the sulfur and carbon analyser

4.3.3 Bomb Calorimeter

The higher heating value (HHV) of the two coals and their coal-chars were determined by using a 6100 oxygen bomb calorimeter according to BS 1016. It was produced by Parr Instrument Co and it is shown in Figure 4.8. The bomb calorimeter consisted of four essential parts which were a) a bomb or metal pressure vessel where the coal is burned, b) a bucket (calorimeter vessel) of measured water with a stirring mechanism where the bomb is placed, c) an insulating jacket to protect the bucket from thermal stresses during the combustion and 4) a thermometer or other

sensor for measuring temperature changes. Within the bomb 1g of coal was combusted in a high pressure oxygen atmosphere and the energy released by this combustion was absorbed by the water surrounding the bomb resulting in its temperature rise. The heat of combustion was then calculated by multiplying the temperature rise by an energy equivalent of approximately 2400 calories for each 1°C rising temperature, which is equal with the HHV of the coal. The LHV of the two coals is derived by subtracting from the HHV the heat of evaporation of water. The calculations are shown in Appendix A.

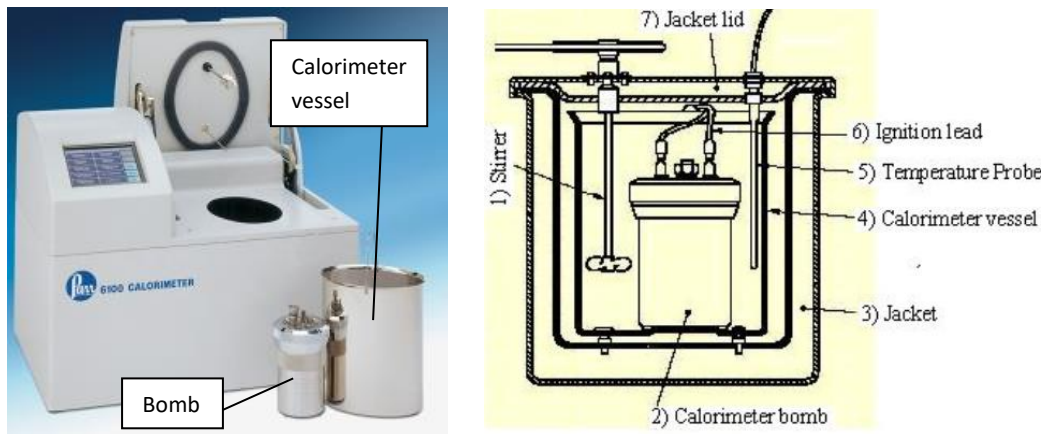


Figure 4.8: Image and schematic of the bomb calorimeter

Table 4.1: Proximate, ultimate analysis and LHV of the coal and char samples

Parameters	Units	Dry steam coal	Dry steam coal char	Anthracite	Anthracite char
Moisture	mass %	0.6	0.1	1.1	0.2
Ash	mass %	3.3	10.1	4.3	8.2
Volatile matter	mass %	13.0	5.4	6.2	2.5
Fixed carbon	mass %	83.2	84.4	88.4	89.1
LHV	MJ/kg	32	31.5	33	32.5
Carbon C	mass %	88.3	99	89.8	99.2
Sulphur S	mass %	0.6	0.9	0.4	0.4

4.4 Description of the experimental process

4.4.1 Char preparation

Char was prepared in the rig in the N₂ environment at atmospheric pressure with a slow heating rate since during the UCG process, the heating rate of the coal seam during pyrolysis is described as slow [6, 9]. The coal samples first were weighed and then were placed on a quartz boat which was introduced into the reactor under the flow of nitrogen (1.5 l/min) and then the right outlet of the reactor was assembled was connected with the gas line as described in Chapter III, section 3.4.1. Then the temperature of the furnace was increased to the required set point temperature at a slow heating rate of 10°C/min and maintained at that temperature for 30 minutes until the volatile matter within the coal was released. During pyrolysis the gases flowed to the exhaust before passing through the tar trap and the gas analyser, which was achieved by switching off the valve in order to minimise contamination in the line. Furthermore the cooler which was connected to the tar trap was turned on around 30 minutes before the start of the gasification in order to allow time to reach its operating temperature of 10° C and cool down the water condenser. The gas analyser was also set to zero and then calibrated every time before each experiment with a zero gas (N₂) and with a span gas respectively. The span gas produced by Air products came with a certificate and it was done gravimetrically in their laboratories. It was a mixture of gases consisting of 15.07% volume of CO, 15.05% volume of CO₂, 5.04% volume of CH₄, 14.96% volume of H₂ and balance of N₂. The O₂ channel in the gas analyser was calibrated with a 100% volume of O₂ cylinder gas. Finally the accuracy of the gas analyser has been cross checked with another span gas produced by BOC which consisted of 0.1% volume of CO, 1% volume of CO₂ and 1% volume by O₂. A few minutes before the start of the gasification experiment the gas analyser was zeroed again and the outlet pipe of the experimental setting was connected to it.

For the pyrolysis experiments the valve which allows the product gas to pass through the gas analyser was opened and the exhaust gas was analysed until the temperature of the furnace was raised from room temperature up to 900 °C where it was maintained for 30 minutes. In order to reduce contamination in the line from the tar, the tar trap was put into a bucket with ice cubes in order to reduce its temperature as low as possible and capture more volatiles and tar as shown in Figure 4.8.



Figure 4.8: The tar trap put into a bucket with ice cubes to drop its temperature

4.4.2 Char gasification at atmospheric pressure

After pyrolysis, the N_2 flow was stopped and the valve, which allows the exhaust gas to pass through the gas analyser, was opened. The required software was set to run and reactant gases comprising CO_2 and steam were introduced into the reactor at a variety of ratios, at atmospheric pressure and temperatures from 600 °C to 900 °C. The chemical species of CO, CH_4 , H_2 and CO_2 that were produced were analysed by the gas analyser. The outlet flowrate of the exhaust gas was monitored with the coriolis flowmeter and its data logger and with a rotameter which was placed at the outlet before the gas analyser. The experiment lasted around 1.5 hours.

For the oxidation experiments the char coal was combusted with O_2 at 900°C and 0.1 MPa. The rest of the procedure was the same with the above.

4.4.3 Char gasification at elevated pressure

For the experiments at pressure, in order to set the required pressure in the rig, the pressure of the regulators of the gases were set to the required pressure, the back pressure regulator was closed down and the inlet flowrate of the gases were set to 10 l/min at the MFC. The on/off valve of the oxidant gas line was turned on to allow the gas to enter into the rig and set the pressure in the rig which took between 1 and 5 minutes depending on the pressure. When the pressure was set, the back pressure regulator was opened slightly in order to allow the exhaust gas to come out and pass

through the coriolis MFM and the gas analyser and at the same time to keep the pressure in the system stable. Then the flowrate of the oxidant gas was set at the value that the MFC was indicating. The flowrate at the outlet, monitored by the rotameter at the outlet and the coriolis MFM which indicated when steam should be injected. The outlet flowrate of the exhaust gas was controlled by the back pressure regulator and monitored by the coriolis MFM and the rotameter at the outlet and was similar for all the experiments at pressure. The experiment lasted around 1.5 hours.

4.4.4 Shut down procedure

After the experiment the on/off valves of the gas lines were turned off to stop the inlet flow of the oxidant gases in the rig, the HPLC pump and the furnace was turned off and all the relevant software was stopped. Then the valve which allows the gases to pass through the gas analyser was turned off and N₂ was introduced into the rig to cool it down more quickly. The cooler was turned off and the outlet pipe of the rig connected to the gas analyser was disconnected and was placed in the exhaust pipe. Then the experimental data was saved.

For the experiments at pressure the back pressure regulator was also turned on slowly to allow the gases to be released more quickly and the pressure at the rear of the rig to be dropped, which was monitored by the pressure gauge at the outlet of the rig.

4.4.5 Post experiment procedure

After three hours the rig has cooled down sufficiently around 100-200 °C for it to be possible to disassemble it by unscrewing the outlet of the rig. Then the quartz boat was pulled half out of the reactor to allow it to cool down. The coal sample was removed to be weighed. The tar trap was also removed and the residue inside the tar trap was weighed.

4.5 Measurements methods

The measurement methods that were used to determine parameters such as carbon conversion (X), carbon conversion of combustible gases (Xa), CGE and LHV of the product gas are described here. This research is primarily concerned with measuring the processes occurring in the reduction zone of the UGC process as described previously. For this reason the following equations were used in order to calculate the carbon conversion (in 90 minutes at steady state) to gas:

$$Ca = C \text{ in } CO + C \text{ in } CH_4 \quad (\text{g}) \quad (\text{Eq. 4.1})$$

$$Xa = \frac{Ca}{Wo} \quad (\text{Eq. 4.2})$$

Equation 4.1 calculates the carbon contained in the combustible (CO and CH₄) product gases Ca and subsequently Equation 4.2 calculates the carbon conversion Xa (in 90 minutes at steady state) provided via these gases from the char, where Wo is the initial mass of carbon contained in the char [83]. (The calculation of Ca is explained more in Appendix D).

The total quantity of char ΔW that has been converted into product gases was also calculated with Equation 4.3 to allow the calculation of the carbon conversion X with Equation 4.4 [84].

$$\Delta W = \text{initial carbon in char} - \text{final carbon in char} = Wo - W \quad (\text{g}) \quad (\text{Eq. 4.3})$$

$$X = \frac{Wo - W}{Wo} \quad (\text{Eq. 4.4})$$

The cold gas efficiency CGE is calculated by Equation 4.5 as the mass of the product gas that is produced per hour (g/h) times the LHV of the product gas (MJ/kg of product gas) over the mass of carbon that is contained in the coal sample (g) times the heating value of the char (MJ/kg of char) [32]. The LHV of the product gas in MJ/Nm³, is the calorific value of the dry gas on a volumetric basis calculated by using Equation 4.6 according to BS EN ISO 6979 methodology and the LHV of the product gas in MJ/kg of product gas is calculated with Equation 4.7.

$$CGE = \frac{(\text{Mass out /h}) \times \text{LHV of product gas}}{\text{Mass in fuel} \times \text{LHV of char}} \times 100 \quad (\%) \quad (\text{Eq. 4.5})$$

$$\text{LHV of product gas} = (\% \text{ Volume of CO} \times \text{LHV of CO}) + (\% \text{ Volume of CH}_4 \times \text{LHV of CH}_4) + (\% \text{ Volume of H}_2 \times \text{LHV of H}_2) \quad (\text{MJ/Nm}^3) \quad (\text{Eq. 4.6})$$

$$\text{LHV of product gas} = (\% \text{ Mass of CO} \times \text{LHV of CO}) + (\% \text{ Mass of CH}_4 \times \text{LHV of CH}_4) + (\% \text{ Mass of H}_2 \times \text{LHV of H}_2) \quad (\text{MJ/kg}) \quad (\text{Eq. 4.7})$$

The LHV of the gases are presented in the Table 4.2 according to BS EN ISO 6979.

Table 4.2: LHV of gases

Gases	LHV (MJ/Nm ³)	LHV (MJ/kg)
CO	12.626	10.9
CH ₄	35.796	50.1
H ₂	10.789	120.1

The reaction constant k (sec⁻¹) of a chemical reaction is exponentially dependent on temperature according to Equation 4.8, where A is the activation energy (sec⁻¹), E is the pre-exponential factor (KJ/mol), R is the ideal gas constant equals to 8.31 J/K mol and T is temperature (K) [82].

$$k = A e^{-(E/RT)} \quad (\text{sec}^{-1}) \quad (\text{Eq. 4.8})$$

Rearranging Equation 4.8 gives

$$\ln k = \ln A - \frac{E}{RT} \quad (\text{Eq. 4.9})$$

By plotting the graph of $\ln k$ versus $\frac{1}{T}$, the slope of the line is equal to $-\frac{E}{R}$ which enable E to be calculated. The intercept of the line gives A .

The reactivity r of Xa was calculated by Equation 4.10 where $\frac{\Delta W}{dt}$ is the reaction rate, which is the change in weight of char with time [67].

$$r = \frac{dXa}{dt} = \frac{1}{W_o} \times \frac{\Delta W}{dt} \quad (\text{g/g} \cdot \text{s}) \quad (\text{Eq. 4.10})$$

4.6 Preliminary experiments to determine the impact of flowrate, sample size and particle size

In order to design the experimental matrix, a series of preliminary experiments were performed to test the presence of any effect of particle size, sample size and flowrate of oxidants to the LHV of the product gas. Initially it was decided to use the lowest possible flowrate of oxidant gas for all the experiments in order to allow more time for the gases to react with the char as well as with themselves. This will enable them to be close to equilibrium because, according to the literature [12], then the LHV of the product gas is reaching its maximum value. The flowrate that was finally used for CO₂ is 0.4l/min due to the limitations of the experimental apparatus.

In order to determine the optimum C/CO₂ ratio, which will determine the required sample size for the experiments for both coals, the stoichiometry for the reaction $C + CO_2 \rightarrow 2CO$ for the flowrate of CO₂ = 0.4 l/min was considered. Experiments were performed for different CO₂/C ratios and constant H₂O flowrate=1.26 ml/min for both coals and finally it was found that the C content, which maximised the LHV of the product gas, was 29.9g (CO₂/C=2.29 m/m) for the dry steam coal and 17.7g (CO₂/C=4.07 m/m) for the anthracite as shown in Figure 4.8 and 4.9 respectively.

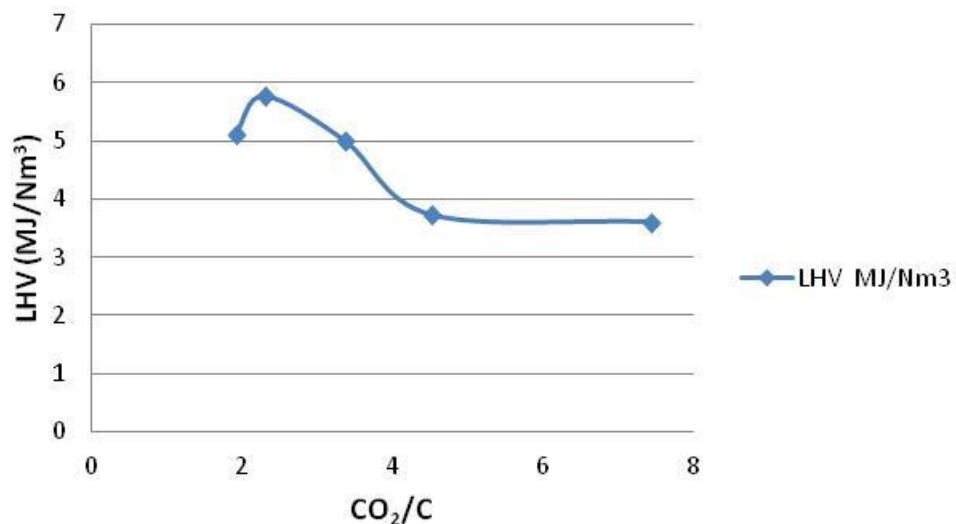


Figure 4.8: Optimum CO₂/C ratio for dry steam coal at fixed CO₂ flowrate=0.4 l/min

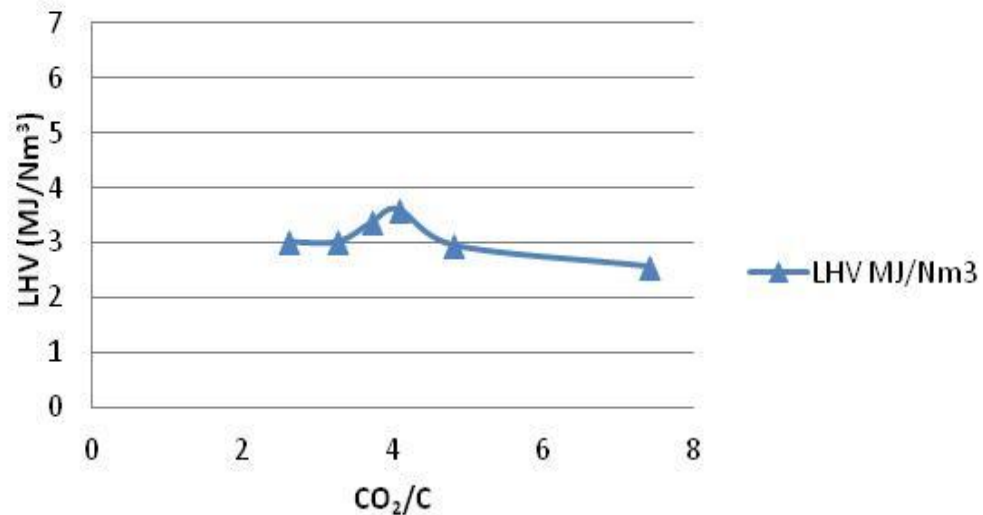


Figure 4.9: Optimum CO₂/C ratio for the anthracite at fixed CO₂ flowrate=0.4 l/min

Furthermore a series of experiments were conducted to determine the effect of particle size with different sizes of coal samples by using the flowrate of gases and the optimum C content that had already been determined as previously described. The results are presented in Table 4.3 where the reactivity is calculated for different sizes of coal samples for both coals. For the dry steam coal the particle sizes that were used were cylinder blocks, angular size blocks and 4-5 mm crushed coal. For the anthracite the particle size of the coal samples that were used were cylinder blocks and 4-5 mm crushed coal.

It is shown in Table 4.3 that there is no significant change between the reactivity of different sizes of char particles as also stated in another study [66] which indicates that the surface area has no impact and that the reactions are chemically controlled [46, 83]. In addition slight variations in the reactivity of different sizes of coal samples is usual because the inherent heterogeneity of the coals and their chars can affect reactivity in different ways due to different chemical and physical properties [73].

It was also observed that the highest reaction rate was achieved with the bigger blocks which were the cylindrical ones and for this reason it was decided to use cylindrical blocks for the experiments. In addition the big cylindrical samples better reflect the UCG process because fragmentation of the coal occurs in a UCG cavity,

which creates big pieces of coal rather than chips and powder that fall into the cavity and form the reduction zone [28].

Table 4.3: Calculated reactivity from experiments with different sizes of coal samples at atmospheric pressure

Experiment	Type of coal	Particle size	Pressure (MPa)	Reactivity (g/g/s)
1	Dry steam coal	cylinder blocks	0.1	4.4E-05
2	Dry steam coal	angular sizes blocks	0.1	2.7E-05
3	Dry steam coal	4-5 mm	0.1	2.4E-05
4	Anthracite	cylinder blocks	0.1	3.6E-05
5	Anthracite	4-5 mm	0.1	2.1E-05

In addition, in order to determine if the particle size has an impact on the reactivity of the coal char at elevated pressure, the optimum operation conditions that were determined at pressure and described in Chapter VI were used to conduct a series of experiments with different particle sizes. The particle sizes that were used were powder and coal blocks and the results are presented in Table 4.4. It is shown in Table 4.4 that again there is no significant change between the reactivity of different sizes of char particles [66] and the slight variations in the reactivity of different sized coal samples can be explained by the different chemical and physical properties of the coal samples [73]. This means that the gas-solid reactions are chemically controlled and lie within regime I conditions and that there is no impact of surface area on the reaction rates at elevated pressure [84].

Finally it can be conclude that there is no contribution of the surface area to the gasification rate at atmospheric and elevated pressure and that the gas-solid reactions take place under the chemical control regime I. These preliminary experiments determined the sample size (C content), particle size for both coals and the flowrate of $\text{CO}_2=0.4$ l/min which will be used for the experiments described in Chapter V and VI at atmospheric and elevated pressure respectively.

Table 4.4: Calculated reactivity from experiments with different sizes of coal samples at elevated pressure

Experiment	Type of coal	Particle size	Pressure (MPa)	Reactivity (g/g/s)
1	Dry steam coal	cylinder blocks	1.65	4.9E-05
2	Dry steam coal	powder	1.6	3.9E-05
3	Anthracite	cylinder blocks	1.0	4.9E-05
4	Anthracite	powder	1.0	3.7E-05

CHAPTER V

EXPERIMENTAL RESULTS AT VARIOUS TEMPERATURES AND COMPOSITIONS OF GASIFYING AGENTS

5.1 Introduction

This chapter presents the results of the experiments conducted for two out of three operating conditions that have the greatest impact on the composition of the product gas, which are temperature and oxidant gas composition [4, 14, 27, 50, 75]. Pressure which is the third most important operating condition will be investigated in the next Chapter. The temperature and oxidant gas composition were tested with two different types of coal by using the methodology described in Chapter IV in order to determine important parameters such as carbon conversion X , CGE and LHV of the product gas, which are parameters that define the gasification performance of the process.

The main objective of this chapter is to better understand how temperature and oxidant gas composition affect the energy conversion of coal char to syngas during the reduction zone of UCG. The reason for that is because most of the gases are produced during the reduction zone [11, 28, 64], which makes it the most important area that needs to be investigated when studying what affects the performance of UCG and potentially how to enhance it. The controlling factor of the gasification in the reduction zone is the reaction of CO_2 with char. CO_2 is mainly produced during the oxidation zone by combustion of char with O_2 [28, 76, 95]. This is an exothermic reaction which raises the temperature for the main gasification reactions to take place in the reduction zone, these are the reaction of char with CO_2 (R3) and with H_2O (R4), which explains why steam is sometimes used as a gasifying agent [94]. Other gases are also produced in the previous zones of UCG (pyrolysis and oxidation) which react with char in the reduction zone except CO_2 and steam, but the latter ones are controlling the rate of chemical reaction. [11, 28, 75]. This justifies why $\text{H}_2\text{O}+\text{CO}_2$ were used as oxidants in this study in order to determine how temperature, gasifying agent composition and pressure affect the performance of the reduction zone in UCG. Then the $\text{O}_2/\text{H}_2\text{O}$ ratio that needs to be injected in order to initiate gasification in the reduction zone can be calculated stoichiometrically according to the experimental results.

Initially experiments were performed at atmospheric pressure in order to determine the impact of temperature and oxidant gas composition on the composition of the product gas in the reduction zone. The optimum values of these operating conditions at atmospheric pressure formed a baseline and were used to perform experiments at elevated pressures. Some of the operating conditions used for all the experiments in Chapter V were determined as described in Chapter IV. These are the flowrate of $\text{CO}_2 = 0.4$ l/min, the sample size of the dry steam coal of 36 g (C content 29.9g) and the anthracite of 20g (C content 17.7g). Furthermore the particle size that was used for both coals were cylindrical blocks.

Section 5.2 presents the results conducted at different temperatures for both coals in order to determine the effect of temperature on the gasification performance of the UCG process. Section 5.3 determines the impact of oxidants gas composition (ratio of $\text{H}_2\text{O}/\text{CO}_2$) on the composition of the product gas at the optimum temperature that was determined in the experiments described in Section 5.2. Section 5.4 compares this study with others and section 5.5 presents the impact of the pyrolysis and oxidation zones on the UCG performance, finally concluding remarks on the experimental results are provided.

5.2 Effect of temperature

The reaction temperature is a significant operating parameter which affects the gasification performance because the endothermic gasification reactions (R3 and R4 presented in Chapter II) are favoured at high temperatures [65, 77, 84]. Studies on underground coal gasification and field trials described in Chapter II highlighted the importance of temperature on the product gas composition and concluded that a reduction in temperature reduces the effectiveness (CGE, LHV and carbon conversion) of the UCG process [10, 13, 50, 76, 93].

The two ranks of coal were tested under different temperatures and the $\text{H}_2\text{O}/\text{CO}_2$ ratio that was used was determined by previous commissioning experiments aiming at maximising the CO and H_2 concentration for each coal as described in Section 5.3.

5.2.1 Experiments with the dry steam coal and anthracite at various temperatures

To study the effect of temperature for the dry steam coal the reactor pressure was fixed to 0.1 MPa (i.e. at atmospheric pressure) and the mass ratio of the H₂O/CO₂ was set to 2:1. Figure 5.1 shows how the concentrations of the produced gases evolved at different temperatures at a)750°C, b)800°C, c)850°C and d)900°C in an atmosphere of CO₂ + H₂O with a CO₂ flowrate of 0.4l/min and H₂O/CO₂ ratio=2:1 (m/m). Similarly the anthracite was tested under the flow of CO₂ + H₂O with a CO₂ flowrate of 0.4l/min, H₂O/CO₂ ratio=2:1 (m/m) at 0.1 MPa and different temperatures at a)760°C, b)800°C, c)850°C and d)900°C. The results are shown in Figure 5.2 where the concentrations of the produced gases over time are plotted.

Figures 5.1 and 5.2 show that during the first 250 seconds of the reaction, the product gas concentrations are changing rapidly due to the steady state condition establishing in the reactor, which was characteristic of all the test conditions examined for both coals. It can be seen when comparing the results at the different temperatures that the concentration of the primary gaseous reactant (the CO₂) is notably lower in the 900°C condition, yielding correspondingly higher concentrations of combustible product gases (notably CO and H₂).

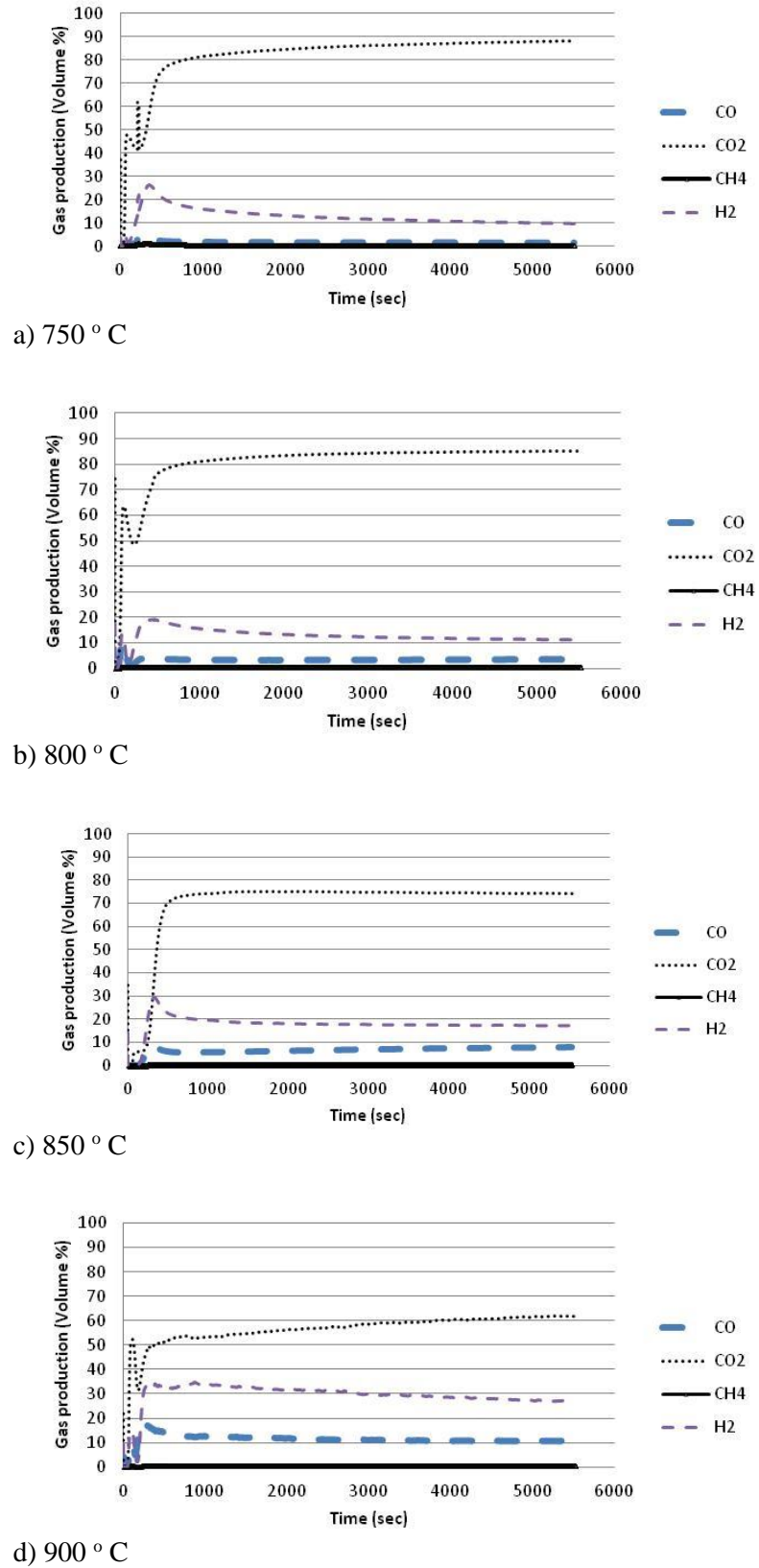
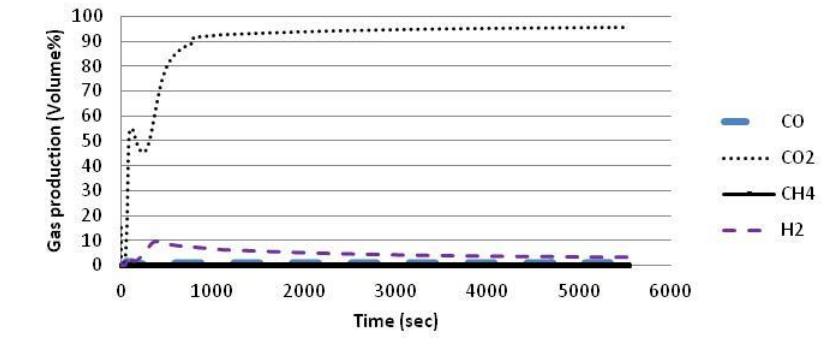
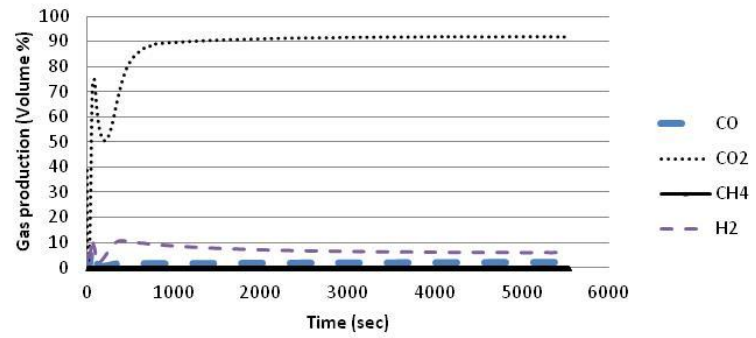


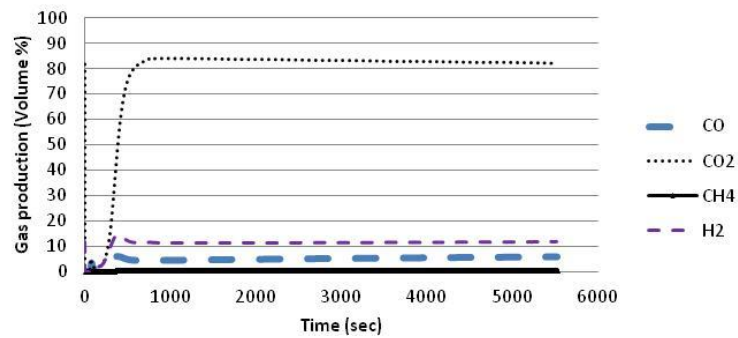
Figure 5.1: Measured rig data showing the variation of concentration of the produced gases (Vol %) over time at a) 750°C, b) 800°C, c) 850°C and d) 900°C under the flow of CO₂+H₂O (H₂O/CO₂=2 (m/m), 0.1 MPa) during gasification of the dry steam coal



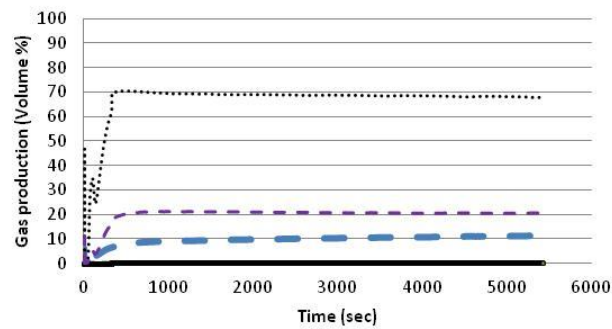
a) 760 ° C



b) 800 ° C



c) 850 ° C



d) 900 ° C

Figure 5.2: Measured rig data showing the variation of concentration of the produced gases (Vol %) over time at a) 760°C, b) 800°C, c) 850°C and d) 900°C under the flow of CO₂+H₂O (H₂O/CO₂=2 (m/m), 0.1 MPa) during gasification of anthracite

5.2.2 Coal samples before and after gasification at atmospheric pressure

Figures 5.3 coal samples before and after gasification with $\text{CO}_2+\text{H}_2\text{O}$ of the dry steam coal and anthracite at atmospheric pressure and 900°C . It is evident in Figure 5.3 that the dry steam coal char samples developed more cracks than those of anthracite which can be explained by dry steam coal having a volatile matter around double than of anthracite which means that there are more free pores available after devolatilisation for the reactant gases to penetrate and reach the internal surface of the porous char. Also after the experimental procedure and shutdown of the experimental rig, it was noticed that the tar was clear and transparent when removing it from the tar trap.

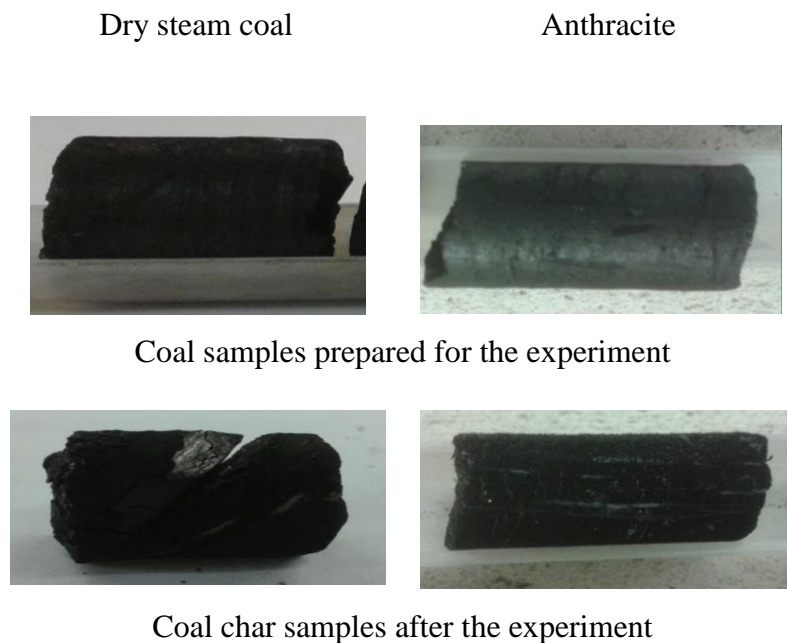


Figure 5.3: Coal samples and coal char samples of the dry steam coal and anthracite before and after gasification at 0.1 MPa under the flow of $\text{CO}_2 + \text{H}_2\text{O}$ (900°C , $\text{H}_2\text{O} / \text{CO}_2=2:1$)

5.2.3 Experimental results / Discussion

5.2.3.1 Effect of temperature on carbon conversion, LHV and CGE

It is subsequently apparent that an increase in temperature favours the carbon reduction reactions, enhancing the concentration of CO and H₂ and increasing the carbon conversion, LHV and CGE of the product gas as shown in Tables 5.1, Table 5.2 for the dry steam coal and Table 5.3 for the anthracite.

Table 5.1 shows that carbon steam gasification is enhanced with the temperature and the highest concentrations of the CO, H₂ and CH₄ when produced for the highest temperature tested which was at 900 °C for both coals.

Table 5.1: Calculated average gas compositions as % vol of dry steam coal and anthracite during the reduction zone for different temperatures at ratio of H₂O/CO₂ = 2 (m/m) and 0.1 MPa.

Type of coal	Gas composition (Vol%)	Temperature (°C)				
		750	760	800	850	900
Dry steam coal	H ₂	13.04	-	13.09	18.81	30.22
	CO	1.80	-	3.44	7.02	11.75
	CH ₄	0.28	-	0.18	0.27	0.54
Anthracite	H ₂	-	4.77	7.20	11.64	20.66
	CO	-	0.86	2.00	5.32	9.81
	CH ₄	-	0.13	0.13	0.24	0.38

As shown in Table 5.2, at 900 °C the LHV of the product gas of the dry steam coal was 4.9 MJ/Nm³ and at 750 °C 1.74 MJ/Nm³. As for anthracite at 900 °C the LHV of the product gas was 3.6 MJ/Nm³ and at 760 °C 0.67 MJ/Nm³ (Table 5.3)

It is also evident how temperature is important for the performance of the UCG by the values of CGE achieved for both coals. The CGE for the dry steam coal at the maximum temperature of 900 °C was 20% which dropped significantly at the value of 5% at 750 °C. Similarly for anthracite the CGE at 900 °C was 18% which also dropped significantly at the value of 2.7% at 760 °C.

The CH₄ concentration remained unchanged implying that the hydro gasification reaction (R5) did not take place to any measurable extent suggesting CH₄ is produced mainly during the pyrolysis step. These results agree with other studies which used different types of gasifiers [23, 28, 50]. In addition, studies on UCG and field trials report that temperatures below 700 °C deteriorated the LHV of the gas composition and reduced the carbon conversion and CGE of the process. [10, 14, 75].

Table 5.2: Calculated gasification parameters of dry steam coal at different temperatures from the rig data (H₂O/CO₂=2 (m/m), 0.1 MPa)

T (°C)		750	800	850	900
Carbon conversion <i>X</i> (in 90 min at steady state)		0.02	0.06	0.10	0.24
LHV	(MJ/Nm ³)	1.7	1.9	3.0	4.9
	(MJ/kg)	1	1.1	2.0	3.9
CGE %		5	6	10	20

Table 5.3: Calculated gasification parameters of anthracite at different temperatures from the rig data (H₂O/CO₂=2 (m/m), 0.1 MPa)

T (°C)		760	800	850	900
Carbon conversion <i>X</i> (in 90 min at steady state)		0.02	0.03	0.11	0.19
LHV	(MJ/Nm ³)	0.67	1.1	2.0	3.6
	(MJ/kg)	0.36	0.6	1.2	2.4
CGE %		2.7	4.5	9	18

The maximum carbon conversion *X* was 0.24 for the dry steam coal and 0.19 for the anthracite at 900 °C. This shows that the dry steam coal is generally more reactive than the anthracite which agrees with other studies where coals ranging from subbituminous to anthracite were tested and it was found that gasification rates diminish for coals of ranks of high volatile bituminous and higher rank [44, 48, 75]. For low rank coals the mineral content determines the gasification rate and not the carbon content [49].

5.2.3.2 Effect of temperature on gasification reaction rate

The effect of reaction temperature on the rates of char conversion to CO and CH₄ during CO₂ / H₂O gasification of the dry steam coal is presented in Figure 5.4 and that of the anthracite in Figure 5.5. It is clear that the gasification rate increases with increased

reaction temperature for both gasification reactions (R3 and R4) and the maximum X_a of 0.13 was achieved for the optimum temperature of 900 °C over the ranges tested for both coals; physical operating constraints from the rig meant that it was not possible to operate above this temperature. These results agree with other studies where the temperature effect on different coal chars under CO_2 and H_2O at atmospheric pressure was investigated and it was found that for the same reaction time (90 minutes at steady state) the carbon conversion increased with increasing temperature [23, 50, 94]. Furthermore in a UCG study the dropped temperature below 700 °C slowed down the reaction speed considerably [76].

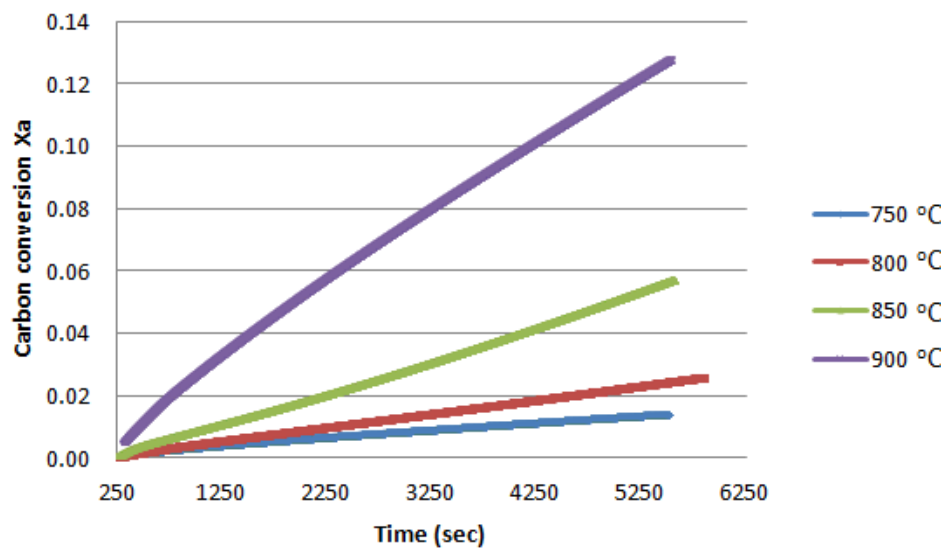


Figure 5.4: Calculated carbon conversion X_a of char to combustible gases ($\text{CO} + \text{CH}_4$) over time during $\text{CO}_2 + \text{H}_2\text{O}$ gasification of the dry steam coal at 750 °C, 800 °C, 850 °C and 900 °C from ($\text{H}_2\text{O}/\text{CO}_2=2$, 0.1 MPa) from raw rig data

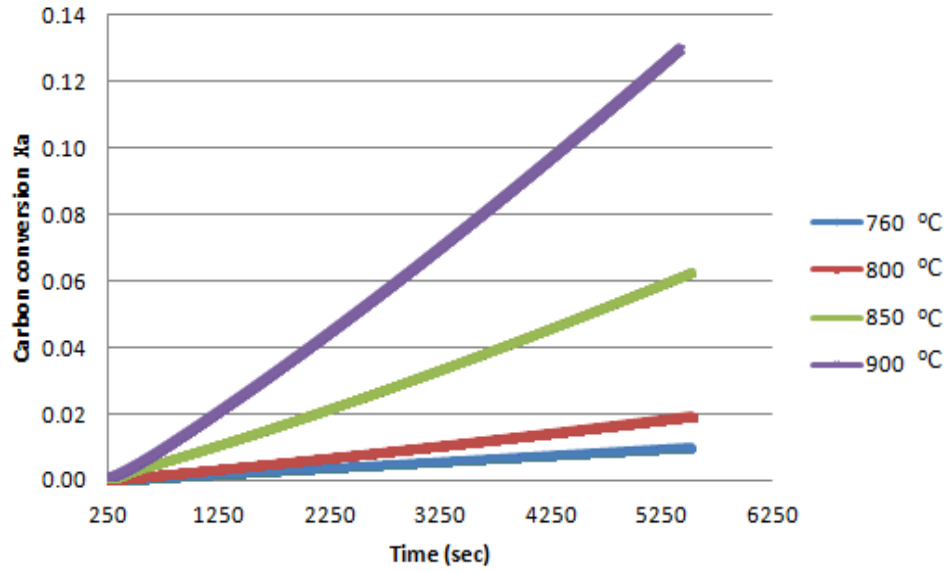


Figure 5.5: Calculated carbon conversion X_a of char to combustible gases ($\text{CO} + \text{CH}_4$) over time during $\text{CO}_2 + \text{H}_2\text{O}$ gasification of anthracite at 760 °C, 800 °C, 850 °C and 900 °C ($\text{H}_2\text{O}/\text{CO}_2=2$, 0.1 MPa) from raw rig data

Figure 5.6 has been produced in order to understand how the chars of the dry steam coal and anthracite react with $\text{CO}_2 + \text{H}_2\text{O}$. It shows the reaction rate of the chars of dry steam coal and anthracite as a function of carbon conversion X_a at 900 °C, which is the temperature where the maximum carbon conversion X_a was achieved under the tested experimental conditions.

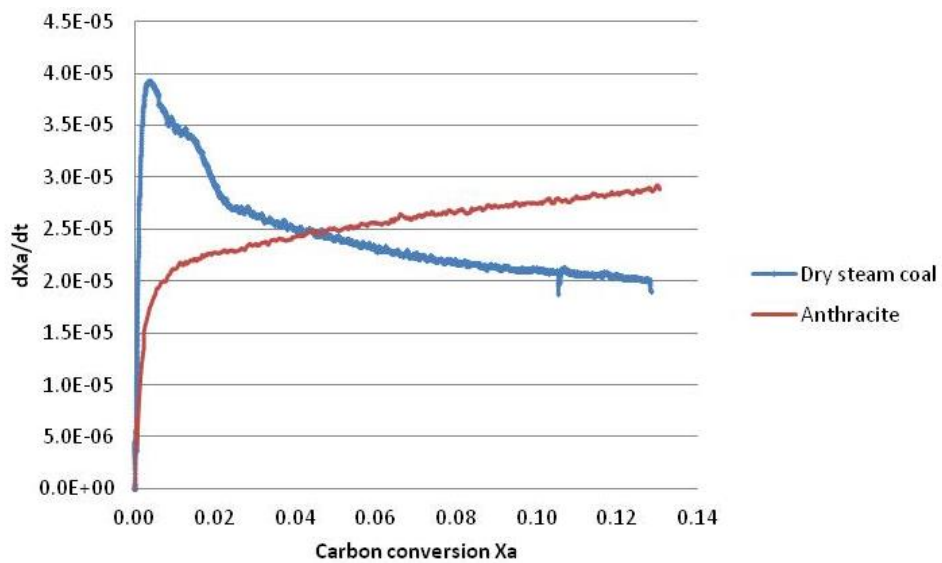


Figure 5.6: Calculated reaction rate of dry steam and anthracite coal char as a function of carbon conversion X_a under the flow of $\text{CO}_2 + \text{H}_2\text{O}$ at 900 °C ($\text{H}_2\text{O}/\text{CO}_2=2$, 0.1 MPa)

The two coal chars demonstrated very different shaped conversion profiles as is evident in Figure 5.6 which are similar with others reported in the literature [66]. The reaction rate of the dry steam coal char increased dramatically with the injection of the gases in the reactor and then it started decreasing during conversion. After approximately 12% conversion X_a the reaction rate seems to decrease very slowly. Anthracite initially demonstrated a slow reaction rate which was increased during conversion and after approximately of conversion $X_a = 4\%$ it was faster than the reaction rate of dry steam coal. It seems that the reaction rate of anthracite continues to increase with a lower rate. Finally it is evident that the dry steam coal char reacts faster than the anthracite char

5.2.3.3 Kinetics calculations

A number of previously published kinetics models were used to describe the gasification on coal particles. In this study the models that are used to interpret the conversion-time data in Figures 5.7 and 5.8 were the progressive conversion model and the shrinking unreacted core model [45] or non-reactive core model [1] which are both based on the first order kinetics and chemical control of the reaction rate due to the low tested temperatures, below 1000 °C. This means that the internal and external diffusion of the gases into the surrounding gas film and inside the char particle is negligible [1, 46]. The progressive conversion model assumes that the reactant gas to some extent enters and reacts with the particle, thus the particle is converted continuously, the particle size remains constant and its density reduces as char conversion proceeds [46]. The shrinking unreacted core model assumes that the reaction occurs first at the outer skin of the particle and then moves into the solid leaving behind converted material and ash. As the reaction progresses the unreacted core keeps shrinking [46].

In Figure 5.7 and Figure 5.8 the conversion X_a of the dry steam coal and anthracite at 900°C are plotted respectively with the shrinking unreacted core model and the progressive conversion model together with the corresponding experimental data. It can be seen that both models fitted the experimental data fairly well because their differences are small but the unreacted shrinking core model is the best fit in the chemical reaction control regime. The progressive conversion model exhibited larger deviations than the shrinking core model for both coals. This conclusion agrees with other studies [43, 46, 96] which evaluates the experimental results and the operation of

the rig. Furthermore the shrinking unreacted core model better describes the behaviour of the coal char of anthracite than that of the dry steam coal because the deviations with the anthracite are smaller.

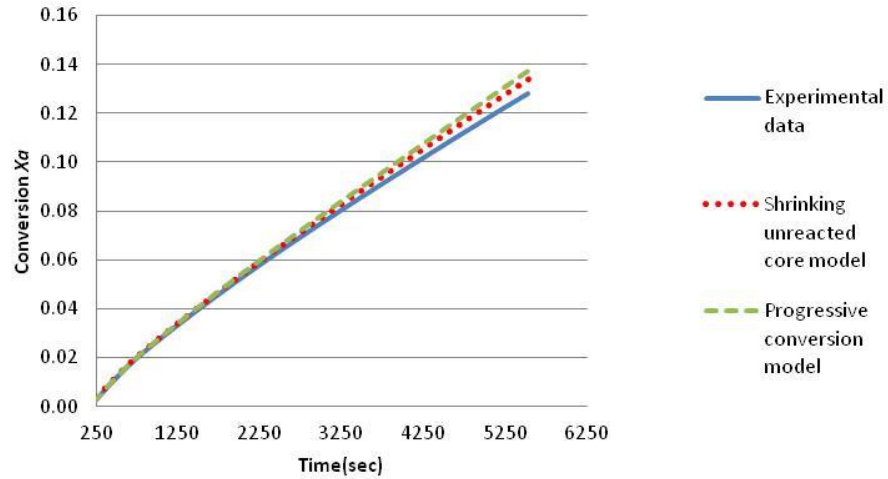


Figure 5.7: Comparison of the conversion X_a at 900 °C of the experimental data with the shrinking core model and the progressive conversion model for the dry steam coal

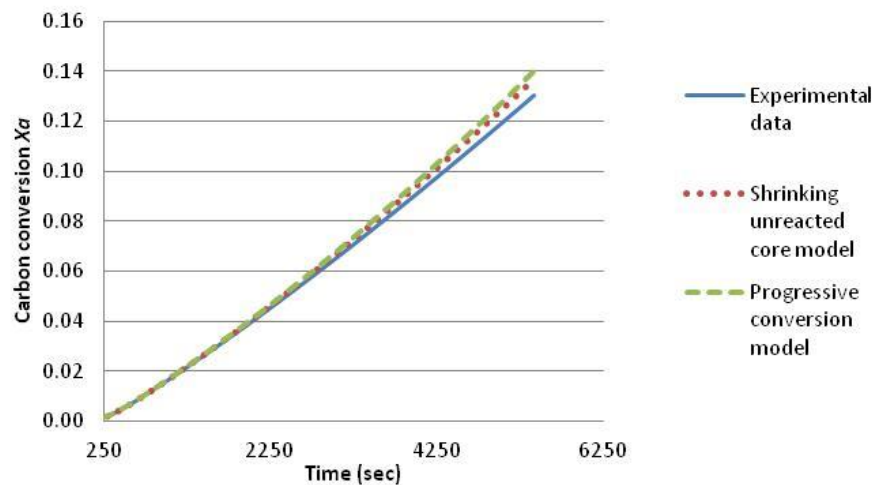


Figure 5.8: Comparison of the conversion X_a at 900 °C of the experimental data with the shrinking core model and progressive conversion model for the anthracite

The reaction rate according to the shrinking unreacted core model is expressed with various equations by different authors [36, 90]. In this study it is shown that the external surface area has no impact on the gasification rate which means that the diffusion of the gases into the surface and through the pores of the particle is happening very quickly because the tested temperatures are below 1000 °C. So the gasification rate is controlled

only by the chemical reactions and for this reason the equation that will be used is shown in Eq. 5.1 which was also considered in other studies [1, 26, 46]:

$$\frac{dXa}{dt} = k (1 - Xa)^{2/3} \quad (\text{Eq. 5.1})$$

Where k is the reaction rate constant and Xa is the carbon conversion of CO and CH₄. The integration of Equation 5.2 results in a linear relationship between $(3(1-(1-Xa)^{1/3}))$ versus the reaction time as follows:

$$3(1-(1-Xa)^{1/3})=k t \quad (\text{Eq. 5.2})$$

In Figure 5.9 it is shown that the plots of $(3(1-(1-Xa)^{1/3}))$ versus time fit the experimental data fairly well and that the shrinking unreacted-core model better describes the gas solid reactions of the dry steam coal particles with CO₂ + H₂O at 0.1 MPa for the temperature range of 750 to 900 °C. Figure 5.10 also shows that the shrinking unreacted core model better describes the reaction of anthracite with CO₂ + H₂O at 0.1 MPa for the temperature range of 760 to 900 °C.

The reaction constant k can be derived from the slope of the straight lines of Equation 5.2 as calculated by Ahn et al., (2001) and Goyal et al., (1989) and shown in Figures 5.9 and 5.10 for the dry steam coal and anthracite respectively [1, 26, 46] . These values are presented in Table 5.4 for the dry steam coal and Table 5.5 for anthracite and it can be observed that it is very similar for the two coals.

Table 5.4: Reaction constants k for CO₂ + H₂O gasification of the bituminous coal-char at 900 °C, 850 °C, 800 °C and 750 °C (H₂O/CO₂=2, 0.1 MPa).

Temperature °C	$k \text{ sec}^{-1}$
900	2.4E-05
850	1.0E-05
800	5.0E-06
750	2.0E-06

Table 5.5: Reaction constants k for CO₂ + H₂O gasification of the anthracite at 900 °C, 850 °C, 800 °C and 760 °C (H₂O/CO₂=2, 0.1 MPa).

Temperature °C	$k \text{ sec}^{-1}$
900	2.3E-05
850	1.0E-05
800	4.0E-06
760	2.0E-06

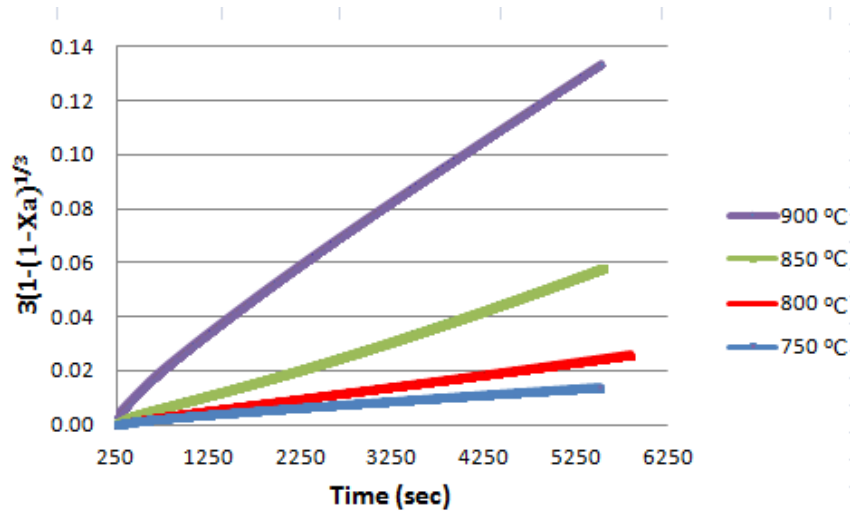


Figure 5.9: Calculated conversion data $3(1-(1-X_a))^{1/3}$ versus reaction time of dry steam coal for $\text{CO}_2 + \text{H}_2\text{O}$ gasification at a total system pressure of 0.1 MPa

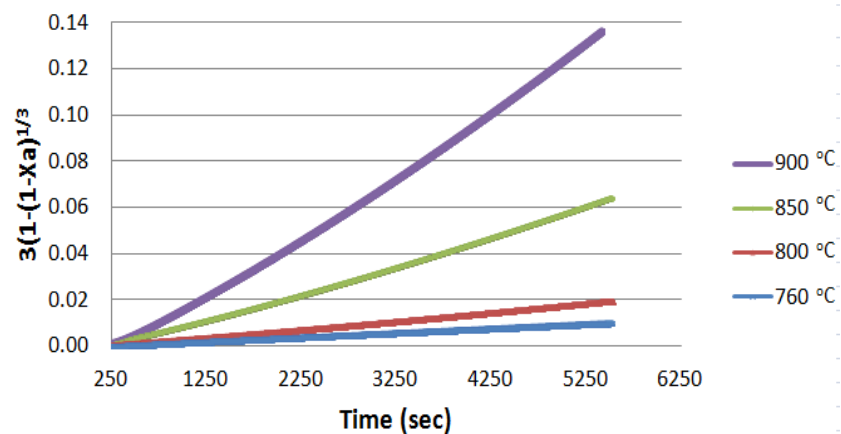


Figure 5.10: Calculated conversion data $3(1-(1-X_a))^{1/3}$ versus reaction time of anthracite for $\text{CO}_2 + \text{H}_2\text{O}$ gasification at a total system pressure of 0.1 MPa

The Arrhenius plot for deriving the kinetic parameters of the reaction constant is illustrated in Figure 5.11 for the dry steam coal and Figure 5.12 for anthracite. The straight lines fit of the reaction constant k at 0.1 MPa pressure and temperature range of 750 to 900°C for both coals indicate that the reactions follow the Arrhenius law and that the variation of the reaction constant k with temperature can be described with the Arrhenius type for both coals as follows in Equation 4.7 described in Chapter IV:

$$k = A e^{-E/RT} \quad (\text{Eq. 4.7})$$

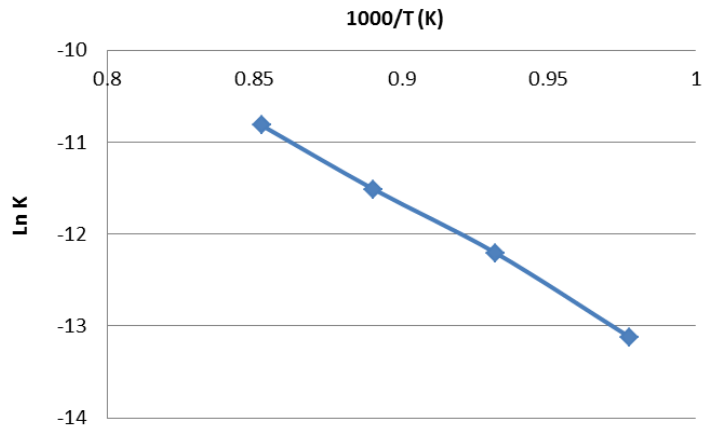


Figure 5.11: Arrhenius plot of the reaction constant k for $\text{CO}_2 + \text{H}_2\text{O}$ gasification of the dry steam coal-char at 900 °C, 850 °C, 800 °C and 750 °C ($\text{H}_2\text{O}/\text{CO}_2=2$, 0.1 MPa)

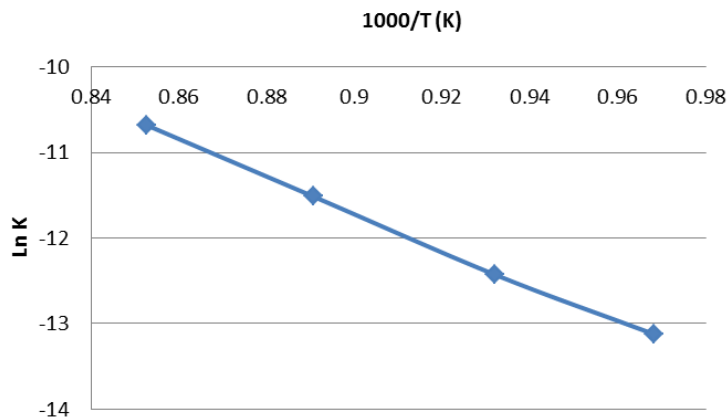


Figure 5.12: Arrhenius plot of the reaction constant k for $\text{CO}_2 + \text{H}_2\text{O}$ gasification of the anthracite coal-char at 900 °C, 850 °C, 800 °C and 760 °C ($\text{H}_2\text{O}/\text{CO}_2=2$, 0.1 MPa)

The kinetic parameters, the activation energy and the pre-exponential factor A calculated for both coals are presented in Table 5.6. The gas-solid reactions of both coals follow the Arrhenius law which means that they are chemically controlled for the temperatures tested for both coals. These values are slightly higher than results published using TGA analysis for substantially smaller samples (100 mg) where char conversion was undertaken with single oxidising gases (such as CO_2 and H_2O) in individual reactions [67]. Furthermore the activation energy calculated in this study is slightly higher than the one calculated for a study where char conversion was undertaken in a fixed bed reactor with char sizes of 0.7 mm by also using single oxidizing gases (such as CO_2 and H_2O) in individual reactions [30]. In addition

chemically control gasification rates reveal true activation energies between 50 to 100 kcal according to literature [83], the ones determined in this study are 83.50 kcal/mole for the dry steam coal and 97.14 kcal/mol for anthracite which again proves that the gas solid reactions are chemically controlled.

Table 5.6: Activation energies and pre-exponential factors for the two coal chars in CO+H₂O at 0.1 MPa and ratio of H₂O/CO₂=2 (m/m).

Coal type	Activation energy E (KJ/mol)	Pre-exponential factor A (1/sec)
Dry steam coal	349.63	5.83x10 ⁴ /sec
Anthracite	406.74	2.63x10 ⁷ /sec

5.2.3.4 Summary

Temperature favours the gasification reactions during the reduction zone and is the most important factor for the gasification performance of UCG. The optimum temperature was determined to be 900 °C for the range of tested temperatures because it maximised the carbon conversion, CGE and LHV of the product gas produced for both coals.

The carbon conversion X (C in CO, CH₄ and CO₂) was 0.24 for the dry steam coal and 0.19 for the anthracite when both coals were tested under their optimum gasification conditions, which shows that the dry steam coal is more reactive than the anthracite. It is worth noting that the maximum carbon conversion X_a (C in CO and CH₄) was 0.13 for both coals with a LHV of 4.9 for the dry steam coal and 3.6MJ/Nm³ for anthracite respectively. This indicates that anthracite may be as suitable for a UCG project as dry steam coal since it produced a similar amount of combustible gases CO and CH₄ under the tested conditions. There are studies which mention that low rank and high volatile coals are preferably for UCG but this study shows that high rank coals can also be considered for a UCG project, if not for energy production certainly for fuel and chemicals production.

The shrinking unreacted core model predicts the gasification conversion of the two coals tested under the flow of CO₂+H₂O at 0.1 MPa and temperatures ranged from 750 to 900° C. The deviations of the shrinking unreacted core model with the experimental data of the anthracite are less than those of the dry steam coal. It is also evident that the gasification rate depends strongly on the temperature indicating chemical reaction rate control within the temperature range tested. From the Arrhenius plot the apparent

activation energy E and the pre-exponential factor A were found to be 349.63 KJ/mol and 5.83×10^4 /sec for the dry steam coal and 406.74 KJ/mol and 2.63×10^7 /sec for the anthracite respectively. These findings could be useful for modelling gasification processes.

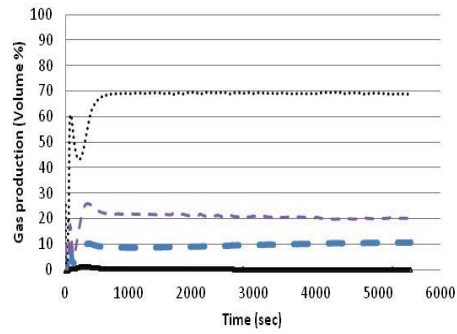
5.3 Effect of gasifying agent composition

The effect of the gasifying agent composition in this work was studied by varying the H_2O/CO_2 concentration in the reactant gas because there was a need to understand better the importance of the reduction zone in UCG where most of the gases are produced. At the start of the UCG process, after the primary combustion is initiated, oxygen is injected into the coal seam in order to initiate gasification by raising the temperature in the cavity through reactions R1 and R2. Oxygen is consumed fairly quickly and the CO_2 , which is the main product gas, reacts with char reaction according to reaction R3. When stable gasification is achieved, H_2O is injected into the cavity to use the extra available heat and enhance the gasification performance with reaction R4. Knowledge of CO_2 supply rates and H_2O/CO_2 ratio determines the composition of the product gas [76, 49] and in addition, the O_2 supply and H_2O/O_2 ratio can also be calculated stoichiometrically. Excess gas dilutes the feed mixture and excess steam decreases the temperature which decreases the performance [14]. This parameter was studied by varying the mass of char in the reactor to determine the optimum CO_2/C ratio in terms of CGE and LHV as described in Section 4.6 and then by varying the H_2O concentration to determine the optimum H_2O/CO_2 ratio as described in this chapter. The results were expressed as a function of H_2O/CO_2 ratio and the temperature that was used for these experiments for both coals was 900 °C which was the optimum temperature as determined in Section 5.2.

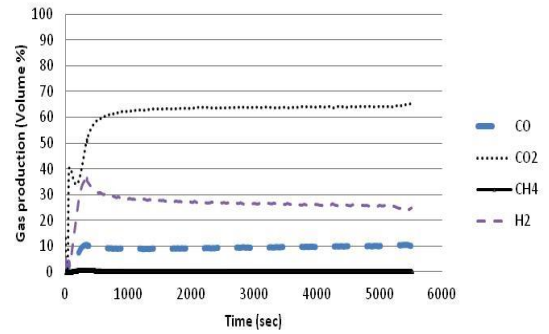
5.3.1 Experiments with dry steam coal and anthracite at various compositions of gasifying agents

Experiments were conducted with the dry steam coal at 900°C and 0.1 MPa under the flow of $CO_2 + H_2O$ at different ratios of H_2O / CO_2 of a)1:1 , b) 1.5:1, c) 2:1, d)2.5:1, e) 3:1 and f) 3.5:1. Similar experiments were also performed for the anthracite at 900°C and 0.1 MPa by using a ratio of H_2O / CO_2 of a)1:1 , b) 1.5:1, c) 2:1, d)2.5:1 and e) 3:1.

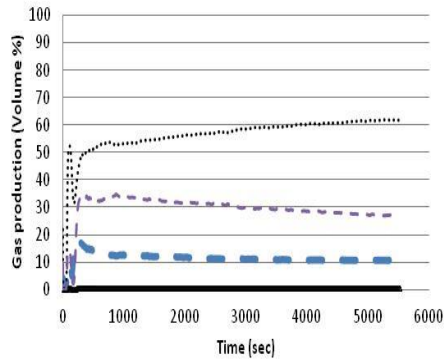
Figures 5.13 and 5.14 show the composition of the product gases during the gasification of the dry steam coal char and anthracite char respectively. During the first 250 seconds of the reaction, the product gas concentrations are changing comparatively quickly due to the steady state condition establishing in the reactor, which was characteristic of all the test conditions examined for both coals. It can be seen that when comparing the results at the different H₂O/CO₂ ratios of the dry steam coal, that the concentration of the primary gaseous reactant (the CO₂) is lower in the H₂O/CO₂ ratios between 1.5:1 to 3:1, yielding correspondingly higher concentrations of combustible product gases (notably CO and H₂). For the anthracite the lower CO₂ concentration was achieved for the H₂O/CO₂ ratios of 1.5:1, 2:1 and 2.5:1 with the highest concentration of combustible gases (CO, H₂ and CH₄) for the H₂O/CO₂ ratio of 2:1. Also it is clear that the reaction of H₂O with coal char is faster than the reaction of CO₂ with coal char because the concentration of H₂ increases rapidly compared to the concentration of CO [11].



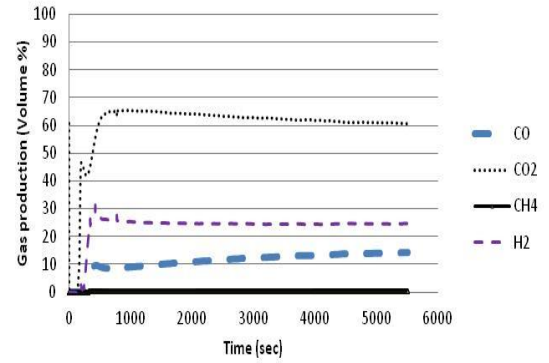
a) Ratio $H_2O/CO_2=1:1$



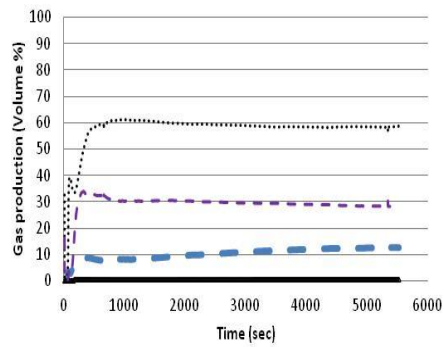
b) Ratio $H_2O/CO_2=1.5:1$



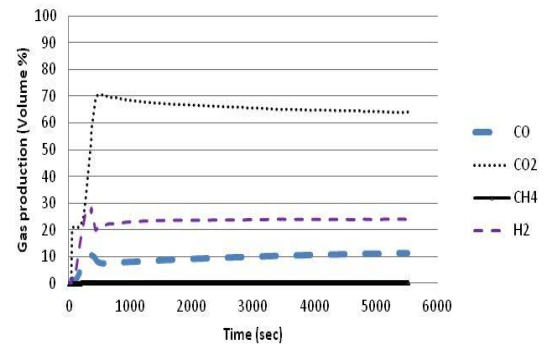
c) Ratio $H_2O/CO_2=2:1$



d) Ratio $H_2O/CO_2=2.5:1$

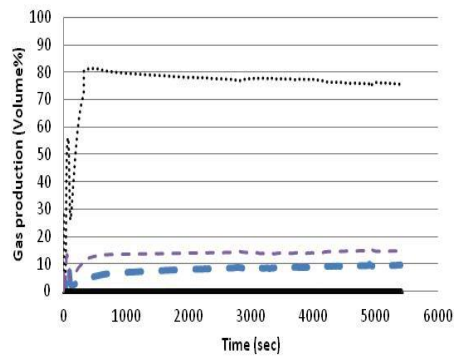


e) Ratio $H_2O/CO_2=3:1$

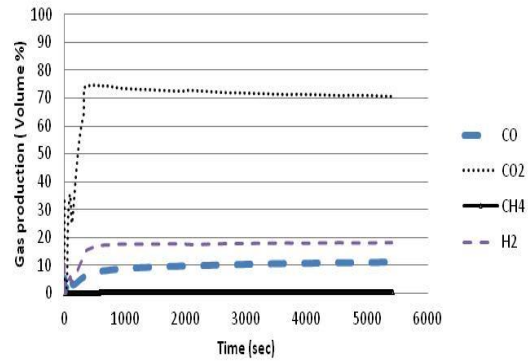


f) Ratio $H_2O/CO_2=3.5:1$

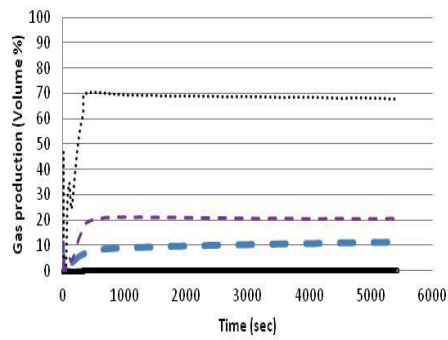
Figure 5.13: Measured rig data showing the variation of concentration of the produced gases (Vol %) during gasification of the dry steam coal char over time for ratio of H_2O / CO_2 of a) 1:1 , b) 1.5:1, c) 2:1, d) 2.5:1, e) 3:1 and f) 3.5:1 under the flow of $CO_2 + H_2O$ (900°C, 0.1 MPa)



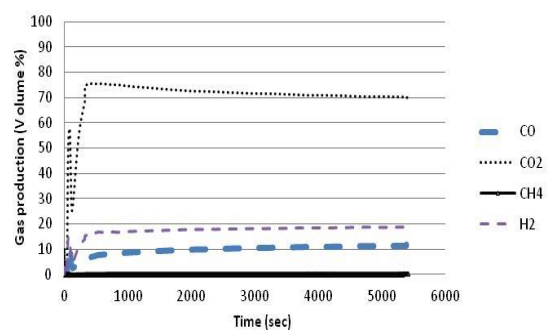
a) Ratio $H_2O/CO_2=1:1$



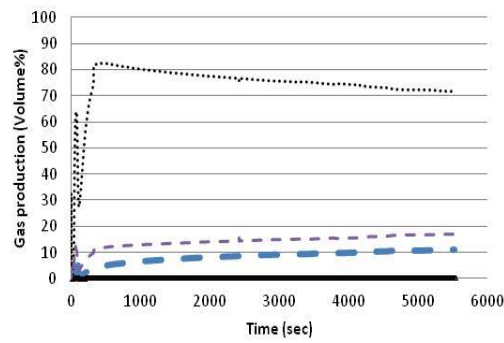
b) Ratio $H_2O/CO_2=1.5:1$



c) Ratio $H_2O/CO_2=2:1$



d) Ratio $H_2O/CO_2=2.5:1$



e) Ratio $H_2O/CO_2=3:1$

Figure 5.14: Measured rig data showing the variation of concentration of the produced gases (Vol %) during gasification of anthracite char over time for ratio of H_2O / CO_2 of a)1:1 , b) 1.5:1, c) 2:1, d)2.5:1 and e) 3:1 under the flow of $CO_2 + H_2O$ ($900^\circ C$, 0.1 MPa)

5.3.1.1 Experimental results / Discussion

5.3.1.2 Effect of gasifying agent composition on gasification reaction rate

In Table 5.7 the gas compositions achieved for the different H₂O/CO₂ ratios for each coal are presented. The carbon steam gasification is enhanced when the H₂O/CO₂ ratio is increasing leading to an increase in the H₂ production for both coals, with their highest concentration achieved at 30.22% and 20.66% for the ratio of H₂O/CO₂=2:1 for the dry steam coal and anthracite respectively. The CO production increases slightly up to the H₂O/CO₂ ratio =2:1 with the value of 11.75% for the dry steam coal and 9.81 for anthracite. At higher H₂O/CO₂ ratios the H₂ and CO production are decreasing. The CH₄ concentration is very small for both coals below 1%, since CH₄ formation is not favoured under this conditions.

Table 5.7: Calculated average gas compositions as % vol of dry steam coal and anthracite during the reduction zone for different ratios of H₂O/CO₂ at 900 °C and 0.1 MPa.

Type of coal	Gas composition (Vol%)	H ₂ O / CO ₂ ratio (m/m)					
		1:1	1.5:1	2:1	2.5:1	3:1	3.5:1
Dry steam coal	H ₂	20.96	27.12	30.22	28.11	29.93	23.82
	CO	9.76	9.53	11.75	11.31	10.44	9.83
	CH ₄	0.59	0.52	0.54	0.52	0.58	0.52
Anthracite	H ₂	13.79	16.94	20.66	17.68	14.75	-
	CO	8.13	9.75	9.81	9.6	8.46	-
	CH ₄	0.24	0.34	0.38	0.34	0.28	-

In Figure 5.15 and Figure 5.16 the carbon conversion (in 90 minutes at steady state) of combustible gases (X_a) is plotted against time for various ratios of H₂O/CO₂ for both coals. In both Figures it is clear that an increase in the H₂O/CO₂ ratio increases the gasification rate for both coals which suggest that the Boudouard reaction (R3) and steam carbon reaction (R4) are favoured. In Figure 5.15 it can be shown that during the gasification of the dry steam coal char the higher gasification rate was achieved with a ratio of H₂O/CO₂=2:1 (m/m) with the highest value of $X_a = 0.13$ as was also shown in Section 5.2.3. As for the anthracite, shown in Figure 5.16, the highest gasification rate

was achieved for the ratios of $H_2O/CO_2=1.5:1$ and $2:1$ suggesting optimum conditions around these points with the highest value of Xa at 0.13 as the dry steam coal, as shown previously in Section 5.2.3. The optimum ratio of H_2O/CO_2 depends on the temperature and the type of the coal and consequently Gregg et al., (1978) [28] believes that it is not possible to make an assumption about the optimum H_2O/O_2 ratio for all the systems and that this optimum ratio should be determined individually for each system and its set of operating parameters. In addition Daggupati et al., (2011) [13] mentions that an optimum H_2O/O_2 ratio exists and this depends on the type of the coal.

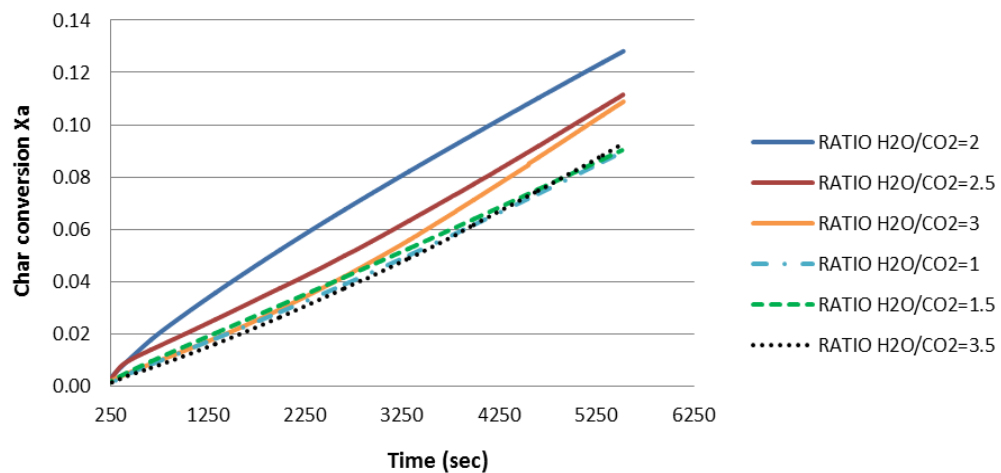


Figure 5.15: Calculated carbon conversion Xa of combustible gases ($CO + CH_4$) over time for various ratios of H_2O/CO_2 ($900^\circ C$, 0.1 MPa) during gasification of the dry steam coal

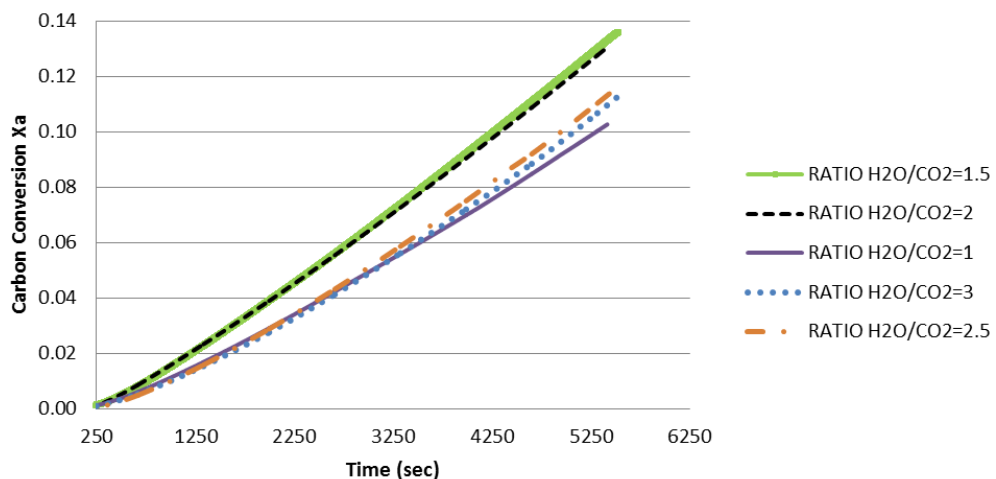
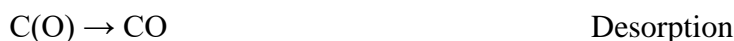


Figure 5.16: Calculated carbon conversion Xa of combustible gases ($CO + CH_4$) over time for various ratios of H_2O/CO_2 ($900^\circ C$, 0.1 MPa) during gasification of anthracite

Above the H₂O/CO₂ ratio of 2:1 for both coals, the higher concentration of steam seems to decrease the gasification rate of the carbon steam reaction which can be explained by the adsorption-desorption mechanism proposed by different authors [2, 44, 51] which is the following (the ΔH of the reactions could not be found):



In this mechanism the retarding effect of the increased production of H₂ is taken into account which inhibits the char-steam reaction by shifting the adsorption reaction to the left according to some studies [67, 83]. Furthermore the decrease in the gasification rate can also be explained by the two-step adsorption-desorption reaction mechanism, widely accepted for the char-CO₂ reaction at atmospheric pressure [3, 86] shown below whereby the increased production of CO slows down the gasification rate of the char-CO₂ reaction by a dynamic exchange in the adsorption reaction to the left [67, 83]. The ΔH of the following reactions could not be found:



According to Ergun et al., (1956), the desorption of the C(O) to CO in both reactions is the rate controlling step which decrease the gasification rate. In addition the reaction of carbon with steam is retarded by H₂ and the reaction of carbon with CO₂ is retarded by both H₂ and CO [52].

5.3.1.3 Effect of gasifying agent composition on carbon conversion, LHV and CGE

Table 5.7 shows the carbon conversion X , LHV and CGE for the dry steam coal and anthracite at 900°C, 0.1 MPa, under the flow of CO₂ and steam at different H₂O/CO₂ ratios. The data indicates that H₂O/CO₂ ratio has a significant impact on the carbon conversion X of the dry steam coal with the maximum values achieved for the range of H₂O/CO₂ ratio between 2:1 to 3:1, which are almost double than those achieved for the H₂O/CO₂ ratios of 1:1 and 3.5:1. The maximum carbon conversion for the dry steam coal was $X = 0.24$ (of which combustibles gases, CO and CH₄, are $X_a = 0.13$) for the H₂O/CO₂ ratio of 2:1 as mentioned in Section 5.2.3. The carbon conversion of anthracite was slightly affected by the various H₂O/CO₂ ratios compared to the dry steam coal

since, as being a high rank coal, is less reactive than the dry steam coal. The maximum carbon conversion for the anthracite was $X = 0.19$ (of which combustibles gases, CO and CH₄, are $X_a = 0.13$) for the H₂O/CO₂ ratio of 2:1 as was also mentioned in Section 5.2.3. It is evident that dry steam coal is more reactive than anthracite in terms of carbon conversion X since the carbon conversion X of dry steam coal is 0.24 and that of anthracite 0.19, but in terms of carbon conversion X_a both coal are similar since both have the same $X_a = 0.13$. This indicates once more that anthracite is theoretically reactive enough to be considered for a UCG project.

Furthermore the data in Table 5.8 indicates that the H₂O/CO₂ ratio has an impact on the CGE of the dry steam coal and anthracite, with the maximum value achieved at 20% for the range of H₂O/CO₂ ratios between 2:1 for the dry steam coal and at 18% for the H₂O/CO₂ ratios of 2:1 to 2.5:1 for anthracite. These results imply that around 20% and 18% of the available chemical energy of the char is converted to gas during this simulated reduction zone of a UCG cavity for the dry steam coal and anthracite respectively. It is worth noting that for the H₂O/CO₂ ratios between 2:1 to 3:1 for dry steam coal and 1.5:1 to 2.5:1 for anthracite the CGE achieved is very similar and these ranges of ratios can be considered as producing a good gas composition of the product gas.

Table 5.8: Calculated gasification parameters of the chars of dry steam coal and anthracite for different H₂O/CO₂ ratios (900 °C, 0.1 MPa)

Coal	H ₂ O / CO ₂ ratio (m/m)	1:1	1.5:1	2:1	2.5:1	3:1	3.5:1
Dry steam coal	Carbon conversion X (in 90 min at steady state)	0.12	0.16	0.24	0.23	0.21	0.12
	LHV (MJ/Nm ³)	3.7	4.3	4.9	4.6	4.7	3.9
	LHV (MJ/Kg)	2.5	3.2	3.9	3.3	3.6	2.8
	CGE (%)	13	16	20	17	18	14
Anthracite	Carbon conversion X (in 90 min at steady state)	0.14	0.19	0.19	0.2	0.15	-
	LHV (MJ/Nm ³)	2.6	3.2	3.6	3.2	2.8	-
	LHV (MJ/Kg)	1.6	2.1	2.4	2.1	1.7	-
	CGE (%)	12	16	18	16	13	-

Figure 5.17 shows the production of the combustible product gases during the gasification of the dry steam coal with H₂O/CO₂ at different ratios. There is an increase in the H₂ concentration with an increase in the H₂O/CO₂ ratio, this decreases when the ratio of H₂O/CO₂ is above 3:1. The higher concentration of CO occurs between the H₂O/CO₂ ratios of 2 to 3 and the CH₄ concentration remains unchanged with a very small increase at high values of H₂O/CO₂ up to 3. This suggests that as the H₂O/CO₂ ratio increases, the homogeneous gasification reactions (R6 and R7) appear favoured to the detriment of Boudouard and steam-carbon reactions (R3 and R4) which can be explained by the adsorption –desorption mechanism explained earlier and the inhibiting effect of H₂ and CO to the gasification rate. Furthermore the following reduction reaction might occur due to the high concentration of steam $2\text{H}_2\text{O} + \text{C} \rightarrow \text{CO}_2 + 2\text{H}_2$ which can cause to CO concentration to decrease and the LHV of the product gas [95]. This phenomenon saturates above a H₂O/CO₂ ratio of 3:1. [23, 95].

Figure 5.18 shows the effect of the H₂O/CO₂ ratio on the LHV (MJ/Nm³) of the product gas during gasification of the dry steam coal char at 900 °C and 0.1 MPa (atmospheric pressure). It can be noted that the range of the H₂O/CO₂ ratios between 2:1–3:1 provided optimum conditions for the dry steam coal char with LHV of 4.9 MJ/Nm³ (H₂O/CO₂ ratio of 2:1) as shown in Table 5.7.

The contribution of H₂ to the maximum resultant LHV of the product gas was 3.3 MJ/Nm³ and that of CO and CH₄ was 1.5 and 0.2 MJ/Nm³ respectively. It is evident that the gas component which most influences the resultant LHV is H₂ since its contribution is comparably higher than that of CO and CH₄ as 67 % ($3.3/4.9=0.67$) of the LHV of the resultant gas is due to H₂ production.

As shown in Figure 5.17 and 5.18, the H₂O/CO₂ ratio of 3:1 has a slightly higher concentration of H₂ than the ratio of 2.5:1, which gives a higher LHV at H₂O/CO₂ ratio of 3:1. This may be due to the small differences of the size of the coal samples, rather than a phenomenon relating to the reactant gas concentrations. As mentioned in section 4.2.2, most of the core samples that were obtained had a length of around 40 mm and a roughly uniform size due to the way the core samples were extracted from the parent blocks by using a coring machine with a diamond core drill. It seems that the small differences in size and small irregularities in some coal samples facilitated the transport of gases to the carbon surface and hence increased the reaction of gases with carbon.

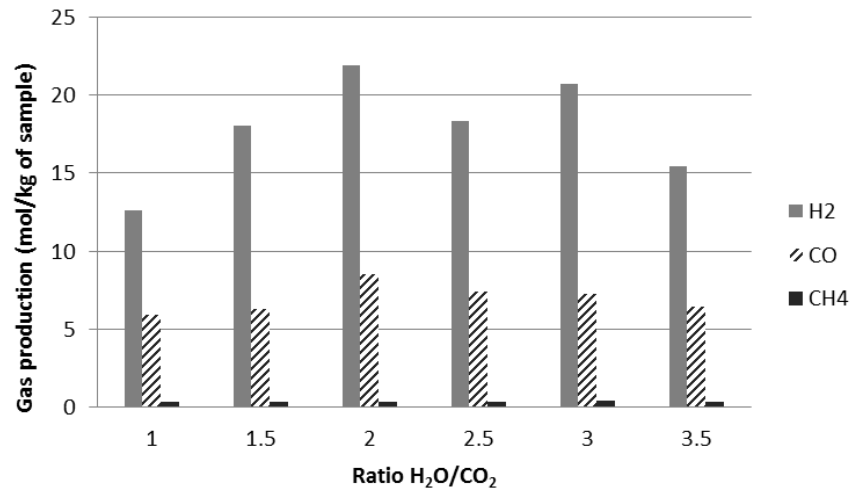


Figure 5.17: Calculated gas production (mol/kg of sample) during gasification of dry steam coal char for various ratios of H₂O / CO₂ (900°C, 0.1 MPa)

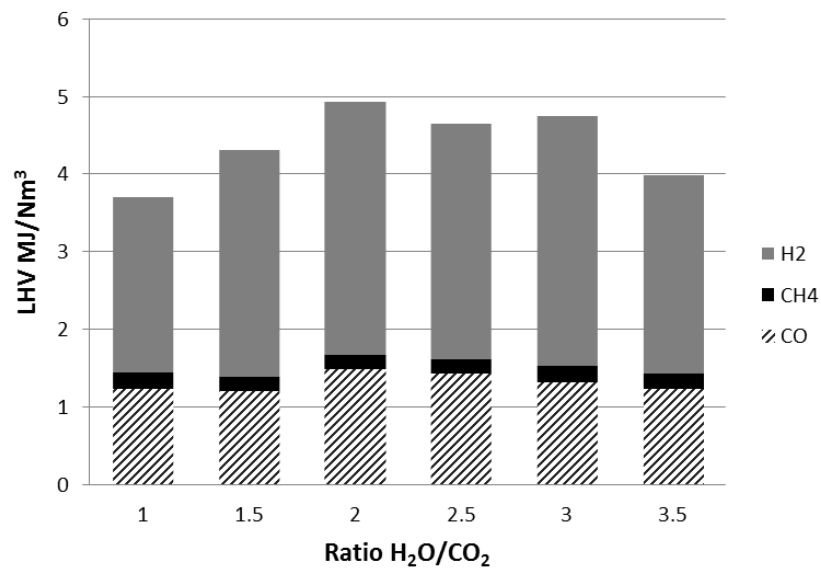


Figure 5.18: Calculated LHV (MJ/Nm³) of the produced gas during gasification of dry steam coal char for various ratios of H₂O / CO₂ (900°C, 0.1 MPa), expressed as the relative contributions of each gas

Similar phenomena are shown in Figure 5.19 where the production of combustible gases for different ratios of H₂O/CO₂ is plotted during gasification of the anthracite with H₂O/CO₂. The H₂ production is increased with an increase in H₂O/CO₂ ratio up to 2:1, above this ratio the H₂ is decreasing. The increase of CO production remained almost constant for H₂O/CO₂ ratios between 1.5:1 - 2.5:1 and the CH₄ concentration remained

unchanged with a small increase for the H₂O/CO₂ ratio of 2:1. At the H₂O/CO₂ ratio of 3:1 it seems that this phenomenon saturates.

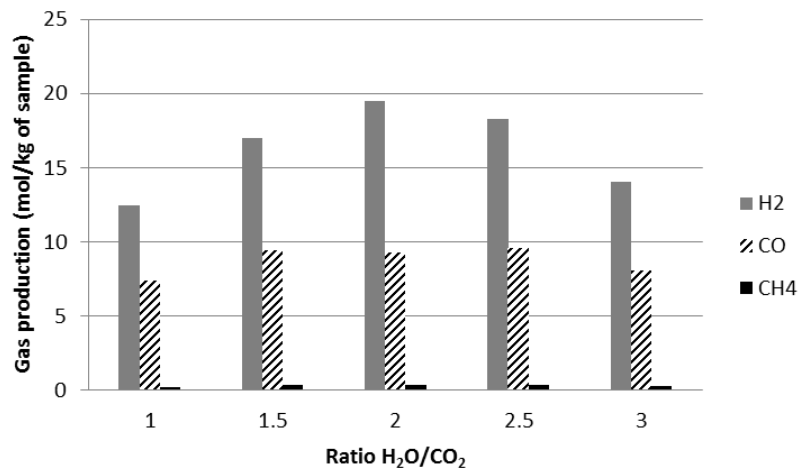


Figure 5.19: Calculated gas production (mol/kg of sample) during gasification of anthracite for various ratios of H₂O / CO₂ (900°C, 0.1 MPa)

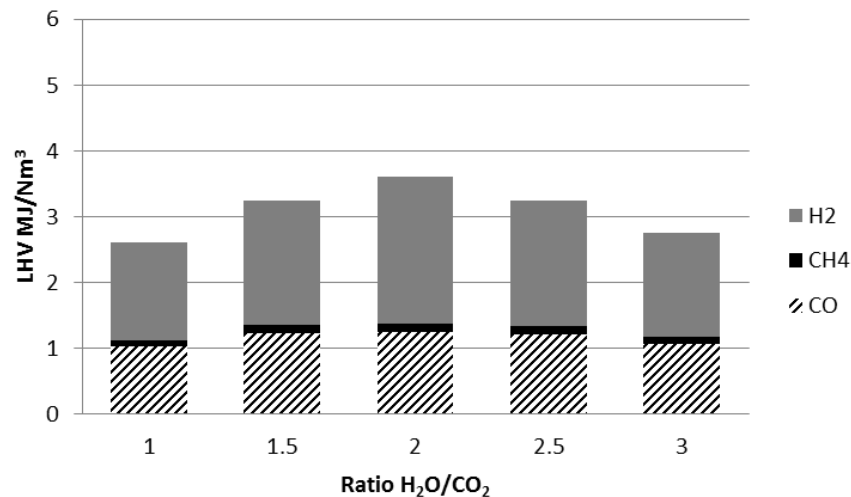


Figure 5.20: Calculated LHV (MJ/Nm³) of the produced gas during gasification of anthracite char for various ratios of H₂O / CO₂ (900°C, 0.1 MPa), expressed as the relative contributions of each gas

The range of H₂O/CO₂ ratio between 1.5:1 to 2.5:1 provided optimum conditions for the anthracite char, with a LHV of 3.6 MJ/Nm³ (H₂O/CO₂ ratio of 2:1) as shown in Table 5.7 and in Figure 5.20 where the effect of the H₂O/CO₂ ratio on the LHV of the product gas is presented. The contribution of H₂ to the maximum resultant LHV of the product gas was 2.2 MJ/Nm³ and that of CO and CH₄ as energetic components on the product gas was 1.2 and 0.1 MJ/Nm³ respectively. It is evident that the gas component which

controls the resultant LHV is H₂ since its contribution is comparably higher than that of CO and CH₄ as 61% ($2.2/3.6=0.61$) of the LHV of the resultant gas is due to H₂ production.

It is evident that the H₂O/CO₂ ratio has an impact on the LHV of the product gas with the maximum values achieved for a certain range of H₂O/CO₂ ratios for both coals. This is the same range of H₂O/CO₂ ratios where the maximum values of carbon conversion X , X_a and CGE were also achieved as shown in Table 5.7. Also the range of H₂O/CO₂ ratios that was determined in this study to produce the maximum LHV of the resultant gas by Nm³ of produced gas (MJ/Nm³), produce also the maximum LHV of the resultant gas by kg of produced gas (MJ/kg) as shown in Table 5.7.

5.3.1.4 Summary

The optimal H₂O/CO₂ ratio was defined for both coals in terms of carbon conversion, CGE and LHV of the product gas produced in the reduction zone. For the dry steam coal the range of the H₂O/CO₂ ratio between 2:1 – 3:1 provided optimum conditions, with a LHV of 4.9 MJ/Nm³ (H₂O/CO₂ ratio of 2:1). The best H₂O/CO₂ ratio for anthracite was between 2:1 and 2.5:1 with a LHV of 3.6 MJ/Nm³ (H₂O/CO₂ ratio of 2:1). The gas component which controls the resultant LHV is H₂ since its contribution is comparably higher than that of CO and CH₄ for both coals. For hydrogen rich gas production the optimum ratio of H₂O/CO₂ is 2:1 for both coals and the ratio of H₂O/O₂ is calculated to be 2.4:1. These results could be useful when deciding the composition of the gasifying agents depending on the end use of the produced gas e.g: power generation, fuels, hydrogen production, chemicals etc. Furthermore the UCG gasification is feasible when operated under optimal conditions.

The gasification rate of the coal chars with CO₂+H₂O is enhanced when the H₂O/CO₂ ratio is increasing. At high H₂O/CO₂ ratios above 2:1 for both coals, it seems that the high concentration of CO and H₂ inhibits the gas solid reactions and it seems that the controlling mechanism is adsorption – desorption. As a result the gasification rate slows down and this phenomenon saturates at even higher H₂O/CO₂ ratios which is above 3:1 for the dry steam coal and 2.5:1 for anthracite.

5.4 Comparison with other studies

In order to be able to assess the experimental results of this study, a comparison was needed with other studies. All the studies and the field trials on UCG were performed by using gasifying agents such as O₂, air and steam or combination of these in order to determine how these gasifying agents affect the composition of the product gas. In this study, CO₂ and steam were used in order to investigate the impact of the reduction zone on the composition of the product gas. So in order to be able to compare the composition of the product gas of this study, studies where O₂ or O₂ with steam were used as gasifying agents were investigated. These studies are described in detail in Chapter II and the composition of their product gas is presented in Table 5.9, which also shows the best gas compositions of this study achieved at the specific conditions for both tested coals.

Table 5.9: Compositions of product gas (%V) of other studies and of this study.

Studies	Coal/char type	Gasifying agents	Gas composition (% Volume)			
			CO ₂	H ₂	CO	CH ₄
1. Stanczyk et al., (2012) [76]	Hard coal (32% V.M)	O ₂ + H ₂ O	56.96	15.28	17.58	3.05
2. Daggupati et al., (2011) [14]	Low rank coal (40% M, 11% V.M.)	O ₂ + H ₂ O	54-44	33-39	9-13	<4
3. Liu et al., (2008) [49]	Lignite (33% M, 25% V.M.)	O ₂ + H ₂ O	27.56	42.95	25.86	3.63
4. Yang et al. (2009) [95]	Gas –fat coal (high V.M.)	O ₂ + H ₂ O	30	40	26	4
5. Stanczyk et al., (2011) [75]	Lignite (53% M)	O ₂	63.6	19.2	6.2	1.7
6. This study Figure 5.12 c)	Anthracite (V.M=6.2%)	CO ₂ + H ₂ O	69	20.7	9.8	0.4
7. This study Figure 5.11 c)	Dry steam coal (V.M=13%)	CO ₂ + H ₂ O	58	30	12	0.5

It is evident that the gas composition of Daggupati et al., (2011) [14] study (no 2), where coal of high moisture content 40% and 11% V.M. was gasified with O₂ and H₂O introduced every ten minutes in a cyclic manner, is in good agreement with the gas composition of this study on the dry steam coal (13% V.M.) as shown in Table 5.8 (no 7). The small differences in the gas compositions can be explained by the high moisture

content of coal in Daggupati et al., (2011) [14] study and because in this study the gas composition derived only from the reduction zone of UCG and not from gases produced during the oxidation and drying/pyrolysis zones which explains the low concentration of CH₄ compared to that of Daggupati.

The gas composition of the Stanczyk et al., (2011) [75] study (no 5) where lignite was gasified in a pilot scale ex-situ reactor with O₂ does not agree with the gas composition of the studies no 3 and 4 where lignite was gasified as well but agrees fairly well with the gas composition of this study on the anthracite (no 6) which is less reactive than lignite as a high rank coal. This can be explained by the high moisture content (53%) of the lignite in Stanczyk et al. study which dropped the temperature and the calculated gasification efficiency of the UCG process and the lignite reacted less with the gases.

Stanczyk et al., (2012) [76] study (no 1) gasified hard coal with high volatile content (32.41%) with O₂ and H₂O separately in alternative stages in a pilot scale ex-situ reactor and the resultant gas composition is comparable with the gas composition with the anthracite in this study as shown in Figure 5.12c) (no 6). The differences can be explained by the high volatile coal in Stanczyk et al. study and because the H₂O was injected in stages.

Liu et al., (2008) [49] (no 3) gasified lignite with O₂ + H₂O in a simulated coal seam and Yang et al. (2009) [96] gasified 'gas-fat' coal of high volatile content with O₂ + H₂O in a model gasifier. The gas compositions of these two studies with similar coal types are in good agreement.

It can be noted from Table 5.8 that the concentrations of CO and H₂ of this study are comparable with other studies, which evaluates the results of this study by using the bespoke high pressure high temperature rig and also reinforces the fact that the majority of the product gas, CO and H₂, is produced during the reduction zone. The concentration of CH₄ of this study is very low compared to the concentration of CH₄ of the other studies and that can be explained since CH₄ is mainly produced during the devolatilisation/pyrolysis zone [28]. It appears likely that many UCG projects are relying heavily on CH₄ which is simply being liberated from the coal and not manufactured in the reactions.

In order to further reinforce that the results of this study are comparable with other studies, Figure 5.21 is presented from Stanczyk et al., (2011) [75] study where the evolution of the produced gases is shown during gasification of lignite with O₂ in a pilot scale ex-situ reactor. It is evident that the concentration of gasifying agent O₂ is very low since most of it is consumed and what is driving the gasification is the CO₂ produced from the combustion of O₂ with carbon and the moisture (H₂O) in the coal which was high. The latter proves experimentally that the controlling factor of the UCG gasification rate is CO₂ and is very similar with the results of this study shown in Figure 5.13c) and Figure 5.14c).

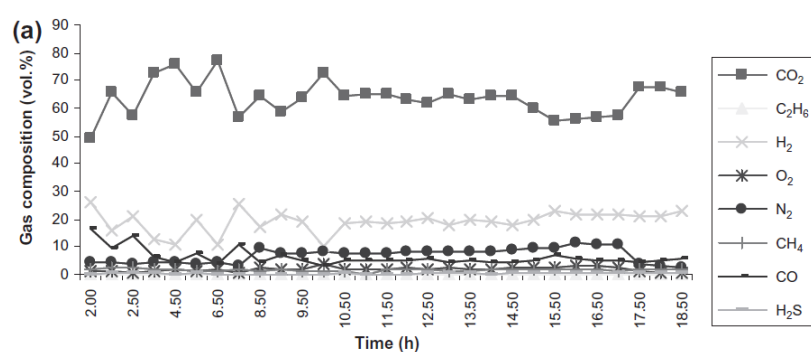


Figure 5.21: Percentage composition of gaseous products during oxygen lignite seam gasification phase [75]

5.5 Experiments at the oxidation and drying - pyrolysis zone

In order to understand how char reacts in the oxidation and during the drying/devolatilisation zone, experiments were conducted under simulating conditions.

Experiments were conducted with both coals under conditions simulating the oxidation zone at UCG by injecting O₂ at the optimum determined operating conditions (temperature of 900° C, ratio of H₂O/CO₂ = 2:1 (m/m) for both coals at 0.1 MPa). The amount of O₂ injected was stoichiometric calculated from the reaction $C + O_2 \rightarrow CO_2$ considering that the flowrate of CO₂ = 0.4 l/min in the previous experiments and it was also found that the flowrate of O₂ = 0.4 l/min, which gives a mass ratio of H₂O / O₂ = 2.4:1. The results are shown in Figure 5.22 and Figure 5.23 for the dry steam coal and anthracite respectively. Experiments were also performed under conditions simulating the drying-pyrolysis zone at UCG by injecting N₂ at 0.1 MPa from room temperature to

900 °C at a heating rate of 5-10 °C/min. The results are presented in Figures 5.24 and 5.25 for the dry steam coal and anthracite respectively.

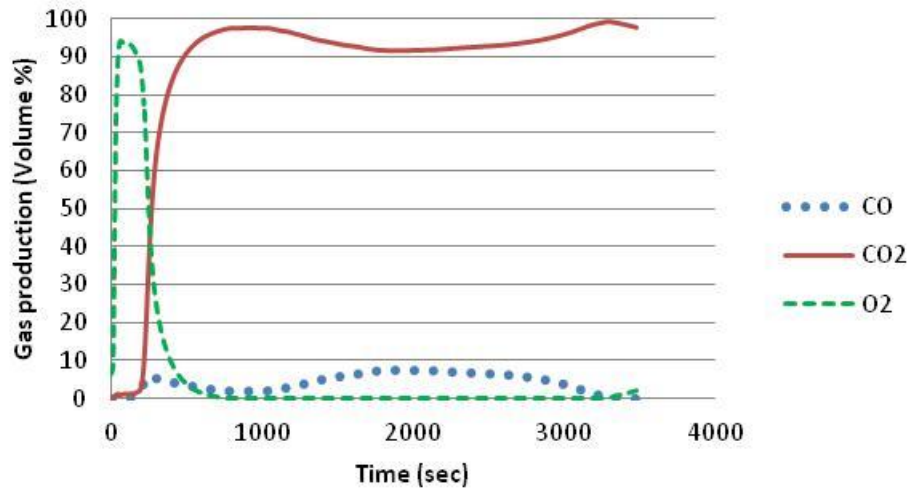


Figure 5.22: Measured rig data showing the variation of concentration of the produced gases (Vol %) during combustion of dry steam coal char over time under the flow of $O_2 = 0.4l/min$ (900°C, 0.1 MPa)

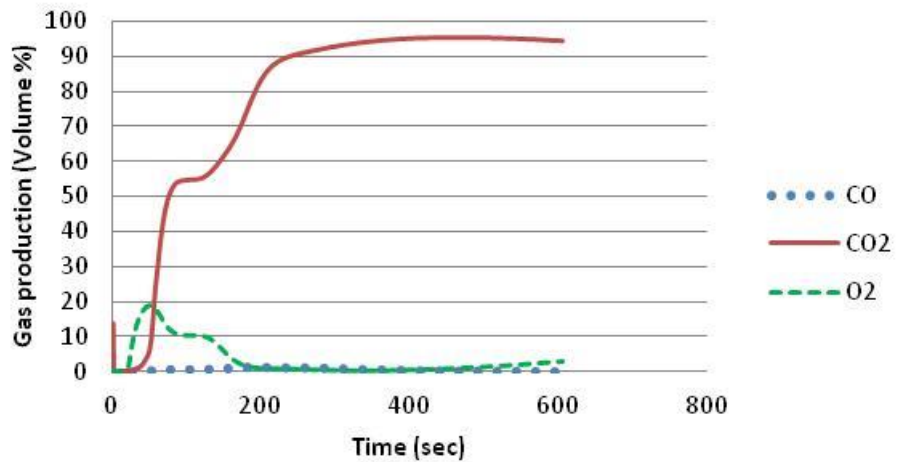


Figure 5.23: Measured rig data showing the variation of concentration of the produced gases (Vol %) during combustion of anthracite coal char over time under the flow of $O_2 = 0.4l/min$ (900°C, 0.1 MPa)

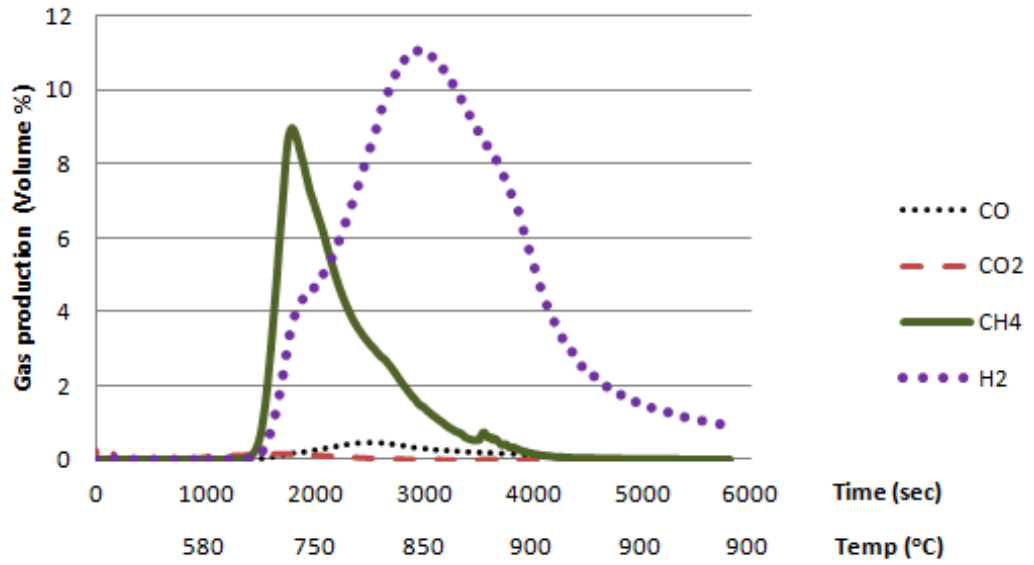


Figure 5.24: Measured rig data showing the variation of concentration of the produced gases (Vol %) during devolatilisation of dry steam coal over time under the flow of N₂ (0.1 MPa)

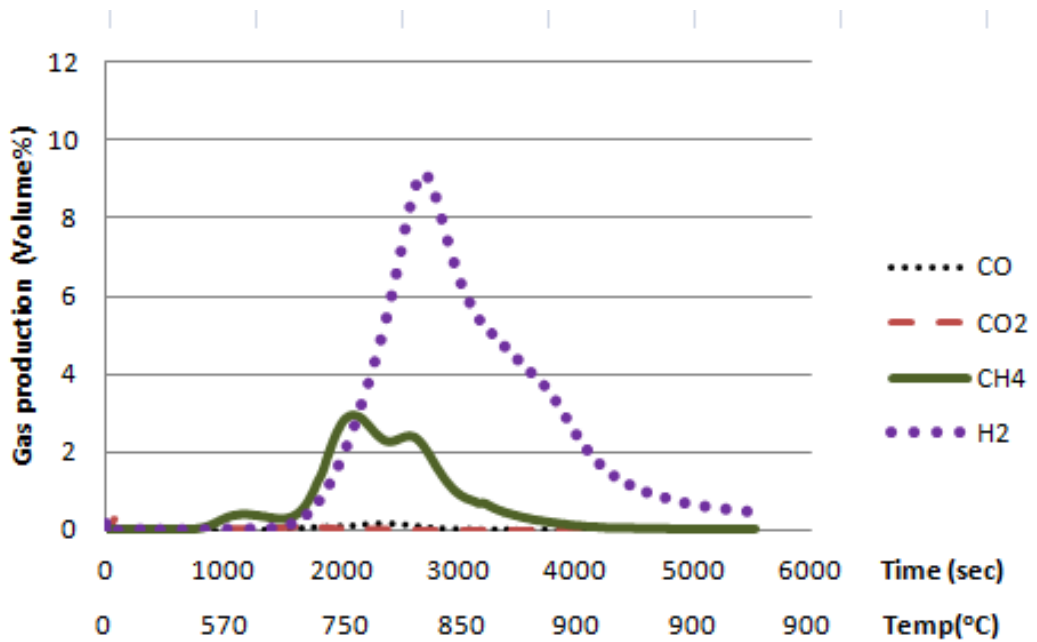


Figure 5.25: Measured rig data showing the variation of concentration of the produced gases (Vol %) during devolatilisation of anthracite coal over time under the flow of N₂ (0.1 MPa)

5.5.1 Experimental results / Discussion

In Figures 5.22 and 5.23 is shown that the O₂ reacting with char was consumed fairly quickly and that it is the CO₂ which is produced that is reacting with the carbon, as

mentioned in Stansyk et al. (2012) [76], and producing CO until the C/O₂ ratio started dropping and as a result the O₂ and CO₂ concentration increasing and decreasing respectively. It is evident that a similar effect is happening during the oxidation zone of UCG, with the O₂ consumed fairly quickly and the produced CO₂ reacting with the char which produces CO during the reduction zone. This again proves that the rate controlling step of the gasification is CO₂, plus the steam that is injected during the UCG process which enhances the gasification performance. Furthermore the carbon conversion determined during the oxidation zone was around 0.45 for the dry steam coal and 0.24 for anthracite as shown in Table 5.10. This shows that enough CO₂ was produced for the gasification reactions to occur at the next reduction zone of the UCG process, since the carbon conversion during the reduction zone was calculated 0.24 for the dry steam coal and 0.19 for anthracite. The contribution of the oxidation zone to the LHV of the product gas is very low since the largest amount of gas produced is CO₂.

In Figures 5.24 and 5.25 it is apparent that the pyrolysis gases are mainly H₂ and CH₄ and that the peak of H₂ production was around 11% and 9% for the dry steam coal and anthracite respectively at temperatures between 840 to 850 °C after which it decreases significantly and approaches zero at around 900 °C. The CH₄ peak was 9% for the dry steam coal and 3% for the anthracite at temperatures around 750 °C after which it decreases and approaches zero at around 900 °C. It is clear that the H₂ and CH₄ are released during the high temperature pyrolysis zone, between 750 to 850 °C. The contribution of the drying/pyrolysis zone to the LHV of the product gas when measured under simulated conditions is shown in Table 5.10, which is 0.88 MJ/Nm³ (0.36 MJ/Kg) for the dry steam coal and 0.47 MJ/Nm³ (0.22 MJ/Kg) for anthracite. These values increase the LHV of the produced gas by 14% and 10% for the dry steam coal and anthracite respectively and are also analogous considering that the volatile matters of the dry steam coal (13% V.M.) is almost double than that of anthracite (6.21% V.M.). It is worth noting that the volatile matter of anthracite is quite significant considering it is a high rank coal with low volatile matter content.

Table 5.10: Calculated gasification parameters during the reduction, oxidation and drying-pyrolysis zone for the dry steam coal and anthracite at 900 °C and 0.1 MPa.

Coal type	Gasification parameters		Reduction zone	Oxidation zone	Drying /pyrolysis zone
Dry steam coal (V.M=13.0 %)	Carbon conversion X		0.24	0.45	0.02
	LHV	MJ/Nm ³	4.9	0.69	0.88
		MJ/kg	3.9	0.28	0.36
Anthracite (V.M=6.2 %)	Carbon conversion X		0.19	0.24	0.015
	LHV	MJ/Nm ³	3.6	0.22	0.47
		MJ/kg	2.4	0.11	0.22

5.5.2 Summary

The optimal H₂O/CO₂ ratio was defined for both coals in terms of carbon conversion, CGE and LHV of the product gas produced in the reduction zone. For the dry steam coal the range of the H₂O/CO₂ ratio between 2:1 – 3:1 provided optimum conditions, with LHV of 4.9 MJ/Nm³ (H₂O/CO₂ ratio of 2:1). The best H₂O/CO₂ ratio for anthracite was between 2:1 and 2.5:1 with LHV of 3.6 MJ/Nm³ (H₂O/CO₂ ratio of 2:1). For hydrogen rich gas production the optimum ratio of H₂O/CO₂ is 2:1 for both coals and the ratio of H₂O/O₂ calculated to be 2.4:1. These results could be useful when deciding the composition of the gasifying agents depending on the end use of the produced gas e.g: power generation, fuels, hydrogen production, chemicals etc.

The gas compositions in Figure 5.13c) and Figure 5.14c) of the dry steam coal and anthracite respectively are comparable to the gas compositions in other studies where O₂ or O₂+ steam were injected as gasifying agents which evaluates the results of this study using the bespoke high pressure high temperature rig.

It is demonstrated that the O₂ injected at the oxidation zone is consumed fairly quickly and the produced CO₂ is reacting with the char and produces CO during the reduction zone which proves that CO₂ is the rate controlling step of the gasification, plus the

steam that is injected which enhances the gasification performance. Furthermore the carbon conversion determined during the oxidation zone was around 45% for dry steam coal and 24% for anthracite which shows that enough CO₂ was produced for the gasification reactions to occur at the next reduction zone of the UCG process.

The contribution of the drying/pyrolysis zone to the LHV of the product gas is 0.88 MJ/Nm³ for the dry steam coal and 0.47 MJ/Nm³ for the anthracite. The contribution of the oxidation zone to the LHV of the product gas is very low since the largest amount of gas produced is CO₂ which is determined to be sufficient for the reduction reactions to occur at the next zone which is the reduction zone (which agrees with Gregg). It is evident that the highest concentrations of the gases are mainly produced during the reduction zone and the rest during the drying and pyrolysis zone, specially for high volatile content coals. It is also shown that the H₂ and CH₄ are released during the high temperature pyrolysis zone, between 750 to 850 °C.

5.6 Chapter Summary

It is shown that temperature and gasifying agents composition affect the performance of the reduction zone in UCG and consequently the overall performance of the process. Temperature favours the gasification reactions during the reduction zone and is the most important factor for the gasification performance of UCG. The optimum temperature was determined to be 900 °C for the range of tested temperatures because it maximised the carbon conversion, CGE and LHV of the product gas produced for both coals.

The optimum operating conditions for both coals which produced the best gas composition were determined at atmospheric pressure and these were 900 °C and a H₂O/CO₂ ratio of 2:1 (H₂O/O₂ ratio of 2.4:1) for both coals with a coal sample of 36g and 20 g for the dry steam coal and anthracite respectively. The maximum LHV of the dry steam coal was 4.9 MJ/Nm³ and 3.6 MJ/Nm³ for anthracite during the reduction zone. These operating conditions are unique for each UCG system.

The gasification rate of the coal chars with CO₂+H₂O is enhanced when the H₂O/CO₂ ratio is increasing. At high H₂O/CO₂ ratios of above 2:1 for both coals, it seems that the high concentration of CO and H₂ inhibits the gas solid reactions and it therefore the controlling mechanism is adsorption – desorption. As a result the gasification rate is

slowed down and the gas phase reactions might be favoured. This phenomenon saturates at even higher H₂O/CO₂ ratios.

H₂ is the gas component which controls the resultant LHV since its contribution is comparably higher than that of CO and CH₄ for both coals. For hydrogen rich gas production the optimum ratio of H₂O/CO₂ is 2:1 for both coals and the ratio of H₂O/O₂ calculated to be 2.4:1. These results could be useful when deciding the composition of the gasifying agents depending on the end use of the produced gas e.g: power generation, fuels, hydrogen production, chemicals etc. Furthermore the UCG gasification is feasible when operated under optimal conditions.

The carbon conversion X (C in CO, CH₄ and CO₂) was 0.24 for the dry steam coal and 0.19 for the anthracite when both coals were tested under their optimum gasification conditions, which shows that the dry steam coal is more reactive than the anthracite. It is worth noting that the maximum carbon conversion X_a (C in CO and CH₄) was 0.13 for both coals which indicates that anthracite may be as suitable for a UCG project as dry steam coal since it produced a similar amount of the combustible gases CO and CH₄ under the tested conditions. There are studies which mention that low rank and high volatile coals are preferably for UCG but this study shows that high rank coals can also be considered for a UCG project, if not for energy production certainly for fuel and chemicals production.

The shrinking unreacted core model predicts the gasification conversion of the two coal chars tested under the flow of CO₂+H₂O at 0.1 MPa and temperatures ranged from 750 to 900° C. The deviations of the shrinking unreacted core model with the experimental data of the anthracite are less than those of the dry steam coal. It is also evident that the gasification rate depends strongly on the temperature indicating chemical reaction rate control within the temperature range tested. From the Arrhenius plot the apparent activation energy E and the pre-exponential factor A were found to be 349.63 KJ/mol and 5.83×10^4 /sec for the dry steam coal and 406.74 KJ/mol and 2.63×10^7 /sec for the anthracite respectively. These findings can be useful for modelling gasification processes.

The contribution of the drying/pyrolysis zone to the LHV of the product gas is 0.88 MJ/Nm³ (0.36 MJ/kg) for the dry steam coal and 0.47 MJ/Nm³ (0.22 MJ/kg) for the anthracite which is around 10% of the max LHV of the product gas produced of both

coals. The contribution of the oxidation zone to the LHV of the product gas is very low since the largest amount of gas produced is CO_2 which is determined to be sufficient for the reduction reactions to occur at the next zone which is the reduction zone. It can be concluded that the highest concentrations of the gases are mainly produced during the reduction zone and the rest during the drying and pyrolysis zone, specially for high volatile content coals. Its worth noting that the gases H_2 and CH_4 are released during the high temperature pyrolysis zone, between 750 to 850 °C.

It is demonstrated that the O_2 injected at the oxidation zone is consumed very quickly and the produced CO_2 is reacting with the char and produces CO during the reduction zone which proves that CO_2 is the rate controlling step of the gasification, plus the steam that is injected which enhances the gasification efficiency.

The gas compositions of the dry steam coal and anthracite are comparable to the gas compositions in other studies where O_2 or O_2 + steam were injected as gasifying agents which evaluates the results of this study using the bespoke high pressure high temperature rig.

CHAPTER VI

EXPERIMENTAL RESULTS ON PRESSURISED GASIFICATION

6.1 Introduction

This chapter presents the results of the experiments conducted at elevated pressure in order to assess the impact of pressure on the composition of the product gas and the performance of the UCG process during the reduction zone. The experiments were performed with dry steam coal and anthracite samples using the methodology described in Chapter IV and the optimal operating conditions that were determined in Chapter IV and V; that is 900 °C temperature, H₂O/CO₂ ratio of 2:1, flowrate of CO₂ = 0.4 l/min and cylindrical blocks for both coals, sample size of the dry steam coal of 36g (C content 29.9g) and that of anthracite of 20g (C content 17.7g). The results were expressed as a function of pressure.

6.2 Effect of pressure

6.2.1 Pressurised gasification experiments with the dry steam coal and anthracite

The effect of pressure on gas production during the gasification of the dry steam coal char at the reduction zone was examined at a reactor temperature of 900 °C and a H₂O/CO₂ ratio of 2:1 and the results are presented in Figure 6.1 for pressures of a) 0.7 MPa, b) 0.9 MPa, c) 1.65 MPa, d) 2.2 MPa, e) 3.0 MPa and f) 3.9 MPa. Similar experiments were also conducted with anthracite at 900 °C and a H₂O/CO₂ ratio of 2:1 at various pressures of a) 0.8 MPa, b) 1.0 MPa, c) 1.65 MPa, d) 2.1 MPa, e) 3.0 MPa and f) 4.0 MPa and the results are shown in Figure 6.2.

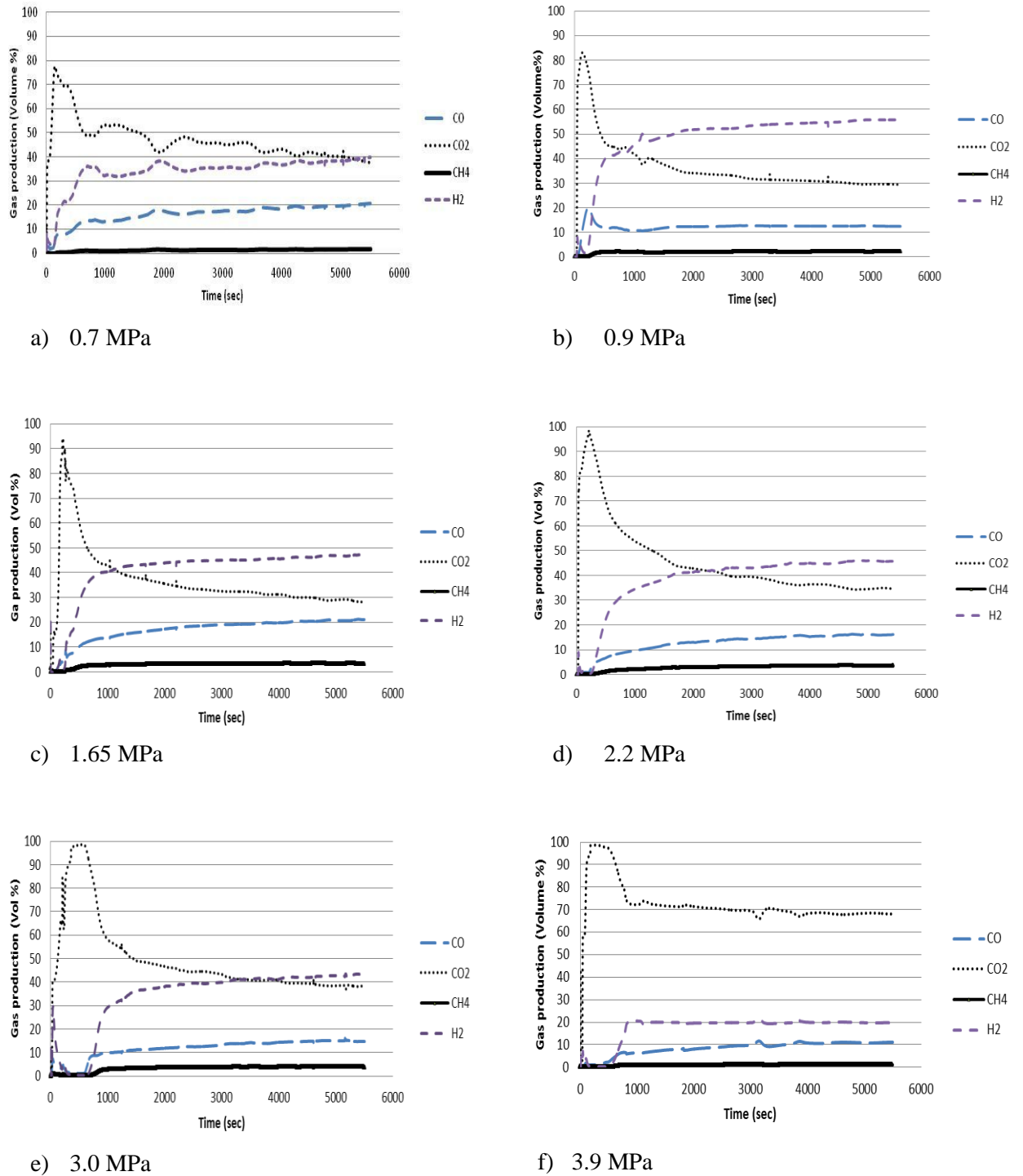


Figure 6.1: Measured rig data showing variation of concentration of the produced gases (Vol %) during gasification of the dry steam coal over time for a) 0.7; b) 0.9 ; c) 1.65; d) 2.2; e) 3.0 and f) 3.9 MPa under the flow of CO₂ + H₂O (900°C, H₂O / CO₂=2:1)

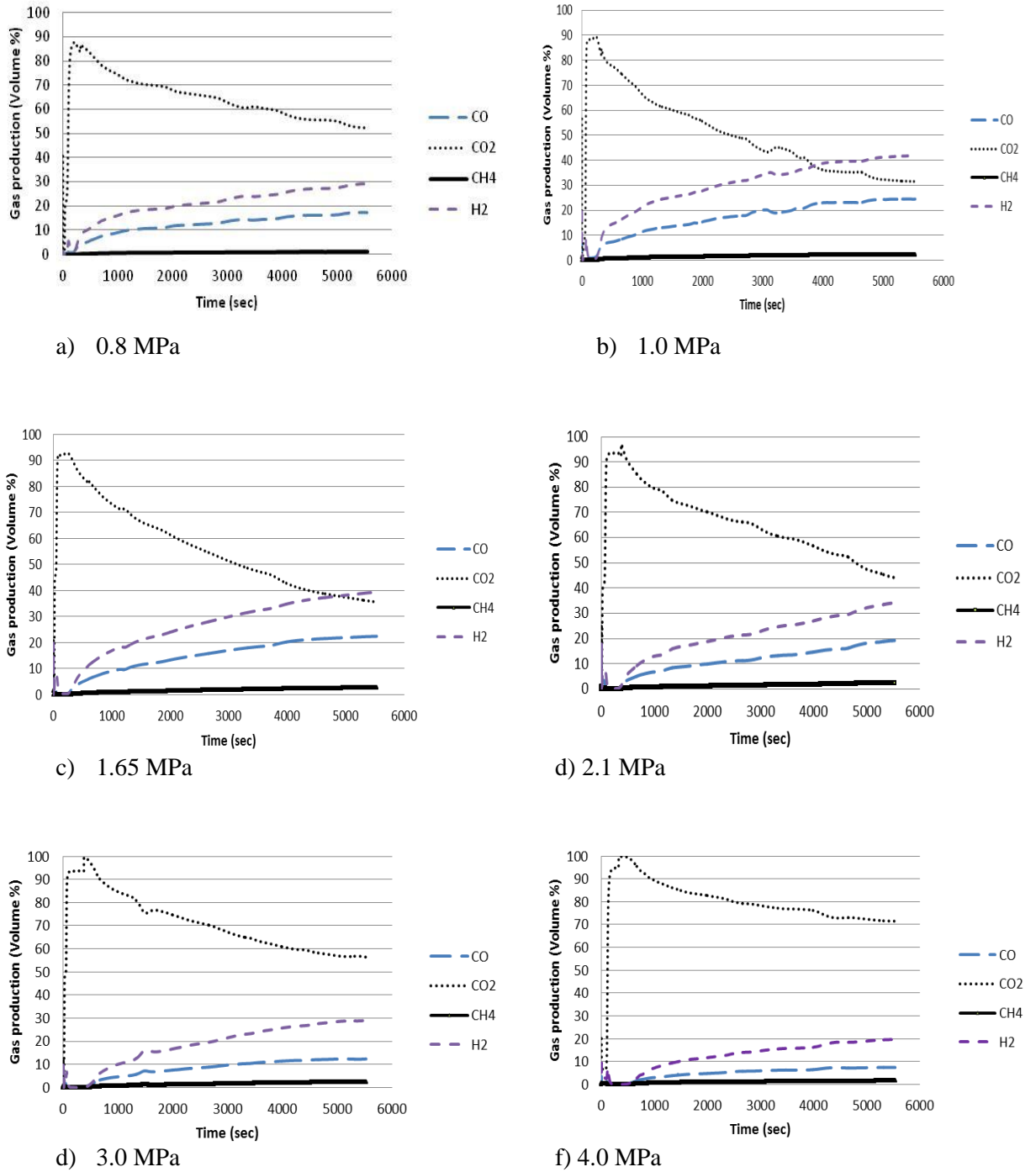


Figure 6.2: Measured rig data showing variation of concentration of the produced gases (Vol %) during gasification of anthracite over time for a) 0.8; b)1.0 ; c) 1.65; d) 2.1; e) 3.0 and f) 4.0 MPa under the flow of CO₂ + H₂O (900°C, H₂O / CO₂=2:1)

6.2.2 Coal samples before and after pressurised gasification

Figures 6.3 and 6.4 show coal samples prepared before the experiment and the coal char samples after gasification with $\text{CO}_2 + \text{H}_2\text{O}$ for both the dry steam coal and anthracite respectively. It is evident in Figure 6.3 that the dry steam coal char samples under pressurised gasification developed a significant amount of cracks which finally fragmented the char samples. Also the dry steam coal developed more cracks than anthracite which is explained by the dry steam coal having a volatile matter around double that of anthracite which means that there are more free pores available after devolatilisation for the reactant gases to penetrate and reach the internal surface of the porous char to consequently react with.

Furthermore the amount of cracks on these coal char samples is much more than those developed in the coal char samples after gasification at atmospheric pressure as discussed in the previous chapter. After the experimental procedure at pressure and the shutdown of the experimental rig, it was noticed that the tar in the tar trap was misty and yellowish compared to the tar produced during the experiments at ambient pressure which was clear and transparent.



Dry steam coal samples



Dry steam coal char samples after gasification

Figure 6.3: Coal samples and coal char samples of the dry steam coal before and after gasification at 1.65 MPa under the flow of $\text{CO}_2 + \text{H}_2\text{O}$ (900°C , $\text{H}_2\text{O} / \text{CO}_2 = 2:1$)



Anthracite sample



Anthracite char sample after gasification

Figure 6.4: Coal sample and coal char sample of anthracite before and after gasification at 1.65 MPa under the flow of $\text{CO}_2 + \text{H}_2\text{O}$ (900°C , $\text{H}_2\text{O} / \text{CO}_2=2:1$)

6.3 Experimental results / Discussion

6.3.1 Pressurised gasification

In Figures 6.1 and Figure 6.2 it can be observed that after approximately 500 seconds, which is the time required to reach steady state conditions in the reactor, the concentrations of CO , CH_4 and H_2 are comparatively higher and CO_2 was lower than that of the atmospheric pressure (0.1 MPa) condition as shown in Figures 5.1d) and 5.2d) for the dry steam coal and anthracite respectively. The reason for this is that pressure increases the gas-solid contact, hence enhances the gas-solid reactions, favouring the CO , CH_4 and H_2 concentrations. Steady state is achieved after an initial period of around 500 sec for the experiments at elevated pressure. During this initial period the product gas concentrations were changing comparatively quickly due to the steady state condition being established in the reactor.

Furthermore, at identical mass flow rates, increasing the pressure increases the residence time so the gases have comparatively more time to react and achieve the best gas composition of the product gas. This phenomenon saturates at higher pressures as is shown for the dry steam coal in Figures 6.1c) at 2.2 MPa, 6.1d) at 3.0 MPa and 6.1e) at 3.9 MPa and for anthracite in Figures 6.2b) at 1.65 MPa, 6.2c) at

2.1 MPa, 6.2d) at 3.0 MPa and 6.3e) at 4.0 MPa, where the resultant concentrations of CO₂ and CH₄ are subsequently higher and the concentrations of CO and H₂ are lower. This agrees with the Le Chatelier-Brauns principal, that under pressure the equilibrium of reactions R5 and R7 will shift to the side with the fewer moles of gas. Furthermore the high concentrations of CO and H₂ have an inhibiting (retarding) effect in the Boudouard and steam carbon reaction respectively. These compounds lower the initial rate and result in a gradually decrease in the reactivity of the char and the CO and H₂ concentrations resulting in increasing the CO₂ and CH₄ concentrations [65]. At the pressure of 3.9 MPa for the dry steam coal and 4 MPa for anthracite as shown in Figures 6.1e) and 6.2e) respectively, the pressure effect seems insignificant and it seems that the gas solid reactions are decreased as the CO and H₂ concentrations are lower compared to their concentrations at the other pressures.

Table 6.1 and 6.2 shows the calculated average gas composition and LHV of product gas in CO₂ + H₂O gasification at 900°C at the tested pressures of the dry steam coal and anthracite respectively from the measured rig data.

Table 6.1: Calculated average gas composition and LHV of product gas in CO₂ + H₂O gasification at 900°C of dry steam coal at a range of pressures from measured rig data

Pressure (MPa)	Gas composition				LHV	
	CO % (vol)	CH ₄ % (vol)	H ₂ % (vol)	CO ₂ % (vol)	MJ/Nm ³	MJ/kg
0.7	16.4	1.38	34.7	47.4	6.3	5.4
0.9	12.3	1.9	49.1	36.7	7.5	7.4
1.65	17.4	2.9	42.1	37.6	7.8	7.5
2.2	12.9	2.8	38.9	37.6	6.8	6.1
3	11.9	3.1	34.7	49.7	6.4	5.7
3.9	8.5	0.9	17.6	73.0	3.3	2.0

Table 6.2: Calculated average gas composition and LHV of product gas in CO₂ + H₂O gasification at 900°C of anthracite at a range of pressures from measured rig data

Pressure (MPa)	Gas composition				LHV	
	CO % (vol)	CH ₄ % (vol)	H ₂ % (vol)	CO ₂ % (vol)	MJ/Nm ³	MJ/kg
0.8	12.3	0.9	21.3	65.5	4.2	2.7
1.0	17.3	1.6	30.4	50.7	6.0	4.2
1.65	15.1	1.61	26.7	56.6	5.4	3.2
2.1	11.4	1.6	21.1	65.9	4.2	2.4
3.0	8.4	1.8	18.8	71	3.6	1.8
4.0	5.1	1.0	12.9	81	2.4	1.3

It can be noted that there was a significant reduction of the CO₂ concentration in the product gas for the pressures tested compared to the ambient pressure as was determined in Chapter V. The CO₂ concentration at atmospheric pressure for the dry steam coal was around 58% and it was reduced to 37-38% for pressures between 0.9-3.0 MPa. For anthracite the CO₂ concentration was around 69% at 0.1 MPa and for pressures between 0.8-1.65 MPa it was reduced to 51-57%. This shows again that there is a range of pressures which enhances the gas-solid reactions and this range depends on the type of coal. Dry steam coal which is a lower rank coal with a higher volatile content than anthracite is reactive at a wider range of pressures than anthracite.

Figure 6.5 and Figure 6.6 present the gas production as a function of pressure for the dry steam coal and anthracite respectively. It is interesting to note that the maximum concentrations of H₂ and CO were produced at the range of pressures between 0.9-1.65 MPa for the dry steam coal and at 0.1-1.65 MPa for anthracite respectively. Above these pressures their concentrations are decreasing and it seems that there is a range of pressures which maximise the production of H₂ and CO for both coals. The concentration of CH₄ is increasing as the pressure increases with the maximum

achieved at 3.0 MPa for both coals at a value of 3.1% and 1.8% for the dry steam coal and anthracite respectively, as shown in Tables 6.1 and 6.2.

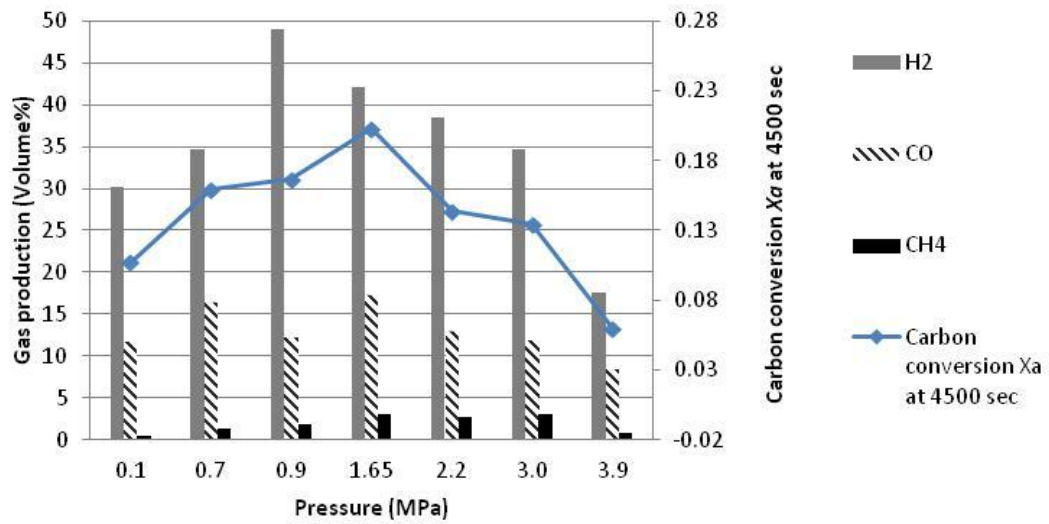


Figure 6.5: Calculated concentrations (Vol %) of the combustible product gases over pressure of dry steam coal from measured rig data

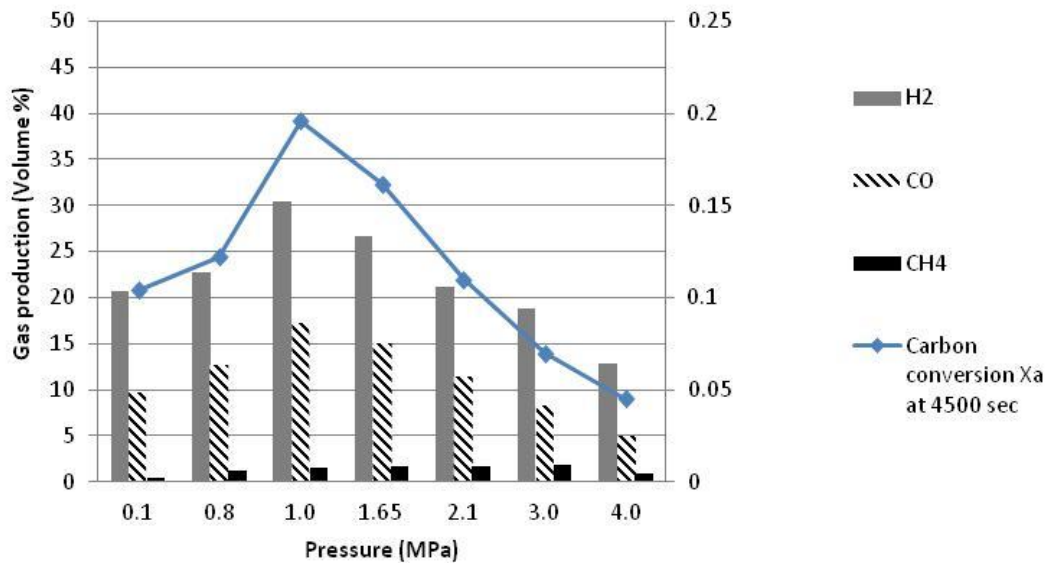


Figure 6.6: Calculated concentrations (Vol %) of the combustible product gases over pressure of anthracite from measured rig data

The carbon conversion X_a of combustible gases (CO and CH₄) at 4500 sec calculated as described in Chapter IV was also plotted for the tested pressures for the dry steam coal and anthracite in Figures 6.5 and 6.6 respectively. The maximum X_a at 4500 sec was achieved at 1.65 MPa and 1.0 MPa for the dry steam coal and

anthracite respectively where the total maximum concentration of CO+CH₄ was achieved as shown in Table 6.1 and 6.2. Above the mentioned pressures, the X_a decreases for both coals which can be explained by the decrease of the combustibles gases concentration. It is interesting to note that the X_a for both coals is around 0.2 which means that approximately 20% of the initial carbon content in the coal samples of both coals is converted to combustible gases after 4500 sec of CO₂+H₂O gasification. Furthermore anthracite seems to produce at different pressures the same amount of combustible gases with dry steam coal which means that under the right operating conditions anthracite can be as reactive as the dry steam coal.

6.3.2 Effect of pressure on gasification reaction rate

In order to demonstrate the effect of pressure on the gasification rate, the carbon conversion X_a (as C in CO and CH₄) of the dry steam coal at 900°C and pressures from 0.7-3.9 MPa and that of anthracite at 900°C and pressures from 0.8-4.0 MPa have been plotted with the maximum X_a as determined at atmospheric pressure in the previous chapter, these are shown in Figures 6.7 and 6.8 respectively. In order to be able to compare the gasification rate at atmospheric and elevated pressures, the data has been normalised to take account of slightly different total mass flow rates through the reactor which was caused by the effect of the pressure regulator located at the outlet of the rig. In undertaking this normalisation the data is expressed as the mass ratio of combustible gas species relative to the total product gas flow rate achieved at ambient pressure for both coals. The results of this normalisation are shown in Figure 6.7 and 6.8 for the dry steam coal and anthracite respectively.

Figure 6.7 shows that the gasification rate for the dry steam coal is enhanced for the pressure range between 0.7-1.65 MPa which then drops further at higher pressures. At 2.2 MPa the gasification rate decreases and at 3.0 MPa it reduces less which shows that the effect saturates (over the conditions tested herein) [40]. Finally at 3.9 MPa the carbon conversion is significantly reduced and is lower than the one achieved at atmospheric pressure which shows that there is a negative pressure dependency.

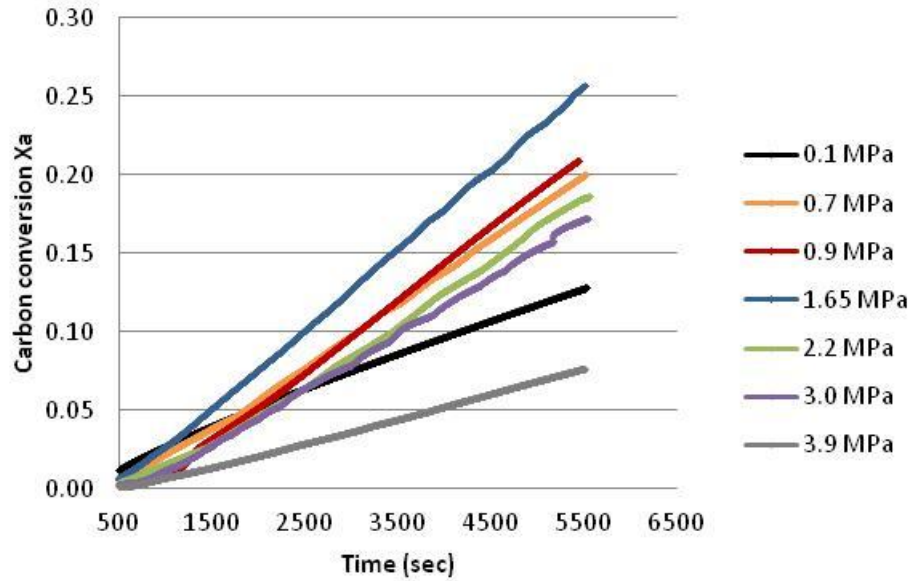


Figure 6.7: Calculated carbon conversion X_a of combustible gases ($\text{CO} + \text{CH}_4$) over time normalised to the total product gas mass flowrate during $\text{CO}_2 + \text{H}_2\text{O}$ gasification of dry steam coal at 900°C and 0.7, 0.9, 1.65, 2.2, 3.0 and 3.9 MPa from measured rig data

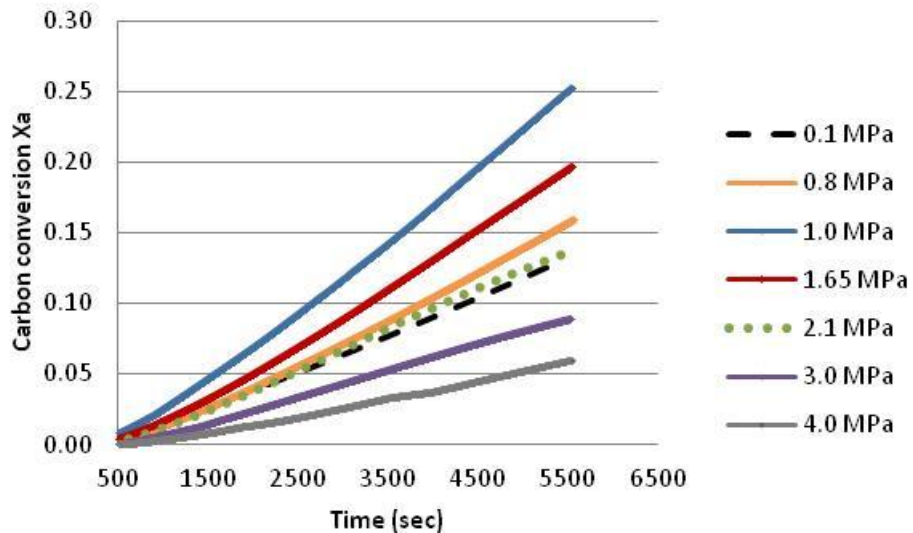


Figure 6.8: Calculated carbon conversion X_a of combustible gases ($\text{CO} + \text{CH}_4$) over time normalised to the total product gas mass flowrate during $\text{CO}_2 + \text{H}_2\text{O}$ gasification of anthracite at 900°C and 0.8, 1.0, 1.65, 2.1, 3.0 and 4.0 MPa from measured rig data

A similar phenomenon also occurred for the anthracite. Figure 6.8 shows that the quantity of carbon converted X_a of the anthracite is notably increased by progressively higher pressures up to 1.0 MPa, above this pressure the carbon

conversion decreases at 1.65, 2.1 at almost uniform increments and at 3.0 MPa the increment becomes smaller which shows that the effect saturates (over the conditions tested herein) [40]. At further high pressure of 4.0 MPa the carbon conversion becomes even smaller which suggests that there is a negative pressure dependency as discussed in Liu et al., (2004) [48]. This finding also agrees with the carbon conversion Xa at 4500 sec plotted in Figures 6.5 and 6.6 for the dry steam coal and anthracite respectively.

It can be noted for both coals that the time to achieve a specified extent of conversion increased above 1.65 MPa for the dry steam coal and 1.0 MPa for anthracite, implying diminished gasification rates at higher pressures. For example the time needed for 0.15 carbon conversion Xa for the dry steam coal was around 4,400, 4,300 and 3,500 sec for 0.7, 0.9 and 1.65 MPa respectively which shows that the gasification rate increases as the time needed for $Xa=0.15$ is decreasing as pressure increases. For the pressures of 2.2 and 3.0 the time required to reach $Xa=0.15$ was around 4,600 and 5000 sec respectively and at 3.9 MPa the highest carbon conversion reached only 0.08 at around 5500 sec which shows that the gasification rate is diminishing as the time for $Xa=0.15$ conversion increases above the 1.65 MPa.

Similarly for anthracite the time required for 0.15 of Xa was around 5,200 and 3,500 sec for 0.8 and 1.0 MPa respectively. For the pressure of 1.65 the time required to reach 0.15 of Xa was increased at 4,500 and for 2.1, 3.0 and 4.0 MPa pressures the time was above 5,500 sec which was the duration of the experiment. This shows again that above 1.0 MPa the gasification rate of anthracite decreases.

The results of this study are in agreement with other studies. In Ma et al., (1992) [53] a similar apparatus and coal (F.C=76.92%, V.M.=6.48%) was used with this study to test the reactivity of carbon with steam and it was concluded that at the tested pressures up to 1.4 MPa the reactivity increased with increased pressure. In this study the tested pressures were up to 4.0 MPa and it was found that the reactivity increased in low pressures up to 1.65 MPa for the dry steam coal char and 1.0 MPa for the anthracite char with $\text{CO}_2 + \text{H}_2\text{O}$ and then decreased in higher pressures. This result is also in agreement with Muhlen et al., (1985) [58] where the reactivity of a bituminous char with steam and CO_2 up to 7.0 MPa was tested with a pressurized

thermo balance and found out that the reactivity increased until low pressures. The study of Goyal et al., (1989) [26] is worth noting where the reactivity of bituminous char with steam, steam + H₂ and with synthesis gas mixtures (H₂, CO, CO₂ and H₂O) was tested with a thermo balance reactor from 0.4 to 2.8 MPa and concluded that the total pressure had negligible effect in the char reactivity. In this study it is shown that the reactivity of carbon with CO₂ +H₂O is sensitive to low pressures up to 1.0 and 1.65 MPa for the anthracite and dry steam coal respectively which effect saturates at higher pressures at the range of 3.0 MPa and becomes negligible at further higher pressures around 4.0 MPa.

6.3.3 Reaction mechanism at pressure

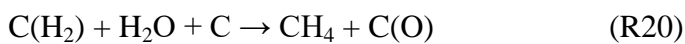
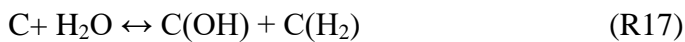
From atmospheric pressure up to 1.65 MPa and 1.0 MPa for the dry steam coal and anthracite respectively, the coal char heterogeneous gasification reactions can be explained by the two-step reaction mechanism of adsorption – desorption which is shown as the following. This reaction mechanism for the Boudouard reaction (R3) is expressed with reactions R8 and R9 and for the carbon steam gasification reaction (R4) with reactions R10 and R11 [2, 3, 52, 60, 69, 86, 89]. The ΔH values of the following reactions could not be found.



C(O) are the adsorbed oxygen surface complexes which consist of an adsorbed atom or molecule chemically bonded with an unsaturated atom in the solid which are the active sites. The concentration of these active sites which are measured with the number of dissociative oxygen chemisorptions onto these sites controls the reaction rate of reactions R3 and R4. As the C(O) concentration increases the reaction rate also increases since the gas-solid reactions does not occur over the entire solid surface but only at the active sites [24]. At low pressures the C(O) concentration is low and the reaction mechanism is controlled by the forward adsorption reactions R8 and R10. From these reactions the C(O) that is produced is then desorbed to CO with

the reactions R9 and R11. By increasing the pressure, the number of C(O) active sites formed is increasing, resulting in an increase in the reaction rate which is proportional to the number of these active sites [16, 19, 21]. It's worth noting that the reaction of char with steam generates more active sites than the reaction of char with CO₂ [19] due to the weak bond of hydrogen in a steam molecule compared to the double bonds forming a CO₂ molecule [22].

At higher pressures such as at 2.2 and 3.0 MPa for the dry steam coal and 1.65, 2.1 and 3.0 MPa for anthracite, the formation of CO₂ and CH₄ has been observed from reactions R3 and R4 respectively as well a decrease of CO and H₂ concentrations. This can be explained by the inhibiting effect of hydrogen and carbon monoxide on the steam and carbon monoxide reactions respectively [36, 89]. These compounds, CO and H₂, in high concentrations lower the initial rate and result in a gradual decrease in reactivity of the char and in the carbon conversion X_a . Reaction mechanisms proposed by different authors [2, 3, 22, 44, 57, 88] include additional steps (reactions) to explain the inhibiting effect of hydrogen and carbon monoxide on the steam and carbon dioxide reactions respectively which are mentioned below. Reactions R12-R16 and reactions R17-R20 can express the reaction mechanism of the R3 and R4 reactions respectively at higher pressures and the reactions R17 and R20 show the formation of CO₂ and CH₄ respectively.



According to the above set of reactions R12-R16, the C(O) and C(CO) concentration on the carbon surface approaches unity and saturation as pressure increases, which means that further increases in pressure will not lead to the formation of more C(O) and C(CO) and the reaction rate will not increase so the impact of pressure will become less significant to independent [68, 89]. It seems that at 3.9 MPa for the dry steam coal and 4.0 MPa for anthracite the carbon surface is saturated with C(O) and C(CO) since the reaction rate is decreased further. A similar phenomenon is occurring with reactions R17-R20 for the carbon steam gasification reaction where the C(O) and C(H₂) concentrations on the carbon surface approaches unity and saturation as pressure increases which means that further increase in pressure will not increase the gasification rate.

This study proves that the reaction rate changes at pressure due to the change of the reaction mechanism and to a different set of reactions occurring at high pressures which agree with other studies [2,3, 58, 45, 60, 85]. This is not in agreement with studies where it is believed that the effects of pressure are more a result of some physical limitation imposed by a property of the char and not due to a fundamental change in the reaction mechanism [67].

6.3.4 Kinetic calculations at pressure

In order to determine which model describes better the behaviour of the two coal chars with CO₂ + H₂O under total pressure, the maximum conversion Xa that was achieved at 1.65 MPa and 1.0 MPa the dry steam coal and anthracite respectively were plotted with the shrinking unreacted core model and the progressive reaction model together with the corresponding experimental data as shown in Figures 6.9 and 6.10.

It can be seen that between the two models the unreacted shrinking core model is the better fit in the chemical reaction control regime. The progressive reaction model exhibited larger deviations than the shrinking core model for both coals. This agrees with other studies [44, 47, 97] which evaluates the experimental results and the operation of the rig.

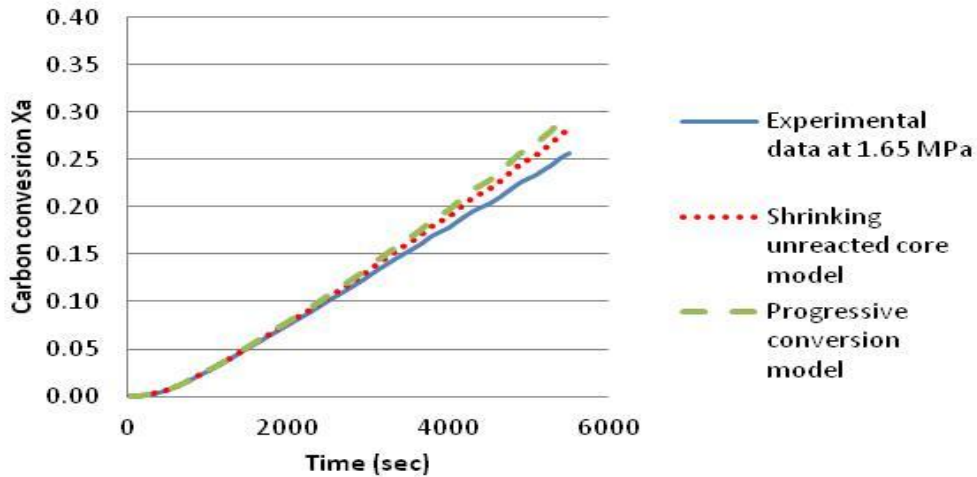


Figure 6.9: Calculated comparison of the conversion X_a at 1.65 MPa and 900 °C of the experimental data with the shrinking core model and the progressive reaction model for the dry steam coal from measured rig data

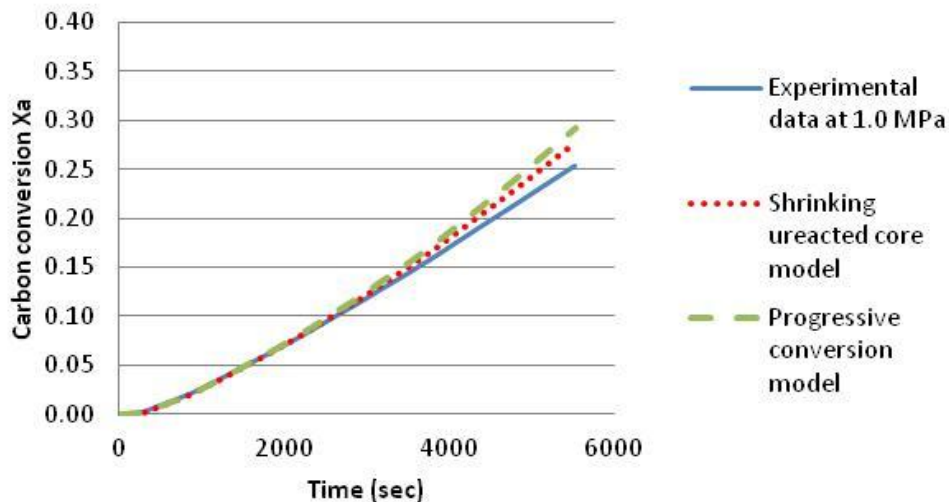


Figure 6.10: Calculated comparison of the conversion X_a at 1.0 MPa and 900 °C of the experimental data with the shrinking core model and the progressive reaction model for the anthracite from measured rig data

The reaction rate according to the shrinking unreacted core model is calculated by integrating Equation 4.7 of k . The reaction constant k can be derived as described in Chapter IV at section 4.5, from the slope of the straight lines in Figures 6.11 and 6.12 as calculated by Ahn et al., (2001) [1] and Goyal et al., (1989) [26] and shown in Tables 6.3 and 6.4 for the dry steam coal and anthracite respectively.

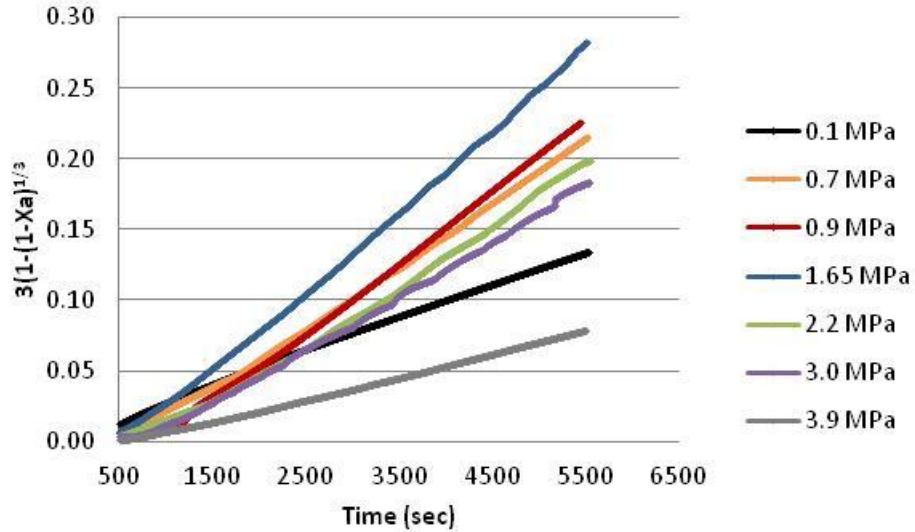


Figure 6.11: Calculated carbon conversion X_a of combustible gases ($\text{CO} + \text{CH}_4$) over time during $\text{CO}_2 + \text{H}_2\text{O}$ gasification of dry steam coal at 0.1, 0.7, 0.9, 1.65, 2.2, 3.0 and 3.9 MPa (900°C , $\text{H}_2\text{O}/\text{CO}_2=2:1$) from measured rig data

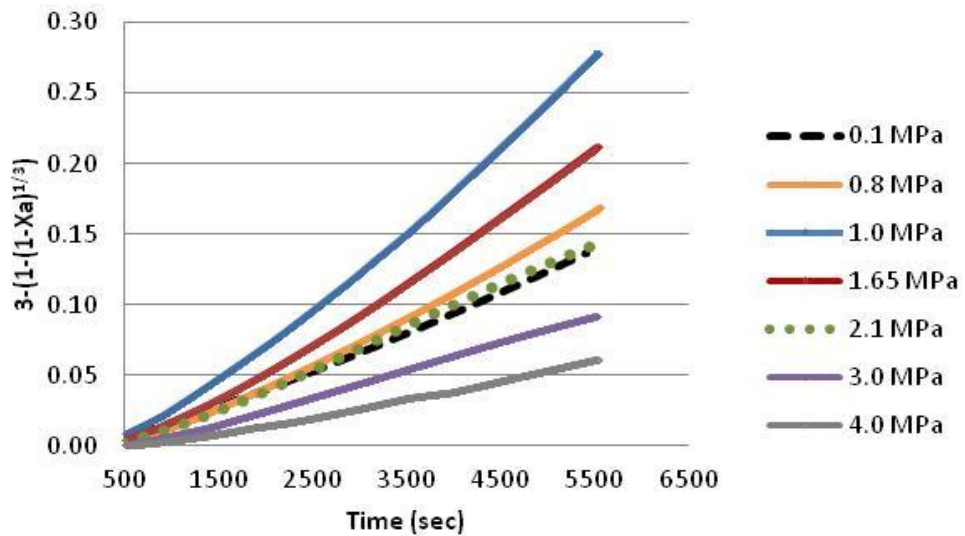


Figure 6.12: Calculated carbon conversion X_a of combustible gases ($\text{CO} + \text{CH}_4$) over time during $\text{CO}_2 + \text{H}_2\text{O}$ gasification of anthracite coal at 1.0, 1.65, 2.1, 3.0 and 4.0 MPa (900°C , $\text{H}_2\text{O}/\text{CO}_2=2:1$) from measured rig data

It can be observed that the reaction constants are very similar for the two coals from atmospheric pressure to 1.0 MPa and that above 1.65 MPa pressure the reaction constant of the dry steam is higher than anthracite. These values are comparable with results published using a thermobalance reactor for substantially smaller samples (-

20 to +40 mesh fraction) where char conversion was undertaken with a mixture of gases (such as CO₂, CO, H₂ and H₂O) at various pressures [26]. Furthermore these values are comparable with results published using a packed bed balance reactor for sample sizes of 0.25-0.42 mm where char conversion was undertaken with single oxidising gases (such as CO₂ and H₂O) in individual reactions [46].

Table 6.3: The values of the reaction constant k for the dry steam coal at various pressures (900°C, H₂O/CO₂=2:1)

Pressure (MPa)	k (sec ⁻¹)
0.1	2.4E-05
0.7	4.1E-05
0.9	4.5E-05
1.65	5.4E-05
2.2	3.9E-05
3.0	3.6E-05
3.9	1.5E-05

Table 6.4: The values of the reaction constant k for anthracite at various pressures (900°C, H₂O/CO₂=2:1)

Pressure MPa	k (sec ⁻¹)
0.1	2.3E-05
0.8	4.0E-05
1.0	5.0E-05
1.65	4.0E-05
2.1	3.0E-05
3.0	2.0E-05
4.0	1.2E-05

An Arrhenius type plot of the reaction constant k as calculated in Ahn et al., (2001) [1] is illustrated in Figures 6.13 for the dry steam coal and anthracite.

It is evident from Figures 6.13 that the reaction rate constant k is increasing as the total pressure increases from 0.1 up to 1.65 MPa for the dry steam coal and 0.1 up to 1.0 MPa for anthracite respectively. Above these pressures the rate constant k is decreasing for both coals.

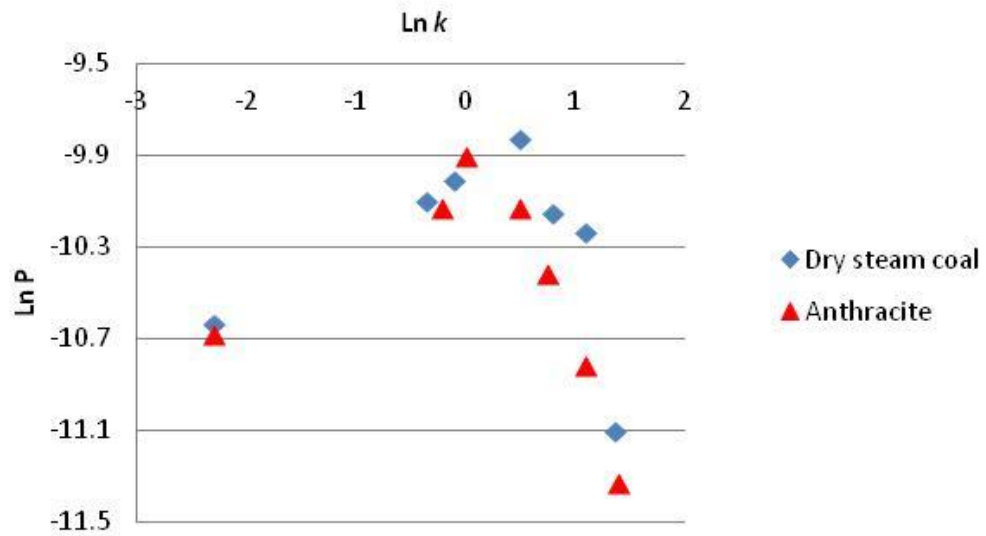


Figure 6.13: Pressure over the reaction constant k for $\text{CO}_2 + \text{H}_2\text{O}$ gasification of dry steam coal char at 0.1, 0.7, 0.9, 1.65, 2.2, 3.0 and 3.9 MPa and anthracite at 0.1, 0.8, 1.0, 1.65, 2.1, 3.0 and 4.0 MPa (900°C, $\text{H}_2\text{O}/\text{CO}_2=2:1$) from measured raw data

In the present study the carbon conversion with time is described as $dXa/dt = k(1-Xa)^{2/3}$ as in other studies [26, 72] which is modified to be $dXa/dt = k P_{\text{total}}^m (1-Xa)^{2/3}$ in order to describe the impact of pressure to the gasification rate as calculated by Ahn et al. (2001) [1]. As shown in Figure 6.13, from the slope of the log-log plot of k versus total pressure the correlation exponent which describes the effect of pressure on the increasing reaction rate of dry steam coal char from 0.1 to 1.65 MPa was found 0.287. So the reaction rate of the dry steam coal with $\text{CO}_2 + \text{H}_2\text{O}$ at 900 °C and total system pressure from 0.1 MPa to 1.65 MPa may be expressed as:

$$dXa/dt = k P_{\text{total}}^{0.287} (1-Xa)^{2/3} \quad (\text{Eq 6.1})$$

Ahn et al., (2001) [1] concludes in his study that due to the fact that the reaction rate coefficient k changes as the total system pressure changes, the value of k is not appropriate to be used at elevated pressures. In this study as shown in Figure 6.13 there is good linearity between the reaction constant k and a pressure range from atmospheric up to 1.65 MPa. For this reason considering the activation energy and the pro-exponential factor that were derived at atmospheric pressure for the dry steam coal in Chapter V, Eq. 6.1 can become:

$$dXa/dt = 5.83 \times 10^4 e^{-(349.63/RT)} P_{\text{total}}^{0.287} (1-Xa)^{2/3} \quad (\text{Eq 6.2})$$

As for anthracite the increasing reaction rate with CO₂ + H₂O at 900 °C and total system pressure from 0.1 to 1.0 MPa, due to good linearity between the reaction constant k and the pressures from atmospheric to 1.0 MPa as shown in Figure 6.13, might be expressed as Eq 6.3. From the slope of the log-log plot of k versus total pressure, the correlation exponent which describes the effect of pressure on the increasing rate of anthracite char from 0.1 to 1.0 MPa was found 0.3. So the increasing reaction rate of anthracite with CO₂ + H₂O at 900 °C and total system pressure from 0.1 to 1.0 MPa may be expressed with the following equation Eq 6.3 but more investigation is needed.

$$dXa/dt = k P_{\text{total}}^{0.3} (1-Xa)^{2/3} \quad (\text{Eq 6.3})$$

By substituting the activation energy and the pre-exponential factor that were derived at atmospheric pressure in Chapter V can be incorporated in Eq 6.4 as follows but again more experimental data is required to evaluate the following equation.

$$dXa/dt = 2.63 \times 10^4 e^{-(406.74/RT)} P_{\text{total}}^{0.3} (1-Xa)^{2/3} \quad (\text{Eq 6.4})$$

The results show that there is positive pressure dependency on the reaction rate under chemical control conditions for both coal chars up to a certain pressure which is 1.65 MPa for the dry steam coal and 1.0 MPa for the anthracite. After these specific pressures the reaction rate is not linear and diminishes (remained below the straight line).

Kajitani et al., (2002) [38] tested the gasification rate of a bituminous char with CO₂ and steam at 1300 °C and total pressures from 0.2 to 2 MPa and found positive pressure dependence only with steam gasification. Ahn et al., (2001) [1] tested the gasification rate of a sub-bituminous coal char with CO₂ at 1300 °C for pressures between 0.5-1.5 MPa and found diminishing gasification rates as pressures increases. This study tested the gasification rates of a dry steam coal and anthracite char for a wider range of pressures than the above mentioned studies, from 0.7 to 4 MPa and found that there is positive pressure dependency but only up to 1.65 MPa and 1.0 MPa for dry steam coal char and anthracite char respectively. The decrease of the gasification rate was explained in Ahn et al., (2001) [1] by the assumption that the

diffusion resistance of reactant gas into the pore structure of char increases as the total system pressure increases since their experiments were run at 1300 °C under both diffusion and chemical control regime II. In this study the experiments took place at 900 °C and under chemical control conditions and the increase and then decrease of the gasification rates can be explained by the adsorption-desorption mechanisms explained previously. In summary it seems that in low pressures up to 1.65 MPa for the dry steam coal and 1.0 MPa for anthracite the number of the active sites is increasing and so is the reaction rate but at higher pressures the number of active sites stops increasing since the carbon surface saturates and for this reason the gasification rate decreases.

6.3.5 Effect of pressure on Carbon Conversion, CGE & LHV

In this section important parameters were calculated which indicate the performance of the coal under pressure during the simulated reduction zone of UCG. These parameters are carbon conversion, CGE and LHV of the produced gas.

6.3.5.1 Carbon conversion X and X_a

Figures 6.14 and 6.15 show the carbon conversion of the dry steam coal and anthracite respectively at 900°C under the flow of CO₂ and steam at different pressures. The data in Figure 6.14 indicates that pressure does not have a significant impact on the carbon conversion X of the dry steam coal with a slight increase between 0.9 and 1.65 MPa at a maximum value of $X = 0.28$, at higher pressures, above 2 MPa the carbon conversion decreases further. Figure 6.15 shows that pressure has almost the same impact on anthracite's carbon conversion X compared to the dry steam coal with the maximum achieved for the 1.0 MPa pressure at a value of $X = 0.27$. Above this pressure the carbon conversion decreases with the highest decrease of 0.16 at 4.0 MPa for anthracite.

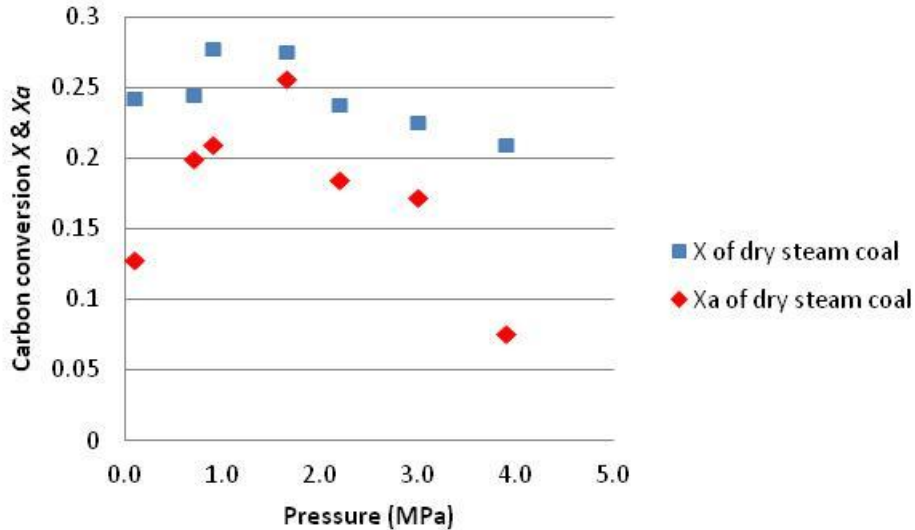


Figure 6.14: Calculated carbon conversion X and Xa at 900°C as a function of pressure for the dry steam ($\text{H}_2\text{O}/\text{CO}_2=2:1$) from measured rig data

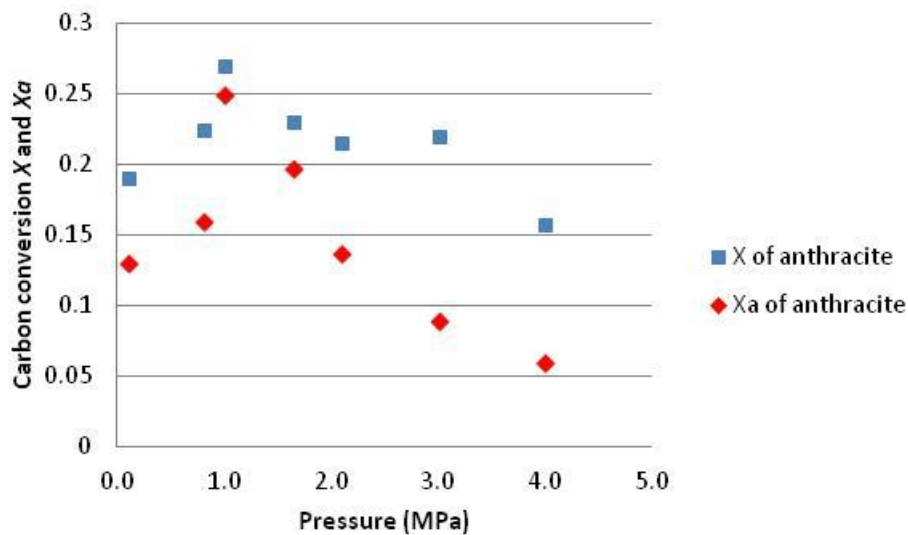


Figure 6.15: Calculated carbon conversion X and Xa at 900°C as a function of pressure for anthracite ($\text{H}_2\text{O}/\text{CO}_2=2:1$) from measured rig data

It is evident in Figures 6.14 and 6.15 that the carbon conversion Xa of combustible gases CO and CH_4 of both coals is affected significantly by pressure (in Figure 6.14 the carbon conversion Xa achieved at all the tested elevated pressures, except the pressure of 3.9 MPa, is higher than that at atmospheric pressure). The maximum Xa achieved for the dry steam coal was 0.26 (0.16/h) at 1.65 MPa pressure which is approximately double than the value of 0.13 achieved at atmospheric pressure.

Furthermore at 1.65 MPa the $X = 0.28$ and $Xa = 0.26$ which means that from 28% of carbon converted to gas, 26% was converted to CO and CH₄ which is a very efficient conversion of 92% of the total carbon converted to gas.

A similar result was also determined for anthracite, as is evident from Figure 6.15, that pressure affects significantly its carbon conversion Xa . The maximum Xa was 0.25 (0.15/h) at 1.0 MPa which means that from 27% of the total carbon converted to gas the 25% was converted to CO and CH₄ which is a similar conversion to the dry steam coal of 92%. The carbon conversion Xa at atmospheric pressure for anthracite was around 0.13 which almost double the value of 0.25 at 1.0 MPa.

Above the pressure of 1.65 and 0.1 MPa for the dry steam coal and anthracite respectively, the Xa decreases with the highest decrease of $Xa=0.08$ achieved at 3.9 MPa for the dry steam coal and for anthracite of $Xa=0.09$ at 4.0 MPa pressure. This result agrees with the decrease of the gasification rate above the pressure of 1.65 MPa for the dry steam coal and 1.0 MPa for anthracite which indicates that the pressure effect saturates and becomes insignificant above the pressure of 3.0 MPa for the dry steam coal and 2.2 MPa for anthracite over the conditions examined here.

It can be concluded that there are no significant differences between the carbon conversions X of the two coals at various pressures. It seems that carbon conversion increases at low pressures but not significantly and above 2.0 MPa for the dry steam coal and 1.65 MPa for anthracite it decreases. Pressure does have a significant impact on the carbon conversion Xa for both coals with the maximum Xa for the dry steam coal at 1.65 MPa and 1.0 MPa for anthracite being double the Xa achieved at atmospheric pressure which is calculated to be 92% of the X total carbon converted to gas for both coals. At pressures above 3.0 and 2.1 MPa for the dry steam coal and anthracite respectively the pressure effect on carbon conversion is less than that achieved at atmospheric pressure so UCG field trials aiming to gasify coal seams at higher pressures will not achieve a better carbon conversion.

Therefore pressure enhances the gas-solid reactions and the contact between gases and coal char and increases the residence time so gases have more time to react up to a certain pressure which is 3.0 for the dry steam coal and 2.1 MPa for anthracite. In addition it was shown that pressurised gasification enhances fragmentation of the

coal sample which enables the transport of gases to the internal surface of the char and hence enhances the gas solid reactions and the carbon conversion Xa .

It can be concluded that anthracite can be as reactive as dry steam coal in terms of carbon conversion X and Xa operating under specific conditions as has been determined in this study. Further discussions will take place on this in the next chapter.

6.3.5.2 LHV of product gas

The LHV of the product gas is presented as a function of pressure in Figure 6.16 and the gas production in mass per kg of coal sample over pressure in Figure 6.17 for the dry steam coal. The data shows that pressure increases the LHV of the product gas of the dry steam coal, with the highest value of 7.8 MJ/Nm^3 (7.5 MJ/Kg) at 1.65 MPa compared to 4.9 MJ/Nm^3 (3.9 MJ/Kg) at 0.1 MPa . The energy embodied in a gas is being converted to an equivalent ratio of 100 W . Figure 6.16 also indicates that the LHV of the product gas had its highest value between 0.9 to 1.65 MPa and it seems that above around 2 MPa the LHV decreases which is in good agreement with the carbon conversion and CGE result.

In addition it is also evident that the CH_4 concentration increases with pressure up to 3.0 MPa as shown in Figures 6.16 and 6.17. Above this pressure it seems that the pressure effect on the CH_4 concentration is insignificant for the dry steam coal. The H_2 concentration also seems to be enhanced at the pressure of 0.9 MPa which is useful information when UCG process is aiming at hydrogen production.

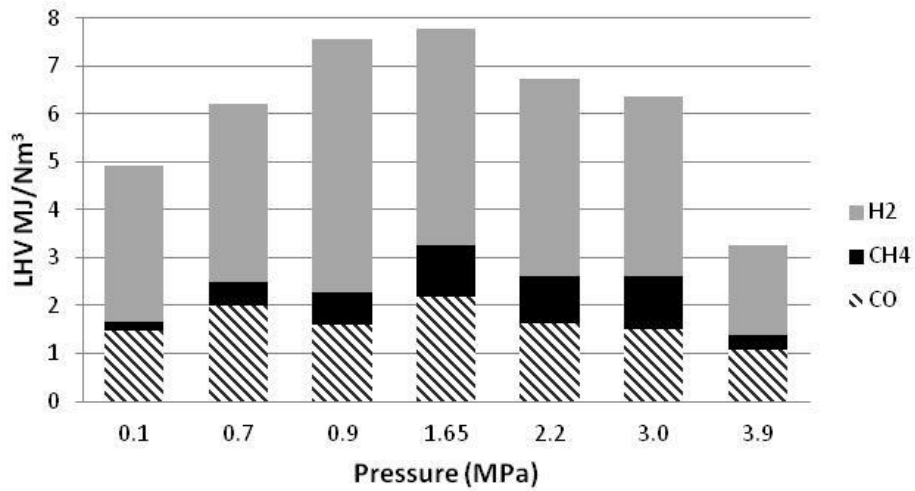


Figure 6.16: Calculated LHV of the gas produced versus pressure during the reduction zone of a simulated UCG process expressed as energy contribution to the overall heating value of the resultant product gas of dry steam coal from measured rig data

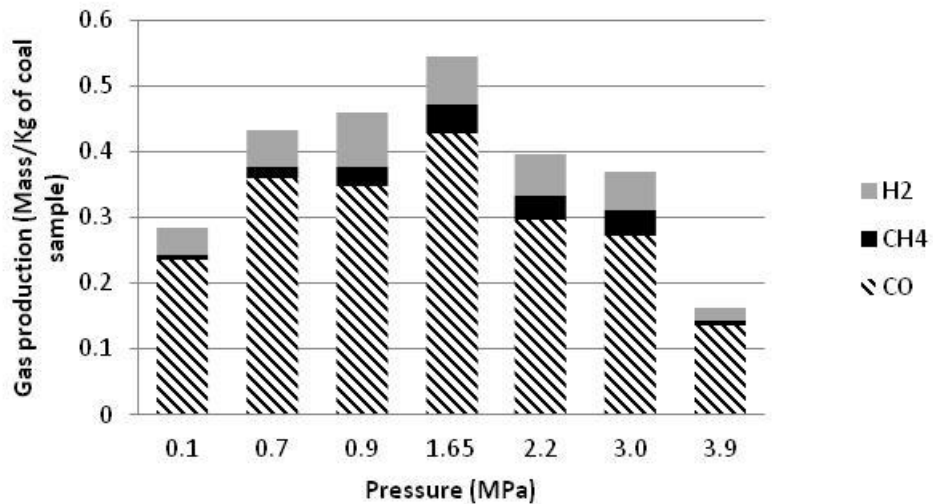


Figure 6.17: Gas production (mass/ kg of coal sample) during gasification of dry steam coal sample for various pressures at 900 °C

The LHV of the product gas of anthracite is also presented as a function of pressure in Figure 6.18 and the gas production in mass per kg of coal sample over pressure in Figure 6.19. It is clear that pressure increases the LHV of the product gas of the dry steam coal with the highest value of 6.0 MJ/Nm³ (4.2 MJ/Kg) at 1.0 MPa compared to 3.4 MJ/Nm³ (2.9 MJ/Kg) at 0.1 MPa. The energy embodied in a gas is being converted to an equivalent ratio of 49 W. Above 1.0 MPa pressure, the LHV

decreases which is in good agreement with the carbon conversion and CGE result. It is also evident that the CH_4 concentration is enhanced with increasing pressure as shown in Figures 6.18 and 6.19 but up to the pressure of 1.65 MPa, above this pressure the pressure the CH_4 concentration is decreasing but is still higher than that at atmospheric pressure.

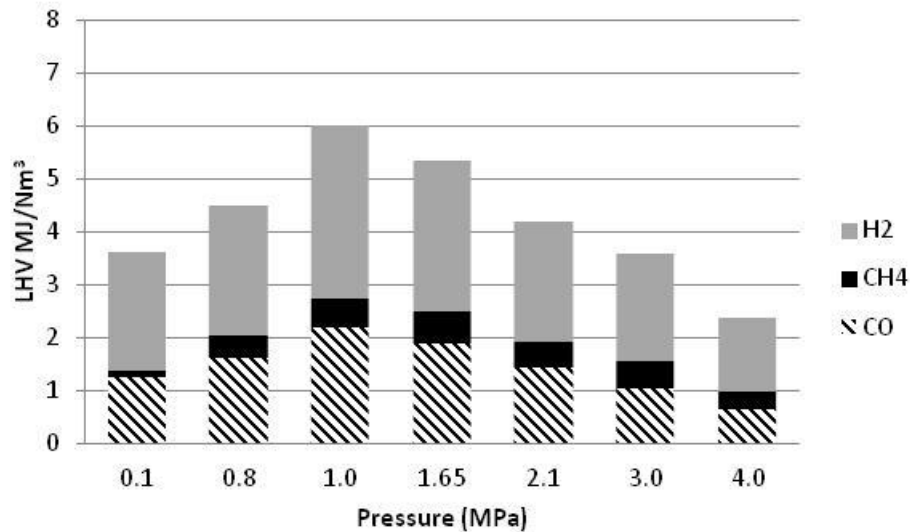


Figure 6.18: Calculated LHV of the gas produced versus pressure during the reduction zone of a simulated UCG process expressed as energy contribution to the overall heating value of the resultant product gas of anthracite from measured rig data

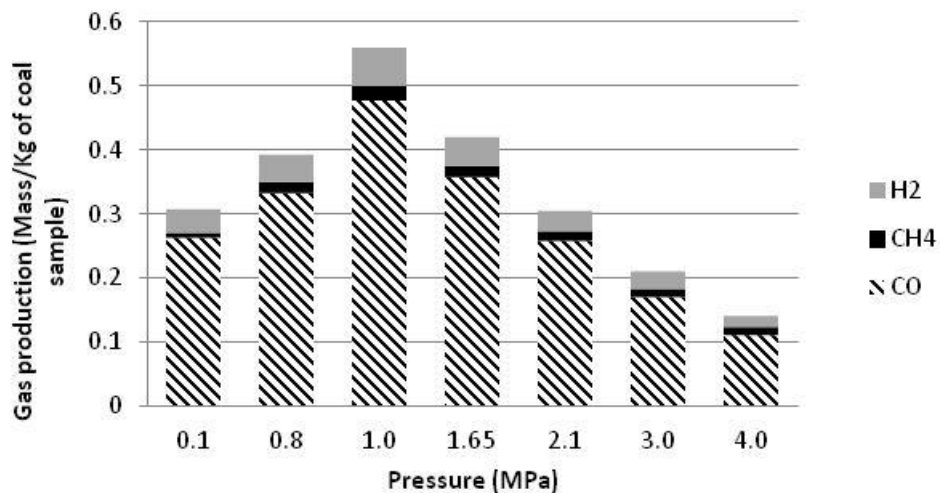


Figure 6.19: Gas production (mass/ kg of coal sample) during gasification of anthracite for various pressures at 900 °C

The LHV of the dry steam coal is higher than that of anthracite mainly due to its higher concentration of H₂ production as shown in Figures 6.16-6.19. This can be explained by the greater number of active sites generated by the C-steam reaction of the dry steam coal char, as a lower rank coal with higher porosity and volatile matter, than anthracite [19]. In addition steam is more reactive with carbon than CO₂ because the hydrogen bonds in the steam molecules are weaker compared to the bonds formed in CO₂ molecules which are double and stronger [22].

It also seems that H₂O and CO₂ do not occur at the same active sites since the carbon conversion Xa of both coals is very similar as shown previously and the H₂ concentration in their product gas of dry steam coal is higher than that of anthracite. This is in agreement with a study where it was found that the reactions of char with CO₂ and H₂O occur simultaneously on separate sites [22].

Finally it is evident from Figures 6.16-6.19 that the dry steam coal is reactive to a wider range of pressures than anthracite which agrees with the carbon conversion, CGE and gasification reaction rate result

6.3.5.3 Cold Gas Efficiency

The CGE is presented as a function of pressure in Figure 6.20. It is evident that pressure enhances the CGE and the performance of the UCG process. The maximum cold gas efficiency was achieved for the dry steam coal for the range of pressures between 0.9 to 1.65 MPa and above around 2.0 MPa the CGE decreases with the highest decrease achieved at 4.0 MPa. The maximum CGE for the dry steam coal char was measured at 39% over the range of conditions tested, which implies that around 39% of the available chemical energy of the char is converted to combustible gas per hour during this simulated reduction zone of a UCG cavity for the dry steam coal.

For the anthracite char it seems that CGE is also increased at low pressures up to 1.0 MPa with a maximum value of 32% which decreases beyond that pressure. The impact of pressure on the CGE is insignificant at pressures higher than 3.0 MPa for the dry steam coal and 2.1 MPa for anthracite. The maximum CGE of dry steam coal is higher than that of anthracite and the reason for this is because the H₂ concentration produced during gasification of the dry steam coal is higher, as

discussed previously and shown in Figures 6.16-6.19, which increases the LHV of the product gas and hence the CGE.

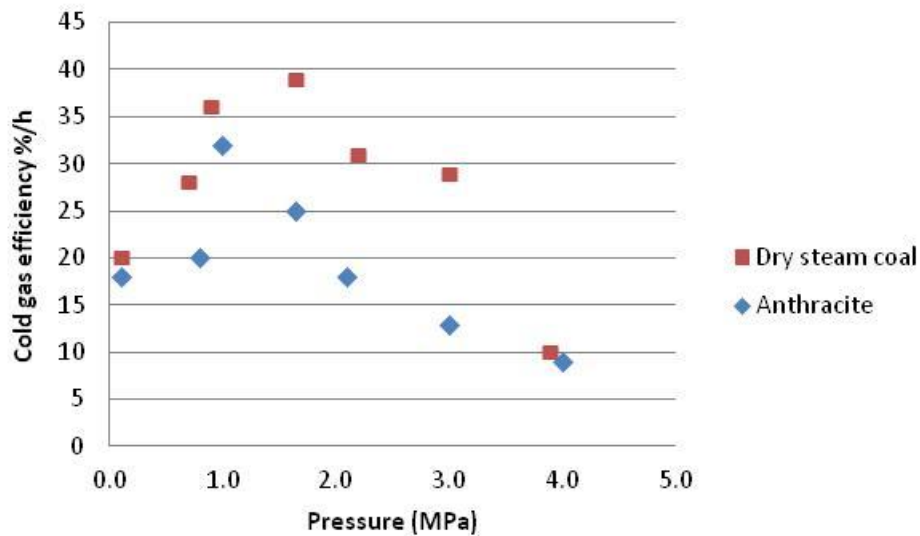


Figure 6.20: Calculated CGE as function of pressure at 900 °C for both coal chars from measured rig data

Figure 6.21 presents the CGE determined by gasifying 1 kg of each coal operating under the specific conditions determined in this study. The maximum CGE was achieved at 32% for the dry steam coal which means that the energy content in the produced gas is 32% of the energy in the parent coal after gasification of the dry steam coal with $\text{CO}_2 + \text{H}_2\text{O}$ at 1.65 MPa and 900 °C. Similarly for anthracite the maximum CGE was achieved at 27% for the 1.0 MPa and 900 °C. These results agree with the previous results of carbon conversion, LHV and CGE.

The determined CGE of the coals and chars can provide information about the efficient performance of a UCG project and the required coal resources for a specific power plant. Further discussions will take place on this in the next chapter.

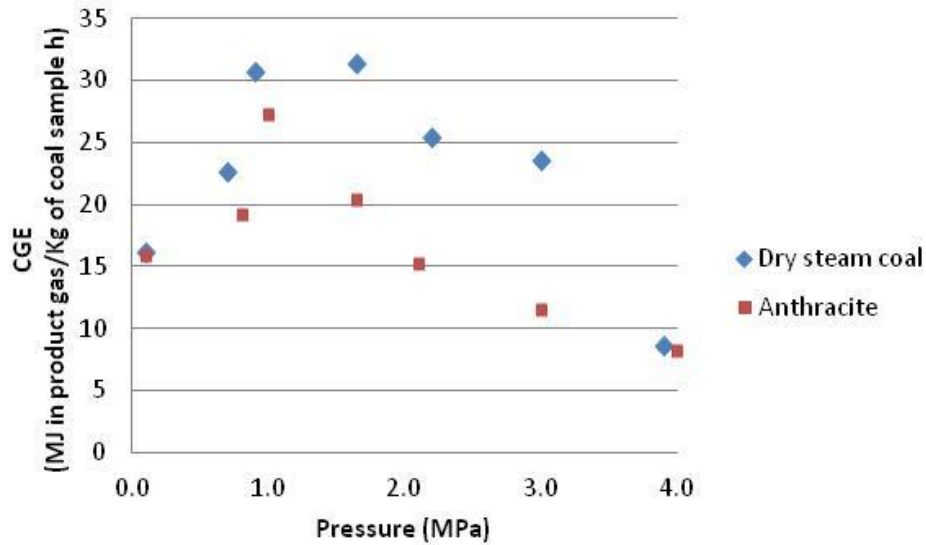


Figure 6.21: Calculated CGE as function of pressure at 900 °C for both coals from measured rig data

6.4 Comparison with other studies at pressure

It can be concluded that the chemical kinetics are improved with pressure resulting in a product gas with a LHV higher by more than 50% than that at ambient pressure in the reduction zone of UCG. This can be explained mainly by the improved contact of gases with carbon under pressure due to the longer residence time, resulting in higher concentrations of combustible gases. But it was also shown that the higher the pressure does not also increase the LHV of the product gas. It seems that there is an optimum operating pressure which produces the maximum carbon conversion X and Xa , CGE and LHV of the product gas which differs for each coal. Therefore UCG projects aiming at going to higher pressures will not achieve an increase in the output for these types of coals.

The above finding in this study agrees with a semi industrial test conducted with a coking coal (60% F.C 16% V.M., LHV 26 MJ/kg) gasified with O_2 -enriched and steam, aiming to investigate the effect of cyclically changing the operational pressure in terms of the composition of the product gas [90]. The highest concentration of H_2 and CO was produced for the pressure of 0.8 MPa and the heating value of the syngas and the gasification rate was increased compared with the fixed pressure operation. The gas composition at pressures of 0.2, 0.4, 0.6, 0.8, 1.0 and 1.2 MPa was 15-25% CO, 5-8% CH_4 and 10-30% H_2 which is in good agreement with the gas

composition produced at pressures in this study for CO and H₂ during gasification of dry steam coal with CO₂ and H₂O as shown in Table 6.1 and Figure 6.1. The concentration of CH₄ is lower in the present study because CH₄ is mainly outgassed during the pyrolysis stage (Table 6.1), which was not considered in the research herein.

Also there are numerical studies predicting the gas composition of the UCG process where the increase in pressure has always a positive impact on the coal gasification [17, 27, 28, 64, 89] by using the Grashof number (which determines the rate of mass transfer from the bulk gas to coal surface) which is proportional to temperature and to the square of pressure. Numerical studies modeled mass transfer from the bulk gas to the coal wall using a correlation for natural convection and hence using the Grashof number which is significant in flow due to natural convection [63]. Maybe this is appropriate only for low rank coals since there is no evidence of saturation of the effect of pressure for low rank coals as it is for high rank coals [49], which is in agreement with this study.

6.5 Chapter Summary

Pressure enhances the chemical kinetics and so the efficient energy conversion of coal to gas because it increases the heating value, carbon conversion, CGE and gasification rate of the dry steam coal and anthracite. It seems that there is an optimum operating pressure which produces a peak in carbon conversion X and Xa , CGE and LHV of the product gas, over the conditions tested which differs for each coal. Therefore UCG projects aiming at going to higher pressures will not achieve an increase in the output for these types of coals - unless there are some new effects occurring above 4 MPa.

The optimum reduction conditions determined for the dry steam coal were H₂O / CO₂ = 2:1 (H₂O / O₂ = 2.4:1), 900°C at 1.65 MPa. Under such conditions the product gas consists by volume of 17% CO, 3% CH₄ and 42% H₂ with a LHV of 7.8 MJ/Nm³ and 7.5 MJ/kg. The maximum carbon conversion was 0.28 (in 90 minutes at steady state) of which 0.26 (0.16/h) are CO and CH₄ and the maximum CGE was 39%. As for the anthracite the maximum LHV of 6 MJ/Nm³ was achieved at 1.0 MPa with H₂O / CO₂ = 2:1 (H₂O / O₂ = 2.4:1) at 900°C. The gas composition

consists by volume of 17.3% CO, 1.6% CH₄ and 30.4% H₂. The maximum carbon conversion was 0.27 (in 90 minutes at steady state) of which 0.25 are CO and CH₄ and the maximum CGE was 32%. These findings can provide information about the efficiency performance of a UCG project and the required coal resources for a specific power plant.

It should be noted that the results have allowed for the consistent analysis of the reduction processes, which yield combustible products directly from the solid phase char. This does not include the contribution of the volatile matter, hence this has in part demonstrated that typical UCG operations on low rank coals provides a combustible syngas product that relies heavily on releasing the volatile matter from the coal.

It can be concluded that there are no significant differences between the carbon conversions X of the two coals at various pressures. It seems that carbon conversion increases at low pressures but not significantly and above 2.0 MPa for the dry steam coal and 1.65 MPa for anthracite it decreases. Pressure does have a significant impact on the carbon conversion Xa for both coals with the maximum Xa for the dry steam coal at 1.65 MPa and 1.0 MPa for anthracite being double the Xa achieved at atmospheric pressure which is calculated to be 92% of the X carbon converted to gas for both coals. At pressures above 3.0 and 2.1 MPa for the dry steam coal and anthracite respectively the pressure effect on carbon conversion is lower than the carbon conversion achieved at atmospheric pressure. So UCG field trials aiming to gasify coal seams at higher pressures will not achieve a better carbon conversion.

Therefore pressure enhances the gas-solid reactions and the contact between gases and coal char and increases the residence time so gases have more time to react up to a certain pressure which is 3.0 for the dry steam coal and 2.1 MPa for anthracite. In addition it was shown that pressurised gasification enhances fragmentation of the coal sample which enables the transport of gases to the internal surface of the char and hence enhances the gas solid reactions and the carbon conversion Xa .

Pressure maximises the H₂ production with a maximum measured concentration of 49% Vol at 0.9 MPa for the dry steam coal and 30.4% Vol at 1.0 MPa for the anthracite. At higher pressures it appears that the effect of pressure saturates and only the CH₄ production is favoured with a maximum of 3% Vol for the dry steam

coal and 1.8% Vol for the anthracite at 3.0 MPa. This is explained by the change in the reaction mechanism. At low pressures there is a two step adsorption-desorption reaction mechanism that enhances the process up to 1.65 MPa for the dry steam coal and 1.0 MPa for the anthracite by increasing the active sites on the carbon surface. At higher pressures up to 3.0 MPa the mechanism changes by different set of reactions occurring producing CO₂ and CH₄ and the gasification rate is decreasing. At 3.9 and 4.0 MPa for the dry steam coal and anthracite respectively the reaction rate decreases further and it seems that there is a negative pressure dependency.

There is positive pressure dependency on the gasification rates Xa of a dry steam coal and anthracite char for the tested pressures but only up to 1.65 MPa for dry steam coal and 1.0 MPa for anthracite. This effect saturates at higher pressures at the range of 3.0 MPa and reduces more at further higher pressures around 4.0 MPa. In this study the experiments took place at 900 °C under chemical control conditions and the increase of the gasification rates can be explained by the adsorption-desorption mechanisms as explained above. At higher pressures such as at 2.2 and 3.0 MPa for the dry steam coal and 1.65, 2.1 and 3.0 MPa for anthracite, the formation of CO₂ and CH₄ has been observed from reactions R3 and R4 respectively as well a decrease of CO and H₂ concentrations. This can be explained by the inhibiting effect of hydrogen and carbon monoxide on the steam and carbon monoxide reactions respectively [36, 88]. It seems that these compounds, CO and H₂, lower the initial rate and result in a gradual decrease in reactivity of the tested chars.

The shrinking unreacted core model was modified to take into account the effect of total pressure to the gasification rate of the two coals tested under the flow of CO₂+H₂O at 900 °C and elevated pressures ranged from 0.7 to 4.0 MPa. The reactions constants k were also calculated at different pressures for the two coals and could be useful data for modelling of coal gasification at elevated pressures. The reaction rate of the dry steam coal with CO₂ + H₂O at 900 °C and total system pressure from 0.7 to 1.65 MPa may be expressed as $dXa/dt = k P_{\text{total}}^{0.287} (1 - Xa)^{2/3}$ or as $dXa/dt = 5.83 \times 10^4 e^{-(349.63/RT)} P_{\text{total}}^{0.287} (1 - Xa)^{2/3}$ due to the good linearity between the reaction constant at atmospheric pressure and those at 0.7 to 1.65 MPa.

As for anthracite the increasing reaction rate with $\text{CO}_2 + \text{H}_2\text{O}$ at $900\text{ }^\circ\text{C}$ and total system pressure from 0.1 to 1.0 MPa, due to good linearity between the reaction constant k and the pressures from atmospheric to 1.0 MPa might be expressed with the following equation but more investigation is needed.

$$dXa/dt = k P_{\text{total}}^{0.3} (1 - Xa)^{2/3} \text{ or as } dXa/dt = 2.63 \times 10^4 e^{-(406.74/RT)} P_{\text{total}}^{0.3} (1 - Xa)^{2/3}$$

It seems that anthracite can be as reactive as the dry steam coal in terms of carbon conversion X and Xa operating under specific conditions as shown in this study, and can produce almost the same amount of combustible gases, CO and CH_4 , as the dry steam coal. However the LHV of anthracite is lower than that of dry steam coal mainly due to the lower H_2 concentration produced during gasification because anthracite has fewer pores available and hence less active sites for the gases to react with. This also affects its CGE which is also lower than that of dry steam coal, nevertheless if anthracite is not suitable for a UCG producing energy it is certainly suitable for hydrocarbons production which is currently needed and certainly more in the near future.

CHAPTER VII

ENERGY AND MASS BALANCE IN ORDER TO DEMONSTRATE PRACTICAL FEASIBILITY OF REAL UCG OPERATIONS

7.1 Introduction

The purpose of this chapter is to evaluate the experimental results of this study and the operation of the bespoke high pressure high temperature rig using a mass and energy balance which was developed. In addition the data of this study is compared with the data from UCG field trials and parameters which determine the performance of the UCG process such as are carbon conversion, CGE and LHV of the product gas are discussed. Finally the LHV and CGE determined in this study are used to calculate the output of small and large potential UCG power plants in order to demonstrate practical feasibility of real UCG operations. Information about the required coal resources and the size of the UCG models are also provided.

7.2 Mass and energy balance

The purpose of the mass and energy balance is to calculate how much mass and energy are spent during gasification of the simulated reduction zone of UCG and also how much mass and energy are left in order to evaluate the experimental results. The experimental conditions and results that will be used for the mass and energy balance will be those determined for the experiment presented in Figure 5.1d) in Chapter V which was performed at 900° C and 0.1 MPa.

7.2.1 Energy balance

Figure 7.1 illustrates the energy balance through a Sankey diagram which is explained in the following paragraph. The calculations are presented in Appendix B.1.

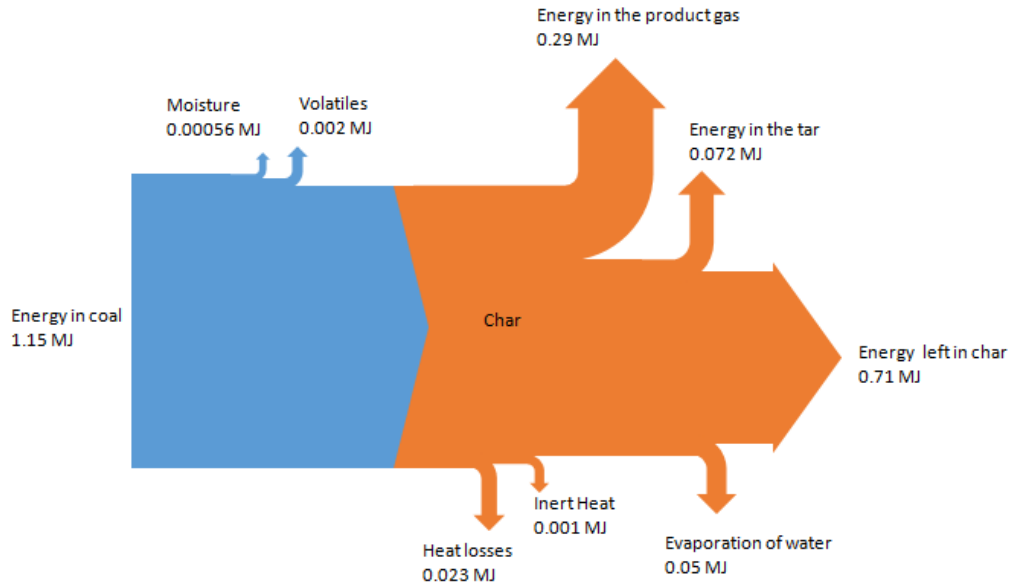


Figure 7.1: Energy balance of the experimental process presented in a Sankey diagram

Considering the 35.58 g of coal sample and the heating value of the coal the input energy is 1.15 MJ/kg. When the temperature starts increasing above 100° C, drying of the coal takes place and the moisture in the coal is released. As the temperature increases above 300° C, devolatilisation occurs and the volatiles in the coal are released. The energy that is needed for those two processes to occur is 0.00056 MJ for the drying and 0.002 MJ for devolatilisation (per 36 g). The energy that is left in the coal for gasification is 1.147 MJ which is the heating value of the created char.

When the temperature reaches 900° C, then 0.4 l/min of CO₂ is introduced in the reactor for 92 min and then 1.26 g/min of water. The injected water is 112.14 g and the water that comes out is 89.7 g, hence the energy needed for the evaporation of the consumed water is $(112.14-89.7) \times 22.6 \text{ MJ/kg}=0.05 \text{ MJ}$ where 22.6 MJ/kg is the heat of water evaporation.

Also the energy that is consumed by heating the ash is calculated at 0.001 MJ and the heat losses to the environment through conduction are 0.023 MJ where 10% additional heat losses from convection and radiation are included, as calculated in Appendix B.2.

In addition the energy consumed by the liquid volatiles (tar) and the light hydrocarbons is calculated as $0.002 \times 36 = 0.072$ MJ, where 36 MJ/kg is the heating value of the tar and 0.002 kg is the approximately weight of the tar and the light hydrocarbons. The calculations are shown in Appendix B.3.

Finally the energy that is left in the 0.224 g of char after 92 minutes of gasification is $0.224 \times 31.5 = 0.71$ MJ. By performing energy balance the calculated energy in the product gas is derived at around 0.29 MJ. The LHV of the product gas determined from the experiment was found as 3.87 MJ/kg of product gas and the mass of the product gas was 75g, therefore the energy in the product gas is calculated as $0.075 \times 3.87 = 0.29$ MJ which is the same as the 0.29 MJ of energy in the product gas calculated from the energy balance.

7.2.2 Mass balance

Figure 7.2 represents the mass balance in a Sankey diagram which is explained below.

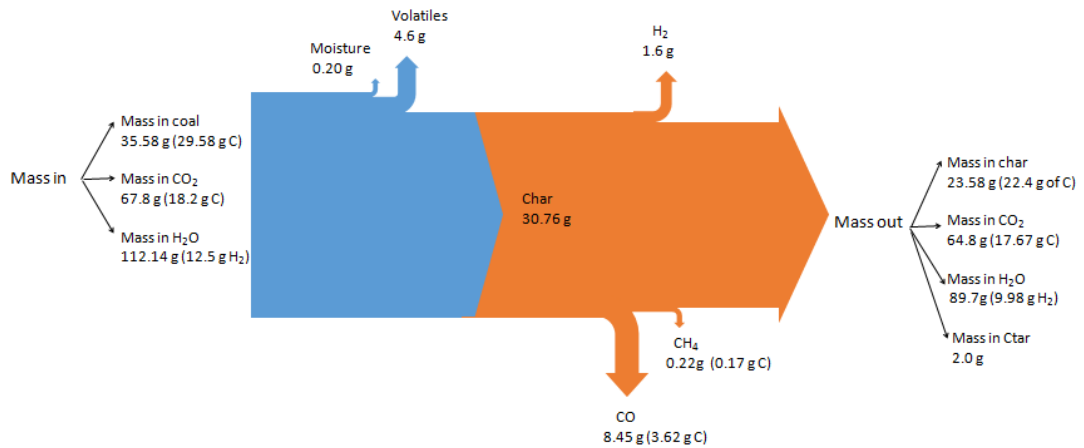


Figure 7.2: Mass balance of the experimental procedure presented in a Sankey diagram

The inlet mass consists of the 35.58 g mass of coal sample plus the mass of CO₂ injected which is 67.8 g (18.2 g of C) and the mass of H₂O (12.5 g of H₂) which is 112.14 g as shown in Figure 7.2.

Through the drying and devolatilisation of the coal moisture and volatiles are released which are 0.20 g and 4.6 g respectively. Subtracting the masses of volatiles and moisture from the mass of coal leaves the mass of char with ash which is 30.76 g ($35.58 - 0.20 - 4.6 = 30.76$ g).

The char reacts with the gases and produces 8.45 g of CO (3.62 g of C), 0.22 g of CH₄ (0.17 g of C) and 1.6 g of H₂ as calculated from the experiment.

The masses of CO₂ and H₂O that were produced are 64.8 g (17.67 g of C) and 89.7 g (9.98 g of H₂) respectively.

The mass of char that was left after the experiment weighed 23.58 g (22.4 g of unreacted char + 1.18 g ash).

The C in tar and the light hydrocarbons is calculated approximately 2 g. The calculations are shown in Appendix B.3.

By calculating the mass balance of carbon, the mass of C that goes in is 47.78 g ($18.2 + 29.58 = 47.78$ g) and the mass of C that comes out is 45.86 g ($17.67 + 3.62 + 0.17 + 22.4 + 2.0 = 45.86$). Similarly by calculating the mass balance for the H₂, the mass of H₂ that goes in is 12.5 g and the mass of H₂ that goes out is 11.64 g ($9.98 + 1.6 + 0.055 = 11.64$ g).

Finally it can be concluded that there is good agreement between the calculated and the experimental values of mass and energy balances of the experimental process and the small differences are within the boundaries of experimental error.

It is evident that the gas composition produced during the experiments with the dry steam coal and anthracite is due to the reactions of gasified chars with the oxidant gases under specific conditions during the simulated reduction zone of UCG.

7.3 Application of data to UCG field trials

This section compares the gas composition produced during the experiments with the gas composition produced from field trials performed under similar operational conditions to those used in the experiments.

In this study it was found that the highest carbon conversion for the dry steam coal and anthracite was achieved at 28% and 27% respectively during the reduction zone

which means that around 72% of the char was not gasified. In order to determine the C which oxidises at the oxidation zone of a UCG process, the enthalpy of the reactions 1-4 has been considered and it was found that out of 1 kg of char, 0.31kg of char needs to be combusted in order to gasify the rest 0.68 kg ($1-0.31=0.68$ kg) of char as shown in Appendix B.4. This means that for this study, the char combusted during the oxidation zone should be around 12% stoichiometric for both coals, which means that the amount of char affected (combusted and gasified) or the carbon converted is 40% and the char left is 60% for these type of coals. The carbon conversion during the devolatilisation of the dry steam coal and anthracite was determined at around 2% in Chapter V, which makes the total carbon conversion for both coals 42%.

Considering the data from the Rocky Mountain 1 field trial (where oxygen and steam were the oxidants) [5, 15] and the El Tremedial field trial (where oxygen and nitrogen were the oxidants) [10] the carbon conversion was calculated as 54% (coal type 32% F.C, 32% V.M., HV=20 MJ/kg) and 55% (coal type 36% F.C, 27.5% V.M., HV=18 MJ/kg) respectively [10, 27]. It must be borne in mind that these field trial values were achieved by including the volatile coal components and was reacted over 3 months for Rocky Mountain 1 and 12.1 days for El Tremedial. These field trials indicated that the carbon converted was approximately around 55% which means that 45% of char was left underground. It seems that carbon conversion is not significantly affected by the type of coal and that the carbon converted during UCG is between approximately 45% for high rank coals, as determined in this study, up to 55% for low rank coals as calculated from field trials data. This means that approximately 45 to 55% of char is left underground and that the carbon conversion seems not to be as high as reported for some field trials, around 95% [82].

The maximum LHV of the product gas as measured in this laboratory investigation was found to be 7.5 MJ/kg at 1.65 MPa. Making an assumption that if the gases produced during oxidation and the volatile fraction released during typical UCG operations were included, this coal would provide an LHV of around 10 MJ/kg [64] and hence the resultant CGE becomes around 45% -50%. The dry steam coal tested had an LHV of 32 MJ/kg (V.M=13%, F.C=83.2%), which is somewhat different to the coals used in the field trials under consideration. If the tested coal had the same

LHV as in the Rocky Mountain 1 field trial (HV=20 MJ/kg) and the El Tremedral field trial (HV=18 MJ/kg) then the resulting CGE would have been 60 and 66% respectively [40]. Low rank coals with comparatively low heating values and high volatile matter content tend to have a high CGE, but it should be borne in mind that the presence of volatile matter in UCG product gas is contributing significantly to the predicted CGE from the process, when compared with the conversion of fixed carbon to CO and CH₄.

Figures 7.3 and 7.4 presents a comparison between the gas compositions of this study with the gas composition of field trials operated at similar pressures. In Figure 7.3 plots the gas composition (mole %) of the Centralia field trial [10] and Rocky Mountain 1 [15] which were run at an operating pressure of 0.37 - 0.43 MPa and 0.5-0.7 MPa respectively with oxygen and steam used as oxidants, alongside a plot of the gas composition produced at the reduction zone of this study by gasifying the dry steam coal and anthracite with CO₂ and steam at 0.7 and 0.8 MPa respectively. Furthermore in Figure 7.4, the gas composition of El Tremedal [10] (operating pressure of 5.4 - 5.6 MPa with oxygen and nitrogen as oxidants) is plotted together with the gas composition of the product gas of this study produced by gasifying the dry steam coal and anthracite with CO₂ and steam at 3.9 and 4.0 MPa respectively.

It can be noted from both Figures 7.3 and 7.4 that the concentrations of CO and H₂ of this study are comparable with those in the field trials, which reinforces the fact that the majority of the product gas, CO and H₂, is produced during the reduction zone. The concentration of CH₄ of this study is very low compared to the concentration of CH₄ of the field trials which can be explained by CH₄ being mainly produced during the pyrolysis zone [11, 28].

It should be noted that the results have allowed for the consistent analysis of the reduction processes, which yield combustible products directly from the solid phase char. This does not include the contribution of the volatile matter, hence this has in part demonstrated that typical UCG operations on low rank coals provides a combustible product gas that relies heavily on releasing the volatile matter from the coal.

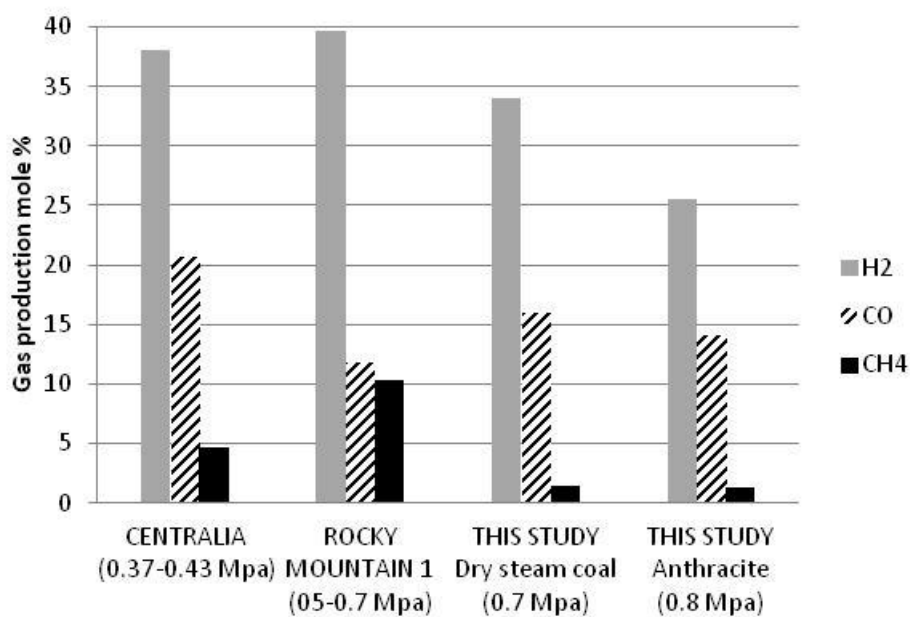


Figure 7.3: Gas composition of Centralia field trial, Rocky Mountain 1 field trial together with the study of the dry steam coal at 0.7 MPa and anthracite at 0.8 MPa

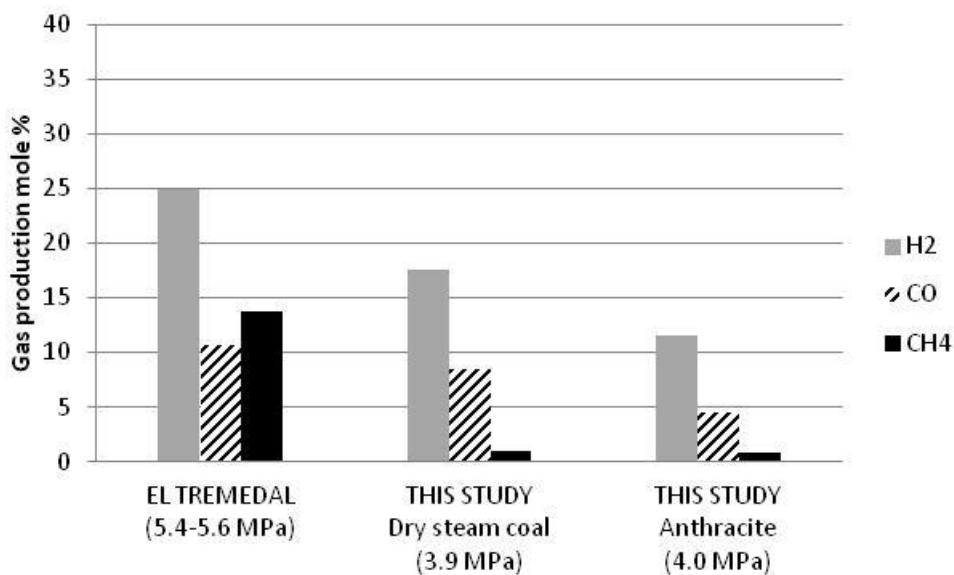


Figure 7.4: Gas composition of El Tremedal field trial together with the study of the dry steam coal at 3.9 MPa and anthracite at 4.0 MPa

7.4 Commercialisation of UCG

In this section the experimental data from this study will be used to calculate the output of a potential UCG project and determine information for a potential UCG power plant including the size and the required coal resources for this specific power plant. This initial information about a UCG project could enable industry to decide whether a UCG project is feasible.

7.4.1 Advance drilling technology (CRIP method)

Every UCG project is planned for an end user which is usually a power plant. But in order for any UCG project to be assessed as feasible and economically viable it needs to be commercial, which means that it needs to be able to provide the required amount of product gas to the power plant at steady state so that the power plant can produce the required amount of energy. This commercialisation can be achieved with the Controlled Retracting Injection Point (CRIP) method [79, 84].

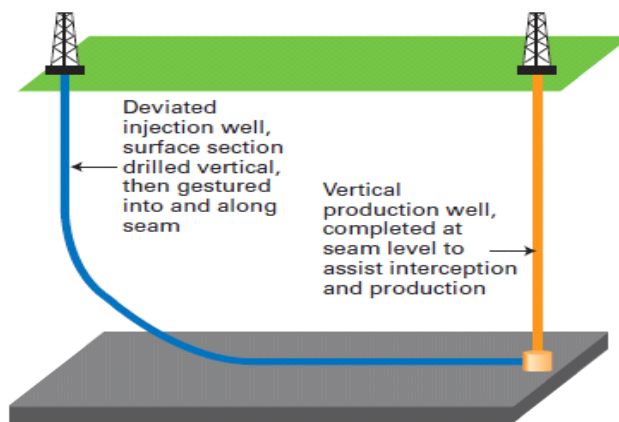


Figure 7.5: Schematic of the CRIP method [16]

With the CRIP process, the production well is drilled vertically, and the injection well is a deviated, curved well through the overburden and into the coal seam which connects to the production well, as shown in Figure 7.5 [16].

Once the channel is established, a gasification cavity is initiated at the end of the injection well in the horizontal section of the coal seam by the use of an attached burner which is used to burn through the borehole casing and ignite the coal [15, 18].

When the coal near the cavity is used up, the injection point which can be moved to any desired location in the injection well, is retracted and a new gasification cavity is initiated upstream and gasification is carried out with a succession of cavities as shown in Figure 7.6. The product gas passes through the used cavities and over an increasing distance as the CRIP is withdrawn before reaching the vertical production well. [12, 16].

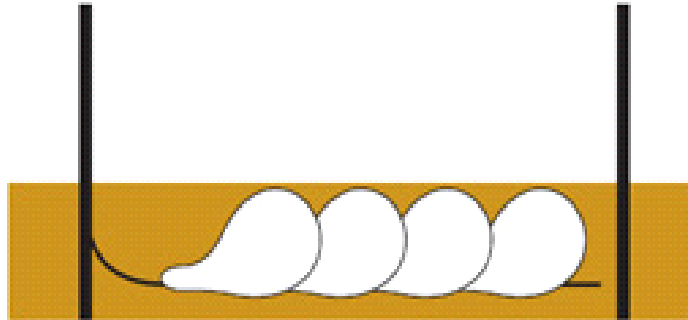


Figure 7.6: Multiple gasification cavities produced by the CRIP technique [16]

7.4.2 UCG model

For a commercial UCG project the coal is gasified by panels which are parallel and operate simultaneously (Figure 7.7). Each panel consist of a number of modules as shown in Figure 7.8, these modules simulate the successive cavities discussed previously.

The panels are gasified with the CRIP method which allows multiple gasification cavities to be created from a single injection borehole such that the maximum volume of coal is gasified between the two wells. Also in this manner, precise control over the progress of gasification is obtained [12, 15, 16].

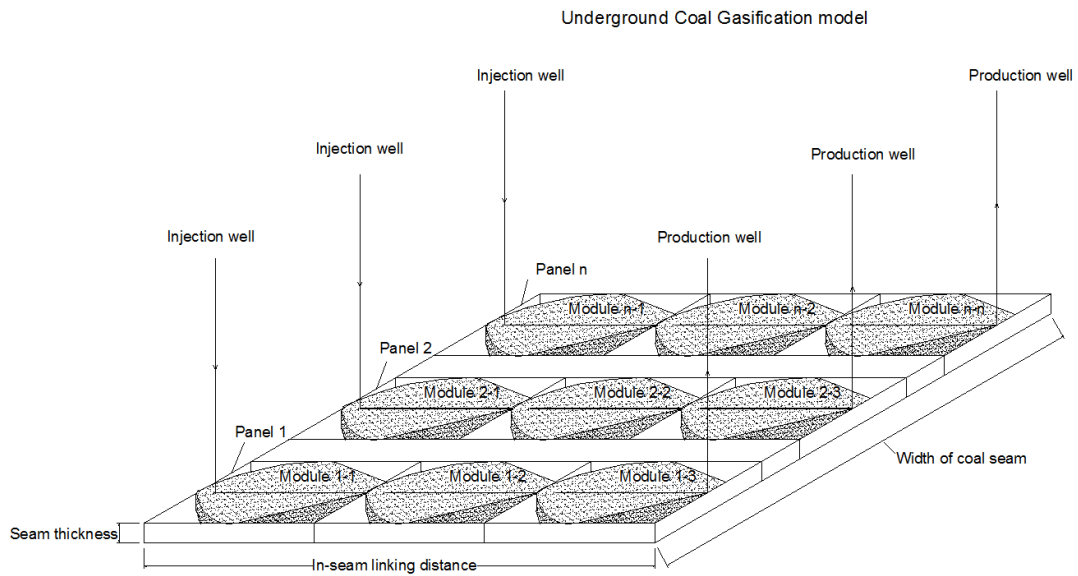


Figure 7.7: UCG model underground by employing the CRIP method

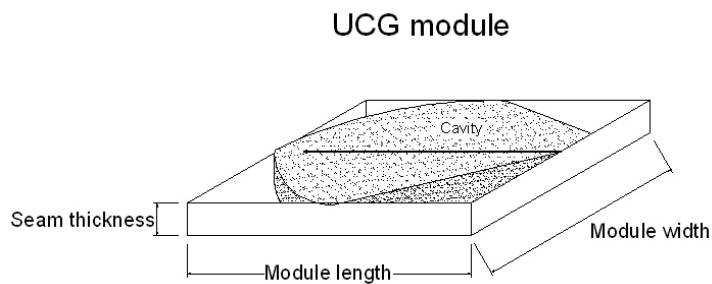


Figure 7.8: UCG module

The in-seam linking distance shown in Figure 7.7 is the distance between the injection and the production well of each panel which can be up to 3000 m since the in-seam drilling technology is well developed. The coal seam thickness needs to be between 2 to 10 m according to DTI criteria (2001). Between the panels there are coal seam pillars to reduce the amount of surface subsidence as shown in Figure 7.7. These pillars are considered in the sweep efficiency which is a factor determining the total coal resources required for a UCG project with a value between 40-60% [12]. The total coal resources required can be calculated by the following formula:

Total coal resources required = Affected (gasified) coal + ungasified coal in the cavities + coal of the pillars = Affected coal / sweep efficiency.

For an average sweep efficiency of 0.5 the total coal resources is equal to Affected coal x 2. In this study it was determined that the carbon conversion during UCG was found approximately between 42% for high rank coals to 55% for low rank coals which means that around 45 to 58% of char is left underground (ungasified) which is in agreement with the values of sweep efficiency.

7.4.3 Coal resources gasified per panel and energy produced by panel

The Review of feasibility of UCG in the UK [16] presented the outputs of a 120 MWth \approx 50 MWe and 720 MWth \approx 3000MWe power plants operated for 20 years. The gasified coal resources required were 5.4 Million tonnes for the 120 MWth and 19.6 Million tonnes for the 720 MWth power plant and it was calculated that for both power plants each panel needs to gasify around 112 t of coal/day. This means that each panel provides around 18 MWth and 30 MWth of energy for small and large UCG power plants respectively.

In addition it was calculated that each panel gasified around 815,000 to 820,000 t of coal in 20 years of the power plants operation. Also the company Carbon Energy stated that for their proposed Blue Gum Gas Project around 40 panels of 500 metres long x 30 meters wide will be required to generate 25 PJ of syngas per annum, based on their experience with their demonstration project at Bloodwood Creek in Australia. It was calculated that to produce 25 PJ/year \approx 792 MWth \approx 330 MWe with 40 panels, then each panel needs to produce $792/40=20$ MWth, this agrees with the Review of feasibility of UCG in the UK.

It can be concluded that the amount of coal gasified per panel for different size UCG power plants is around 105-125 t/panel/day and the energy provided from each panel is around 20-25 MWth. Finally, the in-seam linking distance can be considered from 500 to 1000 m. In the following section all this information will be used to calculate the output of a potential UCG power plant and to determine the UCG model.

7.4.4 Calculating the output of small and large UCG power plants

In order for a UCG power plant to be economically viable it needs to provide between 50-300 MWe of energy [16]. Two case studies will be examined to assess this, the first case study will calculate the output of a 120 MWth \approx 50 MWe power plant and the second one that of a 500MWth \approx 200 MWe. The target coal seam that will be considered is located in the Port Talbot area which is the UCG resource in Wales as suggested in the reports ‘Review of the feasibility of UCG in UK’ [16] and ‘UK coal resource for new exploitation technology’ [37] both produced for DTI. The heating value of the produced gas in Case Study 1 will be considered to be the one determined from this study (although the suggested coal seam is of a lower rank than the dry steam coal tested in this study which means that the heating value of the product gas of the proposed coal seam is higher). For Case Study 2, due to the larger size of the power plant, the heating value of the product gas will be considered to be similar to the one determined in the European field trial El Tremedial which was 11 MJ/Kg, also the target coal seam and the coal seam at the El Tremedial field trial belong to the same coal rank.

Case Study 1

The characteristics of the potential power plant that will be constructed as follows:

- Size of power plant: 120 MWth \approx 50MWe
- Years of operation of power plant: 20
- Load factor of power plant: 90%
- Thickness of target coal seam: 7 m
- Available coal resources: 220 Million tonnes, 169 Million m³
- Available resource area: 24 km²
- In-seam linking distance: 800 m
- Type of coal: dry steam coal
- LHV of coal 32.5 MJ/kg of coal
- LHV of char: 31.5 MJ/kg of char
- Density of coal: 1.32 t/m³
- Heating value of product gas: 7.5 GJ/t of gas
- CGE: 39%

The hours of operation of the power plant are $24 \times 365 \times 20 \times 0.90 = 157680$. So the total MWh thermal and the total energy GJ that will be produced from the 120 MWth power plant are respectively $120 \times 157680 = 18921600 = 18.9$ Million MWh_{th} and $18.9 \times 10^6 \times 3.6 = 71902080 = 68.04$ Million GJ and 3.4 Million GJ/year or 9320 GJ/day.

The required amount of energy the power plant needs per day will be provided by gasifying a certain amount of coal per day through the UCG process. According to the experimental results, the optimum reduction operating conditions determined for the dry steam is at 900°C and 1.65 MPa where 36.24 g of dry steam coal (30.15 g of char) was gasified for around 90 min under $\text{CO}_2 = 0.4$ l/min and a ratio of $\text{H}_2\text{O} / \text{CO}_2 = 2:1$. Under such conditions the product gas consisted by volume of 17% CO , 3% CH_4 and 42% H_2 with a LHV of 7.8 MJ/Nm³ and 7.5 MJ/kg of gas. Also the CGE is 39% which means that $31.5 \times 0.39 = 12.3$ MJ of gas is produced from every kg of char or 10.2 MJ of gas is produced from every kg of coal (10.2 GJ/t of coal).

Therefore in order to produce the required amount of energy needed for the 120 MW power plant per day, which was calculated as 9320 GJ, the amount of coal that needs to be gasified is $9320 \text{ GJ} / 10.2 \text{ GJ} = 914$ t of coal/ day gasified. Considering that the amount of energy that each panel can provide can be assumed to be around 25 MW which corresponds to approximately 105-125 t of coal per panel per day, the number of panels will be 9-7. Assuming 8 panels, then the coal that needs to be gasified every day from each panel to provide the required amount of energy to the power plant is 115 t of coal/day/ panel.

So the required coal resources which are the affected coal resources for the 120 MW power plant is $115 \times 12 \times 365 \times 20 = 6.72$ Million tonnes but considering the sweep efficiency of around 50%, then the total required coal resources is around 13.43 Million tonnes. Considering that the coal has a density of 1.32 t/m³ then the total required coal resources is 10.18 Million m³. Allowing that the in seam linking distance is 800 m and the coal seam thickness 7 m, then the width of coal seam will be 1817 m. If the in-seam linking distance was 1000 m then the width of the coal seam could be 1454 m.

Furthermore the outlet flow during the experiment was 0.6 l/min, therefore for 92 min which was the duration of the experiment, 0.055 m³ of product gas was

produced. Therefore by gasifying 1000 g of coal char instead of 36 g, 1.52 Nm³ of product gas is produced which gives a value of gas yield of 1.52 Nm³ of product gas/Kg of coal and for 6.72 Million tonnes of affected coal the product gas that can be produced is 10.2 Million Nm³ or 1399 Nm³/day . The mass of product gas per hour was 48 g from the 36 g of coal which gives a gas yield of 1.33 gas/kg of coal, hence the product gas from 6.72 Million tonnes of affected coal is 8.9 Million tonnes or 1224 tonnes/day

Considering that from the 10.2 m³ required resources for the 120 MWth power plant the 1/3 will be in the pillars and the 2/3 in the panels (since the sweep efficiency was considered 50%), then the critical panel width is calculated as 120 m and the pillar width 70 m. The width of the panels is in agreement with Gregg et al., (1976) [27] who states that the width of the panel =a x h where h is the coal seam thickness and a=5-10 if air is injected but if air is enriched with oxygen then the panel width could be bigger. Table 7.1 represents the information determined for the 120 MWth power plant.

Table 7.1 Information determined for the 120 MWth power plant

Product gas produced	10.2 Million Nm ³	8.9 Million tonnes
Total required coal resources	10.18 Million m ³	13.43 Million tonnes
Affected coal	6.7 Million tonnes	
Gasified coal/ day t/day	914 t/day	
MWh/t	2.8	
Proposed size of UCG model	1000 x 1454 x 7 m ³	
Number of panels	8	
Size of panels	1000 x 120 x 7 m ³	
Size of pillars	1000 x 70 x 7 m ³	

Case study 2

The characteristics of the potential power plant that could be constructed are the following:

- Size of power plant: 500 MW_{th}≈200MWe
- Years of operation of power plant: 25
- Load factor of power plant: 90%
- Thickness of target coal seam: 7 m
- Available coal resources: 220 Million tonnes, 169 Million m³
- Available resource are: 24 km²
- In-seam linking distance: 800 – 1000 m
- Type of coal: sub bituminous
- Density of coal: 1.32 t/m³
- Heating value of product gas: 11 GJ/t
- CGE:55%

The CGE is calculated at 55% due to the LHV of 11 GJ/t. By performing similar calculations as in Case study 1 (which are shown in Appendix C) the information that was determined for the 500 MW_{th} power plant is presented in Table 7.2

Table 7.2: Information determined for the 500 MW_{th} power plant

Product gas produced	37.4 Million Nm ³	32.7 Million tonnes
Total required coal resources	37.3 Million m ³	49.3 Million tonnes
Affected coal	28.4 Million tonnes	
Gasified coal/ day	3110 t/day	
MWh/t	3.2	
Proposed size of UCG model	1000 x 5329 x 7 m ³	
Number of panels	25	
Size of panels	1000 x 150 x 7 m ³	
Size of pillars	1000 x 74 x 7 m ³	

The 3.2 MWh/t of the 500 MW power plant is matching the 3.2 MWh/t calculated in the ‘Review of the feasibility of UCG in the UK’, (2004) which evaluates the result. It also shows that the 500 MW power plant is performing better than the 120 MW

power plant in terms of the amount of gasified coal and the energy that is produced with the 500 MW power plant producing 3.2 MWh from every tonne of coal compared with 2.8 MWh per tonne of coal produced by the 120 MW power plant. The difference lies in the higher heating value of the product gas used for the 500 MW power plant which relates to a low rank coal and it shows how important the heating value of the product gas is for a UCG project. However if the 120 MW power plant is not to be considered suitable for power generation certainly it would be suitable for the production of hydrocarbons which are greatly needed in the chemical industry.

7.5 Chapter Summary

Mass and energy balance was conducted and it is evident that the gas composition produced during the experiments performed with the dry steam coal and anthracite is due to the reactions of gasified chars with the oxidant gases under specific conditions during the simulated reduction zone of UCG.

It seems that carbon conversion is not affected by the type of coal significantly and that the carbon converted during UCG is approximately between 45% for high rank coals up to 55% for low rank coals. This means that approximately 45 to 55% of char is left underground and that the carbon conversion would not to be as high as reported for some field trials. Furthermore the high heating value produced by low rank coals during underground coal gasification is mainly due to the high volatile matter content (H_2 and CH_4) of the low rank coals and not from the reaction of char with the oxidant gases. For the same reason the CGE is high for low rank coals as well.

The composition of the produced gas in this study is comparable with those in the field trials, which reinforces the fact that the majority of the product gas, CO and H_2 , is produced during the reduction zone. The concentration of CH_4 in this study is very low compared to the concentration of CH_4 in the field trials and that can be explained by CH_4 being mainly produced during the pyrolysis zone. It should be noted that the results have allowed for the consistent analysis of the reduction processes, which yield combustible products directly from the solid phase char. This

does not include the contribution of the volatile matter; hence this has in part demonstrated that typical UCG operations on low rank coals provide a combustible product gas that relies heavily on releasing the volatile matter from the coal

The experimental results used to calculate the output and size of a potential small and large size UCG power plants produced realistic solutions and information about the required coal resources and the UCG models is also provided.

CHAPTER VIII

CONCLUSIONS AND RECOMMENDATIONS

The purpose of this chapter is to present the conclusions drawn from this study and propose recommendations for future research

8.1 Conclusions

8.1.1 Experimental apparatus

A bespoke high pressure high temperature rig was developed as part of this study which operates up to 900 °C temperature and pressures up to 5 MPa and is capable of producing results and data with a high level of accuracy for a broad range of coal samples sizes from powder and crushed coal, to blocks of around 10 mm height x 10 mm width with a length up to 200 mm. This experimental rig simulates the UCG process for a broad range of underground conditions and depths up to 500 m in order to investigate how temperature, gasifying agent composition and pressure affect the overall performance of UCG. Of these operating parameters, pressure is the least investigated. In addition the experimental rig provides a better insight and understanding of the UCG process by simulating each UCG zone individually. Furthermore the condensates produced can be analysed to assess the environmental impact of UCG process under various operating conditions. Although the experimental rig was developed to simulate and investigate the UCG process it can also be used for other applications such as surface gasification, combustion and pyrolysis experiments.

8.1.2 Effect of temperature and gasifying agents composition at atmospheric pressure

Temperature favours the gasification reactions during the reduction zone and is the most important factor for the gasification performance of UCG. The H₂O/CO₂ ratio of the gasifying agents enhances the gasification rate of the coal chars but above 2:1 (m/m) for both the coals tested, dry steam coal and anthracite, it decreases.

The optimum operating conditions which produced the best gas composition for both coals are determined at atmospheric pressure which are 900 °C and a H₂O/CO₂ ratio of 2:1 (H₂O/O₂ ratio of 2.4:1) with a coal sample of 36g for the dry steam coal and 20 g for anthracite. The maximum LHV is 4.9 MJ/Nm³ (3.9 MJ/kg) for the dry steam coal and 3.6 MJ/Nm³ (2.4 MJ/kg) for anthracite during the reduction zone. In addition the range of the H₂O/CO₂ ratio (m/m) is between 2:1 – 3:1 for the dry steam coal and between 2:1 and 2.5:1 for anthracite which produces a gas with a good LHV. These operating conditions are unique for each UCG system and have been determined for the first time for these types of coals allowing them to be considered in future field trials and UCG projects. In addition important information is provided about UCG of higher rank coals for which there is little research.

H₂ is the gas component which controls the resultant LHV since its contribution is comparably higher than that of CO and CH₄ for both coals. For hydrogen rich gas production the optimum ratio of H₂O/CO₂ is 2:1(m/m) for both coals and the ratio of H₂O/O₂ calculated stoichiometric to be 2.4:1 (m/m). These results could be useful when deciding the composition of the gasifying agents depending on the end use of the produced gas e.g: power generation, fuels, hydrogen production, chemicals etc.

The carbon conversion X (C in CO, CH₄ and CO₂) was determined as 0.24 for the dry steam coal and 0.19 for the anthracite when both coal chars were tested under their optimum gasification conditions at atmospheric pressure, which shows that the dry steam coal is more reactive than the anthracite. It was also found that the maximum carbon conversion X_a (C in CO and CH₄) was 0.13 for both coals which is an important finding and indicates that anthracite may be just as suitable for a UCG project as dry steam coal since it produced a similar amount of the combustible gases CO and CH₄ under the tested conditions. There are studies which mention that low rank and high volatile coals are preferable for UCG projects but this study concludes that high rank coals can also be considered for a UCG project, if not for energy production certainly for fuel and chemicals production.

The shrinking unreacted core model predicts well the gasification conversion of the two coal chars tested under the flow of CO₂+H₂O at atmospheric pressure and temperatures ranging from 750 to 900° C. The gasification rate depends strongly on the temperature, indicating chemical reaction rate control within the temperature

range tested. Reaction constants k were determined for different temperatures for both coals and the apparent activation energy E and the pre-exponential factor A were calculated to be 349.63 KJ/mol and 5.83×10^4 /sec for the dry steam coal and 406.74 KJ/mol and 2.63×10^7 /sec for the anthracite. These findings can be useful for modelling gasification processes. These values are slightly higher than results published using TGA analysis for substantially smaller samples (100 mg) where char conversion was undertaken with single oxidising gases (such as CO_2 and H_2O) in individual reactions [66]. Furthermore the activation energy calculated in this study is slightly higher than that calculated for a study where char conversion was undertaken in a fixed bed reactor with char sizes of 0.7 mm by also using single oxidizing gases (such as CO_2 and H_2O) in individual reactions [30].

The contribution of the drying/pyrolysis zone to the LHV of the product gas is 0.88 MJ/Nm³ (0.36 MJ/kg) for the dry steam coal and 0.47 MJ/Nm³ (0.22 MJ/kg) for anthracite which is around 10% of the maximum LHV of the product gas produced for both coals during gasification with $\text{CO}_2 + \text{H}_2\text{O}$ at atmospheric pressure. The contribution of the oxidation zone to the LHV of the product gas is very low since the largest amount of gas produced is CO_2 which is determined to be sufficient for the reduction reactions to occur at the next zone, which is the reduction zone. It can be concluded that the highest concentrations of the gases are mainly produced during the reduction zone and the rest during the drying and pyrolysis zone, specially for high volatile content coals. Its worth noting that the gases H_2 and CH_4 are released during the high temperature pyrolysis zone, between 750 to 850 °C.

It is demonstrated that the O_2 injected at the oxidation zone is consumed fairly quickly and the CO_2 produced reacts with the char which produces CO during the reduction zone proving that CO_2 is the rate controlling step of the gasification and that the reduction zone is responsible for the uniform quality of the product gas together with the overall mass and energy balance in UCG process. The reason that steam is also injected is to use the available energy in the cavity and react with the char to form H_2 and CO which enhances the gasification efficiency.

8.1.3 Effect of pressure

The optimum reduction conditions determined for the dry steam coal were $\text{H}_2\text{O} / \text{CO}_2 = 2:1$ ($\text{H}_2\text{O} / \text{O}_2 = 2.4:1$), 900°C at 1.65 MPa. Under such conditions the product gas consists by volume of 17% CO , 3% CH_4 and 42% H_2 with a LHV of 7.8 MJ/Nm^3 . The maximum carbon conversion was 0.28 (in 90 minutes at steady state) of which 0.26 are CO and CH_4 and the maximum CGE was 39%. For anthracite the maximum LHV of 6 MJ/Nm^3 was achieved at 1.0 MPa with $\text{H}_2\text{O} / \text{CO}_2 = 2:1$ ($\text{H}_2\text{O} / \text{O}_2 = 2.4:1$) at 900°C . The gas composition consists by volume of 17.3% CO , 1.6% CH_4 and 30.4% H_2 . The maximum carbon conversion was 0.27 (in 90 minutes at steady state) of which 0.25 are CO and CH_4 and the maximum CGE was 32%. These operating conditions are useful for industry and UCG applications.

The max LHV of the product gas and CGE for the tested coals at pressure are increased significantly by over 50% than that at ambient pressure in the reduction zone of UCG. Above the pressure of 2.0 MPa for the dry steam coal and 1.65 MPa for anthracite the LHV and CGE decrease. At pressures above 3.0 for the dry steam coal and 2.1 MPa for anthracite the pressure effect on LHV of the product gas and CGE becomes insignificant

Pressure enhances the carbon conversion X and increased from 0.24 at atmospheric pressure to the maximum value of 0.28 at 1.65 MPa for the dry steam coal and from 0.19 to 0.27 at 1.0 MPa for anthracite. There are no differences between the carbon conversions X of the two coals at various pressures and it seems that carbon conversion is enhanced at low pressures and above 2.0 MPa and 1.65 MPa for the dry steam coal and for anthracite it decreases.

It can be concluded that pressure does have a significant impact on the carbon conversion X_a of combustible gases for both coals with the maximum X_a achieved at 0.26 and 1.65 MPa for the dry steam coal and at 0.25 and 1.0 MPa for anthracite. These values are double the value of $X_a = 0.13$ achieved for both coals at atmospheric pressure and are calculated to be 92% of the maximum value of carbon converted X to gas at pressure for both coals.

It seems that there is an optimum operating pressure which produces a peak in carbon conversion X and X_a , CGE and LHV of the product gas, over the conditions

tested which differs for each coal. Therefore UCG projects aiming at operating to higher pressures will not achieve an increase in the output- unless there are some new effects occurring above 4 MPa. This finding agrees with the results of a study based on a semi industrial test but there are numerical studies in the available literature predicting the gas composition of the UCG process for low rank coals which report that the increase in pressure has always a positive impact on the heating value of the product gas. This may occur only for low rank coals since in the literature there are not enough studies reporting saturation [88] of the effect of pressure for such coals during coal gasification whilst high rank coals do show saturation as also shown in this study.

It is evident that pressurised gasification enhances fragmentation of the coal sample which facilitates the transport of gases to the internal surface of the char and hence enhances the gas solid reactions and the carbon conversion X and Xa and as a result increases the LHV of the product gas and CGE.

Pressure maximises the H_2 production with a maximum measured concentration of 49% Vol at 0.9 MPa for the dry steam coal and 30.4% Vol at 1.0 MPa for the anthracite. At higher pressures it appears that the effect of pressure saturates and only the CH_4 production is favoured with a maximum of 3% Vol for the dry steam coal and 1.8% Vol for the anthracite at 3.0 MPa which is explained by the adsorption-desorption mechanism at pressure.

There is positive pressure dependency on the gasification rates Xa of both coal chars for the tested pressures but only up to 1.65 MPa for dry steam coal and 1.0 MPa for anthracite where adsorption-desorption is the controlling mechanism which increases the active sites on the carbon surface. This effect saturates at higher pressures at the range of 3.0 MPa, where the mechanism changes by a different set of reactions occurring, producing CO_2 and CH_4 as the gasification rate is decreasing. It seems that this might be explained by the inhibiting effect of hydrogen and carbon monoxide on the steam and carbon dioxide reactions occurring respectively, which effect result in a gradual decrease in the reactivity of the chars and their gasification rate. At further higher pressures around 4.0 MPa the pressure effect becomes less significant since further increases in pressure will not lead to the formation of more

active sites. This study proves that pressure enhances the reaction rates and that there is a peak pressure above which the gasification rate reduces and the effect of pressure saturates.

The shrinking unreacted core model was modified to take into account the effect of total pressure on the gasification rate of the two coals tested under the flow of $\text{CO}_2 + \text{H}_2\text{O}$ at $900\text{ }^\circ\text{C}$ and elevated pressures ranged from 0.7 to 1.65 MPa. The reaction constants k were also calculated at different pressures for the two coals and could be useful data for modelling of coal gasification at elevated pressures. The reaction rate of the dry steam coal with $\text{CO}_2 + \text{H}_2\text{O}$ at $900\text{ }^\circ\text{C}$ and total system pressure from 0.7 to 1.65 MPa may be expressed with the following equation

$$dXa/dt = k P_{\text{total}}^{0.287} (1 - Xa)^{2/3} \text{ or as } dXa/dt = 5.83 \times 10^4 e^{-(349.63/RT)} P_{\text{total}}^{0.287} (1 - Xa)^{2/3}$$

As for anthracite the increasing reaction rate with $\text{CO}_2 + \text{H}_2\text{O}$ at $900\text{ }^\circ\text{C}$ and total system pressure from 0.1 to 1.0 MPa, due to good linearity between the reaction constant k and the pressures from atmospheric to 1.0 MPa, might be expressed as

$$dXa/dt = k P_{\text{total}}^{0.3} (1 - Xa)^{2/3} \text{ or as } dXa/dt = 2.63 \times 10^4 e^{-(406.74/RT)} P_{\text{total}}^{0.3} (1 - Xa)^{2/3} \text{ but more investigation is needed on anthracite.}$$

It can be concluded that anthracite can be as reactive as the dry steam coal in terms of carbon conversion X and Xa operating under specific conditions at atmospheric pressure or elevated and can produce almost the same amount of combustible gases, CO and CH_4 , as the dry steam coal. However the LHV of anthracite is lower than that of dry steam coal mainly due to the lower H_2 concentration produced during gasification which can be explained by the greater number of active sites generated by the C-steam reaction of the dry steam coal char which is a lower rank coal with higher porosity and volatile matter than anthracite. This also affects its CGE, which is also lower than that of dry steam coal, nevertheless if anthracite is not suitable for a UCG producing energy it is certainly suitable for hydrocarbon production which is currently needed and will be needed even more in the near future. CGE and the LHV of the produced gas are parameters that determine the effective gasification efficiency but the carbon conversion is equally important when considering the end use of the product gas.

8.1.4 Application of data to UCG field trials

The mass and energy balance showed very good agreement between the calculated and the experimental values which evaluates the results of this study. It is evident that the gas composition produced during the experiments performed with the dry steam coal and anthracite is due to the reactions of gasified chars with the oxidant gases under specific conditions during the simulated reduction zone of UCG.

The composition of the produced gas of this study is comparable with those in the field trials, which reinforces the fact that the majority of the product gas, CO and H₂, is produced during the reduction zone. The concentration of CH₄ in this study is very low compared to the concentration of CH₄ of the field trials which can be explained since CH₄ being mainly produced during the pyrolysis zone.

It should be noted that the results have allowed for the consistent analysis of the reduction processes which yield combustible products directly from the solid phase char. This does not include the contribution of the volatile matter, hence this has in part demonstrated that typical UCG operations on low rank coals provides a combustible syngas product that relies heavily on releasing the volatile matter from the coal and not from the reaction of char with the oxidant gases. This is the main reason that the LHV and CGE of low rank coals is higher than high rank coals and not the reaction of char with the oxidant gases. This also explains why the carbon conversion of coals used in UCG is not as high as expected and reported by some field trials. The carbon conversion for the high rank coals was determined around 45% in this study and was calculated around 55% for the low rank coals from two field trials data. It seems that carbon conversion is not significantly affected by the type of coal, that 45 to 55% of char remains underground after a UCG process and that the carbon conversion seems not to be as high as reported for some field trials, around 95%.

The experimental results were used to calculate the output and size of a potential small (120 MW) power plant, also the results from El Tremedial field trial were used to calculate a large (500 MW) size plant and both of these produced realistic solutions which agreed with the literature. In addition information about the required

coal resources and the UCG models is also provided and this knowledge might be useful in future projects.

8.1.5 Overall conclusions

The overall conclusions that can be drawn from this research study are presented below:

- A bespoke high pressure high temperature rig was developed as part of this study which operates up to 900 °C temperature and pressures up to 5 MPa and is capable of producing results and data with high level of accuracy for a broad range of coal samples sizes from powder to crushed coal and blocks of around 10 mm height x 10 mm width and length up to 200 mm. This experimental rig can simulate the UCG process for a broad range of underground conditions and depths up to 500 m and assess the pressure affect on the overall performance of UCG which is the least investigated.
- Optimal operating conditions were provided for the dry steam coal and anthracite which produced the best gas composition both at atmospheric and elevated pressure for both coals at 900 °C during gasification with CO₂+H₂O. In addition operating conditions which enhance the H₂ and CH₄ production were also provided. These operating conditions which are unique for each UCG system, have been determined for the first time for these types of coals and can be considered in future field trials and UCG projects. In addition information about UCG on a high rank coal is provided for which there is little information in the available literature.
- It seems that there is an optimum operating pressure which produces a peak in carbon conversion X and X_a , CGE and LHV of the product gas over the conditions tested which differs for each coal. Therefore UCG projects aiming at reaching to higher pressures will not achieve an increase in the output, unless there are some new effects occurring above 4 MPa. This pressure is determined to be 1.65 MPa for the dry steam coal and 1.0 MPa for anthracite.
- Pressure enhances the gas solid reactions and has a significant impact on the carbon conversion X_a of combustible gases for both coals with the maximum

value of Xa achieved at pressure being double the maximum value of Xa achieved at atmospheric pressure, which is calculated to be 92% of the maximum value of carbon converted X to gas at pressure.

- There is positive pressure dependency on the gasification rates Xa of a dry steam coal and anthracite char at low pressures (1.0 MPa for anthracite and 1.65 MPa for dry steam coal) where adsorption-desorption is the controlling mechanism. This effect saturates at higher pressures at the range of 3.0 MPa because the mechanism changes by different set of reactions occurring producing CO_2 and CH_4 which decrease the gasification rate. At further higher pressures around 4.0 MPa the pressure effect becomes negligible.
- The behaviour of the pyrolised chars of dry steam coal and anthracite with $\text{CO}_2+\text{H}_2\text{O}$ at 900 °C and atmospheric pressure was best described with the shrinking unreacted core model at atmospheric pressure and kinetic parameters were determined for each coal which can be useful for improving the modelling of the UCG process or other gasification applications.
- The shrinking unreacted core model was modified to take into account the effect of total pressure to the gasification rate of dry steam coal under the flow of $\text{CO}_2+\text{H}_2\text{O}$ at 900 °C and elevated pressures ranged from 0.7 to 1.65 MPa. Hence reaction constants for various pressures were determined and a new equation has been derived which might be useful in numerical simulations. Reaction constants at various pressures were also determined for anthracite but more investigation is needed on the impact of total pressure on its gasification rate.
- The contribution of the oxidation zone to the LHV of the product gas is very low and that of the drying/pyrolysis zone is around 10% of the LHV of the product gas produced in the reduction zone from both coals at atmospheric pressure. It can be concluded that the highest concentrations of the gases are mainly produced during the reduction zone and the rest during the drying and pyrolysis zone, specially for high volatile content coals. It is worth noting that the gases H_2 and CH_4 are released during the high temperature pyrolysis zone, between 750 to 850 °C.

- The composition of the produced gas of this study is comparable with those in the field trials of low rank coals, which reinforces the fact that the majority of the product gas, CO and H₂, is produced during the reduction zone. The concentration of CH₄ in this study is very low compared to the concentration of CH₄ in the field trials which can be explained by CH₄ being mainly produced during the pyrolysis zone.
- It should be noted that the results have allowed for the consistent analysis of the reduction processes which yield combustible products directly from the solid phase char. This does not include the contribution of the volatile matter, hence this has in part demonstrated that typical UCG operations on low rank coals provides a combustible product gas that relies heavily on releasing the volatile matter from the coal and not on the carbon conversion of char to gas.
- For the reason above it seems that carbon conversion X is not significantly affected by the type of coal and that the carbon converted during UCG is between approximately 45% for high rank coals, as determined in this study, up to 55% for low rank coals as calculated from field trials data. This means that approximately 45 to 55% of char remains underground and that the carbon conversion seems not to be as high as reported for some field trials, around 95%.
- It is evident that pressurised gasification enhances fragmentation of the coal sample which facilitates the transport of gases to the internal surface of the char and hence enhances the gas solid reactions and the carbon conversion X and Xa and as a result increases the LHV of the product gas and CGE.
- It can be concluded that anthracite can be as reactive as the dry steam coal in terms of carbon conversion X and Xa operating under specific conditions at atmospheric or elevated pressure and can produce almost the same amount of combustible gases, CO and CH₄, as the dry steam coal. However the LHV of anthracite is lower than that of dry steam coal mainly due to the lower H₂ concentration produced during gasification. This also affects its CGE which is also lower than that of dry steam coal, nevertheless if anthracite is not suitable for a UCG producing energy it is certainly suitable for hydrocarbon

production which is currently needed and will be needed even more in the near future.

- CGE and the LHV of the product gas are parameters that determine the effective gasification efficiency but the carbon conversion is equally important when considering the end use of the product gas.
- The experimental results were used to calculate the output and size of a potential small power plant and the results from a field trial were used to calculate a large size plant and both of these produced realistic solutions which agreed with the literature. In addition information about the required coal resources and the UCG models is also provided and this knowledge might be useful in future projects.

8.2 Recommendations

Recommendations for future research work identified from this study are suggested in the following paragraphs:

- It would be valuable to run similar experiments with low rank coals in order to assess the behaviour of low rank coal chars with $\text{CO}_2+\text{H}_2\text{O}$ at atmospheric and elevated pressures in order to enable comparison with the results and findings of this study.
- Furthermore this work could be further extended by performing experiments simulating the UCG process by injecting $\text{O}_2+\text{H}_2\text{O}$ and $\text{air}+\text{H}_2\text{O}$ at pressures of up to 50 bar and for temperatures from 500-900 °C for both the dry steam coal and anthracite that were used in this study. This will enable a comparison with other studies and will also determine the contribution of the oxidation zone to the UCG performance through comparison with the findings of this study which will allow better understanding of the UCG process by investigating the role of each zone separately. Kinetic data can also be derived for different temperatures at pressure which could help numerical simulation of the UCG process. In addition the resultant condensates from drying/pyrolysis experiments can be analysed in order to

identify and quantify contaminants and the impact of temperature and pressure on their concentration.

- It would be useful if the future research work described above was also carried out with low rank coals. This would enable a data base to be created for the performance of different coal types during UCG process with the contaminants that are created.
- The structure of the resultant char at different pressures for various types of coals is connected to the char reactivity and analysis of this structure might help better understand the mechanism controlling the effect of pressure.
- The experimental rig can also be used for other applications such as surface gasification, combustion and pyrolysis applications. Kinetic data for devolatilisation, oxidation and gasification at various pressures, temperatures and sample sizes is also needed to measure char gasification rates at high pressure and for developing mathematical models to predict the rates of carbon conversion for IGCC (Integrated gasification combine cycle) power plants.

REFERENCES

1. Ahn, D. H., Gibbs, B.M., Ko, K.H., Kim, J.J. 2001. Gasification kinetics of an Indonesian sub-bituminous coal-char with CO₂ at elevated pressure. *Fuel*, 80(11), p. 1651-1658.
2. Blackwood, J. D., McGroary, F. 1958. The carbon steam reaction at high pressure. *Australian Journal of Chemistry*, 11(1), p. 16-33.
3. Blackwood, J. D., Ingeme, A. J. 1960. The reaction of carbon with carbon dioxide at high pressure. *Australian Journal of Chemistry*, 13, p.194-209.
4. Bhutto, A.W, Bazmi, A.A, Zahedi, G. 2013. Underground Coal Gasification: From fundamentals to applications. *Progress in Energy and Combustion Science*, 39(1), p. 1-26.
5. Britten, J.A., Thorsness, C.B., 1988. The Rocky Mountain 1 CRIP (Controlled Retracting Injection Point) experiment: Comparison of model predictions with field data. *14th Annual Underground Coal Gasification Symposium*.
6. Britten, J.A., Thorsness, C.B., Upadhye, R.S., Field, J.E. 1986. Development of a reliable method for in-situ ignition of coal through a lined borehole. *Lawrence Livermore National Laboratory*. UCRL-93888
7. Burton, E., Friedmann, J., Upadhye, R. 2006. *Best practices in underground coal gasification*. *Lawrence Livermore National Laboratory*.
8. Cambell, J. H. 1978. Pyrolysis of sub bituminous coal in relation to in-situ coal gasification. *Fuel*, 57, p. 217-224.
9. Cena, R. J., Thorness, C. B. 1981. Underground coal gasification data base. *Lawrence Livermore National Laboratory* UCID -19169.
10. Chappell, M., Mostade, M. 1998. The El Tremedal underground coal gasification field test in Spain first trial at great depth and high pressure. *Fifteenth annual international Pittsburgh coal conference*, Pittsburgh, USA.
11. Couch, G. 2009. Underground coal gasification. *IEA Clean Coal Centre*. Report No: Contract No: CCC/151.
12. Creedy, D., Garner, K, Holloway, S., Jones, N., Ren, T. X. 2001. Review of underground coal gasification technological advancements. *DTI Cleaner Coal Technology Transfer Programme*. Report No: COAL R211.

13. Daggupati, S., Mandapati, R., N., Mahajani, S., M., Ganesh, A., Mathur, D. K., Sharma, R. K., Aghalayam, P. 2010. Laboratory studies on combustion cavity growth in lignite coal blocks in the context of underground coal gasification. *Energy*, 35(6), p. 2374-2386.
14. Daggupati, S., Mandapati, R., N., Mahajani, S., M., Ganesh, A., Sapru, R., Sharma, R. K., Aghalayam, P. 2011. Laboratory studies on cavity growth and product gas composition in the context of underground coal gasification. *Energy*, 35(3), p. 1776-1784.
15. Dennis, D. 2006. Rocky Mountain 1 underground coal gasification test project Hanna, Wyoming: Final technical report for the period 1986 to 2006. *U.S. Department of Energy & National Energy Technology Laboratory*.
16. DTI. Review of the feasibility of UCG in the UK. 2004. *Department of Trade and Industry*.
17. DTI. Review of environmental issues of UCG. 2004. *Department of Trade and Industry*. Report No: COAL R272.
18. Environmental protection agency US, Advanced Resources International. *Directional drilling technology*.
19. Ergun, S. 1956. Kinetics of the reaction of carbon with carbon dioxide. *Journal of Physical Chemistry*, 60 (4), p. 480-485
20. European Commission. 2011. *Energy roadmap 2050*, [COM/2011/885]. EU.
21. European Commission. 2014. *European Energy Security Strategy*, [COM/2014/330]. EU.
22. Everson, R. C., Neomagus, W.J. P., Hein, Kasaini, H., Njapha, D. 2006. Reaction kinetics of pulverized coal-chars derived from inertinite-rich coal discards: gasification with carbon dioxide and steam. *Fuel*, 855(11), p. 1076-1082.
23. Fermoso, J., Arias, B., Plaza, M. G., Pevida, C., Rubiera, F., Pis, J. J., Garcia-Pena, F., Casero, P. 2009. High-pressure co-gasification of coal with biomass and petroleum coke. *Fuel Processing Technology*, 90(7-8), p. 926-932.
24. Fogler, H. S. 2004. *Elements of Chemical Reaction Engineering*. Pearson New International Edition
25. Friedmann, S. J., Upadhye, R., Kong, F. M. 2009. Prospects for underground coal gasification in carbon-constrained world. *Energy Procedia*, 1, p. 4551-4557.

26. Goyal, A., Zabransky, R. F., Rehmat, A. 1989. Gasification kinetics of Western Kentucky bituminous coal char. *American Chemical Society, Ing. Eng. Chem. Res*, 28, p. 1767-1778.
27. Gregg, D. W., Hill, R. W., Olness, D. U. 1976. An overview of the Soviet effort in underground coal gasification. *Lawrence Livermore National Laboratory*, UCRL-52004.
28. Gregg, D. W., Edgar, T. F. 1978. Underground coal gasification. *American Institute of Chemical Engineers Journal*, 24(5), p. 753-81.
29. Haggin, J. 1983. Key tests set for underground coal gasification. *Chemical & engineering news*, 61(29), p. 15-24.
30. Harris, D. J., Smith, I. W. 1991. Intrinsic reactivity of petroleum coke and brown coal char to carbon dioxide, steam and oxygen. *23rd Symposium (International) on Combustion, the Combustion Institute*, 23(1), p. 1185-1190.
31. Haynes international. *Tubular products and capabilities*. Haynes international, Inc, 2015, H-1030F.
32. Higman, C., Van der Burgt, M. 2008. *Gasification*. Elsevier Science.
33. Hill, R. W., Shannon, M. J. 1981. The controlled retracting injection point (CRIP) system a modified stream method for in situ coal gasification. *Lawrence Livermore National Laboratory*, UCRL-85852.
34. International Energy Agency. 2014. World energy outlook 2014. OECD/IEA
35. Irfan, M., Usman, M., Kusakabe, K. 2011. Coal gasification in CO₂ atmosphere and its kinetics since 1948: A brief review. *Energy*, 36(1), p.12-40.
36. Johnson, J L. Kinetics of bituminous coal char gasification with gases containing steam and hydrogen. 1974. *Advances in Chemistry*, Ser.131, p. 145-178.
37. Jones, N., Holloway, S., Creedy, D., Garner K, Smith, N. P. J., Browne, M. A. E., Durucan, S. 2004. UK coal resource for new exploitation technology. *Department of Trade and Industry*. Commissioned report CR/04/015N.
38. Kajitani, S., Hara, S., Matsuda H. 2002. Gasification rate analysis with a pressurized drop tube furnace. *Fuel*, 81, p. 539-546

39. Katta, S., Keairns, D. L. 1981. Study of kinetics of carbon gasification reactions. *Industrial and Engineering Chemistry Fundamentals*, 20(1), p. 6-13.
40. Konstantinou, E., Marsh, R. 2015. Experimental study on the impact of reactant gas pressure in the conversion of coal char to combustible gas products in the context of Underground coal gasification. *Fuel*, 159, p. 508-518.
41. Knight, A. T., Sergeant, G. D. 1980. Reactivity of Australian coal derived chars to carbon dioxide. *Fuel*, 61, p. 145-149.
42. Kristiansen, A. 1996. Understanding coal gasification. IEA Coal Research, 1996.
43. Kwon, T.-W., Kim S. D, Fung D.P.C. 1988. Reaction kinetics of char-CO₂ gasification. *Fuel*, 67, p. 530-536.
44. Laurendeau, N. M. 1978. Heterogeneous kinetics of coal char gasification and combustion. *Progress in Energy and Combustion Science*, 4(4), p. 221-270.
45. Levenspiel, O. 1999. *Chemical reaction engineering*. John Wiley & Sons, 3rd edition.
46. Li, S., Sun, R. 1994. Kinetic studies of a lignite char pressurized gasification with CO₂, H₂ and steam. *Fuel*, 73(3), p. 413-417.
47. Lim, J.-Y., Chatzakis, I. N., Megaritis, A., Cai, H.Y., Dugwell, D.R. 1997. Gasification and char combustion reactivities of Daw Mill coal in wire-mesh and 'hot rod' reactors. *Fuel*, 76(13), p. 1327-1336
48. Liu, G.-S., Niksa, S. 2004. Coal conversion submodels for design applications at elevated pressures. Part II. Char gasification. *Progress in Energy and combustion science*, 30, p. 679-717.
49. Liu, S.-Q., Wang, Y.-Y., Zhao, Y.N. 2008. Enhanced-hydrogen gas production through underground gasification of lignite. *Mining Science and Technology*, 19 (3), p. 384-395.
50. Liu, T., Fang, Y., Wang, Y. 2008. An experimental investigation into the gasification reactivity of chars prepared at high temperatures. *Fuel*, 87(4-5), p. 460-467.

51. Long, F. J., Sykes, K. W. 1948. The mechanism of steam carbon reaction. *Proceeding of Royal Society of London A: Mathematical, Physical and Engineering Sciences*, 193(1034), p. 377-399. The Royal Society.
52. Ma, Z.-H., Zhang, C.-F., Zhu, Z.-B., Sun, E.-L. 1992. A study on the intrinsic kinetics of steam gasification of Jincheng coal char. *Fuel Processing technology*, 31(1), p. 69-77.
53. Mandapati, R., Daggupati, S., Mahajani, S. M., Aghalayam, P., Sapru, R. K., Rakesh, K. S., Ganesh, A. 2012. Experiments and kinetic modelling for CO₂ gasification of Indian coal chars in the context of underground coal gasification. *Industrial Engineering Chemical Research*, 51(46), p.15041-15052.
54. Marsh, R., Steer, J., Fesenko, E., Cleary, V., Rahman, A., Griffiths, T., Williams, K. 2008. Biomass and waste co-firing in large-scale combustion systems.. *Proceedings of the Institution of Civil Engineers, Energy*, 161 (EN3), p. 115
55. Moilanen, A., Muhlen H.-J. 1996. Characterization of gasification reactivity of peat char in pressurized conditions. *Fuel*, 75(11), p. 1279-1286.
56. Morris, J. P., Buscheck, T. A., Hao, Y. 2009. Coupled geomechanical simulations of UCG cavity evolution. *International Pittsburgh Coal Conference (LLNL-CONF-414700)*.
57. Mühlen, H., van Heek, K. H., Jüntgen, H. 1985. Kinetic studies of steam gasification of char in the presence of H₂, CO₂ and CO. *Fuel*, 64, p. 944-949.
58. Mühlen, H., van Heek, K. H. 1991. Fundamental issues in control of carbon gasification reactivity. In: Lahaye J., Ehrburger P. Dordrecht: Kluwer Academic publishers, p.1
59. Nozaki, T., Adschiri, T., Fujimoto, K. 1992. Coal char gasification under pressurized CO₂ atmosphere. *Fuel*, 71, p. 349-350.
60. Olness, D., Gregg, D. W. 1977. The historical development of underground coal gasification. *Lawrence Livermore National Laboratory, UCRL-52283*.
61. Perkins, G., Sahajwalla, V. 2005. A numerical study of the effects of operating conditions and coal properties on cavity growth in underground coal gasification. *Energy & Fuels*, 20, p. 596-608.

62. Perkins, G., Sahajwalla, V. 2007. Modelling of heat and mass transport phenomena and chemical reaction in underground coal gasification. *Chemical Engineering Research and Design*, 85(A3), p. 329-343.
63. Perkins, G., Sahajwalla, V. 2008. Steady-state model for estimating gas production from underground coal gasification. *Energy and Fuels*, 22(6), p. 3902-3914.
64. Perry, R. H., Green, D. W. 1999. *Perry's chemical engineers' handbook*, M.Graw-Hill Companies Inc.
65. Porada, S., Czernski, G., Dziok, T., Grzywacz, P., Makowska, D. 2015. Kinetics of steam gasification of bituminous coal in terms of their use for underground coal gasification. *Fuel Processing technology*, 130, p. 282-291.
66. Roberts, D. G. 2000. *Intrinsic reaction kinetics of coal chars with oxygen, carbon dioxide and steam at elevated pressure*. PhD Thesis, University of Newcastle, UK.
67. Roberts, D. G, Harris D. J. 2000. Char gasification with O₂, CO₂, and H₂O: Effects of pressure on intrinsic reaction kinetics. *Energy and Fuels*, 14(2), p. 483-489.
68. Roberts, D. and D. Harris. 2006. A kinetic analysis of coal char gasification reactions at high pressures. *Energy and Fuels*, 20(6), p. 2314-2320.
69. Roberts, D. and D. Harris, Wall, T. F. 2003. On the effects of high pressure and heating rate during coal pyrolysis on char gasification reactivity. *Energy and Fuels*, 17, p. 887-895.
70. Sha, X.-Z., Chen, Y.-G., Cao, J., Yang, Y.-M., Ren, D.-Q. 1990. Effects of operating pressure on coal gasification. *Fuel*, 69, p. 656-659.
71. Shafirovich, E., Varma, A. 2009. Underground coal gasification: A brief review of current status. *Industrial Engineering Chemistry Research*, 48(17), p. 7865 - 7875.
72. Shufen, L., Xinyan, X. 1993. Gasification reactivity of three Chinese coal chars with steam at elevated pressure. *Fuel*, 72(9), p. 1351-1353.
73. Smith, I.W., The combustion rates of coal chars: A review. 1982. In *Symposium International on Combustion*. 19(1), p.1045-1065.
74. Stańczyk, K., Smoliński, A., Kapusta, K., Wiatowski, M., Świądrowski, J., Kapusta, K., Grabowski, J., Kotyrba, A., Rogut, J. 2010. Dynamic

- experimental simulation of hydrogen oriented underground gasification of lignite. *Fuel*, 89(11), p. 3307-3314.
75. Stańczyk, K., Howaniec, N., Smoliński, A., Świądrowski, J., Kapusta, K., Wiatowski, M., Grabowski, J., Rogut, J.. 2011. Gasification of lignite and hard coal with air and oxygen enriched air in a pilot scale ex-situ reactor for underground coal gasification. *Fuel*, 90(5), p. 1953-11962.
 76. Stańczyk, K., Kapusta, K., Wiatowski, M., Świądrowski, J., Smoliński, A., Rogut, J., Kotyrba, A. 2012. Experimental simulation of hard coal underground gasification for hydrogen production. *Fuel*, 91(1), p. 40-50.
 77. Tangsathitkulchai, C., Junpirom, S., Katesa, J. 2012. Comparison of kinetic models for CO₂ gasification of Coconut-shell chars: carbonization temperature effects on char reactivity and porous properties of produced activated carbons. *Engineering Journal*, 17(1), p. 14-27.
 78. Taylor, H. S. 1925. A theory of the catalytic surface. *Proceedings of the Royal Society of London*, Series A, 108(745), 105, p. 105-111.
 79. Thorsness, C. B., Hill, R. W., Britten, J. R. 1988. Execution and performance of the Crip process during the rocky mountain 1 UCG field test. *Lawrence Livermore National Laboratory*, UCRL-98641.
 80. Thorsness, C. B., Rozsa, R. 1977. In-situ coal gasification: Model Calculations and Laboratory Experiments. *Society of Petroleum Engineers Journal*, 18, p.105-116.
 81. Turdogan, E.T., Vinters, J.V. 1969. Kinetics of oxidation of graphite and charcoal in carbon dioxide. *Carbon*, 7, p. 101-117.
 82. Van der Riet, M. 2008. Underground coal gasification. *South Africa Institute of Electrical Engineers Generation Conference*.
 83. Von Fredersdorff, C. G., Elliott, M. A. 1960. *Coal gasification*. Institute of Gas Technology.
 84. Walker, I. K. 2007. Commercial development of underground coal gasification. *Proceedings of the Institution of Civil Engineers (ICE)-Energy*, 160(4), p. 175-180.
 85. Walker, P.L., Rusinko, F., Austin, L.G. 1959. Gas reactions of carbon. *Advances in Catalysis*, 11(590), p. 133.

86. Walker, P. L. Jr., Hippo, E. Factors affecting reactivity of coal chars. 1975. *American Chemical Society, Fuel Chemistry Division*, 20(3), Conference: 170.
87. Wall, T., Guisu, L., Wong, W.-W. 2002. Effect of pressure on ash formation during pulverised coal combustion and gasification. *Progress in Energy and Combustion Science*, 5, p. 405-443.
88. Wall, T., Liu, G.-S., Wu, H.-W., Roberts, D. G., Benfell, K. E., Gupta, S., Lucas, J. A., Harris, D. J. 2002. The effects of pressure on coal reactions during pulverised coal combustion and gasification. *Progress in energy and combustion science*, 2, p. 405-433.
89. Wang, Q., Wang, Z.T., Feng, B. 2009. Semi industrial tests on enhanced underground coal gasification at Zhong-Liang-Shan coal mine. *Asia pacific journal of chemical engineering*, 4, p. 771-779.
90. Wen, C. Y. 1968. Non catalytic heterogeneous solid fluid reaction models. *Industrial Engineering Chemistry*, 60(9), p. 34-54.
91. Wiatowski, M., Stanczyk, K., Swiadrowski, J., Kapusta, K., Cybulski, E., Krause, E., Grabowski, J., Rogut, J., Howaniec, N., Smoliński, A. 2012. Semi-technical underground coal gasification (UCG) using the shaft method in Experimental Mine “Barbara”. *Fuel*, 99(1), p. 170-179.
92. Yang, L., Liang, J., Yu, L. 2003. Clean coal technology - Study on the pilot project experiment of underground coal gasification. *Energy*, 28(14), p. 1445-1460.
93. Yang, L. 2006. The dynamic temperature field of two stage underground coal gasification. *Energy Sources, Part A Recovery, Utilisation and Environmental Effects*. 28(7), p. 667-680.
94. Yang, L., Zhang, X., Liu, S., Yu, L., Zhang, W. 2008. Field test of large-scale hydrogen manufacturing from underground coal gasification. *International Journal of Hydrogen Energy*, 33, p. 11.
95. Yang, L. H., Zhang X., Liu S. 2009. Underground coal gasification using oxygen and steam. *Energy sources, Part A* (31), p. 1883-1893.
96. Ye D, Agnew J, Zhang D. 1997. Gasification of a South Australian low-rank coal with carbon dioxide and steam: kinetics and reactivity studies. *Fuel*, 77(11), p. 1209-1220.

97. Yeary, D. 1987. *Experimental study of lateral cavity growth mechanisms in underground coal gasification*. MSc Thesis, Texas Tech University, Chemical Engineering Department, US.

Appendix A

Calculation of LHV

LHV=HHV- Heat of vaporisation of water

HHV is determined by the Bomb Calorimeter at 33.49 MJ/Kg

Heat of vaporisation of water= mass of water* h_{fg}

Where h_{fg} is the latent heat of vaporisation of water which is 2.465 MJ/Kg of water

The percentage of Hydrogen content in the coals is 4% and 3% for the dry steam coal and anthracite respectively which means that in 1 Kg of coal the steam content is 0.4 Kg for the dry steam coal and 0.3 Kg for the anthracite.

LHV of dry steam coal= $33.49-0.4 \times 2.465 = 32.50$ MJ/Kg

LHV of dry steam coal= $33.74-0.3 \times 2.465 = 33.00$ MJ/Kg

Or alternatively the following formula could be used

LHV=HHV-24.44(9%H+M%) KJ/Kg

Appendix B

B.1 Energy balance calculations

MASS and ENERGY BALANCE			
VARIABLES			
Type of coal	Steam coal		
Mass of coal	Kg		0.036
Fixed Carbon %	%		83.200
Volatiles %	%		12.940
Moisture %	%		0.584
Ash %	%		3.290
CV of parent coal	MJ/kg		32.500
CV of parent char	MJ/kg		31.500
Initial temperature	C		25
Final temperature	C		900
Water injected	kg		0.115
Water coming out	kg		0.089
Char gasified during the experiment	kg		0.007
Char left after the experiment	kg		0.022
Specific heat of water	KJ/Kg K		2.680
Specific heat of bitumen	KJ/Kg K		0.448
Specific heat of ash	KJ/Kg K		0.840
Heating energy of tar	MJ/kg		36
CALCULATIONS			
Energy in the coal	MJ/kg	$0.036 \times 83.2\% =$	1.154
STAGE 1: Temperature is rising			
1.1 DRYING	MJ/Kg coal	$2.68 \times 0.584\% \times 0.036 =$	0.00056
1.2 DEVOLATILISATION	MJ/Kg coal	$0.448 \times 12.94\% \times 0.36 =$	0.002
Energy left in the coal		$1.154 - 0.001 - 0.002 =$	1.151
STAGE 2: Injecting water + Gasification of char			
2.1 EVAPORATION OF WATER	MJ	$2.26 \times (0.115 - 0.089) =$	0.05
2.2 GASIFICATION OF CHAR			
$C + CO_2 \rightarrow 2CO$	MJ		14.400
$C + H_2O \rightarrow CO + H_2$	MJ		14.500
$C + 2H_2 \rightarrow CH_4$	MJ		-6.250
Actual energy needed for gasification	MJ	$0.007 \times 14.5 =$	0.104
Inert heating	MJ	$3.29\% \times 0.84 \times 0.036 \times (8.32\% \times (90 - 25)) / 1000 =$	0.001
Losses to the environment	MJ		0.023
Energy in the char	MJ	$0.0224 \times 31.5 =$	0.71
Energy in the tar	MJ	0.002×36	0.072
Energy in the product gas	MJ	$1.151 - 0.05 - 0.001 - 0.023 - 0.71 - 0.072 =$	0.29

B.2 Calculation of the heat losses to the environment through conduction

$Q = 2 \pi K L (T_F - T_o) (1.1) / \ln (r_o/r_i)$ W or Btu/hr where

K is the thermal conductivity coefficient in 8.9 W/m K or 62 Btu in/ft² hr F

L the length of the reactor in m or ft

1.1 is an additional 10% for convection and radiation heat losses

r_o is the outer radius of the reactor in m or inches

r_i is the inner radius of the reactor in m or inches

Also 1 W = 3.412 Btu and 1 ft = 12 inches

B.3 Calculation of the C in tar and hydrocarbons

The C in the tar and in the light hydrocarbons (C_{t+h}) can be calculated by the Fixed Carbon=83.2% of the coal determined from the proximate analysis and the C content =88.4% determined from the ultimate analysis.

In 100 g of coal, the Fixed Carbon (F.C) is 83.2 g and the C=88.4, the $C_{t+h} = 88.4 - 83.2 = 5.1$ g in 100 g of coal. In 35.58 g of coal sample the C_{t+h} is approximately 2 g.

B.4 How much char is needed to oxidise in order to initiate gasification
if we have 1 kg of char on an ash free basis

1. Oxidation of char

$C + O_2 \rightarrow CO_2$	$\Delta h = -32.8$	MJ/Kg
Total energy released	$\Delta h = -32.9$	MJ/Kg

2. Gasification of char

$C + CO_2 \rightarrow 2CO$	$\Delta h = 14.4$	MJ/Kg
$C + H_2O \rightarrow CO + H_2$	$\Delta h = 14.5$	MJ/Kg
$C + 2H_2 \rightarrow CH_4$	$\Delta h = -6.25$	MJ/Kg
Total energy needed for gasification	$\Delta h = 14.5$	Considering only $C + H_2O \rightarrow CO + H_2$

RESULTS

Combusted char (y) $y = 1 - x$	$32.8 \cdot (1 - x) = 14.5x$	$x = 0.69$
Gasified char (x)	$1 - 0.69 = 0.31$	$y = 0.31$

Appendix C

Case study 2

The hours of operation of the power plant are $24 \times 365 \times 20 \times 0.90 = 157680$, so the total MWh thermal and the total energy GJ that will be produced from the 500 MWth power plant are respectively $500 \times 157680 = 78.84$ Million MWhth and $78.84 \times 10^6 \times 3.6 = 283.82$ Million GJ and 14.2 Million GJ/year or 38880 GJ/day.

Each panel will produce 25 MWth and the number of panels are $500/25 = 20$. The energy that needs to be produced every day from each panel is 1944 GJ/day panel, and the LHV of the product gas per kg of char is $55\% \times 31.5 = 17.3$ MJ and 14.4 MJ/kg of coal. Hence the amount of coal that needs to be gasified is $1944 \text{ GJ} / 14.4 \text{ GJ/t} = 135$ t of coal/day panel and the amount of affected coal for 25 years is 24.6 Million tonnes. Considering the sweep efficiency at a value of 0.5, then the total amount of coal required is 49.3 Million tonnes or 37.3 Million m^3 considering a density of 1.32 t/m^3 for sub bituminous coal which is less than the available coal resources.

Considering that the in-seam linking distance is 800 m the width of coal seam will be 6666 m, if the in-seam linking distance was 1000 m than the width of the coal seam would be 5329 m. The required resource area is calculated at 6.2 km^2 which is less than the available resource area.

The outlet flow during the experiment was 0.6 l/min which means that for 92 min which was the duration of the experiment 0.055 m^3 of product gas was produced. Therefore by gasifying 1000 g of coal char instead of 36 g, 1.52 Nm^3 of product gas is produced which gives a value of gas yield 1.52 Nm^3 of product gas/Kg of coal and for 24.6 Million tonnes of affected coal the product gas that can be produced is 37.4 Million Nm^3 or $4098 \text{ Nm}^3/\text{day}$. The mass of product gas per hour was 48 g from the 36 g of coal which gives a gas yield of 1.33 gas/kg of coal, hence the product gas from 24.6 Million tonnes of affected coal is 32.7 Million tonnes or 3585 tonnes/day

Appendix D

Experimental data

The experimental data is provided on the CD included with this thesis.

Calculation of the C in C_a

The C contained in CO and CH₄ per second was calculated by dividing the amount of CO and CH₄ determined from the experiments per second by 12, which is the molarity of C. Then the C calculated in CO and CH₄ per second were added together and then also added cumulatively for every second to determine the final C_a - which is the total C contained in the CO and CH₄ produced from the experiments for both coals.